JPL Publication 88-28

Interplanetary Particle Environment

Proceedings of a Conference

Joan Feynman
Stephen Gabriel
Editors

April 15, 1988

National Aeronautics and
Space Administration

Jet Propulsion Laboratory
California Institute of Technology
Pasadena, California

JPL Publication 88-28

Interplanetary Particle Environment

Proceedings of a Conference

Joan Feynman
Stephen Gabriel
Editors

April 15, 1988

NASA
National Aeronautics and
Space Administration

Jet Propulsion Laboratory
California Institute of Technology
Pasadena, California

This publication was prepared by the Jet Propulsion Laboratory, California Institute of Technology, under a contract with the National Aeronautics and Space Administration.

ABSTRACT

A workshop entitled the Interplanetary Charged Particle Environment was held at the Jet Propulsion Laboratory (JPL) on March 16 and 17, 1987. The purpose of the Workshop was to define the environment that will be seen by spacecraft operating in the 1990s. It focused on those particles that are involved in single event upset, latch-up, total dose and displacement damage in spacecraft microelectronic parts. Several problems specific to Magellan were also discussed because of the sensitivity of some electronic parts to single-event phenomena. Scientists and engineers representing over a dozen institutions took part in the meeting.

The workshop consisted of two major activities, reviews of the current state of knowledge and the formation of working groups and the drafting of their reports. Fifteen presentations were made during the first part of the meeting. Two working groups were then convened, one on solar events and particles accelerated by shocks within the heliosphere and the other on galactic cosmic rays. The working groups made recommendations as to what models should now be used in the assessment of interplanetary particle environments and also recommended what steps should be taken in the future to upgrade the environmental models. This volume contains the reports of the working groups, presentations or extended abstracts of presentations given at the meeting, and a list of the participants.

CONTENTS

PREFACE

A workshop entitled the Interplanetary Charged Particle Environment was held at JPL on March 16 and 17, 1987. The purpose of the Workshop was to define the environment that will be seen by spacecraft operating in the 1990's. It focused on those particles that are involved in single event upset, latch-up, total dose and displacement damage in spacecraft microelectronic parts. Several problems specific to Magellan were also discussed because of the sensitivity of some electronic parts to single-event phenomena. These included shielding of the spacecraft, by Venus, from solar particles, the ability to predict the occurrence of proton events 24 hours in advance, earth-based real-time forecasting for the entire Magellan mission, and the use of a particle detector on the spacecraft to shut off circuit elements in case of the arrival at Venus of a major proton event.

Although the conference was called on extremely short notice, twenty-five scientists and engineers representing over a dozen institutions responded to the JPL call for a two-day meeting on March 16 and 17, 1987. The workshop consisted of two major activities, reviews of the current state of knowledge and the formation of working groups and the drafting of their reports. Fifteen presentations were made during the first part of the meeting. Two working groups were then convened, one discussing solar events and particles accelerated by shocks within the heliosphere and the other discussing galactic cosmic rays. The working groups were asked to make recommendations as to what models should now be used in the assessment of interplanetary particle environments and also to recommend what steps should be taken in the future to upgrade the environmental models. This volume contains the reports of the working groups and presentations or extended abstracts of presentations given at the meeting as well as a list of the participants.

As conveners we would like to thank all the participants for their participation and cooperation. Because of the relevance to the Magellan emergency the workshop was called with only a few weeks notice. In spite of the pressure of their previously planned work the participants responded enthusiastically with their well-considered papers and their intense and dedicated work as members of the working groups.

We would also like to thank R.E. McGuire of the NASA Goddard Space Flight Center who, in preparation for this workshop, carried out an analysis of his data addressed to the Magellan problem specifically but was unable to attend the conference. His work was however used in the conference discussions. Special thanks are due to M.A. Shea who chaired the solar particle working group and R.A. Mewaldt who chaired the galactic cosmic ray working group.

WORKING GROUP REPORTS

Toward a Descriptive Model of Solar Particles in the Heliosphere

M. A. Shea and D. F. Smart
Air Force Geophysics Laboratory
Hanscom AFB, Bedford, Mass 01731

J. H. Adams Jr.
Naval Research Laboratory
Washington, D. C. 20375

D. Chenette
Aerospace Corporation
2350 East El Segundo Blvd.
El Segundo, California, 90245

J. Feynman
Jet Propulsion Laboratory
4899 Oak Grove Drive
Pasadena, California 91109

Douglas C. Hamilton
University of Maryland
College Park, MD 20742

G. Heckman
NOAA/ERL/SEL
325 Broadway
Boulder, Colorado 80303

A. Konradi
NASA/Johnson Space Center
Houston, Texas 77058

M. A. Lee
University of New Hampshire
Durham N. H. 03824

D. S. Nachtwey
NASA/Johnson Space Center
Houston, Texas 77058

E. C. Roelof
Applied Physics Laboratory
Johns Hopkins University
Johns Hopkins Road
Laurel, Maryland 20810

ABSTRACT

During a workshop on the interplanetary charged particle environment held in 1987, a descriptive model of solar particles in the heliosphere was assembled. This model includes the fluence, composition, energy spectra, and spatial and temporal variations of solar particles both within and beyond 1 AU. The ability to predict solar particle fluences was also discussed. Suggestions for specific studies designed to improve the basic model were also made.

1. INTRODUCTION

In March 1987 a two-day Workshop on the Interplanetary Charged Particle Environment was held at the Jet Propulsion Laboratory in California. The objective of this workshop was to review current models of the interplanetary charged particle environment in the energy range above approximately 1 Mev/nucleon in an effort to provide to system design engineers a composite model of the spatial environment for planning future space missions; see Robinson (1988) for a short summary of some of the proposed NASA mission. Of particular concern was the ability to estimate the energetic charged particle environment a spacecraft is likely to experience so that the effects of these particles on microelectronic devices operating in space can be predicted and adverse effects can be mitigated. Although the participants were initially requested to provide data and/or models appropriate for the projected Magellan mission (an eight-month mission around Venus), the scope of the workshop was extended to include a descriptive energetic charged particle environment for the heliosphere.

The workshop participants were divided into two working groups, one to consider galactic cosmic rays (Mewaldt et al., 1988) and one to consider solar particles. This is a report of the solar particle working group, written from notes prepared during the workshop itself and does not include an extensive review of the literature. This report is confined to a brief description of the fluence, composition, spectra, spatial and temporal variations of solar particles within approximately 5 AU. The ability to predict solar particle fluences from solar observations was also discussed in conjunction with a "detect and avoid" scenario. Areas where future research is necessary were identified, and suggestions for future workshops and/or symposia were also made.

2. SOLAR PARTICLE EVENTS

2.1 Events and Fluences

Solar particle events can occur at any time in the solar cycle although the events containing the highest fluences are likely to occur during the "active years" distributed around sunspot maximum (see Figure 1). There are basically three solar cycles of solar particle event data. The major events during the 19th solar cycle occurred prior to routine spacecraft measurements, and the fluxes, fluences and spectra for those events must be inferred from the ionospheric response to solar particles and from ground-based neutron monitor data.

There are basically three different solar particle fluence models. The original proton fluence model, which was based on solar cycle 20 spacecraft measurements, was derived by King (1974); this model has also been incorporated in the Adams (Adams et al., 1981; Adams, 1986) model. There exists a heavy ion, primarily iron, fluence model based on solar cycle 21 measurements (Chenette, 1984). Finally, there is a new proton fluence model, developed by Feynman (1988a,b), based on a composite of all available proton measurements, both direct and inferred, from 1955 through 1985.

For the purposes of this workshop we established a working definition of "major" proton events as those having a fluence of more than 1.0×10^{10} protons with energies greater than 10 MeV. The frequency with which this type of major event might be experienced is dependent upon the model chosen. The group consensus was that the most conservative estimate was three such major events in 21 years, a conclusion based on the frequency of events during solar cycles 19-21. The least conservative estimate would be one such event in 12 years. This was based on the frequency of events which occurred during the "active years" of cycles 20 and 21. For purposes of this report, the "active years" included the period from two years prior to solar sunspot maximum through four years after solar sunspot maximum.

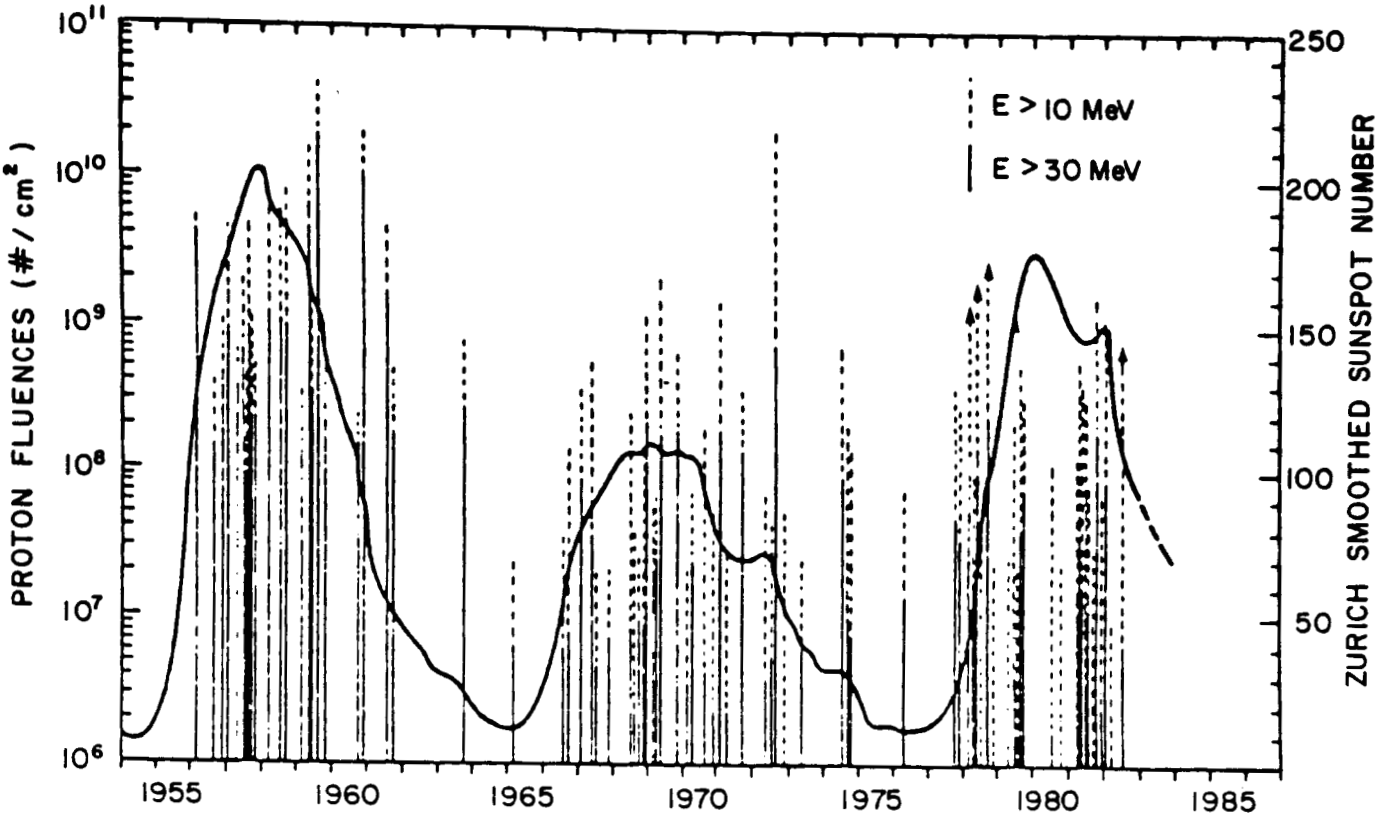

Figure 1. Occurrences of solar proton events as observed at the earth. The vertical bars indicate the fluence for each event. The sunspot number is the dark curve and is labeled on the right axis.

2.2 "Worst Case" Scenarios

The group was also asked to consider the "worst case" scenario for long term mission planning. The group consensus was that a "worst case" scenario would be three "major events" in seven years.

The "worst case" scenario also includes an estimate of what would be the heavy ion component. The consensus view deviated slightly from the estimates given by the Adams model. It has been observed, from the available data, that the heavy iron to hydrogen ratios are dependent on the "size" of the events. The "smaller" events have a higher average ratio than the "larger" events. The ratio of Fe/H utilized by Adams is 4.1×10^{-5} taken from the results published by Mason (1980). More recent data (Cook et al., 1984), acquired at around 10 MeV/nucleon, allows derivation of a Fe/H ratio of 3.4×10^{-5}.

The group was asked to consider a "worst case" heavy ion scenario. In this "worst case" scenario, we projected the Fe/H ratio to be $4.1\ 10^{-4}$ (an anomalously high ratio) for the ions with energies greater than 1 MeV/nucleon. A 90% "worst case" proton event would have fluences exceeding 2.5×10^{7} protons/cm2 with energies greater than 10 MeV. However, the probability of having a "worst case" solar particle event possessing a "worst case" Fe/H ratio was estimated to be 1 in 100 years. This is a committee "guesstimate" prepared at the request of the meeting sponsors and is very uncertain.

2.3 SHOCK ACCELERATED EVENTS

There was a general consensus that the shock acceleration phenomena exist (see Lee, 1988 for a more detailed discussion), and that they play a role in modifying the energetic charged particle population flux and spectra. However, there was no consensus as to the exact manner in which an interplanetary shock (or an ensemble of several shocks) would modify a specific energetic charged particle population, or to the longitudinal extent of such a modification. There was general agreement that the solar flare generated energetic particle flux observed at the earth after the occurrence of the 4 August 1972 solar flare was modified by the presence of converging interplanetary shocks. It may be such a sequence of relatively rare events (frequency about once a solar cycle) that is responsible for the largest observed fluences. Some of the extraordinary large solar particle fluences observed in the 19th solar cycle may have been the result of sequences of events in which the solar energetic particle population was modified by the presence of interplanetary shocks.

3. SPECTRAL FORM OF ENERGETIC PARTICLE EVENTS

An estimate of the spectral form is required in order to extrapolate the models to various energies. Rather than derive new and independent spectral models, the group considered that the available models were generally useful for mission planning and, with care, can be extrapolated to other positions in the heliosphere. The group further recommends that certain models might be more appropriate for specific applications. We recommend the Adams (1981, 1986, 1988) model employing a Fe/H ratio of 3.4×10^{-5} rather than an extreme worst case scenario for computing peak flux estimates and for computing single event upset (SEU) probabilities. We recommend use of the Feynman (1988a, 1988b) model for computing probable fluences that will be experienced during a specific mission and for computing the probability of "latch up" events.

4. SPATIAL DEPENDENCE OF SOLAR FLARE GENERATED ION FLUXES IN THE HELIOSPHERE

Most of the available data base of ion fluxes consists of measurements made on spacecraft orbiting the earth at one Astronomical Unit. There are some data extending out into the heliosphere, and some limited data between 1 and 0.3 AU; however, the preponderance of data on which the models are based are from spacecraft observations at about 1 AU near the ecliptic plane. Future plausible mission profiles range from near-sun missions to the most distant heliosphere at latitudes considerably beyond the ecliptic plane. Therefore, the committee was tasked to give recommendations of how to extrapolate the current 1 AU based models to other positions in the heliosphere.

4.1 RADIAL DEPENDENCE OF IONS

The data base from which the following recommendations are derived is based on measurements in the energy range of 10 to 70 MeV from 1 to 5 AU. The committee was unable to reach a consensus for a specific relationship to be recommended when extrapolating solar particle fluxes and fluences from 1 AU to other distances in the heliosphere. Previous workshops considering a similar problem suggested several methods of estimating the particle flux at distances close to the sun (Neugebauer et al., 1978), however, each method produced significantly different results. For this workshop Hamilton (1988) has prepared a more discussion of the radial dependence of the solar energetic particle flux. The committee recommends using a power law function to extrapolate to other distances.

4.1.1 Flux Extrapolations

To extrapolate proton fluxes from 1 AU to other distances in the heliosphere, the following are recommended in lieu of more accurate knowledge:

From 1 AU to > 1 AU, use a functional form ranging from R^{-4} to R^{-3}.

From 1 AU to < 1 AU, use a functional form ranging from R^{-3} to R^{-2}.

For heavier ions, use the existing elemental abundance ratios to extrapolate from proton fluxes to expected heavy ion fluxes. Table 1 lists observed (normalized to hydrogen) elemental abundance ratios derived by several independent investigators.

4.1.2 Fluence Extrapolations

To extrapolate proton fluence from 1 AU to other distances in the heliosphere, the following are recommended in lieu of more accurate knowledge:

From 1 AU to > 1 AU, use a functional form ranging from R^{-3} to R^{-2}.

From 1 AU to < 1 AU, use a functional form ranging from R^{-3} to R^{-2}.

For heavier ions, use the existing elemental abundance ratios to extrapolate from proton fluences to expected heavy ion fluences. The elemental abundance ratios given in Table 1 can also be used to extrapolate to heavy ion fluences.

4.2 ANGULAR DEPENDENCE AT THE SAME RADIAL DISTANCE

The committee view was that the "worst case" solar particle events would be those events that are "well connected" to the solar flare source region. The intrinsic assumption is that the interplanetary magnetic field topology basically follows an Archimedean spiral structure that has not been substantially modified by interplanetary shocks, and that the flow of energetic particles is along the interplanetary magnetic field lines. With these assumptions it is possible (at least to a zeroth order approximation) to "map" the interplanetary magnetic field lines from an observational point in space to a high coronal source. "Well connected" means that the flare position is close to the "root" of the Archimedean spiral path extending to the observation location.

For a position at 1 AU and for a "nominal" solar wind we assume that the "well connected" location is at about one radian west of the central meridian on the sun (i.e. at about 57 degrees west). For observational points at other radial distances it would be necessary to compute the probable "foot point" of the Archimedean spiral path based on observed or nominal solar wind speeds using some appropriate method such as the EQRH approximation (i.e. ballistic solar wind) originally derived by Nolte and Roelof (1973).

The following is a possible recipe for estimating solar particle fluxes and/or fluences at various angular distances from the flare site.

1. Using the Archimedean spiral concept, compute the longitude on the sun from which the interplanetary magnetic field line passing through the spacecraft position would originate. This heliolongitude would be the location from which the maximum flux would be expected if the flare were to occur at that position.

2. Determine the heliocentric angular distance (i.e. the "great circle" distance) between the location of the solar flare and the solar longitude of the "root" of the idealized spiral field line passing through the spacecraft.

3. Estimate the expected ion flux from the solar flare.

4. Extrapolate the ion flux expected along the Archimedean spiral path leading from the flare site to the Archimedean spiral path passing through the spacecraft by applying a "coronal gradient". In the absence of a known coronal gradient assume an average of one order of magnitude decrease in flux per radian angular distance away from the flare site using the expression $10^{-(F-A)}$ where F is the heliographic position of the flare and A is the heliographic position of the "root" of the Archimedean spiral passing through the spacecraft. Both F and A are expressed in radians. Extrapolate to other angular positions using the same functional form.

4.2.1 Longitudinal Dependence at the Same Radial Distance

Follow the general procedure outlined above assuming a coronal gradient of one order of magnitude per radian. Find the longitudinal difference between the spacecraft location and the flare location and extrapolate to the spacecraft longitude.

4.2.2 Latitudinal Dependence at the Same Radial Distance

Follow the general procedure outlined above assuming a coronal gradient of one order of magnitude per radian. Find the latitudinal difference between the spacecraft location and the flare location and extrapolate to the spacecraft latitude.

There is a systematic variation in the heliolatitude of solar flares throughout the solar cycle. A rough estimate of the flare latitude early in the solar cycle would be approximately 30 degrees from the solar equator. The average flare latitude decreases towards the equator throughout the solar cycle; late in the solar cycle the average flare latitude may be about 5 degrees from the solar equator.

5. REVIEW OF PROTON PREDICTION METHODS

It was the consensus of the panel that there is no useful ability to predict flares that will release protons into space 24 hours in advance of the event. However, when a flare occurs, it is possible to use the electromagnetic emission characteristics to predict the probable proton fluxes. In the United States both the major forecast centers have prediction algorithms to predict the proton flux expected at the earth after the occurrence of a "significant" solar flare. These predictions are usually within an order of magnitude of the observed flux. Statistics available from the jointly operated NOAA/USAF Space Environment Forecast Facility at Boulder, Colorado indicate a reasonable skill in forecasting if a specific flare will be a proton producer. Proton prediction statistics are available for the time period 1976 through 1984. During this time period predictions were made for 2247 solar flare occurrences. The "significant" particle flux threshold was that protons with energies greater than 10 MeV would exceed a flux of 100 protons/cm^2/sec/ster. The prediction results show that no significant event was predicted 2184 times; only 4 of these events exceeded the "significant" threshold. There were 63 predictions of a "significant" proton flux of which 44 events were actually observed; there were 19 cases where a significant proton event was predicted but not observed. This prediction skill is predicated upon being able to observe the solar flare position and the electromagnetic emission characteristics. Approximately 20% of the observed proton events at the position of the earth cannot be predicted because the flare occurs on the "invisible" hemisphere of the sun as viewed from the earth (Smart et al., 1976). It was the consensus of the group that there is no way to use earth-based real-time forecasts for the entire Magellan mission especially when the spacecraft has a large angular separation from the earth-sun line.

6. DETECT AND AVOID SCENARIO

It was the consensus group opinion that "detect and avoid" is a plausible operational scenario. If there are components on board that would be adversely affected by a large solar particle flux, automatic protective sequences would be preferable to remote decision and command sequences. Typical times from solar flare observation to maximum particle flux at 1 AU for 10 MeV protons are a few hours. As the energy of the ions increases, the time from solar flare observation to particle maximum may decrease to less than 30 minutes for GeV protons. The shortest observed times at 1 AU from relativistic GeV proton onset to maximum during ground-level events is six minutes. These short times may not allow enough time for remote observations of the particle environment to exceed some critical threshold which, in turn, would result in a specific command sequence from the spacecraft control center to the satellite for preventative action. This is particularly true for a spacecraft orbiting another planet which would not be in radio line of sight to the earth for a portion of its orbital period. If there should happen to be sensors whose possible malfunction during a large solar particle event would be mission threatening and it is possible to "shut down" these sensors, then an automatic on-board environmental shut down sequence could be actuated. Figure 2 illustrates a suggested scenario. The conditions are that there would be a threshold above which the sensors are likely to malfunction. As the particle flux approaches this threshold, simple on-board detectors would sense the particle flux and initiate the protective sequence. This protective sequence would remain in effect until either the flux drops below a specified "resume function" level or until specifically commanded from the spacecraft control center. The type of particle sensor envisioned would be a

simple reliable omni-directional detector rather than a complex state-of-the-art system capable of accurately resolving particle energies and species.

7. RECOMMENDATIONS FOR FUTURE WORK

1. The current data bases of energetic solar particle events should be enhanced. These data should be analyzed to determine the peak ion fluxes and fluences for all available energy channels.

a. The alpha particle measurements have not been organized in the same manner in which the solar proton event data have been organized. These data should be analyzed to determine the distribution of event fluxes and fluences.

b. The heavy ion particle data should be organized, as much as possible, in a manner similar to the solar proton event data. These data should be analyzed to determine the distribution of event fluxes and fluences.

c. Historical studies of major events should be added to the data base to determine the extreme values of the solar accelerated ion distribution functions. This would include ancient historical data from ice core results, moon rocks, fossil records, etc.

2. A model to predict solar alpha particle fluxes should be developed similar to the proton prediction model. This would include the time of particle onset at a point in space, the expected time of maximum and the expected maximum intensity.

Such a model would remove the ambiguity currently present by normalizing heavy ion fluxes to proton fluxes because the observed ratio of helium to heavy ions is less variable than the observed ratio of hydrogen to heavy ions. This alpha particle model would be the baseline for the development of a model for heavy ion prediction.

3. The radial dependence of peak ions fluxes and fluences within 1 AU should be determined. The HELIOS 1 and 2 data, together with the earth-orbiting IMP data, could be used to accomplish this.

4. The currently available measurements beyond 1 AU should be consolidated in an effort to determine a more accurate radial gradient of solar particle fluxes beyond 1 AU.

5. There is a need for study groups, workshops, and symposia to focus on the problems identified above. A Chapman-type conference on the state of the present knowledge of solar particle events would be useful; however, the leaders of such a conference should be required to produce a comprehensive review paper on the subject.

Table 1. NORMALIZED ABUNDANCES OF SOLAR ENERGETIC PARTICLE EVENTS

		Adams Mason et al (1980) 1 MeV	Gloeckler (1979) 1-20 MeV	Cook et al (1984) 10 MeV	McGuire et al (1985) 6.7-15 MeV
1	H	1.0	1.0	1.0	1.0
2	He	2.2 E-2	1.5 E-2		1.5 E-2
3	Li		1.0 E-7	4.8 E-8	2.8 E-6
4	Be		1.5 E-7	6.0 E-9	1.4 E-7
5	B		1.5 E-7	1.2 E-8	1.4 E-7
6	C	1.6 E-4	1.2 E-4	9.6 E-5	1.3 E-4
7	N	3.8 E-5	2.8 E-5	2.7 E-5	3.7 E-5
8	O	3.2 E-4	2.2 E-4	2.2 E-4	2.8 E-4
9	F		4.3 E-7	1.0 E-8	1.4 E-7
10	Ne	5.1 E-5	3.5 E-5	3.1 E-5	3.6 E-5
11	Na	1.6 E-6	3.5 E-6	2.6 E-6	2.4 E-6
12	Mg	3.9 E-5	3.9 E-5	4.3 E-5	?.2 E-5
13	Al	3.5 E-6	3.5 E-6	3.1 E-6	3.3 E-6
14	Si	3.8 E-5	2.8 E-5	3.5 E-5	4.2 E-5
15	P	2.3 E-7	4.3 E-7	1.7 E-7	4.0 E-7
16	S	1.8 E-5	5.7 E-6	7.8 E-6	6.5 E-6
17	Cl	1.7 E-7		7.1 E-8	
18	Ar	3.9 E-6	8.7 E-7	7.3 E-7	4.6 E-6
19	K	1.3 E-7		1.0 E-7	
20	Ca	2.3 E-6	2.6 E-6	3.1 E-6	3.2 E-6
21	Sc			7.8 E-9	
22	Ti	1.0 E-7		1.2 E-7	
23	V			1.2 E-8	
24	Cr	5.7 E-7		5.0 E-7	
25	Mn	4.2 E-7		1.8 E-7	
26	Fe	4.1 E-5	3.3 E-5	3.4 E-5	
27	Co	1.0 E-7		4.8 E-7	
28	Ni	2.2 E-6		1.2 E-6	
29				1.4 E-8	
30				3.8 E-8	

REFERENCES

Adams, J. H. Jr., R. Silberberg, and C. H. Tsao, Cosmic Ray effects on Microelectronics, Part 1: The near-earth particle environment, NRL Memorandum Report 4506, Naval Research Laboratory, Washington, D. C., August 25, 1981. (ADA103897)

Adams, J. H. Jr., Cosmic Ray effects of Microelectronics, Part IV, NRL Memorandum Report 5901, Naval Research Laboratory, Washington, D. C., December 31, 1986.

Adams, J. H. Jr., Current models of the intently ionizing particle environment in space, these proceedings, 1988.

Bremean, H. H. and E. C. Stone, Solar and photospheric abundances from Solar Energetic Particle Measurements, Astrophy. J., 299, L57, 1985.

Chenette, D. L. and W. F. Dietrich, The solar flare heavy ion environment for single event upsets, IEEE Trans on Nucl. Sci., NS-31, 1217, 1984.

Cook, W. R., E. C. Stone and R. E. Vogt, Elemental composition of solar energetic particles, Astrophy. J., 297, 827, 1984.

Feynman, J., T. Armstrong, L. Dao-Gilbner, and S. Silverman, A new proton fluence model, these proceedings, 1988A.

Feynman, J., T. Armstrong, L. Dao-Gilbner, and S. Silverman, A new proton fluence model, IEEE Trans on Nucl. Sci., in press, 1988B.

Gloeckler, G., Composition of energetic particle population in interplanetary space, Reviews of Geophysics, 17, 569, 1979.

Hamilton, D. C., The radial dependence of the solar energetic particle flux, these proceedings, 1988.

King, J. H., Solar proton fluences for 1977-1983 space missions, J. Spacecraft and Rockets, 11, 401, 1974.

Lee, M. A., Particles accelerated by shocks in the heliosphere, these proceedings, 1988.

Mason, G. M., L. A. Fisk, D. Hovestadt, and G. Gloeckler, A survey of ~1 MeV nucleon^{-1} solar flare particle abundances, $1 < Z < 26$, during the 1973-1977 solar minimum period, Astrophy. J., 239, 1070, 1980.

Mewaldt, R. A., A. C. Cummings, J. H. Adams, Jr., P. Evenson, W. Fillius, J. R. Jokipii, R. B. McKibben, and P. A. Robinson, Jr., Toward a descriptive model of galactic cosmic rays in the heliosphere, these proceedings, 1988.

McGuire, R. E., T. T. Von Rosenvinge and F. B. McDonald, The composition of solar energetic particles, Astrophy. J., 301, 938, 1986.

Neugebauer, M., L. A. Fisk, R. E. Gold, R. P. Lin, G. Newkirk, J. A. Simpson, and M. A. I. Van Hollebeke, The energetic particle environment of the solar probe mission, JPL Publication 78-64, Jet Propulsion Laboratory, Pasadena, Calif. 1978.

Nolte, J. T. and E. C. Roelof, Large scale structure of the interplanetary medium, 1: High coronal structure and the source of the solar wind, Solar Physics, 33, 241, 1973.

Robinson, P. A., The effects of high energy particles on planetary missions, these proceedings, 1988.

Smart, D. F., M. A. Shea, H. W. Dodson and E. R. Hedeman, Distribution of proton producing flares around the sun, Space Research XVI, 797, 1976.

Toward A Descriptive Model of Galactic Cosmic Rays in the Heliosphere

R. A. Mewaldt and A. C. Cummings
California Institute of Technology
Pasadena, CA 91125

J. H. Adams, Jr.
Naval Research Laboratory
Washington, D. C. 20375

P. Evenson
Bartol Research Foundation, University of Delaware
Newark, DE 19711

W. Fillius
University of California, San Diego
La Jolla, CA 92093

J. R. Jokipii
University of Arizona
Tucson, AZ 85721

R. B. McKibben
Enrico Fermi Institute, University of Chicago
Chicago, IL 60637

P. A. Robinson, Jr.
Jet Propulsion Laboratory
Pasadena, CA 91109

ABSTRACT

We review the elements that enter into phenomenological models of the composition, energy spectra, and the spatial and temporal variations of galactic cosmic rays, including the so-called "anomalous" cosmic ray component. Starting from an existing model, designed to describe the behavior of cosmic rays in the near-Earth environment, we suggest possible updates and improvements to this model, and then propose a quantitative approach for extending such a model into other regions of the heliosphere.

1. INTRODUCTION:

In March of 1987 a two day *Workshop on the Interplanetary Charged Particle Environment* was held at the Jet Propulsion Laboratory. The purpose of this workshop was to review current models of the interplanetary charged particle environment in the energy range above ~1 MeV/nuc, in an effort to improve our capability to predict the environment that will be seen by future spacecraft. One of the important applications of such models is in predicting the effects that energetic charged particles can have on microelectronic devices operating in space.

The second day of the workshop was divided into two working groups, one to consider solar particles, and a second to consider galactic cosmic rays. We present here a report of the galactic cosmic ray working group, drafted during the workshop itself. Within the somewhat limited time available, a review was conducted of the significant parameters that are required to provide a phenomenological description of the elemental composition, differential energy spectra, and the spatial and temporal variations of galactic cosmic rays (GCRs) in the heliosphere. Also considered was the "anomalous cosmic ray" (ACR) component - thought to represent a sample of the neutral interstellar medium that has been accelerated to energies of ~10 MeV/nuc.

Adams et al. (1981; see also Adams, 1986) have developed a descriptive model of cosmic rays in the near-Earth environment that is based on the extensive measurements of the composition, energy spectra, and solar cycle variations of cosmic rays that have been made from spacecraft, balloon, and ground-based observations over the past two or three decades. As a result of a review of that model, and the data on which it is based, we conclude that it provides a reasonable and essentially complete description of cosmic rays *near Earth* that should be useful for a variety of applications, including predictions of the radiation environment and its effect on a variety of spacecraft components. We find, however, that there are a few areas where improvements and updates to the description of cosmic rays at Earth are now possible.

In addition, recent measurements from the Pioneer and Voyager spacecraft in the outer heliosphere now provide guidance on how descriptive models of cosmic rays can be extended beyond 1 AU to ~50 AU in radius, and up to ~30° in latitude. This report provides some guidance as to how this might be approached, and to what might be expected in the regions beyond. Further detail on the composition, energy spectra, and spatial and temporal behavior of cosmic rays, both at Earth and further out in the heliosphere, can be found in a number of other papers presented at this workshop by the individual authors of this report.

2. APPROACH:

In an effort to provide a mathematical model that can be readily used to make quantitative predictions, we suggest the following approach to modeling the GCR and ACR components. We assume that the differential energy spectrum, $j(Z, E, t, r, \theta, \phi)$, of a given species of nuclear charge Z, kinetic energy per nucleon E, and heliographic coordinates r, θ, and ϕ can be represented by the the following separable function:

$$j(Z,E,t,r,\theta,\phi) = j_o \times F_t(Z,E,t) \times F_r(Z,E,t) \times F_\theta(Z,E,t) \times F_\phi(Z,E,t) \quad (1)$$

where $j_o(Z,E)$ is the 1 AU spectrum of element Z at solar minimum (essentially the current Adams et al. model; see Sections 3.1 and 3.2), and where:

F_t is the time dependence (see Sections 3.4 and 4.1)
F_r is the radial dependence (Section 4.2)
F_θ is the latitude dependence (Section 4.2), and
F_ϕ is the longitude dependence (assumed to = 1).

For lack of any definitive measurements, F_ϕ is presently assumed to be = 1 and will not be discussed further. Preliminary recommendations for the remainder of these factors are described below, along with an indication of their uncertainty. A similar procedure is recommended for the ACR component (see Section 3.3).

3. MODEL FOR 1 AU:

We suggest the following updates and improvements in the model for cosmic rays at 1 AU. These alterations affect the values for $j_o(Z,E)$ but differ only to a minor extent from the current model of Adams et al.

3.1 ENERGY SPECTRA OF GALACTIC COSMIC RAYS

Figure 1 shows energy spectra for several elements as measured at 1 AU during the last solar minimum. Note that below ~50 MeV/nucleon the spectra of N and O (and to a less obvious extent, He) contain contributions from the "anomalous" cosmic ray component, while the spectra of H and C continue to decrease down to at least 10 MeV/nuc, below which solar and interplanetary fluxes typically dominate. Adams et al. (1981) used the measured He spectrum as a generic spectrum to model the flux of galactic cosmic-ray species with $3 \leq Z \leq 16$. We suggest that the measured spectrum of carbon be used for this purpose instead of He. The motivations for this change are that GCR He at some energies may be as much as ~20-30% ^{3}He, which has a different charge to mass ratio than ^{4}He, and that a significant fraction of low energy (<100 MeV/nuc) He is from the ACR component (see Section 3.3). The measured H and He spectra should continue to be used for Z=1 and Z=2 species, while Fe should be used as a model for the spectra of $17 \leq Z \leq 92$ species. Although this is a minor change, it makes better use of the existing cosmic-ray data base.

3.2 COMPOSITION OF GALACTIC COSMIC RAYS

We suggest that the relative abundances of cosmic rays that are an input to the Adams et al. model be reviewed to see that they include the most recent data, including that from the HEAO-C2 ($4 \leq Z \leq 30$; Engelmann et al., 1985) and HEAO-C3 (Z>30; Stone et al., 1987) experiments, and also recent balloon data (e.g., Dwyer and Meyer, 1987). Recent measurements of H and He should also be

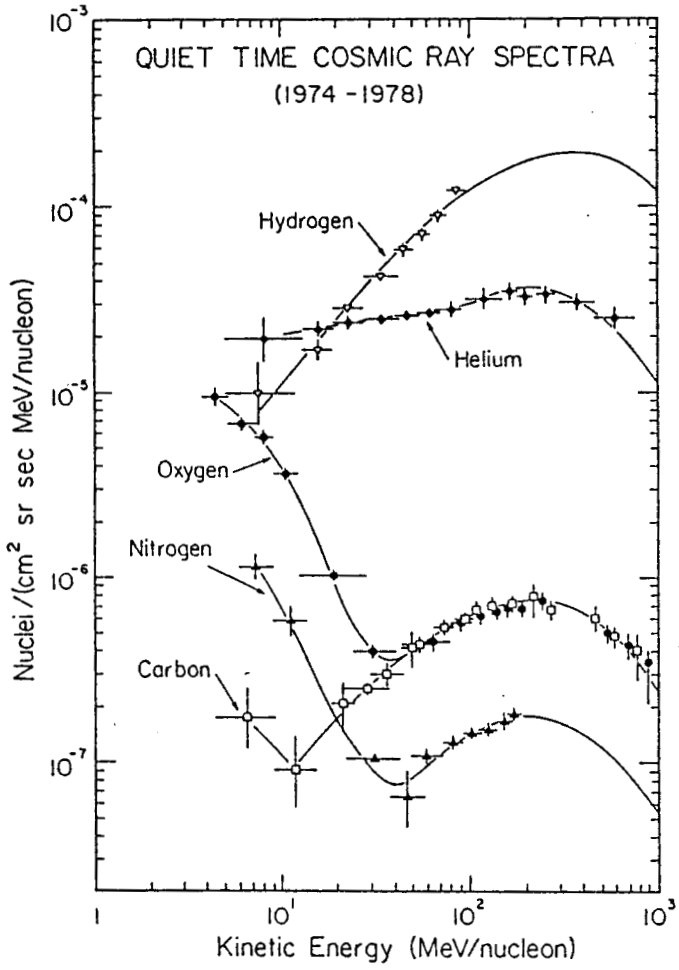

Figure 1: Quiet-time energy spectra for the elements H, He, C, N, and O measured at 1 AU over the solar minimum period from 1974 to 1978 (from Mewaldt et al., 1984). Note the "anomalous" enhancements in the low-energy spectra of He, N, and O. The data are from the Caltech and Chicago experiments on IMP-7 and IMP-8.

reviewed (e.g., Webber et al., 1987a, 1987b), since, ironically, some of the most significant uncertainties in cosmic-ray composition are in the relative flux of H, He, and heavier elements as a function of energy.

3.3 THE "ANOMALOUS" COSMIC RAYS

The anomalous cosmic-ray (ACR) component is now known to consist of six elements, He, C, N, O, Ne, and Ar, with unusual relative abundances in the energy range below ~50 MeV/nuc. Of these, He (Garcia-Munoz et al., 1973) and O (Hovestadt et al. 1973, McDonald et al., 1974) were the first discovered and are the most abundant, while anomalous fluxes of N and Ne are also well established (see also Webber et al., 1975, Klecker et al., 1977, Mewaldt et al., 1976, Webber and Cummings, 1983). Recent Voyager measurements provide evidence that there are small anomalous fluxes of C and Ar (Cummings and Stone, 1987a).

Observations in the outer heliosphere show that the ACR component has a positive radial gradient, larger in magnitude than that of other cosmic ray species (see, e.g., the recent measurements by Cummings et al., 1987; McKibben et al., 1987; and McDonald and Lal 1986). For a review of earlier measurements of the ACR component, see Gloeckler (1979); for more recent reports see Jones (1983), Fisk (1986), Garcia-Munoz et al. (1987) McKibben (1987), and references therein.

A widely held model of the origin of this component, due to Fisk et al. (1974), is that it originates as neutral interstellar gas that drifts into the heliosphere, becomes singly-ionized near the Sun, and is then convected by the solar wind to the outer heliosphere where the ions are accelerated to higher energies. These ions are then observed after they have propagated to the inner solar system from the acceleration site.

This model accounts for the composition of the ACR component. For example, except for carbon, the elements of the anomalous component all have first ionization potentials larger than that of hydrogen and are therefore likely neutral in the interstellar medium. The abundance of anomalous carbon is $<1\%$ of oxygen, consistent with the expectation that most of the carbon gas is already ionized in the interstellar medium because of its low first ionization potential. This ionized gas is prevented from entering the heliosphere by the solar magnetic field embedded in the outward-flowing solar wind. So far, the predicted singly-charged ionization state of the ACR component has not been confirmed by direct measurement; however, there is considerable indirect evidence that this is the case, and experiments have been conducted and more are planned to try to provide this most crucial evidence for the model.

We propose to model the composition and energy spectra of the ACR component at 1 AU in the heliographic equatorial plane by using an energy and flux scaling recipe developed by Cummings et al. (1984) and Cummings and Stone (1987a). Observations indicate that the spectral shape of the ACR component underwent a change at the time of the reversal of the solar magnetic field (in agreement with a model by Jokipii (1986)). It remains to be seen, however, whether the spectrum over the next few years will maintain this new shape or will return to its 1972-1977 shape. Based on data thru 1986, we propose two recipes, one for each half of the solar magnetic cycle. The generic ACR energy spectrum is determined by fitting the ACR helium spectrum to the ACR oxygen spectrum with constant flux and energy scaling factors as free parameters.

Figure 2a shows the appropriate generic ACR energy spectrum for the $qA>0$ solar minimum period ($\sim$1969-1980 and $\sim$1991-2002) measured at 1.8 AU (adapted from Cummings and Stone, 1987b). This spectrum should be normalized to 1 AU by using a radial gradient of 15%/AU (see section 4.2), checking that the resulting spectra are consistent with solar minimum measurements at 1 AU (e.g., Figure 1). Figure 2b shows the complementary ACR spectrum for $qA<0$ ($\sim$1980-1991) at 19.5 AU. This spectrum also requires a normalization to 1 AU using a radial gradient of 15%/AU.

The individual spectra for the various species of the ACR component, $j_A(E)$, at 1 AU can be derived from these generic spectra, $j_G(E)$, by:

$$j_A(E \cdot f_E(A)) = j_G(E) \cdot N(t) \cdot N_1 \cdot f_F(A) \quad (3)$$

where j denotes the differential energy spectrum at E MeV/nuc, N(t) is the time variation normalization factor, N_1 is the correction factor to 1 AU, and $f_E(A)$ and $f_F(A)$ are the energy and flux scaling factors, respectively. The values of N_1, f_E, and f_F are displayed in Table 1 for the various species. As an example of the use of this table, we find ACR abundances of ~5:1:0.18:0.07 for He:O:N:Ne at 10 MeV/nuc for qA>0 periods. The ACR abundances of C and Ar would be less than a few per cent of oxygen at this time (see also Figure 1). The uncertainties in composition derived by this approach should be less than ~20% for He, N, O, and Ne, and perhaps 50% for the rare elements C and Ar.

The intensity of the ACR component is very sensitive to solar modulation, varying by a factor of >100 over the solar cycle. We propose that the intensity of the ACR component can be modeled by scaling from measured neutron monitor rates using the relationship:

$$I = I_o(\frac{NM}{NM_o})^n, \quad (2)$$

where I_o is the intensity of ACR oxygen at some time t_o, NM_o is the neutron monitor count rate at t_o, and I and NM refer to some different time t. Optimal values for I_o, NM_o and the index n have not yet been determined, but Figures 3 and 4 show examples of such fits with $n \simeq 30$ and 40, respectively, using the Mt. Washington neutron monitor.

In Figure 3, ACR oxygen data from 1 AU are compared to the scaled neutron monitor intensity with n=30, while in Figure 4 Voyager 2 data from 1 to 22 AU have been fit with a combined spatial and temporal dependence assuming a constant gradient of 15% per AU (see Section 4.2). In this case the value of n=30 used in Figure 3 is consistent with the 1977 to 1980 data, but the observations after the field reversal in 1980 require a greater value of n, or alternatively, a larger radial gradient. Thus, as noted above, there was a change in the ACR component that apparently took place at the time of the reversal of the solar magnetic field. These examples show that the approach recommended here can give a fairly accurate representation of the time history of the ACR component, but it remains to examine existing data in detail to find optimal parameter values.

3.4 TIME DEPENDENCE AT 1 AU

Perhaps the largest uncertainty in the predictive power of the present Adams et al. model for galactic cosmic rays arises from the difficulties of fitting and predicting the time variations in the flux of cosmic rays over the solar cycle. The current model assumes a sinusoidal time dependence for the galactic cosmic ray flux at Earth, based on a fit to a mixture of neutron monitor and ion chamber measurements accumulated over more than 40 years. We suggest that the Adams et al. model be modified to include a more realistic time dependence. Data from

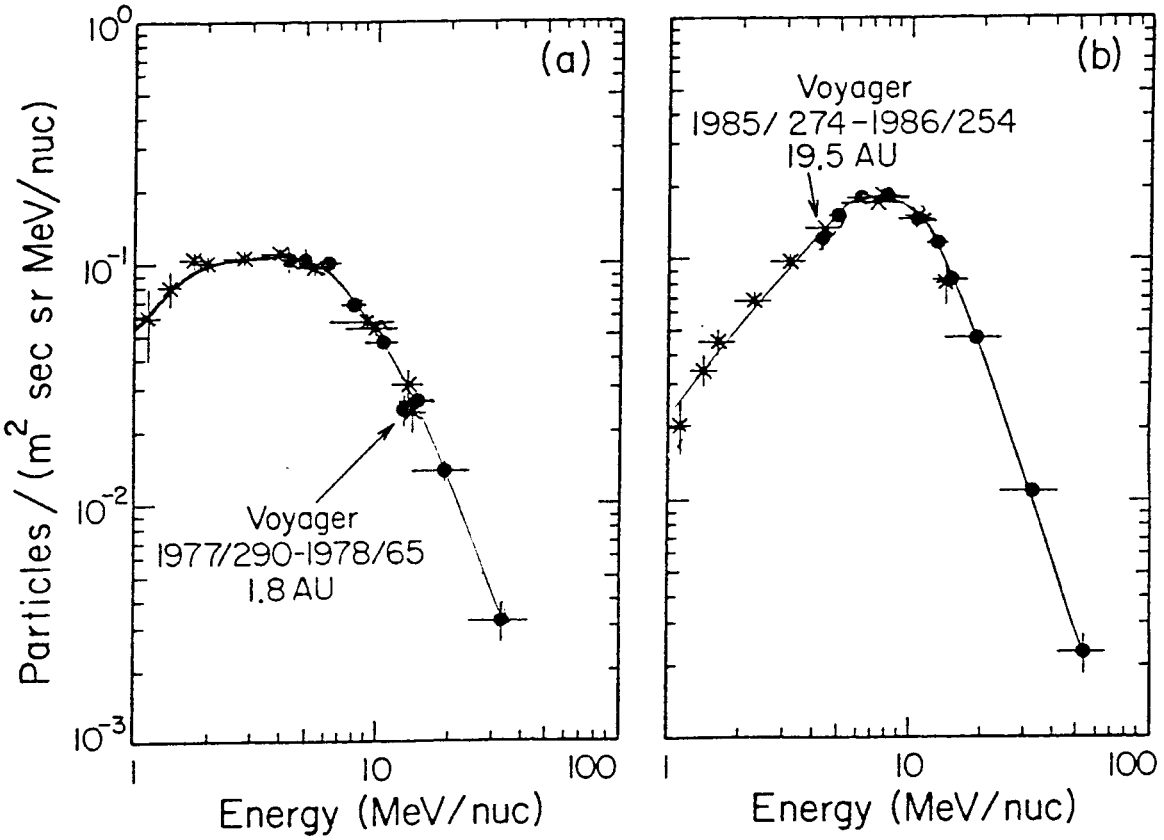

Figure 2: a) Generic ACR energy spectrum from Voyager 1 and 2 representative of ACR oxygen (as described in the text) for the solar minimum period 1977-1978 (qA>0). b) ACR generic spectrum from Voyager 2 for the 1985-1986 period (qA<0).

Table 1. Energy (f_E) and Flux (f_F) Scaling Factors and Correction Factor to 1 AU (N_1) for Anomalous Component Spectra (see Equation 3).

Species	A	qA>0			qA<0		
		f_E	f_F	N_1	f_E	f_F	N_1
He	4	3.50	2.46	0.89	5.31	1.32	0.062
C	12	unknown	unknown	"	1.41	0.0075	"
N	14	0.89	0.21	"	1.14	0.13	"
O	16	1.00	1.00	"	1.00	1.00	"
Ne	20	0.78	0.11	"	0.64	0.12	"
Ar	36	unknown	unknown	"	0.37	0.019	"

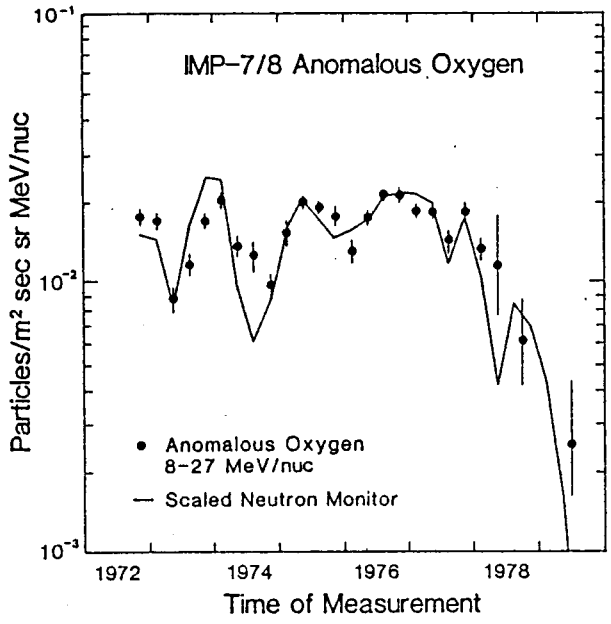

Figure 3: The intensity of 8 to 27 MeV/nuc anomalous oxygen at 1 AU during the years from 1972 to 1979 as measured by IMP-7/8 (see Webber et al. 1981). The solid line is scaled from the Mt. Washington neutron monitor counting rate using the relation $I = I_o(NM/2400)^{30}$ with I_o=0.0174.

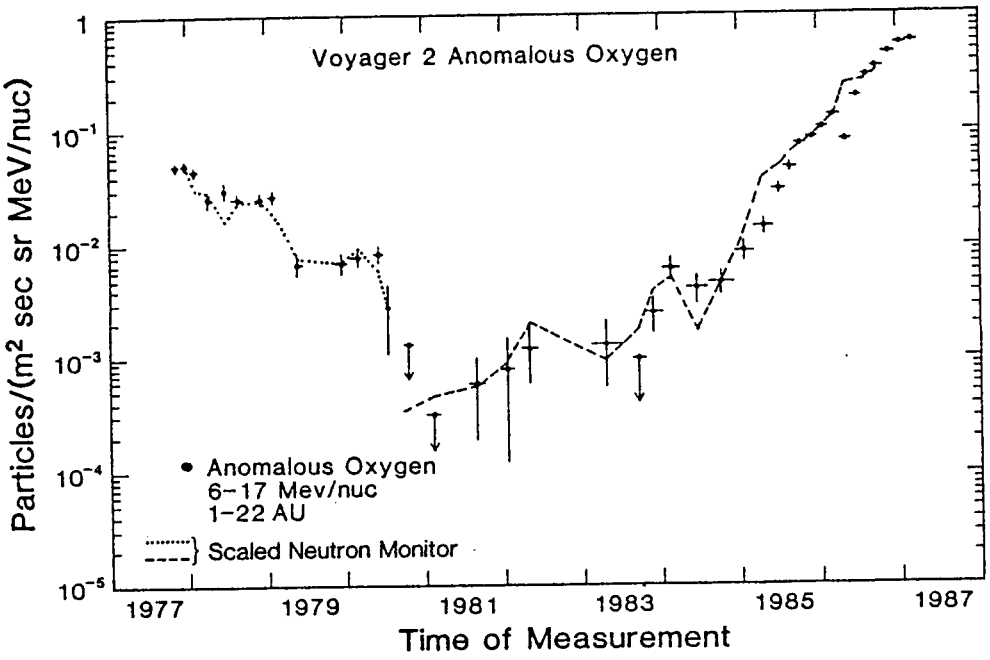

Figure 4: Voyager 2 measurements of 6 to 17 MeV/nuc anomalous oxygen during the years 1977 to 1987 over the radial range from ~1 to 22 AU. The dotted line is scaled from the Mt. Washington neutron monitor using the relationship $I = I_o(NM/2400)^n$ for the intensity at 1 AU, with $I_o = 0.0423$ and $n = 30$. The dashed line for the period after 1980 uses $I_o = 0.330$ at 19.5 AU and $n = 40$. Both fits assume a radial gradient of 15% per AU. It is not possible to achieve a good fit before *and* after 1980 using the same values for n and the radial gradient.

Climax and other neutron monitors (see, e.g., Figure 5) are now available for over 33 years, equivalent to three sunspot cycles and one and one half complete magnetic cycles. While it may be fortuitous, it is interesting that the last eleven years of the data look very much like the first, suggesting that the data be folded, averaged, and smoothed as appropriate to form a "standard" 22 year magnetic cycle. We believe that this approach is likely to give more realistic predictions for future missions than the present approach, and it is essentially guaranteed to be more accurate for *ex post facto* estimates.

It must be kept in mind that the temporal variations of cosmic rays of different rigidity are not perfectly correlated, and there are in some cases systematic phase lags in the behavior of particles with lower rigidity. However, such differences in phase are not likely to be significant when averaging over periods of >1 year. For the purposes of spacecraft and mission design, we recommend that the current approach of the Adams et al. model be continued, namely to construct spectra for maximum and minimum flux levels from the envelope of all measurements and to interpolate between these two spectra using the modeled or actual (as appropriate) neutron monitor level.

4. A MODEL FOR COSMIC RAYS IN THE OUTER HELIOSPHERE:

4.1 TIME DEPENDENCE IN THE OUTER HELIOSPHERE

The cosmic ray intensity does not vary simultaneously throughout the entire heliosphere. However, for many applications, such as the calculation of average doses, it is an appropriate approximation to consider the variation to be simultaneous. Typical deviations from simultaneity occur approximately on the time scale of solar wind propagation through the heliosphere - generally about one year,

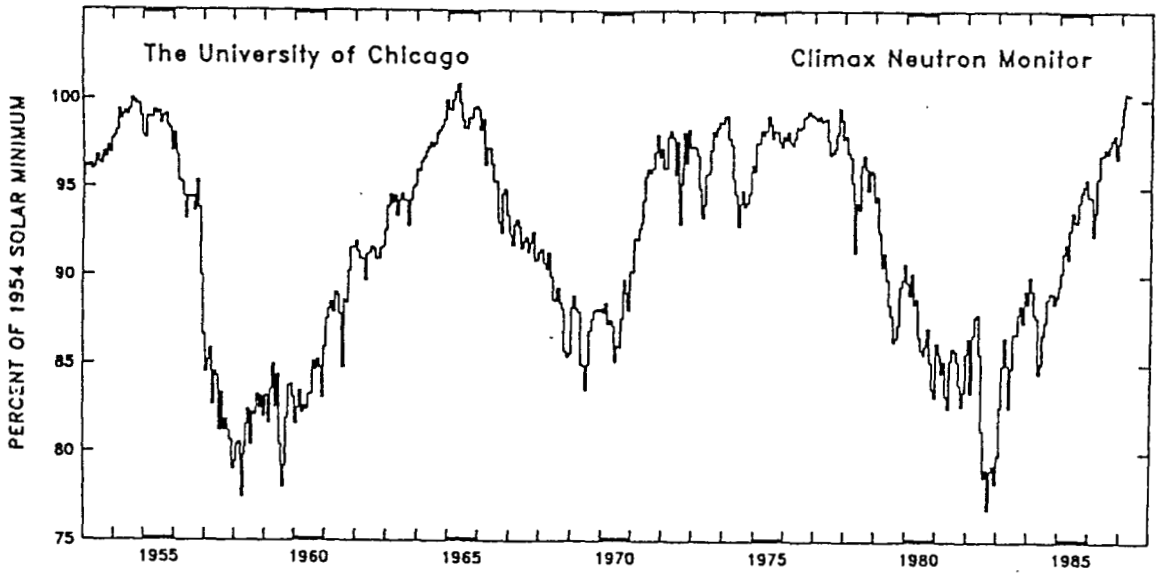

Figure 5: Monthly average counting rates of the Climax neutron monitor for the period 1953 to 1987.

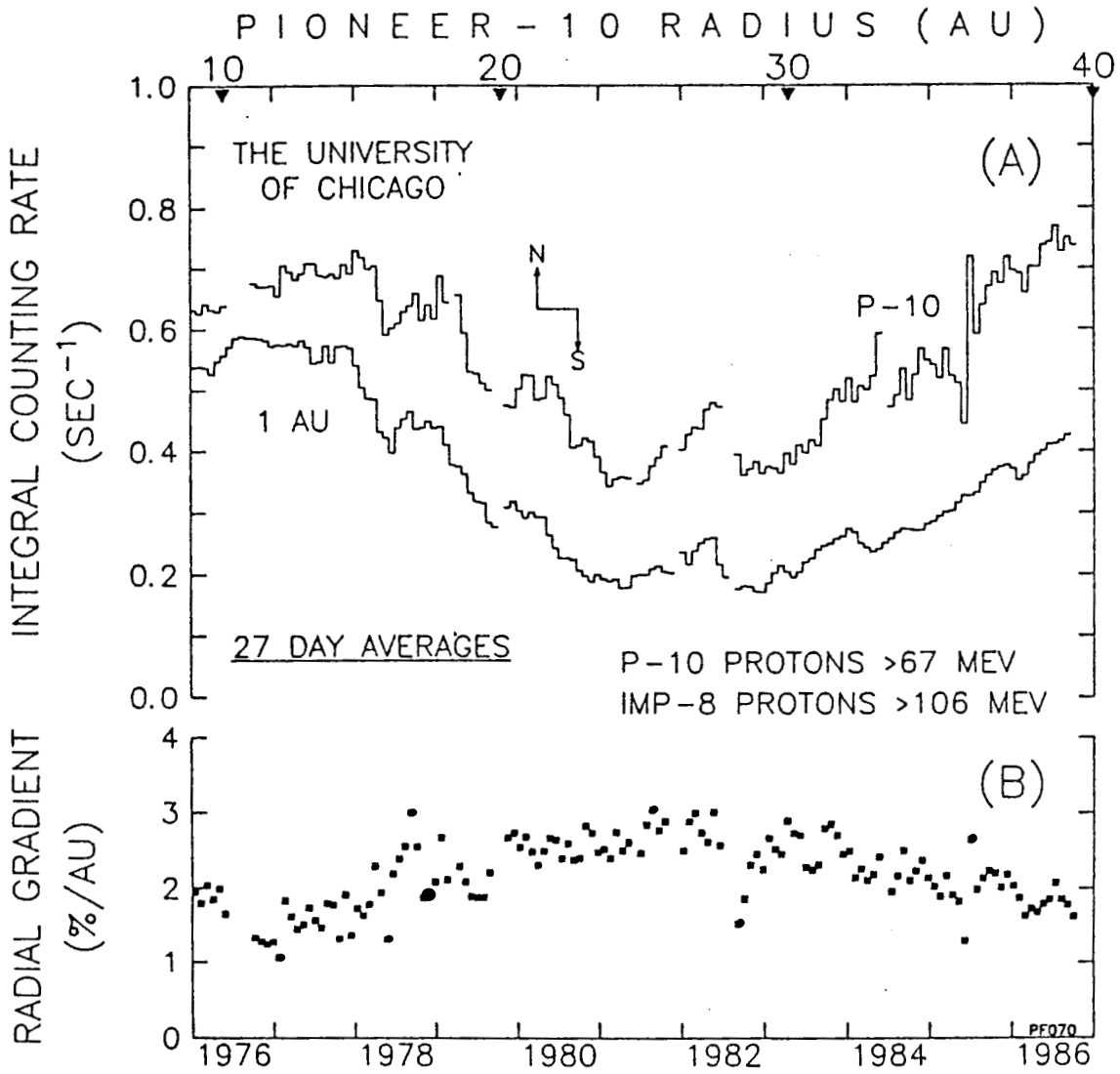

Figure 6: Radial gradient of high-energy protons as measured by Pioneer 10 and IMP-8 (from Lopate et al., 1987). For additional recent cosmic ray gradient measurements see Decker et al. (1987), Fillius et al., (1985), Webber and Lockwood, (1987), McKibben (1987), and references therein.

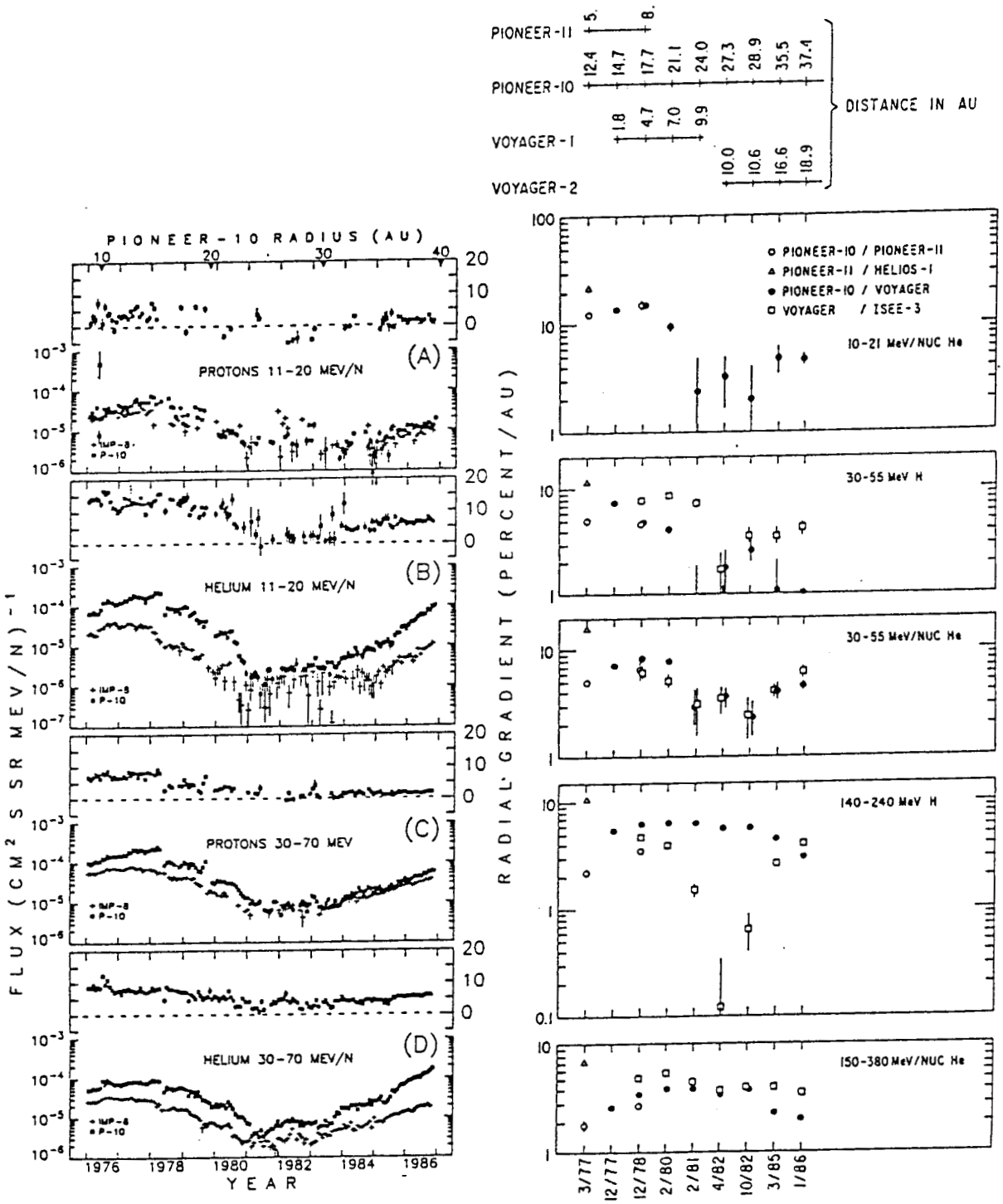

Figures 7a (left) and 7b (right): Radial gradient measurements for low energy H and He nuclei from Lopate et al. (1987; left) and McDonald et al. (1986; right). Note that He nuclei <100 MeV/nuc may contain significant contributions from anomalous cosmic ray He.

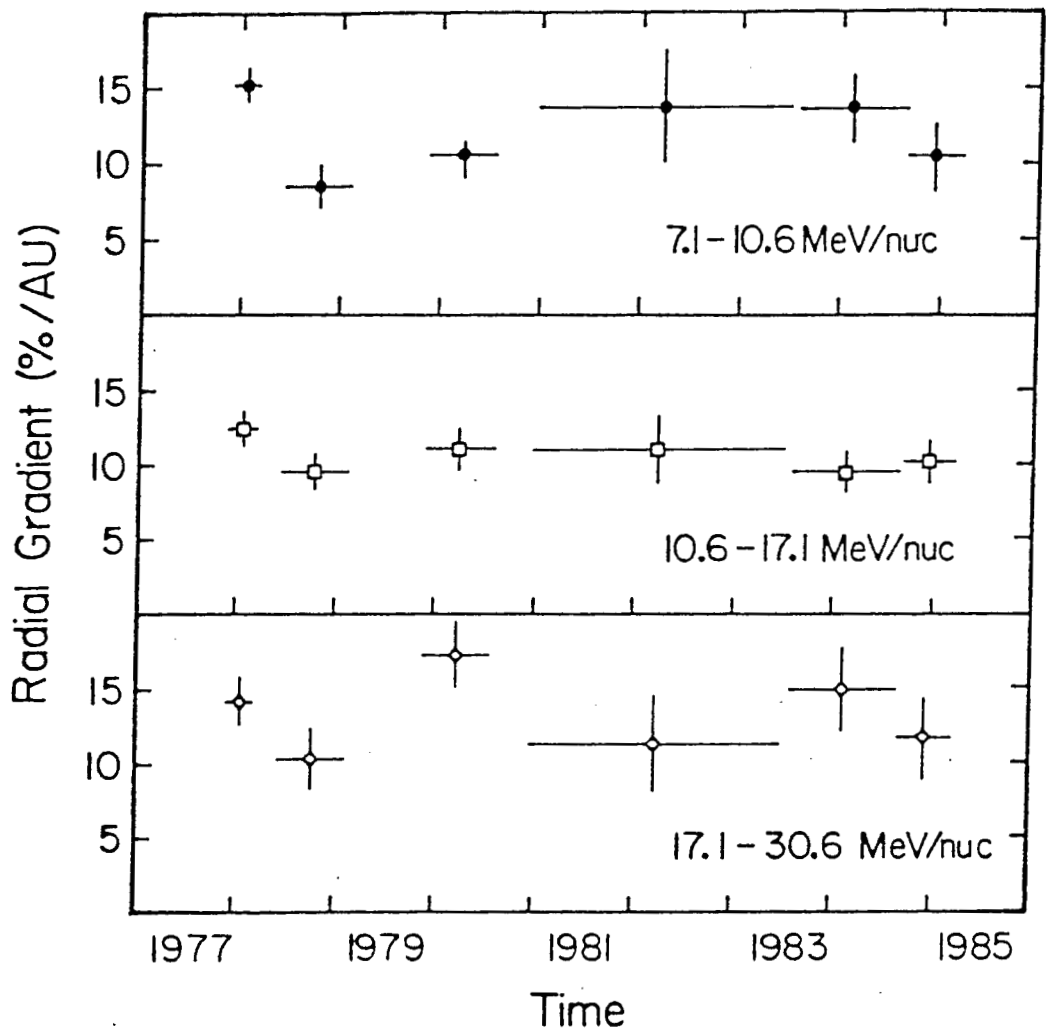

Figure 8: Radial gradient measurements of anomalous oxygen nuclei measured by Voyager 1 and 2 and Pioneer 10 (from Webber et al., 1985).

Table-2 Cosmic Ray Gradients

	G_r (%/AU)	G_θ^* (%/degree)
Low Energy Galactic Cosmic Rays	5(+5,-3)	1 ± 1
Integral Flux (E > 100 MeV/nuc)	2(+2,-1)	1 ± 1
Anomalous Cosmic Rays	15(+8,-7)	5 ± 3

* For 1980-1991; the sign of G_θ apparently depends on the phase of the solar cycle (see text)

an interval that is short compared to the 11-year solar cycle. We therefore suggest that the time dependence throughout the heliosphere be expressed in terms of the behavior at 1 AU, and that the error limits given for radial and latitude dependence contain an allowance for possible time dependence of these parameters as well. Figure 4 is an example of how application of the measured time-dependence of cosmic-ray modulation at 1 AU combined with a constant radial gradient can be used to represent the time behavior of the intensity in the outer heliosphere.

4.2 SPATIAL DEPENDENCE OF COSMIC RAY INTENSITIES IN THE HELIOSPHERE

We assume that the intensity of the GCR and ACR components as a function of position can be described by the function

$$j(Z,E,t,r,\theta) = j_o(Z,E,t)\, e^{G_r(r-1)}\, e^{G_\theta \theta}, \qquad (3)$$

where $j_o(Z,E,t)$ is the intensity of cosmic rays of charge Z and kinetic energy E (MeV/nucleon) at time t observed at 1 AU. Here r is the radial location for which the flux is to be computed, measured in AU from the Sun, θ is the latitude measured in degrees from the heliographic equator, and G_r and G_θ are the radial and latitudinal gradients in percent per AU and percent per degree, respectively. Although G_r and G_θ are observed themselves to be functions of energy and time, the temporal dependence is not well known or understood, and we have therefore tried to simplify our description of these variations as much as possible.

For the purposes of the model, we define G_r and G_θ for the following classes of cosmic rays:

(1) Low energy ($<$ 100 MeV/nuc) galactic cosmic rays.
(2) The integral flux of cosmic rays (E $>$ 100 MeV/nuc), which has a mean energy of ~2 GeV/nuc (median energy ~1 GeV/nuc).
(3) The anomalous cosmic ray component.

The energy dependence of the gradients is reflected by the difference between gradients measured for classes 1 and 2. Radial gradients for class (3) reflect primarily the different spectral form and (presumably) charge state of the anomalous component. The values of the gradient for galactic cosmic rays presumably vary smoothly with energy between the energies characteristic of class (1) and (2), but we have not defined the functional form of the dependence. From a suitable compilation of data, it should be possible to do this in a convenient manner consistent with the available observations. Examples of radial gradient measurements for several species are shown in Figures 6 to 8.

Table 2 summarizes nominal values for G_r and G_θ, including a central value and a range. Essentially all observed values are incorporated within the quoted ranges. There is evidence that the actual gradients may depend on time or the phase of the solar activity cycle, and that the sign of latitude gradients may depend upon the magnetic polarity of the heliosphere (see below). The gradients undoubtedly also vary somewhat with radial position (and possibly heliospheric

longitude). For example, there is evidence that the radial gradient is smaller in the outer heliosphere than in the inner heliosphere (Webber and Lockwood, 1986; see also Cummings et al., 1987), although the exact nature of this variation is not well established. For purposes of predicting the absolute flux of cosmic rays at some location and time this approach (Equation 3) should be generally valid. It is much less likely to give accurate estimates of small *differences* in intensity between spacecraft at various locations in the heliosphere. The reader is warned that this is currently an area of very active research and observations over the next few years can be expected to define the nature of the spatial distribution of cosmic rays in the heliosphere much more clearly.

It should be noted that observations during 1975-1976 indicate that for the solar minimum period of 1972-77, the sign of G_θ for the ACR component was positive (Bastian et al., 1979), while during 1985-1987 it was negative (Cummings et al., 1987). The sign of G_θ presumably reversed sign when the polarity of the solar magnetic field reversed in 1980, and it would thus be expected to be negative again in the solar minimum of 1997-98. The available observations are consistent with the possibility that the sign of G_θ for galactic cosmic rays also reverses sign in the two halves of the solar cycle, but this cannot be established at this time. For purposes of simplicity, we assume here that *all* latitude gradients reverse sign every 11 years. Values quoted for G_θ are for near solar minimum conditions. The values at solar maximum are uncertain, but are presumably transitional between the solar minimum values.

Values in Table 2 are based on observations from Pioneer 10/11, Voyager 1/2, IMP-8, and ISEE-3 over a radial range of 1 to 40 AU, and a latitude range of 0 to 30^{o}N. Measurements by Helios 1 and 2 have shown that the radial gradient given here can be safely extrapolated in to ~0.3 AU. Extrapolation much beyond the range of observations, especially to latitudes $> \pm 30^{o}$, should be considered very uncertain. In any extrapolation, the interstellar spectrum discussed in Section 6 should be considered an upper limit on achievable fluxes, at least for galactic cosmic rays with energies $\geq$ 300 MeV/nuc. At lower energies, the maximum intensity and spectral shape of both the GCR and ACR components at large distances from Earth are very uncertain.

5. LARGE-SCALE STRUCTURE OF HELIOSPHERE OUT TO 1000 AU

A cartoon illustrating the expected large-scale structure of the heliosphere is shown in Figure 9. The solar wind flows radially out to a termination shock, where the velocity decreases suddenly by a factor of ~4. This occurs at a point where the wind ram pressure ($\sim \rho V^2$) equals the interstellar pressure, at 50-100 AU. Beyond this the (now subsonic) solar plasma is forced, by the flow of the interstellar gas, to flow back around the side of the heliosphere into a heliospheric tail. The dashed line is the "contact surface" separating the solar gas from the interstellar gas. Outside the contact surface, we have the interstellar plasma, which flows around the heliosphere at some 20-40 km/sec. If the sound speed in the interstellar gas is less than about 20 km/sec, there will be a second shock in the interstellar gas.

Recent calculations (Jokipii, 1987) indicate that the interstellar spectrum of cosmic rays extends into the contact surface. The outflowing solar gas outside of the termination shock appears to cause a substantial decrease in the cosmic ray intensity. Furthermore, the shock doesn't have a large effect on cosmic ray modulation.

One may conclude that the "modulation boundary" corresponds to the contact surface, and that the termination shock is inside the boundary. Previous models neglecting the shock are probably correct qualitatively. We expect that this contact surface is probably located approximately a factor of $\sim$ 1.5 beyond the solar wind termination shock (i.e., $\sim$100-150 AU). It should be realized that these distance estimates are quite uncertain, other estimates of the distance to the modulation boundary include values as small as $\sim$50 AU (see, e.g., Randall and Van Allen, 1986; Webber, 1987).

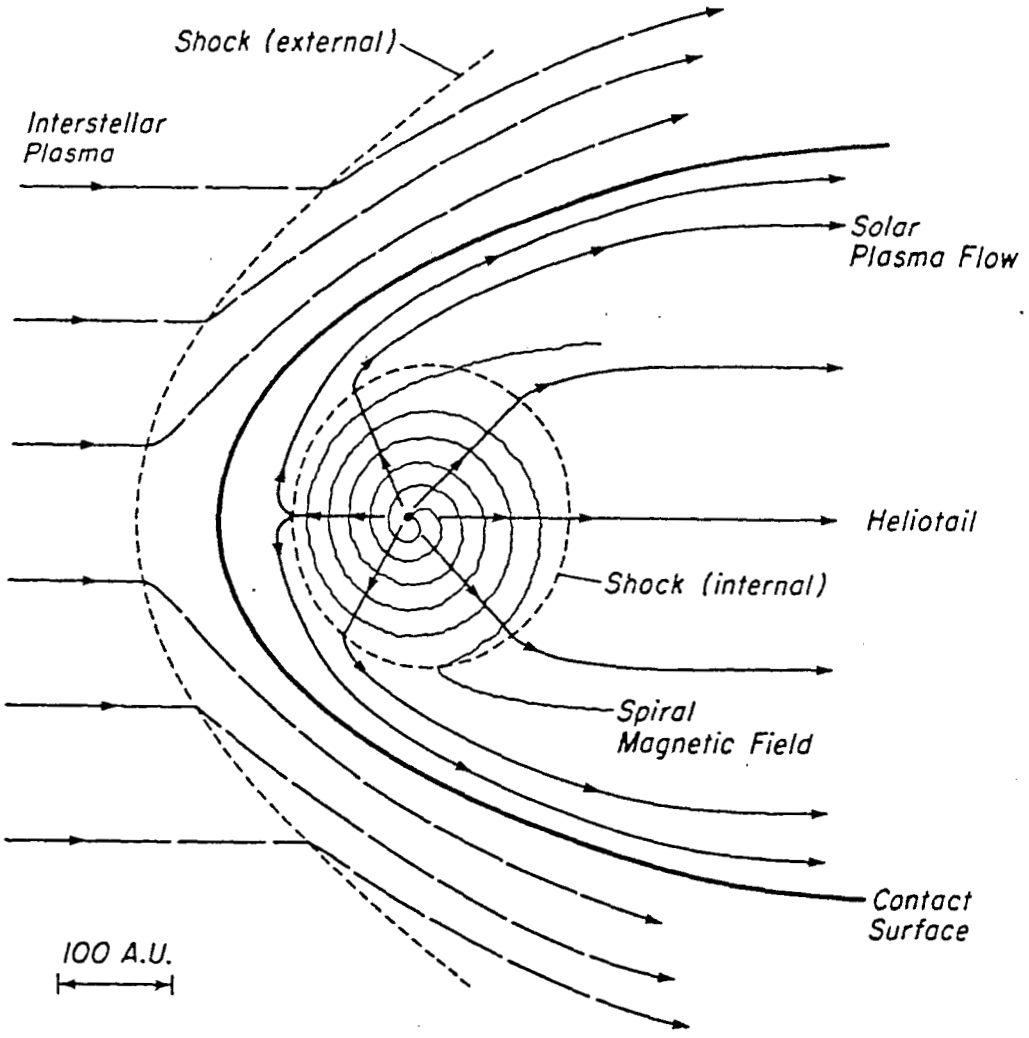

Figure 9: Schematic overview of the heliosphere indicating the solar wind termination shock and the contact surface (from Jokipii, 1987).

6. COSMIC RAYS OUTSIDE THE HELIOSPHERE:

The galactic cosmic ray energy spectrum in interstellar space is essentially unknown. The effect of the solar wind is always to decrease the intensity from the local interstellar value. General equilibrium of the interstellar gas requires that the local interstellar cosmic-ray energy density be not greater than that of the interstellar gas, or about 1 eV/cm^3. If this constant were to be violated, the cosmic rays would not be contained by the Galaxy in a near steady state, as required by meteorite measurements.

Many possible spectra satisfy this energy density constraint. A popular form which is often assumed is:

$$\frac{dJ_i}{dE} = A(E + E_o)^{-2.7}$$

where E is kinetic energy in GeV/nuc, E_o = 0.4 GeV/nuc, and A is chosen to match the high-energy spectrum (>20 GeV/nuc), which is not significantly modulated (as an example, for protons A = 1.5 x $10^4 m^{-2} sr^{-1} sec^{-1} GeV^{1.7}$, while A for He is about a factor of twenty smaller). Using this spectral form (or one of similar shape), and taking into account the time-dependent effects of solar modulation, it has been found to be possible to account in a reasonable manner for observations of the energy spectra of protons, alpha particles, and electrons over the solar cycle (see, e.g., Evenson et al., 1983). It should be kept in mind, however, that because of the significant amount of energy loss that cosmic rays suffer during the solar modulation process, we have almost no information on the local interstellar energy spectrum of cosmic rays below a few hundred MeV/nuc.

7. SUMMARY AND CONCLUSIONS:

We conclude that the current model for galactic and anomalous cosmic rays at Earth (Adams et al., 1981) is reasonably complete and should provide useful estimates of the near-Earth particle environment. The accuracy that can be expected is, of course, a function of both species and energy/nucleon. In particular, it will be much better at energies of several GeV/nucleon and above, where the effects of solar modulation are relatively small, than it will be at low energies (~100 MeV/nuc). For the same reason one can expect the GCR predictions to be considerably more accurate than the ACR predictions. With this in mind we estimate that it should generally be possible to predict the flux of low energy particles at any one time to within a factor of ~2, and to predict integral fluxes (or the flux of GeV particles) to perhaps ±30% at radial distances of 1 ±0.5 AU from the Sun, and near the ecliptic plane. (Note that our comments here are restricted to the GCR and ACR components of the Adams et al. model, and do not pertain to the predictions for solar flare particles.) When averaged over a period of several years we would expect the accuracy of the model to be better, since the greatest uncertainty in the model appears to be in its description of the temporal behavior of cosmic rays. There are several areas that we have indicated, especially for descriptions of the time dependence, and of the ACR component, where the accuracy of this model might be improved, but we do not expect major differences in

predictions of the overall cosmic-ray intensity for the near-Earth environment.

We have also suggested an approach that could be used to predict the behavior of cosmic rays in the outer heliosphere, making use of the wealth of new information that has already been (and continues to be) provided by the Pioneer and Voyager spacecraft. Such an approach should in principle yield predictions for the galactic cosmic ray environment over a wide range of the heliosphere that are of comparable accuracy to those presently available at Earth.

Acknowledgements: This work was supported by NASA under a variety of grants and contracts at the various institutions represented.

REFERENCES

Adams, J. H. Jr., Cosmic ray effects on microelectronics, part IV, *NRL Memorandum Report 5901,* 1986.

Adams, J. H. Jr., R. Silberberg, and C. H. Tsao, Cosmic ray effects on microelectronics, part I: the near-earth particle environment, *NRL Memorandum Report 4506,* 1981.

Bastian, T. S., R. B. McKibben, K. R. Pyle, and J. A. Simpson, Variations in the intensity of galactic cosmic rays and the anomalous helium as a function of solar latitude, *Proc 16th Internat. Cosmic Ray Conf. 12,* 318, 1979.

Cummings, A. C., R. A. Mewaldt, and E. C. Stone, Large-scale radial gradient of anomalous cosmic-ray oxygen from 1 to ~30 AU, submitted to the *20th Internat. Cosmic Ray Conf.* Paper SH 6.4-5, 1987.

Cummings, A. C., E. C. Stone, and W. R. Webber, Evidence that the anomalous cosmic ray component is singly ionized, *Ap. J. Lett., 287,* L99, 1984.

Cummings, A. C., and E. C. Stone, Elemental composition of the anomalous cosmic ray component, submitted to the *20th Internat. Cosmic Ray Conf.,* paper SH6.4-2, 1987a.

Cummings, A. C., and E. C. Stone, Energy spectra of anomalous cosmic ray oxygen, submitted to the *20th Internat. Cosmic-Ray Conf.,* paper SH6.4-4, 1987b.

Decker, R. B., S. M. Krimigis and D. Venkatesan, Latitudinal gradient of energetic particles in the outer heliosphere during 1985-1986, *J. Geophys. Res., 92,* 3375, 1987.

Dwyer, R. and P. Meyer, Cosmic-ray elemental abundances from 1-10 GeV per nucleon for boron through nickel, *Proc. 20th Internat. Cosmic Ray Conf.,* Paper OG 4.1-1, 1987.

Engelmann, J. J., P. Goret, E. Juliusson, L. Koch-Miramond, N. Lund, P. Masse, I. L. Rasmussen, A. Soutoul, Source energy spectra of heavy cosmic ray nuclei as derived from the French-Danish experiment on HEAO-3, *Astron. and Astrophys., 148,* 12, 1985.

Evenson P., M Garcia-Munoz, P Meyer, K. R. Pyle, and J. A. Simpson, A quantitative test of solar modulation theory: the proton, helium, and electron spectra from 1965 through 1979, *Astrophys. J., 275,* L15, 1983.

Fillius, W., I. Axford, and D. Wood, Time and energy dependence of the cosmic ray gradient in the outer heliosphere, *Proc. 19th Internat. Cosmic Ray Conf., 5,* 189, 1985.

Fisk, L. A., The anomalous component, its variation with latitude and related aspects of modulation, *The Sun and Heliosphere in Three Dimensions,* R. G. Marsden (ed.), Reidel, p. 401, 1986.

Fisk, L. A., B. Kozlovsky, and R. Ramaty, An interpretation of the observed oxygen and nitrogen enhancements in low-energy cosmic rays, *Astrophys. J., 190,* L35, 1974.

Garcia-Munoz, M., K. R. Pyle, and J. A. Simpson, The anomalous helium component in the heliosphere: the 1 AU spectra during the cosmic ray recovery from the 1981 solar maximum, *Proc. 20th Internat. Cosmic Ray Conf.,* Paper SH 6.4-11, 1987.

Garcia-Munoz, M., G. M. Mason, and J. A. Simpson, A new test for solar modulation theory: the 1972 May-July low-energy galactic cosmic ray proton and helium spectra, *Astrophys. J., 182,* L81, 1973.

Gloeckler, G., Compositions of energetic particle populations in interplanetary space, *Reviews of Geophys. and Space Phys., 17,* 569, 1979.

Hovestadt, D., O. Vollmer, G. Gloeckler, and C. Y. Fan, Differential energy spectra of low-energy ($\leq$ 8.5 MeV/nucleon) heavy cosmic rays during solar quiet times, *Phys. Rev. Letters, 31,* 650, 1973.

Jokipii, J. R., Particle acceleration at a termination shock 1. Application to the solar wind and the anomalous component, *J. Geophys. Res., 91,* 2929, 1986.

Jokipii, J. R., reported at this workshop, March, 1987.

Jones, F. C., Cosmic ray modulation and the anomalous component, *Rev. Geophys. Sp. Phys., 21,* 318, 1983.

Lopate, C., R. B. McKibben, K. R. Pyle, and J. A. Simpson, Radial gradients of galactic cosmic rays to ~40 AU during declining solar activity, submitted to the *20th Internat. Cosmic Ray Conf.,* paper SH6.3-14, 1987.

Klecker, B., D. Hovestadt, G. Gloeckler, and C. Y. Fan, Composition and energy spectra of cosmic rays between 0.6 and 24 MeV per nucleon during quiet times: transition from a solar to the anomalous component, *Astrophys. J., 212,* 290, 1977.

McDonald, F. B., and N. Lal, Variations of galactic cosmic rays with heliolatitude in the outer heliosphere, Geophys. Res. Letters, 13, 781, 1986.

McDonald, F. B., B. J. Teegarden, J. H. Trainor, and W. R. Webber, The anomalous abundance of cosmic ray nitrogen and oxygen at low energies, *Astrophys. J., 187,* L105, 1974.

McDonald, F. B., T. T. von Rosenvinge, N. Lal, J. H. Trainor, and P. Schuster, The recovery phase of galactic cosmic ray modulation in the outer heliosphere, *Geophys. Res. Letters, 13,* 785, 1986.

McKibben, R. B., K. R. Pyle, and J. A. Simpson, The anomalous helium and oxygen components in the heliosphere: observations at R $>$ 30 AU during recovery from maximum solar modulation, *submitted to the 20th Internat. Cosmic Ray Conference,* Paper, SH6.4-12, 1987.

McKibben, R. B., Galactic cosmic rays and anomalous components in the heliosphere, *Reviews of Geophysics, 25,* 711, 1987.

Mewaldt, R. A., J. D. Spalding, and E. C. Stone, The isotopic composition of the anomalous low energy cosmic rays, *Astrophys. J., 283,* 450, 1984.

Mewaldt, R. A., E. C. Stone, S. B. Vidor, and R. E. Vogt, Isotopic and Elemental

composition of the anomalous low-energy cosmic ray fluxes, *Astrophys. J., 205,* 931, 1976.

Randall, B. A., and J. A. Van Allen, Heliocentric radius of the cosmic ray modulation boundary, *Geophys. Res. Lett. 13,* 628, 1986.

Stone, E. C., C. J. Waddington, W. R. Binns, T. L. Garrard, P. S. Gibner, M. H. Israel, M. P. Kertzman, J. Klarmann, and B. J. Newport, The abundance of ultraheavy elements in the cosmic radiation, submitted to the *20th Internat. Cosmic Ray Conf.,* paper OG4.3-1, 1987.

Webber, W. R., R. L. Golden, and R. A. Mewaldt, A re-examination of the cosmic ray helium spectrum and the $^3He/^4He$ ratio at high energies, *Astrophys. J. 312,* 178, 1987.

Webber, W. R., R. L. Golden, and S. A. Stephans, Cosmic ray proton and helium spectra from 5 -2000 GV measured with a magnetic spectrometer, sumitted to the *20th International Cosmic Ray Conference,* paper OG 4.1-2, 1987.

Webber, W. R., The interstellar cosmic ray spectrum and energy density; interplanetary cosmic ray gradients and new estimate of the boundary of the heliosphere, to be published in *Astronomy and Astrophysics,* 1987.

Webber, W. R., and A. C. Cummings, Voyager measurements of the energy spectrum, charge composition, and long term temporal variations of the anomalous components in 1977-1982. *Solar Wind Five,* NASA Conf. Pub. 2280, M. Neugebauer, ed., 1983.

Webber, W. R., A. C. Cummings, and E. C. Stone, Radial and latitudinal gradients of anomalous oxygen during 1977-1985, *Proc. 19th Internat. Cosmic Ray Conf., 5,* 172, 1985.

Webber, W. R., and J. A. Lockwood, Interplanetary cosmic ray radial and latitudinal gradients derived in 1984 using IMP 8, Voyager, and Pioneer data, *Astrophys. J., 302,* 511, 1986.

Webber, W. R., and J. A. Lockwood, Interplanetary radial cosmic ray gradients and their implication for a possible large modulation effect at the heliospheric boundary, *Astrophys. J., 317,* 534, 1987.

Webber, W. R., F. B. McDonald, J. H. Trainor, B. J. Teegarden, and T. T. von Rosenvinge, Further studies of the new component of cosmic rays at low energies, *Proc. 14th Internat. Cosmic Ray Conference, 12,* 4233, 1975.

Webber, W. R., F. B. McDonald, T. T. von Rosenvinge, and R. A. Mewaldt, A study of temporal and radial dependencies of the anomalous helium and oxygen nuclei, *Proc. 17th Internat. Cosmic Ray Conference, 10,* 92, 1981.

BACKGROUND

The Effects of High Energy Particles on Planetary Missions

Paul A. Robinson Jr.
Jet Propulsion Laboratory
California Institute of Technology

Introduction

NASA is currently planning and building space systems for use in the 90's. An important part of the system design is understanding the environment and its effects on the system. These effects include spacecraft charging, internal charging, and degradation due to radiation. Most of these effects are reasonably well understood and have been studied for a considerable period of time. Voyager, for instance, had an extensive and apparently successful radiation control program which included prediction of the environment, prediction of the effect of the environment on systems and parts, and appropiate engineering response to the assessed degradation of the spacecraft due to the radiation environment.

However, the extensive use of modern, low power, high speed electronics has brought new concerns to the engineering community. Modern electronics have become so fast and so small that a single particle can influence their behavior -- a single particle can cause the electronics to malfunction in contrast to the cumulative effect of a multitude of particles required to cause earlier electronics to malfunction. Over the past five or so years, single event upsets -- situations where a heavy ion causes a flip-flop circuit in the chip to change state, have received a great deal of attention. Several conferences now devote a considerable fraction of their attention to this phenomenon. The IEEE Nuclear and Space Radiation Effects conference in July and the Single Event Effects Annual Symposium in April are two conferences which devote a considerable amount or all of their time to single event phenomena (SEP).

A prime consideration in the calling of this conference on the environment at this time, in addition to the fundamental importance of the environment in planning and designing space missions, is a new development in electronic part sensitivity. In addition to single event upsets, which are primarily soft errors, it is possible for modern electronics to latchup. A latchup many times results in a total failure of the electronic part, and consequently a possible loss of the mission. As will be shown later, this concentrates attention on the behavior of heavy ions in solar flares, and those trapped in the earth's radiation belts.

In this paper, we will review the background and motivation for detailed study of the variability and uncertainty of the particle environment from a space systems planning perspective. The engineering concern raised by each environment will be emphasized rather than the underlying physics of the magnetosphere or the sun. The rest of the papers in this conference will concentrate on the physics and predictions of the environment.

Missions now being planned span the short term range of one to three years to periods over ten years. Thus the engineering interest is beginning to stretch over periods of several solar cycles. Coincidentally, detailed measurements of the environment are now becoming available over that period of time.

Both short term and long term environmental predictions are needed for proper mission planning. Short term predictions, perhaps based on solar indices, real time observations, or short term systematics, are very useful in near term planning --

launches, EVAs (extravehicular activities), coordinated observations, and experiments which require the magnetosphere to be in a certain state.

Long term predictions of both average and extreme conditions are essential to mission design. Engineering considerations are many times driven by the worst case environment. Knowledge of the average conditions and their variability allows trade-off studies to be made, implementation of designs which degrade gracefully under multi-stress environments, the exercise of mission options based on near real time updates to environmental predictions, and prevents rejection of environmental considerations as nescient. Even the bounding of conditions over a mission duration is of considerable importance to mission planning, although that may not be very satisfying to the modeler who is attempting to predict real time variations, or to understand the details of magnetospheric activity.

Current Planning

A specific mission is concerned with the time and spatial variations of the environment along its trajectory. Current planetary missions with destinations as far as 1000 AU and as near as the sun are being planned. In the table below, some of the unmanned missions under consideration are listed, along with possible radiation induced engineering concerns. Many more manned and unmanned missions are possible and perhaps more likely. The point is, all missions need to consider the radiation environment.

Table: Some Current Missions

Project	Purpose	Possible Radiation Concern
Magellan	Radar mapping of Venus	Latchup of digital radar unit and single event upsets in memory especially during large solar flares
Starprobe	Investigation of the sun	Intense solar radiation -- heat shield; solar flares producing radiation damage, single event upsets and latchup.
Mariner Mark II	General purpose research craft planetary exploration	Wide range of possible environments. Concern ranges from single particle phenomena to radiation damage
TAU (Thousand AU)	Explore the outer reaches of the solar system	Extremely long mission and trajectory make tolerance to radiation induced problems a strong concern. Robust system design is called for.

Radiation Effects on Electronics

We review briefly some of the major radiation concerns that have historically been considered in planetary programs. This is followed by a short review of latchups.

Historically, the discovery of the Van Allen belts inaugurated space exploration and simultaneously initiated radiation damage as a concern for future space exploration. Since that time radiation damage to man and electronics has played a role in the planning and implementation of all space programs. The principal concern, until recently, has been the damage that a large number of particles inflict on solid state parts. This concern is usually referred to as a total dose problem.

Total Dose

There are two categories of total dose concern for electronics -- displacement damage and ionization. In one case the charged particle actually displaces an atom in the solid state structure and thereby modifies the mobilities etc. of the device.

Ionization along the track of a particle deposits charge and energy in the device which ultimately influence its operation. For example, thin insulating regions in the device collect charge at the interface between the insulating area and a semiconducting region, and thereby influence the current flow in the semiconductor. Programs have specified total dose tolerance for a number of years. For example, in the Galileo program the electronics radiation requirements are as follows:

Environment	Displacement	Ionization
Protons	4E10p/cm-sq 20MeV equivalent	electrons dominate (except surfaces)
electrons	Ions dominate	150 krads(Si)
Neutrons	5E10 n/cm-sq 1 MeV equivalent	negligible
Heavy ions	protons dominate	electrons dominate
Gamma	Negligible effect	electrons dominate

As can be inferred from this table, each ion species needs to be considered individually. Notice that the total dose effects of all heavy ions are small compared to the total dose of protons or electrons. This is because the number of other species are much smaller than either electrons or protons. Shielding is many times used to eliminate or reduce to acceptable levels total dose effects.

Single Event Upsets

A more recent perturbation to space systems is the phenomenon called single event upsets. In this case, a single particle, by depositing a short but intense charge trail, is able to change the state of a memory device. In the figure below, this is pictured as a single particle depositing enough energy in the depletion region of a bipolar integrated circuit (IC) to cause the flip-flop circuit, of which this is part, to change state (a "bit flip"). It is the combination of small feature size, high speed electronics, with dense ionization tracks by heavy ions, which leads to this phenomenon.

figure: Basic SEU Mechanism

Single Event Upset Mechanism

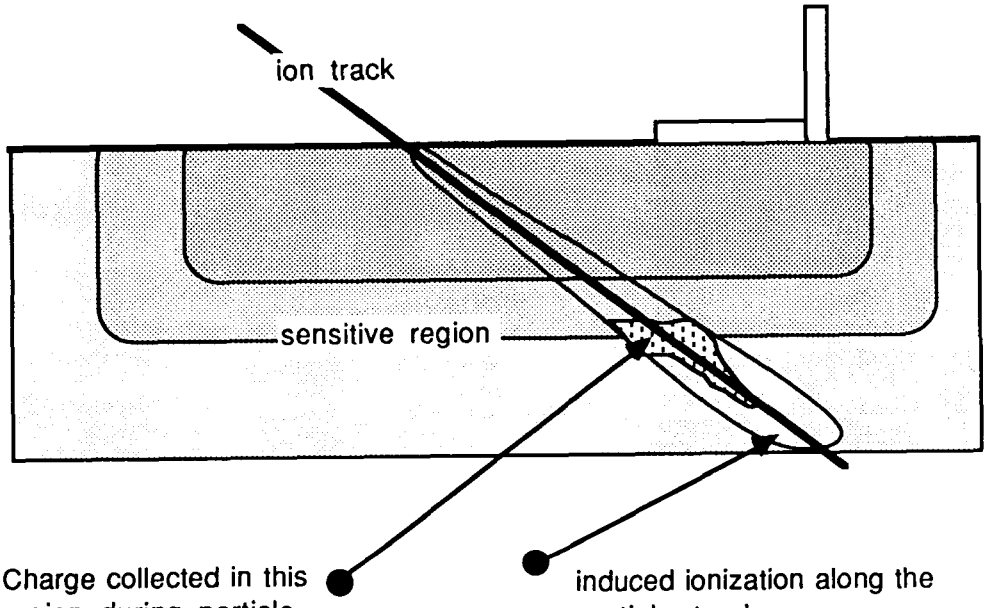

Charge collected in this region during particle transit can trigger a change of state of the memory

induced ionization along the particle track

Sensitive region is typically the depletion region, although charge can be collected a considerable distance from the depletion region.

Importance of Heavy Ions

The reason that heavy ions are of principal concern for single event upsets is seen in the next figure. For a single particle to cause an upset, the charge or energy deposited in the thin depletion region of the device needs to exceed a certain minimum. Thus a high stopping power (dE/dx) or high linear energy transfer (LET) is required.

figure: Stopping Power of Heavy Ions in Silicon

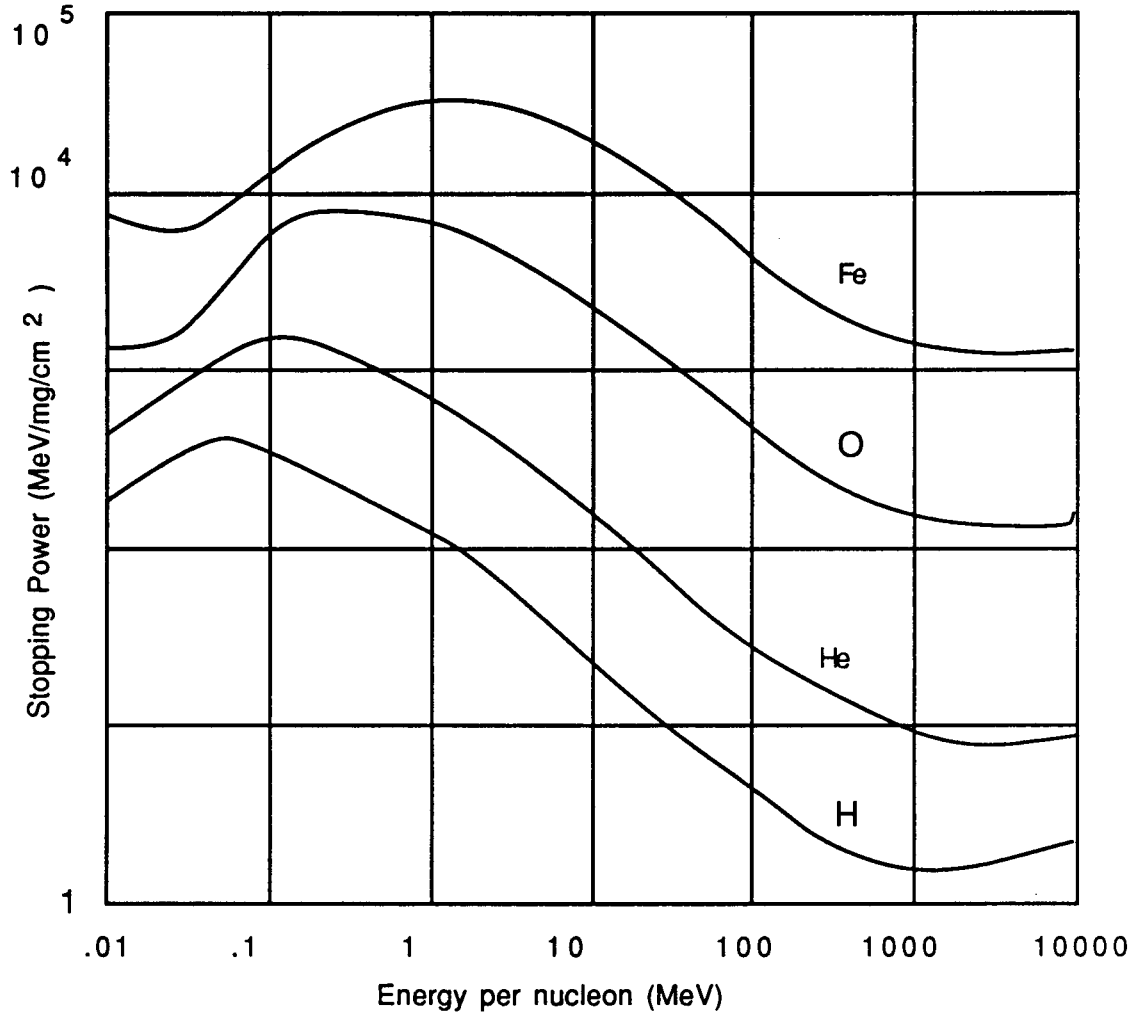

Feature Size Progress

IC (Integrated Circuits) development is tending towards faster logic and lower power. ICs are made faster and more energy efficient by decreasing the size of the features that make up the flip-flop circuit. This amounts to designing ICs in which the charge required to store information is smaller and smaller. As the charge per bit required to store information decreases, the amount of charge needed to cause a change in the stored information also decreases. The diagram below illustrates this trend. The charge used in storing information and the likelihood of upsetting the flip-flop are both related to the ability of a particle to deposit charge in the sensitive region of the device. In its simplest terms the probability of causing a SEU is a threshold phenomenon. All particles with an LET greater than a given amount normally incident on the sensitive volume will cause an upset. (Detailed calculations consider angular distributions, the structure and geometry of the sensitive volume, charge collection mechanisms, and circuit timing, in arriving at a SEU rate.)

figure: IC Feature Size

SEU Critical Charge versus Feature Size

(supplied by Petersen, 1987)

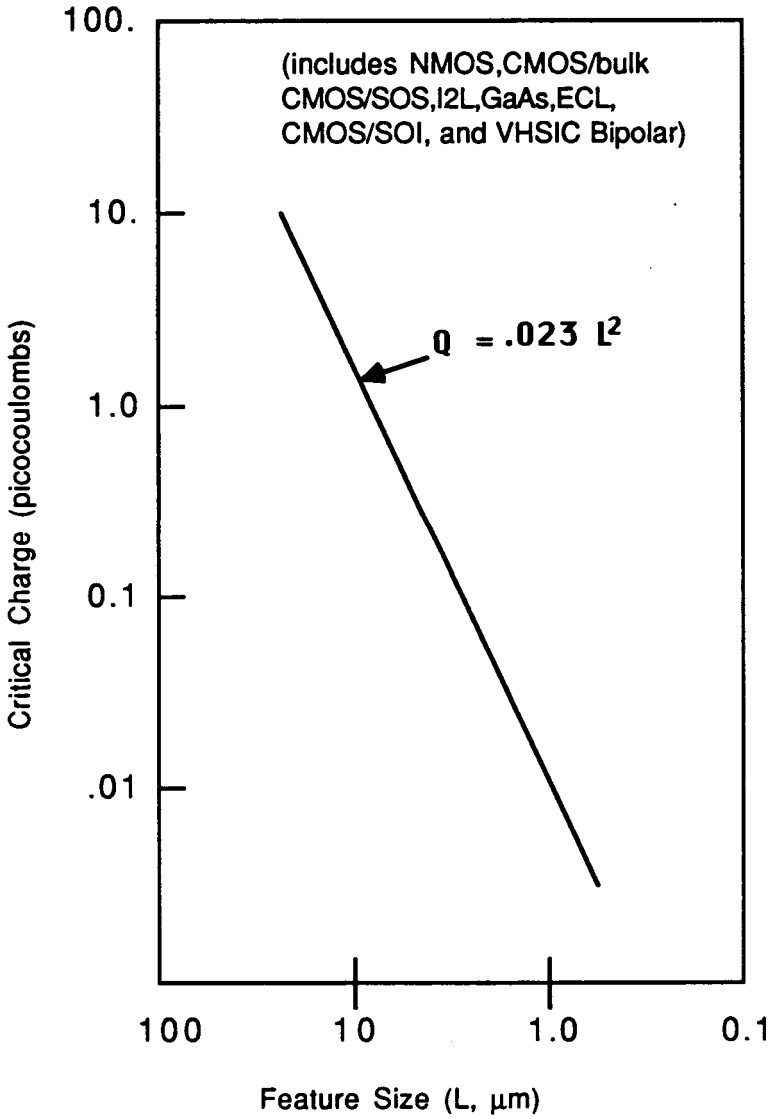

Trends in IC Development

It is unlikely that this push towards smaller, less power consuming, and faster devices will abate in the near future. Future planetary exploration needs the low power requirements, increased capability and performance these devices offer. Therefore future systems designs will need to confront single event phenomena.

Environmental Concern

Since the concern is for high LET particles which can deposit a large amount of charge in a small sensitive volume, the environmental interest is on galactic cosmic rays and heavy ion rich solar flares. The interest is high in the CNO group and above with energies of 2 MeV/nucleon or greater. For example, the particular parts of

interest to the Magellan program have sensitivities beginning around 40 Mev-cm sq/mg. Thus they have a particular interest in elements above the iron group.

Protons or other ions can cause SEUs indirectly when they create higher LET particles via nuclear reactions very near or in the sensitive volume. However, since the cross section for nuclear reactions is small, the proton or other population must be very large for this effect to be important. The figure below illustrates a typical SEU sensitive part prediction. In this case the threshold is low enough to allow proton interactions in the silicon of the chip to cause SEUs. The earth's proton belt is intense enough to make a significant contribution to the total SEU rate over a considerable region of space near earth.

figure: Typical SEU Rate Prediction

SEU Rates for AMD2901B, after Adams, 1986

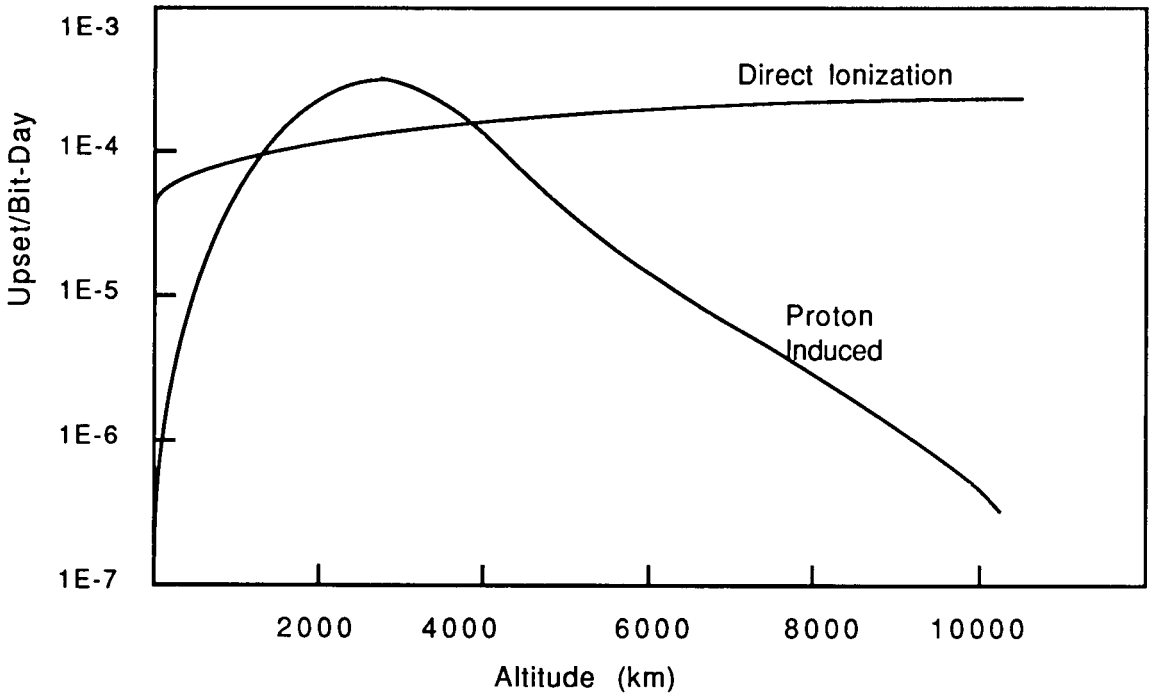

Latchups

Perhaps the primary motivating factor for calling this conference at this time is a concern on the part of several JPL planetary programs for a recently raised concern for single particle induced latchups in modern electronics. Latchups caused by over-voltage or large "gamma-dot" conditions have been known for a long time.

Single Particle Latchups

More recently, it has been shown that single high Z particles can turn "on" part of a integrated circuit in an unintended "latched" condition. Once in this state, electronics are no longer controlled in the way the designer planned, and must be powered down to regain control of the circuit. In addition it is possible for the unwanted circuit to draw enough power through the chip to damage it. Latchups occur when unintended circuits are turned on by a heavy ion. In a typical CMOS geometry these circuits cannot be avoided, although careful designing (guard rings, controlling epi layer thickness etc.) can eliminate or mitigate the problem. The figure below shows a typical CMOS structure. The unwanted "device" which latches up in this example is a pnpn

structure which occurs between Vdd and ground. This will occur whenever one has a p well near devices in the n substrate.

figure: typical CMOS structure

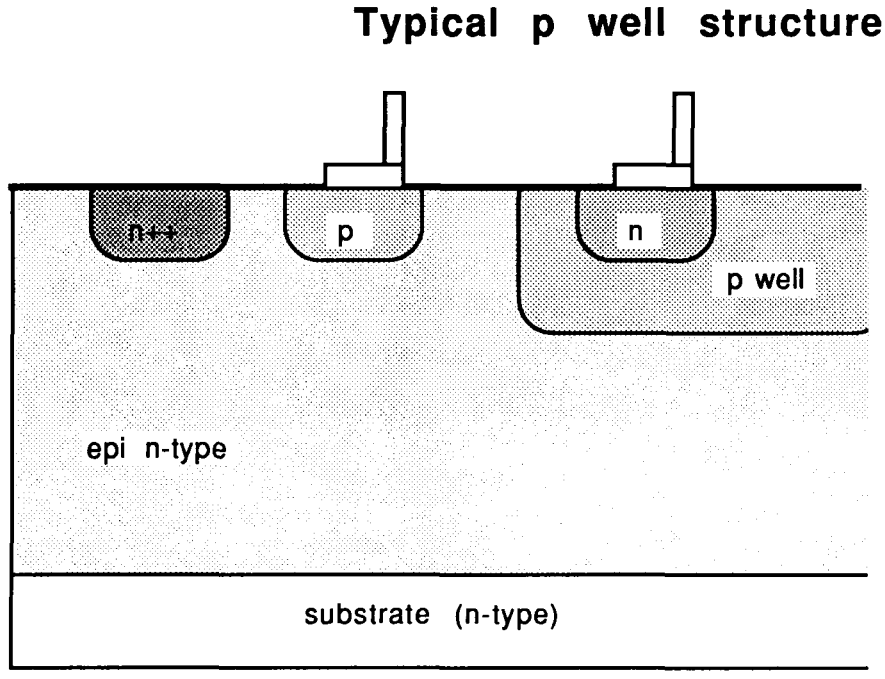

Latchup Mechanism

The current flow in the latched condition is probably quite complex. This is illustrated in the figure below. Some designers consider the pnpn structure to be coupled npn and pnp transistors such that the net gain for the circuit is greater than one (see Troutman). However, this has not been proved. Others consider multiple current paths through the structure which result in large current flow. Apparently multiple current paths are required to set up the conditions which allow the latchup condition. In spite of the fact that the detailed mechanism is not completely understood, latched conditions do exist, and have been triggered by single particles in tests.

figure: latchup circuit

SCR action initiated by single particle

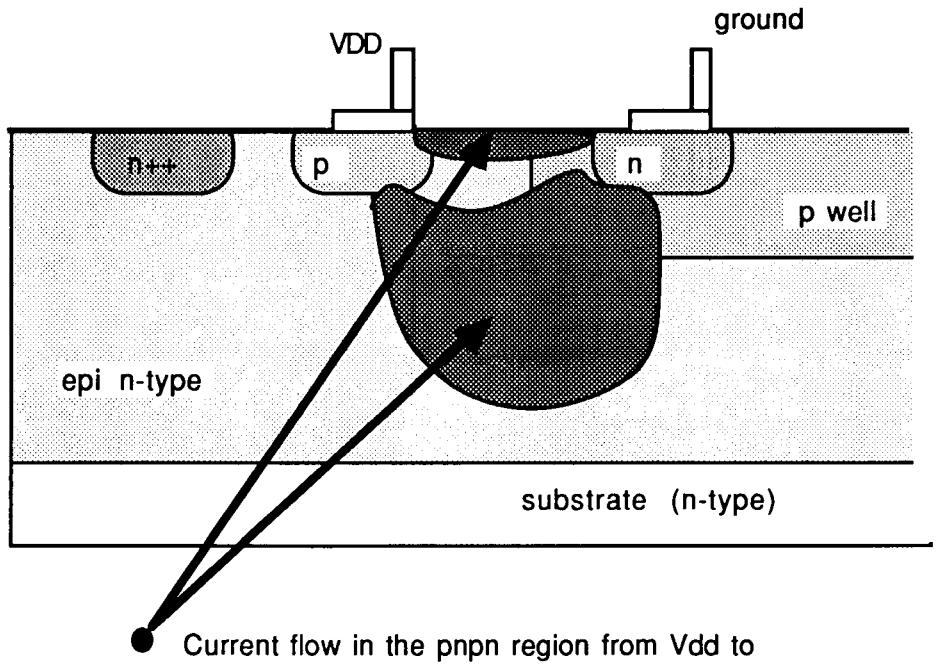

Current flow in the pnpn region from Vdd to ground is uncontrolled

Causes

There are several different ways in which an inadvertent circuit can be activated in a CMOS structure. Three methods of inducing a latchup and a brief description of each are given below:

Single Particle

Single particle induced latchups are similar to a SEU. This could be a limiting factor for Magellan since the part could be destroyed or seriously degraded. For Magellan the interest is concentrated in the Fe group and above. Concern for ions below iron in Z stems from considerations of particles that enter the sensitive volume at grazing angles.

Gamma Dot

This is of concern to those who plan to survive a nuclear attack when a sudden flash of x-rays completely "disorients" the chip. Voltages and voltage differentials are uncontrolled on the chip for a short period. When the voltages settle down it is possible for the chip to be in a latched configuration.

Over-voltage

This is a well-known electronic effect where an external voltage forward biases the p-well boundary and causes the IC to fail. This kind of latchup may or may not be identical to the single particle caused latchup. The electrical characteristics of a latchup are shown in the figure below. The parts of the curve closest to the voltage axis are the normal operations of the pnpn structure in which the diodes are essentially blocking the current. However for large backward bias or forward bias, large (generally unwanted) currents can flow. The dashed portion of the curve is inferred from the existence of the holding current. If the power supply providing Vdd cannot supply at least the holding current, the circuit will drop out of a latched condition. This fact is used in some designs

to prevent latchups. In other cases, resistance in the power circuits limits the current to levels which the part can tolerate. Current limiting may prevent damage to the part, but the power will have to be removed and reapplied for normal operation of the part. It is not clear without calculations or experiments what if any damage will result to a part in a latchup state.

figure: Electrical Characterization

Latchup circuit characteristics

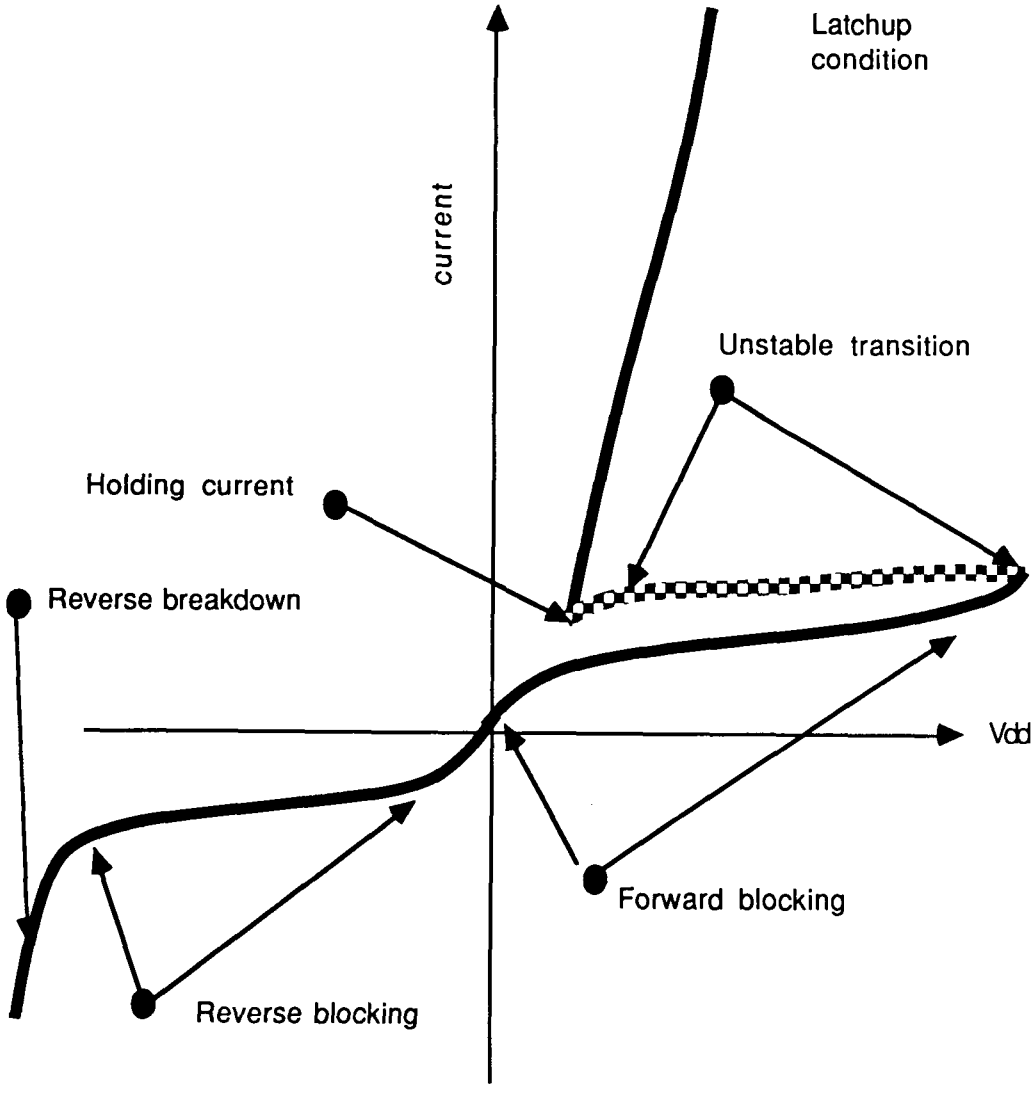

The latchup condition is usually unintended and can result in burn out of the transistor. It always involves a pnpn or npnp situation, and can be initiated by over-voltage, a single particle, or flash x-rays.

Current Status in the Engineering Community

In single event processes it is usually the charge deposited in the electronic part that is the most significant physical parameter. This means that the environment of concern is the high energy heavy ions. Both solar flares and galactic cosmic rays include particles of this sort. This has awakened a considerable interest in the engineering community for a quantified understanding of the variability and uncertainty in the measured and predicted heavy ion environment. In particular there is a desire to understand how frequently systems will be faced with single particle events of engineering importance. The pace of development in the electronics industry is rapid enough that parts will not always be immune to single particle effects. This underscores the importance of knowing the likelihood of significant single particle events.

Currently, engineering models are "worst case." This means that the largest flux estimates and highest occurrence frequencies are used for mission assessments. The danger of overestimates is the avoidance of missions important to planetary exploration, overly pessimistic risk estimates, underutilization of modern technology, and unrealistic demands on part designs. The danger of underestimates is possible mission failure.

Environmental Models Used in Calculations

There are two kinds of environmental models used in SEU and latchup calculations. One describes the worst possible environment and its frequency of occurrence, and the other describes the environment averaged over the mission duration.

Worst case

Worst case models are very useful for "bullet proof" designs. If the environment cannot be any worse than a given model, and the system can tolerate that condition, then the system design has properly considered that environment.

Nominal

For all missions the total expected fluence is used to set electronic part design limitations. A nominal environment includes the uncertainty in the modeling and the natural variability of the environment.

The Magellan Question

Background

At this time (January, 1987), a vital memory chip in the Magellan system can "latch up" when struck by heavy ions. (Since the conference it was determined that the part failed a short time after latching, and that other problems in addition to the latchup problem made that part unusable. That part has been replaced with one which has a much reduced sensitivity to latchup.) Other missions will also face a choice between proceeding with the latchable parts (perhaps the most economical and simple choice) or redesigning the system with new non-latchable parts (and accepting the risks to costs and schedule). Both options have to be considered. Therefore it is vital to have accurate estimates of the SEU or latchup causing environment.

Latchup rates

The latchup rate is calculated by integrating a cross section as a function of LET (linear energy transfer) over the spectra of particles in exactly the same manner as SEU calculations.

The Environments

We believe the heavy ion particle spectra for Magellan will consist of the galactic background plus an occasional contribution due to large solar flares. If the background rate, due to small solar flares and galactic cosmic rays, is large enough, new parts will be needed. Thus, we need your opinion on the magnitude and variability of the background environment, particularly ions with E> 2 MeV/nuc and Z>20.

We also believe that a large solar flare rich in heavy ions would dominate the latchup rate for a day or two. If the background rate is small, a possible system solution would be to fly a detector which would safeguard the system in the event of a large solar flare. No latchups occur when the system is turned off. No data is taken with an off system, so we desire as short an off period as possible. We need to understand if a "detect and avoid" strategy is likely to work. (Contributed ideas on detectors are also desired in case such an option is chosen.)

Engineering Models

What is needed for Magellan or other programs is an engineering model, not a detailed scientific model which illuminates the underlying mechanisms. We have been thinking in terms of simple spectra of the form

$$\frac{dJ}{dE} = A e^{-g}$$

where A is the "magnitude" of the spectra, g (the exponent of E) describes the "shape" of the spectra, E is the energy in MeV/nucleon, and dJ/dE is the flux in particles -nucleons per (centimeter squared - second - steradians - MeV)

Example

Using the models in the references below a simple comparison of models/experience might be as follows:

Model	Fe/O	A	g	Occurrence
C	1.2 to .8	?	2.5 to 4.5	1 in 11 years
A-m	.13		2.9-5.3?	24 in 7 years
A-wc	.4		2.9 - 5.3 ?	1 in 7 years
M	.11 to .06	?	2 to 3 ?	

(!) Fe/O is the iron to oxygen ratio

A is the magnitude parameter in the simple fit in particles/(cm**2-ster-sec-(Mev/nuc)) at 10MeV/nucleon

g is the shape parameter in the simple fit (E is the energy in MeV/nucleon)

occurrence is the number of such flares per year

C is the Chenette model

A - m is the mean model from Adams

A-wc is the worse case model from Adams

M is the McGuire model

The Questions

We would very much appreciate your thoughts on our situation and particularly the following questions:

Background flux

1. What model should be used for the background heavy ion flux?
2. How variable is the "background" heavy ion flux?

Solar Flares

1. What model(s) should be used for solar flares?
2. How frequently can a significant flare be expected?
3. How variable is the solar flare flux?
4. How far in advance can solar flares be predicted/ detected reliably?
5. Will the planet Venus shield the spacecraft from a solar flare when the spacecraft is in eclipse?

References

Adams Jr., J. H., R. Silberberg, and C. H. Tsao, "Cosmic Ray Effects on Microelectronics, Part I: the Near-Earth Particle Environment," NRL Memorandum Report 4506, Naval Research Laboratory, August 1981.

Adams Jr., J. H., J. R. Letaw, and D. F. Smart, "Cosmic Ray Effects on Microelectronics, Part II: the Geomagnetic Cutoff Effects," NRL Memorandum Report 5099, Naval Research Laboratory, May 1983

Adams Jr., J. H. and K. Partridge, "Do Trapped Heavy Ions Cause Soft Upsets on Spacecraft?" NRL Memorandum Report 4846, Naval Research Laboratory, October 1982.

Adams Jr., James H., "Cosmic Ray Effects on Microelectronics, Part IV," NRL Memorandum Report 5901, 1986

Chenette, D. L. and W. F. Dietrich, "The Solar Flare Heavy Ion Environment for Single Event Upsets: A Summary of Observations over the Last Solar Cycle, 1973-1983," IEEE Transactions on Nuclear Science, Vol NS-31 No. 6 December 1984 pp 1217-1222.

McGuire, R. E., private communication for this conference

Troutman R. R., "Latchup in CMOS Technology, The Problem and its Cure," Kluwer Academic Publishers, Boston, 1986

The Effects of High Energy Particles on Man

D.S. Nachtwey

(Title Only)

CURRENT MODELS OF THE INTENSELY IONIZING PARTICLE ENVIRONMENT IN SPACE

N89-28458

JAMES H. ADAMS, JR.
E. O. Hulburt Center for Space Research
Naval Research Laboratory
Washington, D. C.

ABSTRACT

This paper will describe the Cosmic Ray Effects on MicroElectronics (CREME) model that is currently in use to estimate single event effect rates in spacecraft.

1.0 INTRODUCTION

The first models of the intensely ionizing particle environment in space were constructed to estimate the biological effects of these particles. When single event upsets (SEU's) and other single event effects were discovered in the 70's, a detailed model of the intensely ionizing particle environment near the earth's orbit was constructed. The focus of all these models has been the computation of linear energy transfer (LET) spectra, because both the biological and the electronic effects of these particles can be computed from LET spectra. LET is defined as the amount of energy transferred, per unit path length, from an energetic particle to the medium through which it is passing. This energy must be deposited along or near the particle's path. This is different from stopping power (or dE/dx) which is defined as the amount of energy lost, per unit path length, by the energetic particle as it passes through the medium. These two are not the same, since the energy lost may **exceed the energy transferred and, on the microscopic scale, the energy is never deposited in the medium at the same place as it is lost. Nevertheless, LET is nearly equivalent to stopping power, and stopping power (computed in the straight-ahead, continuous-slowing-down approximation) is usually used to approximate LET.**

2.0 HISTORY

Wallmark and Marcus[1], in their 1962 paper on the minimum size of semiconductor devices, were the first to recognize that cosmic rays would interfere with the performance of the miniaturized components that they envisioned for the future. This interference appeared first as SEU's. SEU's are caused by intensely ionizing particles that can produce a burst of charge or a current transient that is large enough to disrupt the logic state of a microelectronic circuit. SEU's were first reported by Binder et al.[2] in 1975. These authors used a scanning electron microscope to simulate the ionization of a stopping Fe nucleus and demonstrate that the anomalies observed in space were indeed due to cosmic rays.

These early papers were ignored by the radiation effects community. It was not until SEU's due to cosmic rays were reported on the NAVSTAR GPS satellite[3] and SEU's due to alpha particles were discovered in the laboratory [4,5] that research into SEU's began.

The importance of such intensely ionizing particles had already been recognized in the radiobiology community[6,7] and a substantial research program on their unique effects was underway in the 60's. As part of this effort, an LET spectrum for galactic cosmic rays was computed by Curtis and Wilkinson[8]. Their spectrum includes the contributions of the elements up through Fe and corresponds to the minimum of the 11 year solar activity cycle (and therefore the maximum of the cosmic ray intensity cycle). Later, Heinrich[9] used the cosmic ray differential energy spectra from Mason[10] to construct differential and integral LET spectra behind various thicknesses of shielding. These LET spectra only included the contributions from the elements carbon through iron. Because the measurements of Mason were made during the maximum solar cycle, these LET spectra describe the space environment at its mildest.

Following the discovery that single event upsets were due principally to cosmic ray heavy ions, the Laboratory for Cosmic Ray Physics at Naval Research Laboratory undertook the project of constructing a comprehensive model of the intensely ionizing particle environment near earth[11] in 1980. This model will be discussed below.

3.0 Galactic Cosmic Rays

The model for the galactic cosmic ray spectra near earth[11] was constructed using all the published data on galactic cosmic rays. It was decided to model the energy spectra of the elements H, He, and Fe. The remaining elemental spectra could then be constructed from these using constant, or energy dependent elemental ratios. The choice of H, He, and Fe for the model spectra was made because: 1) the H spectral form is unique (because of its unique charge to mass ratio); 2) He is, by far, the best measured of the cosmic ray spectra and it has the same form as the heavier primary elements C, O, and Ne; 3) the element Fe is quite abundant and its spectral form differs somewhat from that of He. With only two spectral forms to model all the elemental spectra from He to Ni, it was decided to model the lighter elements with He and the heavier ones with Fe. The best break point was found to be between S and Cl.

All the data on H, He and Fe differential energy spectra were used to define the forms of the spectra at the extremes of solar minimum and solar maximum. It was found that these spectral extremes could be fit to analytic functions. These analytic functions made computation of particle fluxes very fast. The functions are approximate fits to the data as can be seen, in the case of the Fe spectrum, from the solid lines in fig. 1 (taken from [14]). Some details of the fit are in error, such as the turn up in the spectra at low energies and the asymptotic power law fit at high energies. The low energy turn up is not from galactic cosmic rays, but contributed by a quasi-steady interplanetary component.

Following the publication of the data from the HEAO-C experiments (see, for example, [12] and [13]), the model for cosmic rays was updated to include these and other recent results [14]. The updated model fits the HEAO-C data on the elemental spectra above 900 MeV/amu to ±15% for the elements Li to Ni. The data from the HEAO-C-3 experiment[13] allowed the model to be extended to uranium, by using the Fe spectrum as a model for the spectra of all the heavier elements. With this extension, we have a model for all the cosmic ray elemental spectra at solar maximum and solar minimum.

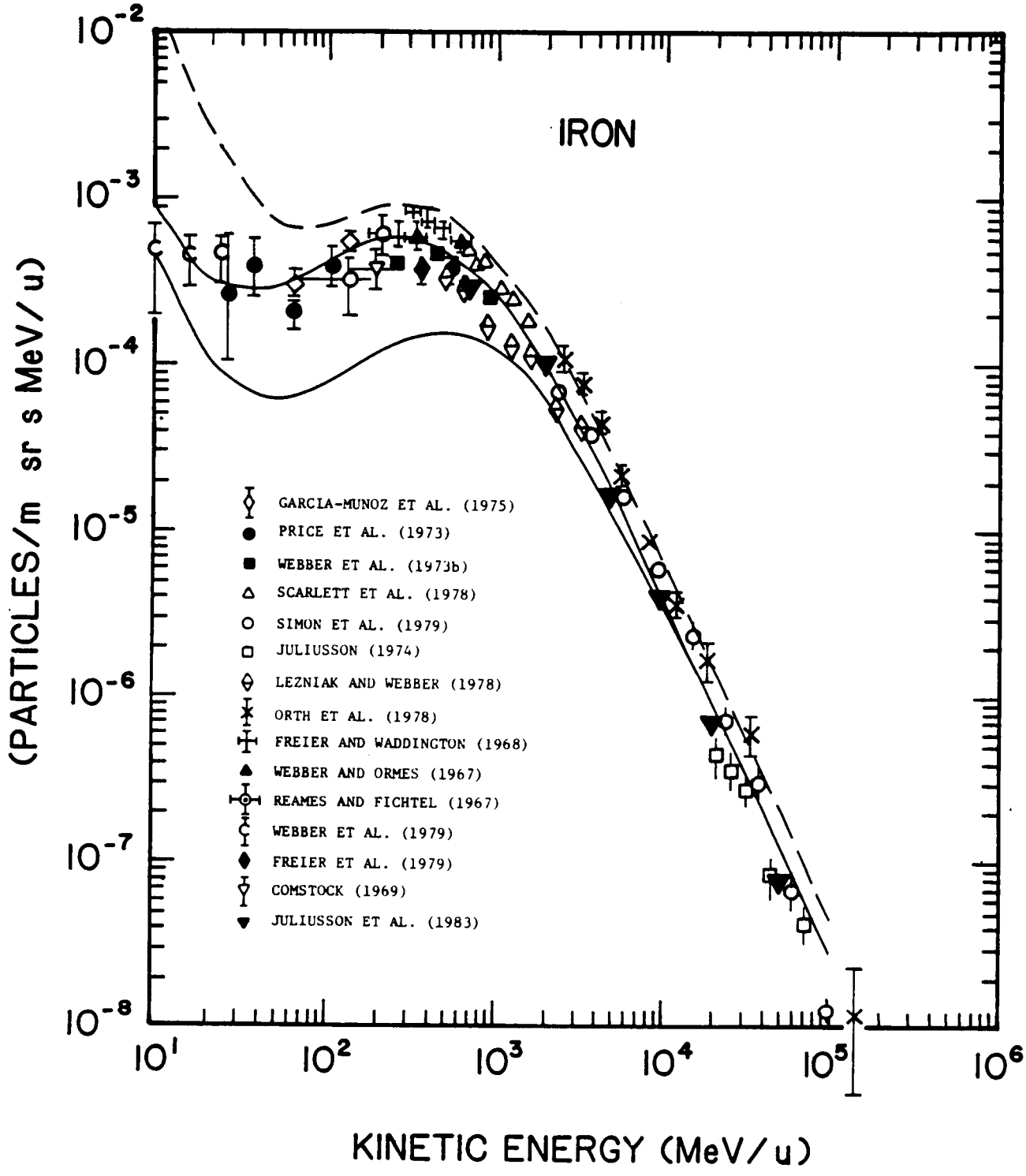

Figure 1. The cosmic ray iron spectrum: The solid curves are for solar maximum (lower) and solar minimum (upper). The dashed curve is the 10% worst case iron spectrum, which is implied by comparison with the cosmic ray helium spectrum. (This figure is taken from ref. [14], refer to this report the references to the data in this figure.)

To describe the cosmic ray spectra at other phases of the solar cycle, we linearly interpolate between the solar maximum and solar minimum spectra with an interpolation factor that is a sinusoidal function of time. The period of

this sine function is set by the sun spot cycle and the phase is adjusted to match the cosmic ray neutron monitor data. Since the actual solar cycle is a poor fit to a sine wave, this method of fitting leads to a factor of 2 uncertainty in predicting future flux levels below 1000 MeV/amu. This is the dominant source of error in the model for galactic cosmic rays. There is little point in improving the spectral fits or the elemental ratio fits so long as we have no better way to predict future levels of solar modulation.

4.0 Intensity Fluctuations at Low Energies

The galactic cosmic ray model discussed above describes the particle intensity during quiet periods at any point in the solar cycle. It often occurs that solar or interplanetary disturbances add to the particle intensity at earth. To account for this we used data from the Univ. of Chicago experiment on IMP-8, [15], to determine a flux level at each energy for the elements H and He, such that the flux measured on IMP-8 exceeded this level only 10% of the time. From these flux levels, we constructed a 10% worst case spectrum for H and He. There was not enough statistical precision in the Fe data from IMP-8 to determine 10% worst case flux levels for Fe, so we assumed that the fluctuations in the Fe spectrum were the same fractional size as those in the He spectrum. This 10% worst case spectrum is shown as the dashed curve in figure 1. The instantaneous Fe flux at any energy should exceed this spectrum only 10% of the time.

5.0 Solar Energetic Particles

The largest increases above the galactic cosmic ray background are due to solar energetic particle (SEP) events, produced by solar flares. For SEP's, the data base on protons is much more extensive and covers a much longer time period than the data on heavy ions. Because of this, we adopted the strategy of modeling the proton differential energy spectra in SEP's and then using the heavy ion to proton ratios to construct the heavy ion spectra. This procedure is not very satisfactory since heavy ions are often found to have different spectra than protons in the same SEP. It is justified only because: 1) the variability in proton flux from one SEP to another is greater than the variability in the heavy-ion-to-proton ratio, and 2) the chronology of well measured proton spectra is four times longer than the one for heavy ion spectra and more complete as well. The proton data, therefore, provide a better description of the variability in SEP size. We followed the method of King[16] to model the proton differential energy spectra in SEP events. Following King, we defined large SEP events as ones with one week integral proton fluences (above 10 MeV) exceeding $2.5X10^7$ protons/cm^2. We also treated the August 1972 SEP's as a special case, as King had done. By using integral measurements of the peak proton flux and total proton fluence above three energy thresholds, we constructed proton differential energy spectra. These spectra were constructed for the peak flux and the total event fluence in three cases: 1) using the means of the log normal distributions of the peak fluxes and total fluences, we constructed spectral models for large SEP's; 2) using these same means + 1.28σ (to reach the 10% probability level in the log normal distributions), we constructed 10% worst case spectral models for large SEP's; 3) Using the published data on the SEP of Aug. 4, 1972, we constructed spectral models for this event, which we called an anomalously large event, as King had done. The 10% worst case spectral models are intended to provide flux and fluence estimates so high that only one large SEP in 10 will produce a peak flux or a fluence that exceeds this model. Following the publication of additional data on SEP's by Chenette and Dietrich[17] and others, the models for the peak SEP fluxes were revised[14].

The heavy ion to proton ratios we adopted were the means of the ratios of individual SEP events that we found in the published data. These mean ratios were used to define spectra for mean SEP composition. We also constructed distributions of these ratios and found that they looked like two half-gaussians (with different standard deviations), joined at the mean. The tail of this distribution was broader toward the heavy ion rich side than toward the heavy ion poor side. We used this distribution to determine heavy ion to proton ratios so large that they should be exceeded by only one SEP in 10. These ratios were used to define spectra with 10% worst case heavy ion enrichment. This work was also updated in ref. [14]. The mean ratios we have adopted are close to those in a recent survey by Mason[18].

6.0 The Anomalous Component

This is a steady feature of the low energy spectra of He, N, O, Ne and Ar. There is some evidence for it in the spectra of C, Mg, Si, and Fe. At the earth's orbit (1 astronomical unit or AU), it exceeds the cosmic ray background only during solar minimum. Even then, it makes a minor contribution to the integral LET spectrum. We have used the published measurements of the anomalous component spectra near 1 AU to produce analytic models of these spectra for the elements He, N, and O in the interplanetary medium.

If the anomalous component is singly ionized as the theory of Fisk et al.[19] suggests, then these ions would have greater access to the inner magnetosphere of the earth. We have included this possibility in our model for the anomalous components of the elements He, C, N, O, Ne, Mg, Si, Ar, and Fe.

The intensity of the anomalous component increases at ~15%/AU with radial distance from the sun. This means that in the outer heliosphere, the anomalous component always exceeds the galactic cosmic ray background and is a major contributor to the LET spectrum at solar minimum.

7.0 Material and Geomagnetic Shielding

The CREME model includes provisions for computing a geomagnetic cutoff transmission function, so that the orbit-averaged particle spectra can be modeled for any spacecraft in any orbit about the earth. This is done by sampling the vertical geomagnetic cutoff at a large number of points along the spacecraft's flight path, and then constructing the transmission function from this sample[20].

The model also computes the differential energy spectra inside the spacecraft. This is done by accounting for energy loss and nuclear interactions in the shielding. The method accounts for ions lost in interactions, but not for the products of those interactions that continue into the spacecraft. This leads to a systematic underestimate of the particle flux, but this underestimate is less than a factor of 2 for shielding of less than 50 g/cm^2 aluminum equivalent. More detailed calculations, which include secondary production are possible, but do not seem to be warranted.

8.0 Computation of LET Spectra

The model differential energy spectra for all the elements, propagated into the spacecraft to the depth of the microelectronic components, are combined to form a single integral LET spectrum[14]. The LET spectrum is simply,

$$F(L) = \int_{L}^{\infty} \sum_{j=1}^{92} (dN_j/dE)(dS_j/dE)^{-1} \, dS$$

Where,

S_j = dE/dx for an ion of atomic number j.

Using the CREME model, the integral LET spectrum can be calculated inside any spacecraft in any orbit of the earth or in interplanetary space near the orbit of the earth. This can be done for a variety of interplanetary "weather" conditions and for any part of the 11 year solar cycle.

9.0 UNCERTAINTIES IN THE CREME MODEL

There are several deficiencies in the data base on the energetic particle environment near earth which affect the estimation of single event effect rates. The ionization state of heavy ions in the interplanetary medium strongly affects their access to the earth's magnetosphere. There is no conclusive direct evidence on these charge states above ~1 MeV/amu. In the case of galactic cosmic rays, there is no doubt that they have passed through about 7 g/cm^2 of interstellar gas. This is more than enough matter to fully ionize all but the very heaviest ions[21]. The theory of Fisk et al.[19] for the origin of the anomalous component predicts that it is singly ionized. There is some indirect evidence that the anomalous component is singly ionized. Several attempts are underway to measure the charge state directly, using the earth's magnetic field. One of these experiments reports preliminary results that favor higher ionization states[22,23]. The charge state of solar energetic heavy ions is also uncertain. Here too, the indirect evidence[24] indicates that that these ions are less than fully ionized. This evidence is consistent with the distribution of charge states measured at low energies[25].

For satellites passing through in the inner Van Allen belt, there is uncertainty about the contribution of trapped radiation to the SEU rate. If there is even a small admixture of heavy ions trapped along with the protons in the inner belt, these heavy ions could be the dominant cause of SEU's. The **data base on trapped heavy ions has been reviewed [26] and it is not possible to rule them out as a dominant source of SEU's in the heart of the inner belt.**

10. CONCLUSIONS

The CREME model provides a description of the radiation environment in interplanetary space near the orbit of the earth that contains no major deficiencies. The accuracy of the galactic cosmic ray model is limited by the uncertainties in solar modulation. The model for solar energetic particles could be improved by making use of all the data that has been collected on solar energetic particle events.

There remain major uncertainties about the environment within the earth's magnetosphere, because of the uncertainties over the charge states of the heavy ions in the anomalous component and solar flares, and because of trapped heavy ions.

The present CREME model is valid only at 1 AU, but it could be extended to other parts of the heliosphere. There is considerable data on the radiation environment from 0.2 to 35 AU in the ecliptic plane. This data could be used to extend the CREME model.

As the electronic and biological effects of intensely ionizing particles are better understood, it is reasonable to expect that LET will no longer provide an adequate description of the radiation. It is therefore important to provide models that contain a complete description of the radiation environment.

REFERENCES

1. J. T. Wallmark and S. M. Marcus, Proc. of the IRE, 286, March, 1962.

2. D. Binder, E. C. Smith and A. B. Holman, IEEE Trans. on Nucl. Sci., **NS-22**, 2675-80, 1975.

3. J. C. Pickel and J. T. Blandford, Jr., IEEE Trans. on Nucl. Sci., **NS-25**, 1166-71, 1978.

4. Timothy C. May and Murray H. Woods, IEEE Trans. on Electron Devices, **ED-26**, 2-9, 1979.

5. David S. Yaney, J. T. Nelson, and Lowell L. Vanskike, IEEE Trans. on Electron Devices, **ED-26**, 10-15, 1979.

6. Frank Attix and William C. Roesch, ed., "Radiation Dosimetry", Vol. 1, Academic Press, New York, 1968.

7. Cornelius A. Tobias and Paul Todd, ed., "Space Radiation Biology and Related Topics, Academic Press, New York, 1974.

8. S. B. Curtis and M. C. Wilkinson, NASA TM X-2440, 1007-14, Jan. 1972.

9. W. Heinrich, Rad. Effects, **34**, 143-8, 1977.

10. G. M. Mason, Ap. J., **171**, 139-61, 1972

11. J. H. Adams, Jr., R. Silberberg and C. H. Tsao, "Cosmic Ray Effects on Microelectronics, Part 1: The Near Earth Particle Environment", NRL Memorandum Report 4506, August 25, 1981.

12. **J. J. Englemann, P. Goret, E. Juliussion, L. Koch-Miramond, P.** Masse, A. Soutoul, B. Byrnak, N. Lund, B. Peters, I. L. Rassmussen, M. Rotenberg and N. J. Westergaard, Proc. of the 18th Intl. Cosmic Ray Conf., **2**, 17-20, 1983.

13. W. R. Binns, R. K. Fickle, T. L. Garrard, M. Israel, J. Klarmann, E. C. Stone, and C. J. Waddington, Ap. J., **247**, L115-8, 1981.

14. James H. Adams, Jr., "Cosmic Ray Effects on Microelectronics, Part IV", NRL Memorandum Report No. 5901, Dec. 31, 1986.

15. K. R. Pyle, private communication, 1981.

16. J. H. King, Journal of Spacecraft and Rockets, **11**, 401-8, 1974.

17. D. L. Chenette, and W. F. Dietrich, IEEE Trans. on Nucl. Sci., **NS-31**, 1217-22, 1984.

18. G. M. Mason, "The Composition of Galactic Cosmic Rays and Solar Energetic Particles", to be Published in Rev. of Geophys. and Sp. Sci., 1987.

19. L. A. Fisk, B. Kozlovsky and R. Ramaty, Ap. J. (Letters), **190**, L35-7, 1974.

20. J. H. Adams, Jr., J. R. Letaw, and D. F. Smart, "Cosmic Ray Effects on Microelectronics, Part II: The Geomagnetic Cutoff Effects", NRL Memorandum Report No. 5099, May 26, 1983.

21. John. R. Letaw, J. H. Adams, Jr., Rein Silberberg, and C. H. Tsao, Astrop. and Sp. Sci., **114**, 365-79, 1985.

22. James H. Adams, Jr., Allan J. Tylka and Bertram Stiller, Trans. Am. Geophys. U., **67**, 341, 1986.

23. James H. Adams, Jr. and Allan J. Tylka, Bull. Am. Phys. Soc., **32**, 1066, 1987.

24. H. H. Breneman and E. C. Stone, Ap. J., **299**, L57-L61, 1985.

25. A. B. Klecker, D. Hovestadt, G. Gloeckler, F. M. Ipavich, M. Scholer, C. Y. Fan, and L. A. Fisk, Adv. Space Res., **4**, 161-4, 1984,

26. J. H. Adams, Jr. and K. Partridge, "Do Trapped Heavy Ions Cause Soft Upsets on Spacecraft?", NRL Memorandum Report No. 4846, October 12, 1982.

Solar Flare Heavy Ion Flux and Fluence Models for Upset and Latchup Rate Estimation

D.L. Chenette
W. F. Dietrich

(Title Only)

N89-28459

A New Proton Fluence Model for E >10 MeV

J. Feynman[1], T. P. Armstrong[2], L. Dao-Gibner[3], S. Silverman[4]

Abstract:

We describe a new engineering model for the fluence of protons with energies >10 MeV. The data set used is a combination of observations made primarily from the Earth's surface between 1956 and 1963 and observations made from spacecraft in the vicinity of Earth between 1963 and 1985. With this data set we find that the distinction between "ordinary proton events" and "anomalously large proton events" made in earlier work disappears. The >10 MeV fluences at 1 AU calculated with the new model are about twice those expected on the basis of models now in use. In contrast to earlier models, our results do not depend critically on the fluence from any one event.

Introduction:

The proton fluence model currently used to evaluate hazards to spacecraft systems is that developed by King in 1974. That model was designed specifically to predict fluence during the period from 1977-1983, i.e. the 21st solar cycle.

Because of this specificity we undertook a review of the King model and as a result of the review, we have developed an updated model for energies > 10 MeV. The model is now being extended to E > 30 MeV. The purpose of this paper is to provide the workshop with an overview of our approach to this problem. We can not report on our work in full detail because of time and space limitations of the workshop and this paper gives only a brief outline of the work.

The King (1974) model for 1977-1983 was based on two assumptions. First King noted that the fluence during the solar cycle that maximized in 1957 (cycle 19, maximum annual sunspot number 190) was much larger than the fluence during the 20th cycle that had just been completed. The fluence during cycle 20 was dominated by a single event, the great proton flare of August, 1972. This lower fluence during cycle 20 (maximum annual sunspot number 107) was in agreement with the notion that was widely held at the time, i.e. that the number of great proton flares during a solar cycle was a function of the cycle's maximum sunspot number. Furthermore, the predictions King used for sunspot maximum for cycle 21 indicated that it would resemble or be smaller than cycle 20. With these assumptions about the relation between sunspot number and major proton flares and about the intensity of cycle 21 it was very reasonable to use the cycle 20 data base to make a conservative prediction of cycle 21 fluence. However, neither of these assumptions have proved valid for cycle 21. There were no major proton events at all during cycle 21 despite the fact that the maximum annual sunspot number in cycle 21 was 155, compared to cycle 20's maximum of about 107. The failure of these assumptions indicates the importance of reviewing the data and producing a new model.

(1) Jet Propulsion Laboratory, Pasadena, CA 91109.
(2) Dept. of Phys. and Astron., U. of Kansas, Lawrence, KS 66045.
(3) Syscon, Pasadena, CA 91109.
(4) Dept of Physics, Boston College, Chestnut Hill, MA 02173.

Data Base

Data on proton fluences come from two major sources. Since 1963 instruments have been observing proton fluxes in space. All of the feasible data from satellite observations have been collected and edited for valid solar particle responses. A nearly time continuous record of daily average fluxes of particles above the thresholds of 10, 30 and 60 MeV has been constructed. The details of the production of this data set are described in Armstrong et al., (1983). These data form one of the two sets used. The second data set is that used by Yucker (1970, 1971) and consists of the events between 1956 and 1962. As is well known, several of these earlier events were said to have fluences comparable to and even larger than the event of August 1972. Because these events occurred before the space era had really begun, and because they were not observed from interplanetary space, it is widely believed that the fluences reported for them were highly inaccurate and exaggerated. To check on the validity of this data set, a careful review of the original papers was undertaken. The care with which these early events were studied can be illustrated by noting that a conference was held on the November 1960 solar-terrestrial events at the then Air Force Cambridge Research Laboratories (now known as the Air Force Geophysics Laboratory). Twelve papers were given at the conference and a 165 page report was produced (Aarons and Silverman, 1962). A second thorough review of the known high fluence events between 1949 and 1961 was reported on in the Solar Proton Manual edited by Frank McDonald (1982). In that publication Malitson and Webber (1962) report that events since 1956 had been carefully studied and 1956 was chosen here as the beginning of our data set. Malitson and Webber reviewed their data in the Solar Proton manual as did Fichtel, Guss and Ogilvie in the next paper in the manual. Fichtel et al, (1962) had as their goal to determine the fluences of individual solar particle events within a factor of two. Fichtel et al. claim that the accuracy obtained is frequently much better. We concluded that the accuracy of the pre-1963 data was good and the data should be included in the new proton fluence model. As a non-scientific aside we would like to mention that the fact that these events were extremely large is not doubted by those observers who are still active in the field and who were concerned with proton events and aurora at the time they occurred. This includes two of the authors of this paper and several of the attendees at this workshop. On the basis of our reviews of the 1956-1962 data set we have included that data in our data base.

Method of Analysis

To analyze the data we followed the general approach used earlier by Yucker (1971) and King (1974). That is, we first studied the distribution of event magnitudes. Malitson and Webber (1962) had stressed that solar flares producing protons occur in groups with several flares occurring over a period of days in the same active center. Since these grouped events can not be assumed to be occurring independently of one another the distribution of fluences in a data set that considers each flare to be a separate event can not be expected to be a random sample of any underlying parent population. We therefore decided to integrate over each group of flares in our definition of "event fluence." Initially we were concerned that there would be a certain amount of arbitrariness in choosing the beginning and end times of events. To check this, beginning and ending times for events were chosen independently by two of the authors (J. F and LDG) but no significant differences were found between the two resulting lists.

Using the event fluences determined in this way we tested to see if the fluences followed a log normal distribution. The events were ordered according to the log of the magnitude and this was plotted vs. the percent of observed events that have a magnitude less than the given event. To be more exact fluences were plotted against (i x 100)/(n+1) where i is the rank value of the events ordered from smallest to largest and n is total number of events used in the data set. The graph paper used to plot the results is ruled so that a log normal distribution will appear as a straight line. The result for the E > 10 MeV data set is shown in Figure 1. Most of the data lies on a straight line. For the lowest fluences shown, the data turns up and the observed fluences become much larger than those expected from any straight line. This is an artifact and is expected whenever a data set is truncated (Nelson, 1982). In our case we have included only those events for which the fluence was greater than 1 x 10^7 particles/cm^2.

The data for fluences above 2 x 10^7 particles/cm^2 is well fit by a straight line. This is in contrast to King's (1974) results where only the data from cycle 20 was considered (for the reasons discussed in the introduction). In that case the 1972 event was so much larger than any other event in the set that it could not be considered part of the same distribution. King had to treat the 1972 event separately from other events. He called the 1972 event an AL (anomalously large) event and all other events OR (ordinary). In the present study the 1972 event is not outstanding and, in fact is not the event with highest fluence. These results for the E > 19 MeV data encourage us to use a single method of analysis for all events in the data set.

Solar Cycle Variation

In King's treatment he distinguished between the maximum and minimum phases of the sunspot cycle. However, "maximum and minimum" phases were not clearly defined. This would have caused difficulty if the 1972 event was to have been predicted. The maximum of cycle 20 occurred in 1968. Thus the event occurred four years after solar maximum and 3 years before solar minimum. If a prediction was to have been made from say 1965, would the appropriate model have been considered to be the maximum or minimum model?

In order to examine the solar cycle dependence in more detail, we used a superposed epoch analysis of the annual fluence for the 30 years covered by our data set. Our approach differed from that of other workers in that we defined the time of cycle maximum accurately to 0.1 years instead of the usual 1 year accuracy. The times of maximum of the 13 months running average sunspot number were supplied by Heckman (Gary Heckman, personal communication). The "years" of the cycle were then also defined as 365 day periods centered on the sunspot maximum correct to 0.1 years, i.e., "years" are not calendar years.

The result of this analysis for E > 30 MeV and for the 3 cycles for which we have data is shown in Figure 2. Notice the clear difference between the 7 years of high fluence and the 4 years of low fluence in each cycle. With only two exceptions, the annual fluences exceeded 10^8 particles/cm^2 during the 3 sets of 7 hazardous years/cycle and were less than that during the other 3 sets of 4 years/cycle. This is true even if no major proton events occurred during a hazardous year of a particular cycle. Furthermore, note that the hazardous period is not centered on sunspot maximum but extends from 2 years before maximum to 4 years after maximum.

This clear result has important implications to space missions. In comparing the fluences to be expected during different missions it is very important to take into account the actual launch date, since we can now be quite secure in predicting negligible fluences during the 4 minimum years of each cycle. Also notice that the dates of the last three cycle maxima occurred 11 years apart to the 0.1 year, so that we can be reasonably confident in predicting the time of the next maximum (about 1991). There is much more variance in the time between minima. The first spots of the new cycle (22) have appeared during the last 6 months (H. H. Sargent, personal communication, 1987).

Solar Cycle Corrected Proton Fluences

With the establishment of such a clear solar cycle variation, the approach to the determination of the best fit to the fluence distribution must be changed somewhat. The distribution should be constructed using data from only the 7 hazardous years in each cycle. The few small events that occurred during the 4 year quiet periods should be dropped from the data set.

The hazardous years' fluence distribution for protons with E > 10 MeV is shown in Figure 3. Again there is a turnup of the points at low fluence due to truncation of the data set. However, even after this is taken into account the rest of the data do not define a single straight line. We have also looked at other types of distribution functions such as type II and III extreme value distributions but the fits to the data were not improved. Our approach to the problem of the non-linearity of the data is to note that it is only those events with large fluences that influence the total fluence during a year. It is therefore more important to fit the large fluence part of the distribution than the low fluence part. We have carried out our analysis using the straight line eyeball fit shown in Figure 3. The turnup of the data at low fluences is an artifact due to the truncation of the data set (Nelson, 1982) and these points are not taken into account in the fit. Note that this fit does not depend crucially on the accuracy of the determination of the fluence from any one event. This is an advantage when compared with the situation faced by King who had to use fluences from only one solar cycle during which there was only a single event with fluences greater than 2×10^{10} particles/cm^2 for E > 10 MeV.

Statistical analyses

Since the high fluence portion of the data can be fit quite well with a straight line, the analysis was carried out along the lines used by King for the so called "ordinary flares." Let f_p be the proton fluence of an event, f_p can be written as $f_p = 10^F$. If f_p is distributed lognormally then F is distributed normally and its density function is commonly expressed as

$$f(F) = \frac{1}{\sqrt{2\pi}\sigma} e^{-\frac{1}{2}\left(\frac{F-\mu}{\sigma}\right)^2} \qquad (1)$$

where σ is standard deviation, and μ is the mean log fluence. These are obtained from the straight line fit to the data. The probability that during a mission length τ the fluence level will exceed f_p is

$$P(>F,\tau) = \sum_{n=1}^{\infty} p(n,w\tau)\ Q(F,n) \qquad (2)$$

where

$p(n,w\ \tau)$ is the probability of n event(s) occurring during mission length τ if an average of w events occurred per year during the observation period. The probability is assumed to follow a Poisson distribution and is calculated as

$$p(n,w\tau) = e^{-w\tau}\frac{(w\tau)^n}{n!} \qquad (3)$$

This choice of occurrence distribution is somewhat different from that of King who used an extension of the Poisson method introduced by Burrell (1971) to account for the small size of the sample of events available to King. Since our sample consists of over 50 events, we have not used the Burrell extension.

Q(F,n) is the probability that the sum of all fluences due to n events will exceed 10^F. Q(F,1) is the probability that the fluence given by that 1 event which occurred is greater than or equal to 10^F. Q(F,2) is the probability that 2 events occurred and the sum of their fluences is greater than or equal to 10^F. Q(F,3) etc....

The values of Q(F,n) are simulated using a Monte Carlo method. The Monte Carlo program utilizes two subroutines given in Press et al. (1986). One is a random number subroutine which generates random numbers with a uniform distribution in the interval of [0,1]. The other is a subroutine which applies the Box-Muller method of inverse transformation to obtain a Gaussian distribution. The inverse transformed method is discussed in detail in Yost, (1985).

The random numbers are assumed to be the inverse function of p(F) which is defined as:

$$p(F) = \int_{-\infty}^{F} \frac{1}{\sqrt{2\pi}\sigma}\, e^{-\frac{1}{2}\left(\frac{F\bullet\ -\mu}{s}\right)^2}\ dF\bullet \qquad (4)$$

which can be written as

$$p(F) = \int_{-\infty}^{z} \frac{1}{\sqrt{2\pi}} e^{-\frac{1}{2}t^2} dt \qquad (5)$$

where $z = \frac{F-\mu}{\sigma}$

The values of mu and sigma used in equation 4 are those obtained from the straight line fit to the log fluence F distribution. As explained above since the larger fluence events were very important in calculating the total expected fluences, the largest events were given greater weight than the small fluence events in determining the fitted straight line. Generating these random numbers and performing the inverse transformed calculations on them will result a set of numbers that are random samples of the fit to the log fluence F distribution.

The actual simulation of Q(F,n) consists basically of two steps. In step one, N sets of random samples from a Gaussian distribution are generated. N is a large number to ensure the randomness (100000). Each set j is a collection of n random numbers x_i. In step two, each set j is assigned a value of 1 if

$$\sum_{i=1}^{n} \left(10^{x_i * \sigma + \mu}\right) \geq 10^{F} \qquad (6)$$

The ratio of the cumulative numbers of set j with value of 1 over the total numbers of generated sets N is the probability of exceeding fluence f_p due to n event(s). This procedure is repeated to determine the value of each Q(F,n) of interest.

Equation (2) has been evaluated for various mission lengths τ and the result is shown in Figure (4).

Results

The procedure described above has been carried out for the active years of the solar cycle and for various mission lengths. Figure 4 shows the results for energies >10 MeV. This figure gives the probability of exceeding a given fluence level over the life of the mission assuming constant heliocentric distance = 1AU. For estimates of fluence at other heliocentric distances a correction must be made for the radial dependence of fluences. This problem is discussed in the report of the solar cosmic ray working group in this proceedings. Figure 4 shows five mission lengths. In calculating mission length only the time that the spacecraft spends in interplanetary space during solar cycle active years should be included.

In Table 1 we compare our new expected fluences with the King value for a mission length of 2 years. The new fluences are about twice the King fluences at energies >10 MeV. The "confidence levels" should be interpreted as meaning that, if 1,000 two year missions were flown at different times during solar cycle active years then 800 of them (or 950 depending on the chosen "confidence level") would have fluences no larger than the fluences shown in the table. (Of course it would take more than 2,000 years to carry out such a statistical study.) The "confidence level" does not include changes that would come about from using slightly different fits to the observed distribution of event fluences in Figure 3.

Energies with lower bounds greater than 30 MeV have not yet been treated in the new model. Until that work is carried out we suggest using the 10 MeV results and extrapolating to higher energy using the 1972 event as a model. This method of dealing with energies >10 MeV (including >60 MeV and >100 MeV) is unsatisfactory and the new work needed to extend the model properly should be undertaken.

Recommendations

As part of this workshop we have been asked to suggest future work to improve the models.

For protons at 1 AU and for energies >10 MeV studies of long term variations in occurrence frequency of major proton events may result in more secure estimates of the number expected in the future. There is some evidence that the occurrence frequency of major proton events changes with the 88 year cycle and this issue requires further study. The question of where we now are in the 88 year cycle should also be studied (Feynman and Fougere, 1985, Feynman and Silverman, 1987). A second opportunity for improvement may exist in the use of more sophisticated statistical methods. We also suggest that the proton flux model be looked at to see if the incorporation of new more extensive data would improve that model.

Several problems exist in extending proton models to regions other than 1 AU. We are very uncertain as to the radial dependence of proton fluences, especially for major events in which perhaps the fluences and certainly the maximum fluxes are influenced by shocks and other disturbances in the solar wind. The effects of interplanetary propagation on major events should be studied.

Very little observational or theoretical information is known for energies less than 10 MeV. There are at least 2 sources of particles at these energies. One is the low energy tail of the solar particle events and the other is particles accelerated out of the solar wind by shocks. Both sources should be incorporated into proton fluence models if we are to prevent both over or under design.

Acknowledgments:

We thank W. R. Yucker for discussions concerning the 1956-1963 data set.

The research described in this paper was carried out by the Jet Propulsion Laboratory, California Institute of Technology, under a contract with the National Aeronautics and Space Administration. The work of one of the authors (T.P.A.) was supported by NSF grant ATM-83-05537.

REFERENCES

Aarons, J. and S. Silverman, Ed. AFCRL Studies of the November 1960 Solar-Terrestrial Events, AFCRL-62-441, April 1962.

Armstrong, T. A., C. Brungardt, J. E. Meyer, Satellite observations of interplanetary and polar cap solar particle fluxes from 1963 to the present, Weather and Climate Responses to Solar Variations, B. M. McCormac, Ed. Colorado Associated University Press, 1983.

Burrell, V. O., The risk of Solar Proton events to space missions, Proceedings of the National Symposium on Natural and Manmade Radiation in Space, Las Vegas, Nevada, March 1-5, 1971, E. A. Warman, Ed., NASA Technical Memorandum, NASA TMX-2440, 1972.

Fichtel, C. E., D. E. Guss and K. W. Ogilvie, Details of individual solar particle events, Chapt 2 appearing in Solar Proton Manual, Frank B. McDonald, ed., NASA Goddard Space Flight Center, X-611-62-122, Greenbelt, MD, 1962.

King, J. H., Solar Proton Fluences from 1977-1983 Space Missions, Journal of Spacecraft Rockets, vol. 11, No. 6, 1974, pp. 401-408. "NASA Sp-8118, Interplanetary Charged Particle Models (1974)."

Malitson, H. H. and W. R. Webber, A summary of solar cosmic ray events, Chapt 1 appearing in Solar Proton Manual, Frank B. McDonald ed., NASA Goddard Space Flight Center, X-611-62-122, Greenbelt, MD, 1962.

Nelson, W., Applied Life Data Analysis, Wiley, 1982.

Press, W. H., Flannery, B. P., Teuikolsky, S. A., Vetterling, W. T. Numerical Recipes, pp. 192, Cambridge University Press, 1986.

Yost, G. P., "Lectures on Probability and Statistics," LBL-16993, Rev. 84/HENP/3, June 1985.

Yucker, W. R., "Statistical Analysis of Solar Cosmic Ray Proton Dose," McDonnell Douglas Report MDCG-0363, June 1970.

Yucker, W. R., Solar cosmic ray hazard to interplanetary and earth-orbital space travel, 345, Proceedings of the National Symposium on Natural and Manmade Radiation in Space, Las Vegas, Nevada, March 1971, E. A. Warman, Ed. NAST TM2440, 1972.

Table 1. 2 Year Mission (E >10 MeV)

Confidence Level, %	King	New
80	1.3×10^{10}	2.5×10^{10}
95	4.0×10^{10}	7.7×10^{10}

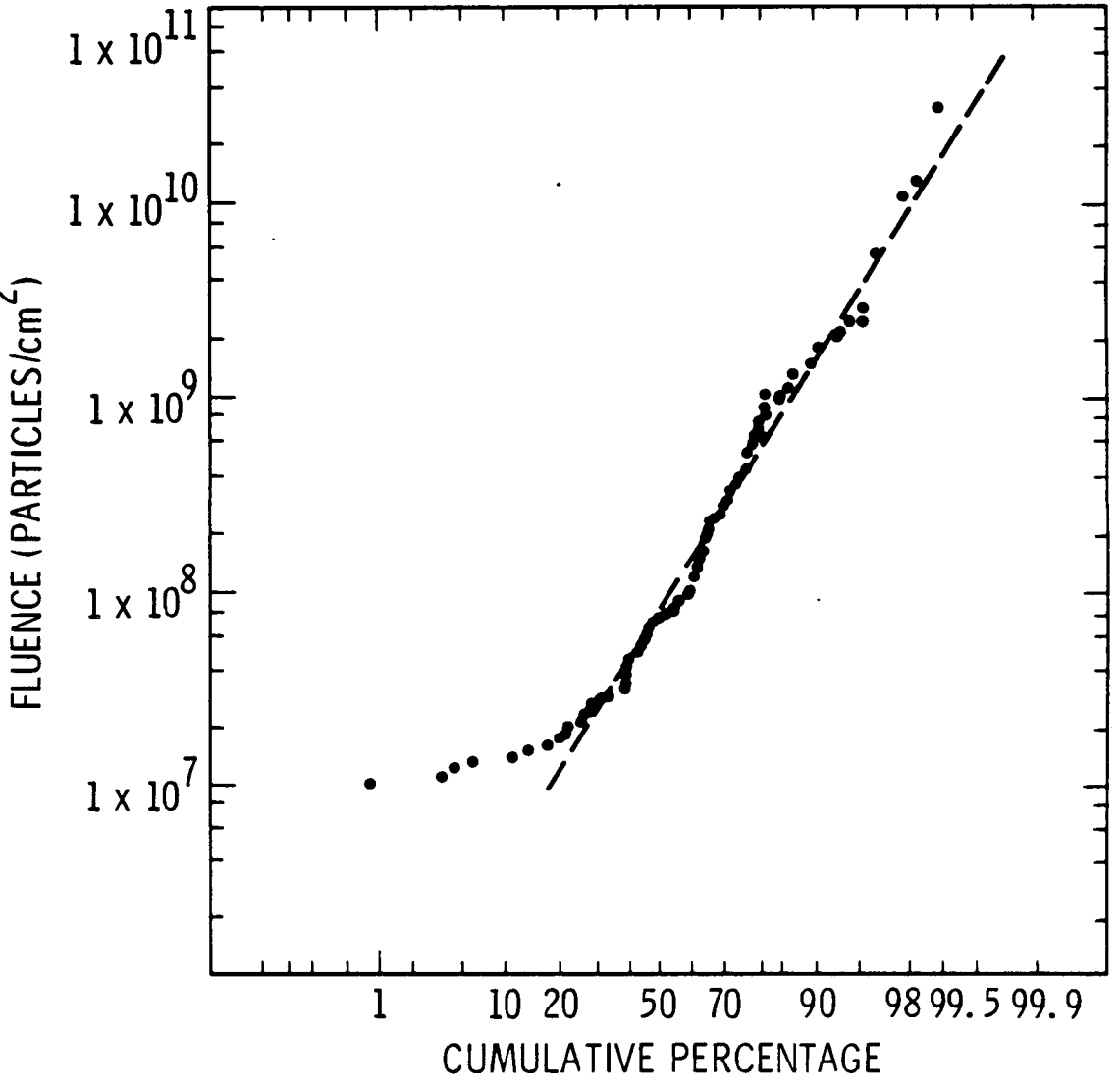

Fig 1 Distribution of fluences for complete data set, 1956-1986, for proton energies >10 MeV.

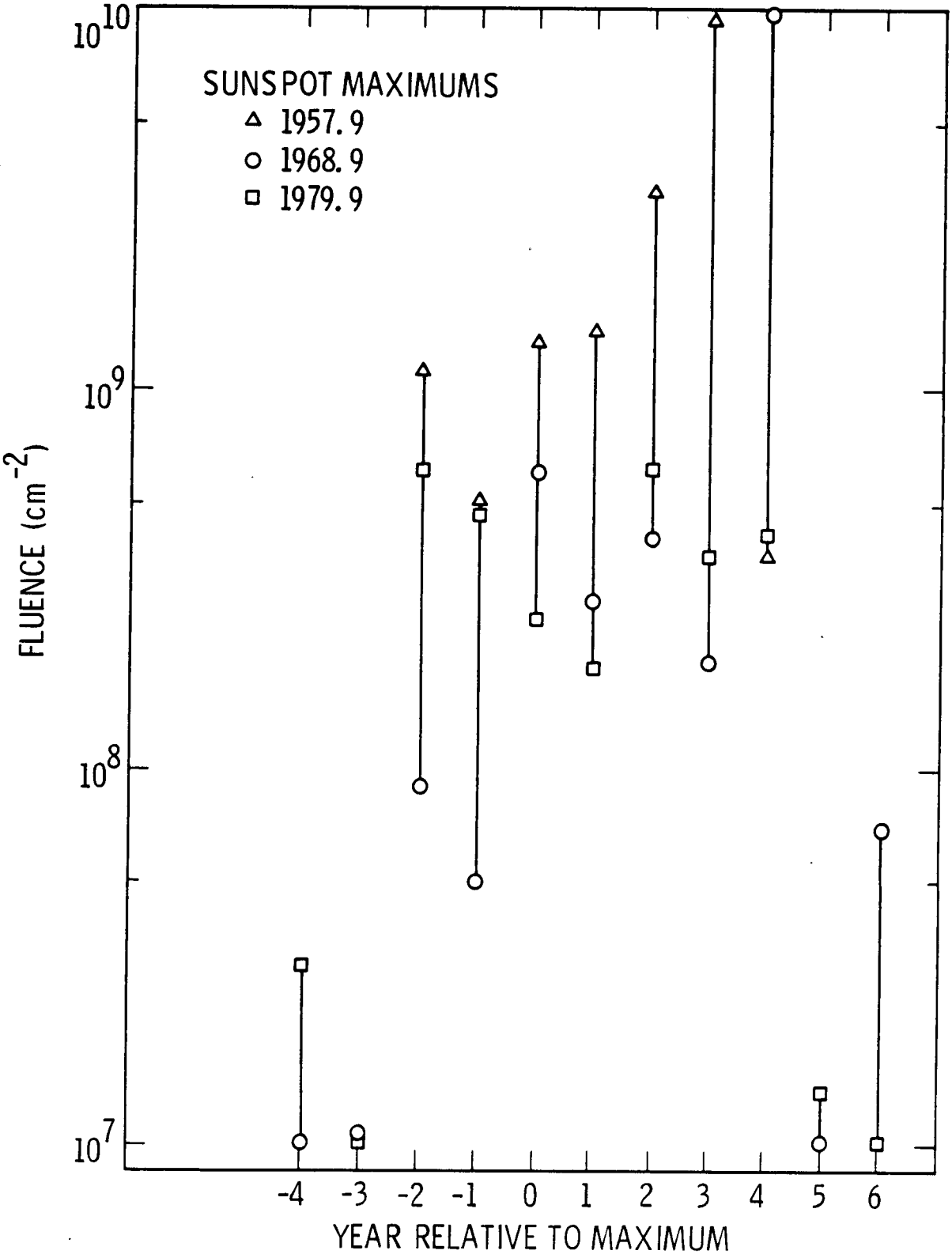

Fig 2 Solar cycle dependence of annual fluences, 1956-1986. See text for definition of "years".

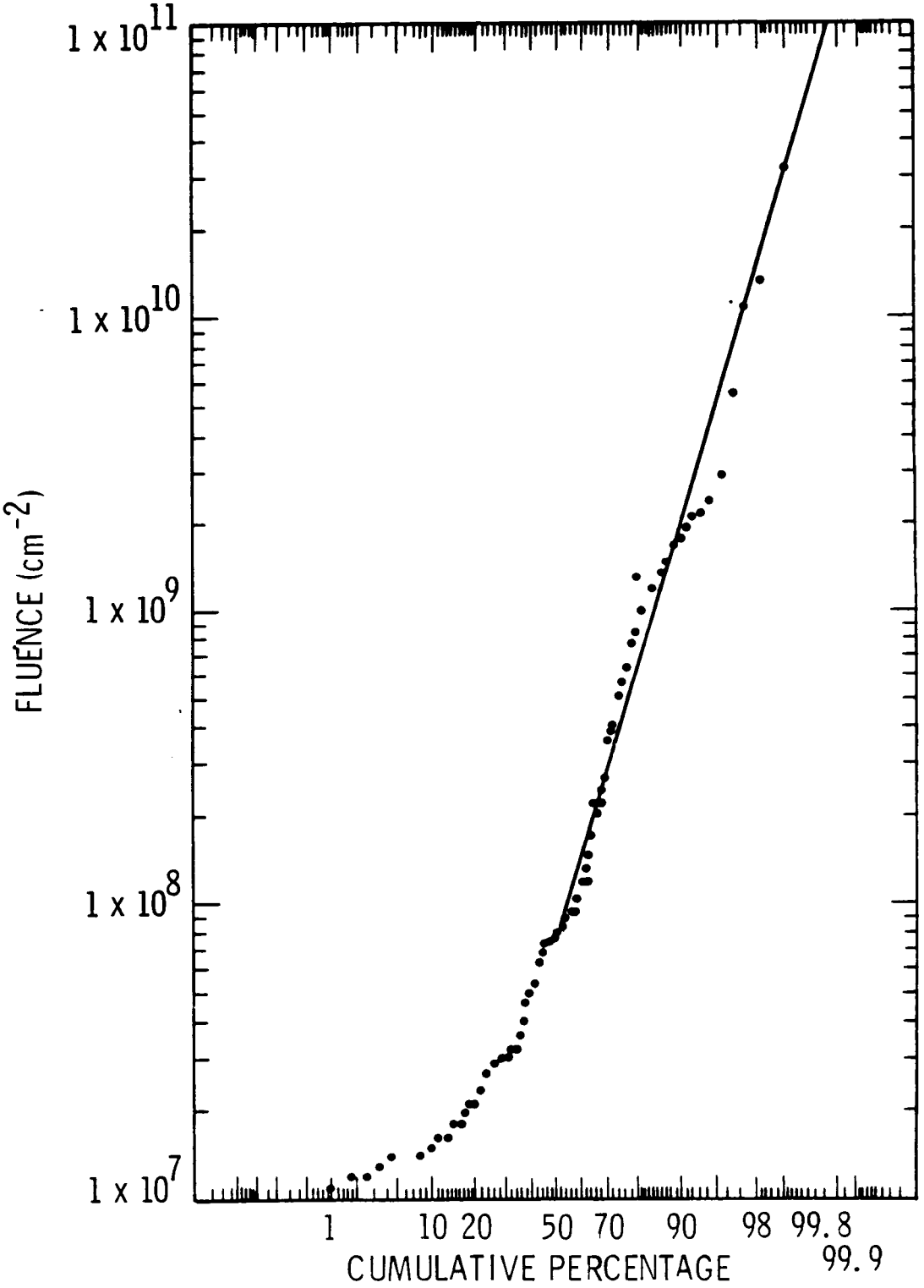

Fig 3 Distribution of fluences for solar cycle active years for proton energies >10 MeV.

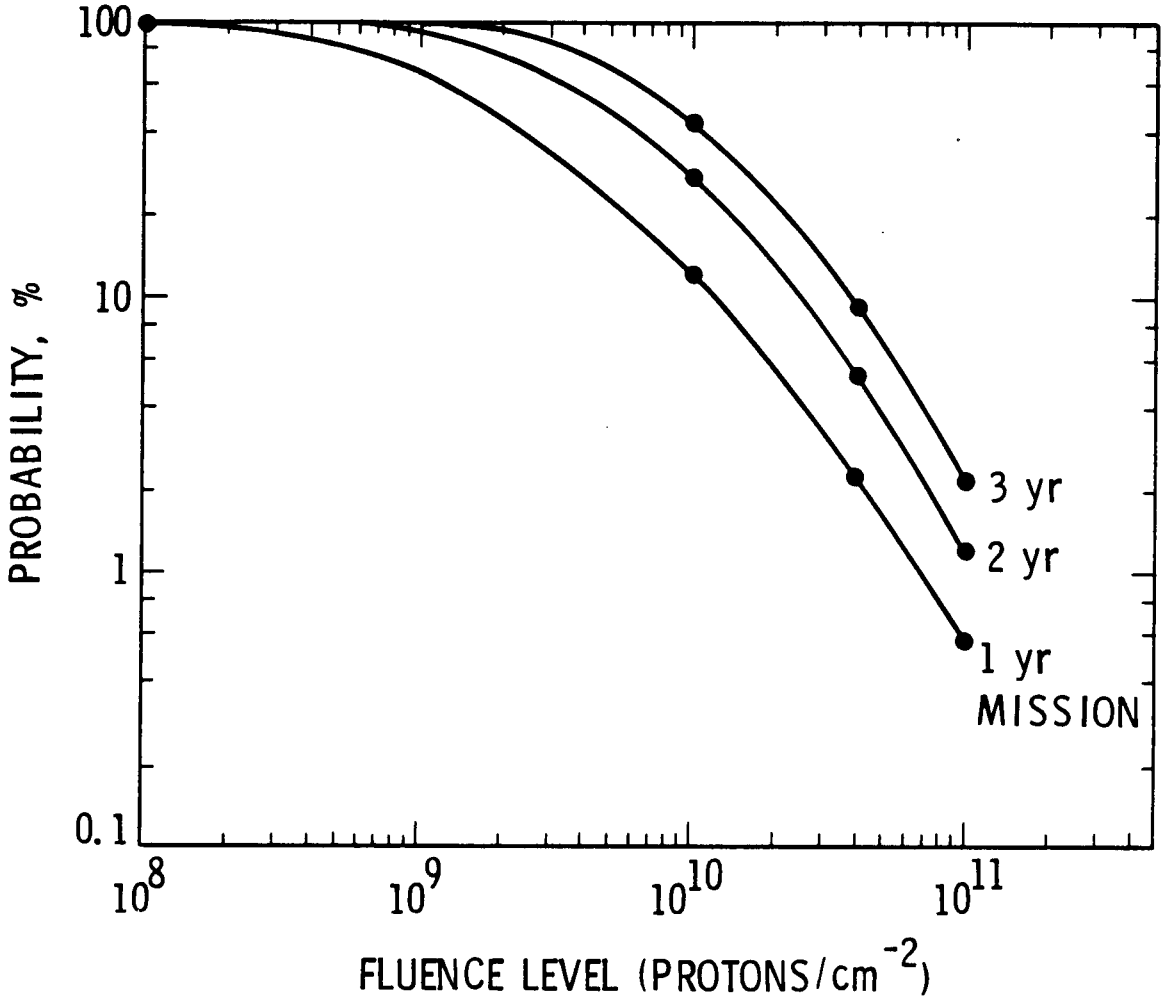

Fig 4 The probability of exceeding selected fluences for different mission lengths for proton energies >10 MeV.

SOLAR PARTICLE EVENTS

INTENSITY/TIME PROFILES OF SOLAR PARTICLE EVENTS AT ONE ASTRONOMICAL UNIT

M. A. SHEA
Air Force Geophysics Laboratory
Hanscom Air Force Base
Bedford, Massachusetts 01731

ABSTRACT

A description of the intensity-time profiles of solar proton events observed at the orbit of the earth is presented. The discussion, which includes descriptive figures, presents a general overview of the subject without the detailed mathematical description of the physical processes which usually accompany most reviews.

1. INTRODUCTION

Major solar flares are often associated with the acceleration of energetic particles at the sun and their injection into the interplanetary medium where they can be detected by a variety of techniques. Only high energy particles could be detected at the earth prior to the space age since the particles had to have enough energy to be able to penetrate to balloon altitudes, or in rare cases, to ground-level detectors. Since the advent of the space era, data obtained from particle sensors on spacecraft throughout the heliosphere as well as improved balloon and ground-based instrumentation have greatly increased our understanding of solar particles and their propagation in the solar system. This paper presents a summary of the intensity/time profiles of particle events as detected at the earth's orbit.

2. SOLAR EMISSIONS

Solar flares are associated with electromagnetic emissions, acceleration of electrons and ions, and, if conditions are favorable, the injection of these particles into space. Each solar flare is unique, and the generation of these emissions can differ from event to event. Figure 1 is a representation of the propagation time of various types of solar emissions from the sun to the earth. Solar X-rays and other types of electromagnetic radiation reach the earth at essentially the speed of light - i.e. in approximately eight minutes. To a first order approximation, the intensity of the radio and soft X-ray emissions observable at one Astronomical Unit is independent of the location of the flare on the visible disk of the sun. Energetic solar particles reach the orbit of the earth from a few minutes, if the particles are relativistic, to hours for the lower energy particles. Both the measured onset time and maximum intensity of these particles are a function of the solar longitude of the flare with respect to the detection location. Enhanced solar plasma usually propagates to the earth within one or two days and can manifest itself by the occurrence of aurora and geomagnetic disturbances, the magnitude of which are dependent upon the interplanetary plasma and field characteristics at the time of the arrival of the plasma at the earth. Figure 2 illustrates the relative time of arrival of solar particle emissions at the earth. Note that the 1-8 Angstrom soft X-ray emission is often detected prior to the recorded onset of the solar flare in H-alpha; this is primarily a difference in the recording sensitivities.

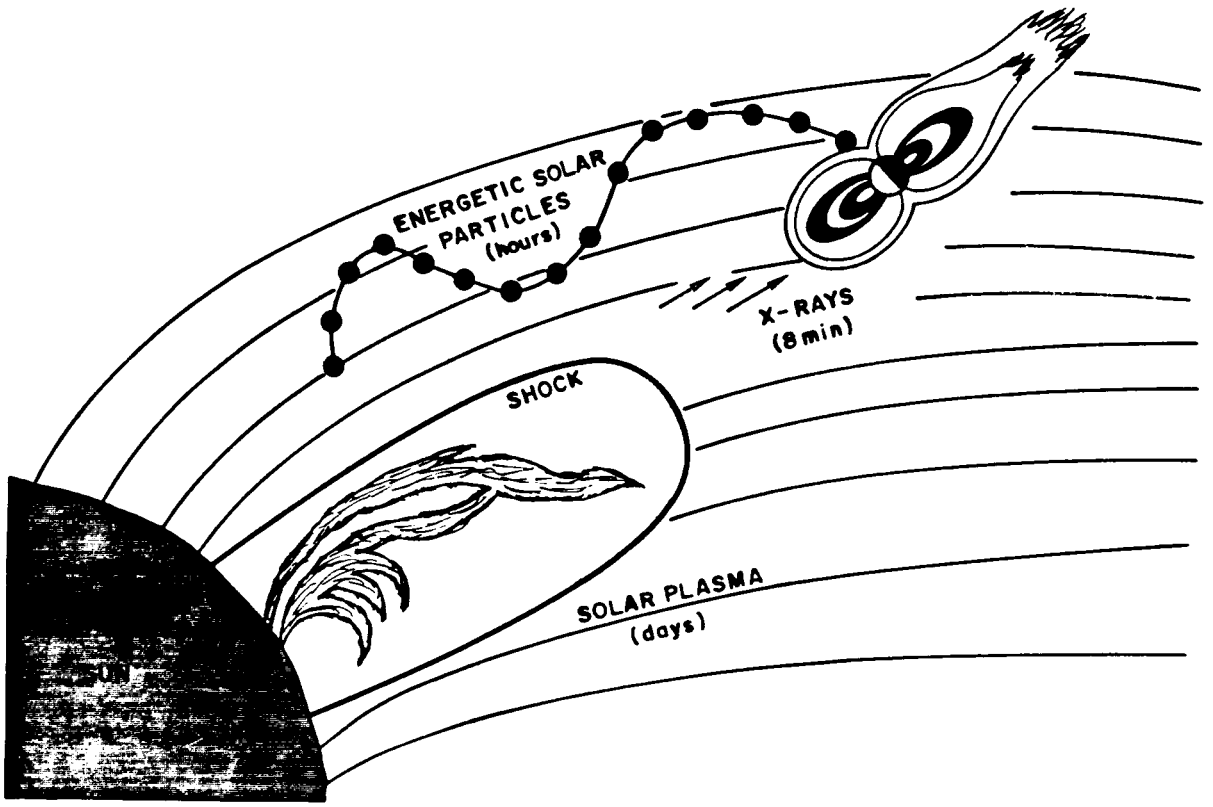

Figure 1. Pictorial representation of energetic particle propagation from the sun to the earth. The relative time scales are noted.

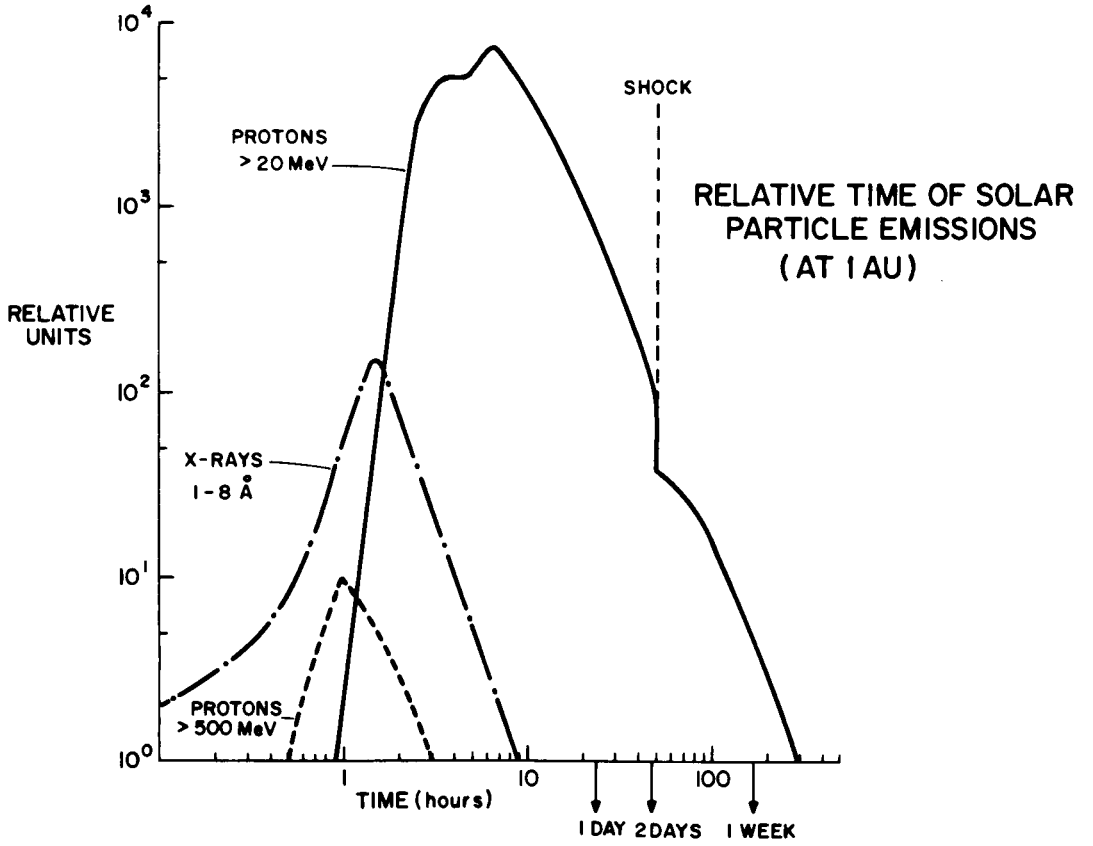

Figure 2. Time scales of solar particle fluxes at 1 AU.

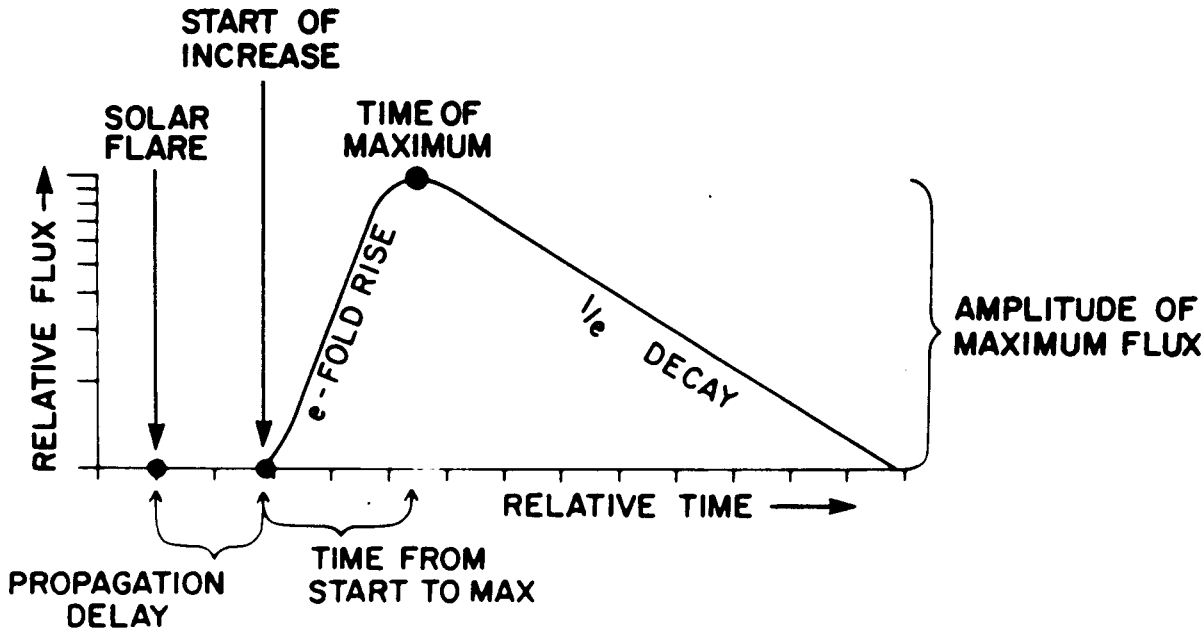

Figure 3. Characteristic solar particle intensity/time scale profile.

Although the general shape of the intensity/time profile, as shown in Figure 3, will differ from event to event and also with respect to the location of the flare on the sun with respect to the location of the detection point in the heliosphere, particle events can be characterized by the following: a propagation delay between the onset of the solar flare in H-alpha emission and the onset of the particle increase; a relatively rapid rise in intensity to a maximum value; and a slow decay to the background level. Although actual event profiles can be complicated by multiple particle injections or interplanetary perturbations, this simplified picture is appropriate for any one isolated event.

3. SOLAR PARTICLE PROPAGATION

The concept of solar particle propagation is discussed elsewhere in these proceedings (Smart, 1988) and will not be discussed in detail here. The essential fact is that solar particles propagate into the interplanetary medium along the interplanetary magnetic field lines. If a solar particle producing flare occurs near the "footpoint" of the interplanetary magnetic field line connecting the earth with the sun (which is nominally around 60° west longitude on the sun), then a detector located along this field line, e.g. the earth, should record the earliest onset time and the highest intensity of any detector located at the same radial distance but at different heliolongitudes. Figure 4 illustrates this favorable propagation path. If a flare occurs at any other solar longitude, the particles which reach the earth are first transported through the solar corona to the interplanetary field line connecting the sun with the earth whereupon they propagate along the field line to the earth.

Figures 5 and 6 illustrate typical intensity/time profiles that would be recorded at one Astronomical Unit from identical flares at different locations on the sun. The intensity/time profile shown on the right side of Figure 5 is typical for a flare that occurred at the "footpoint" of the interplanetary magnetic field line connecting the sun with the earth. Notice the rapid rise to maximum intensity. The particle flux would be maximum along the favorable propagation path (shown by the larger dots) whereas particles that diffuse through the solar corona to other field lines would have a smaller flux (shown by smaller dots).

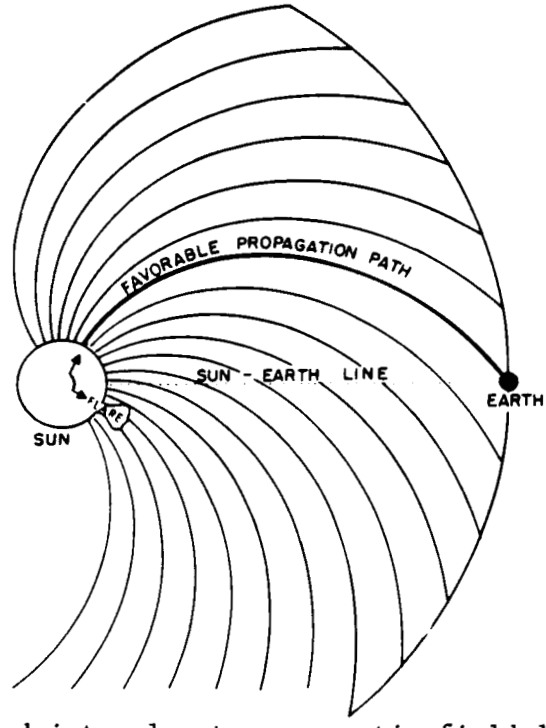

Figure 4. Idealized interplanetary magnetic field line between the sun and the earth with the favorable propagation path indicated.

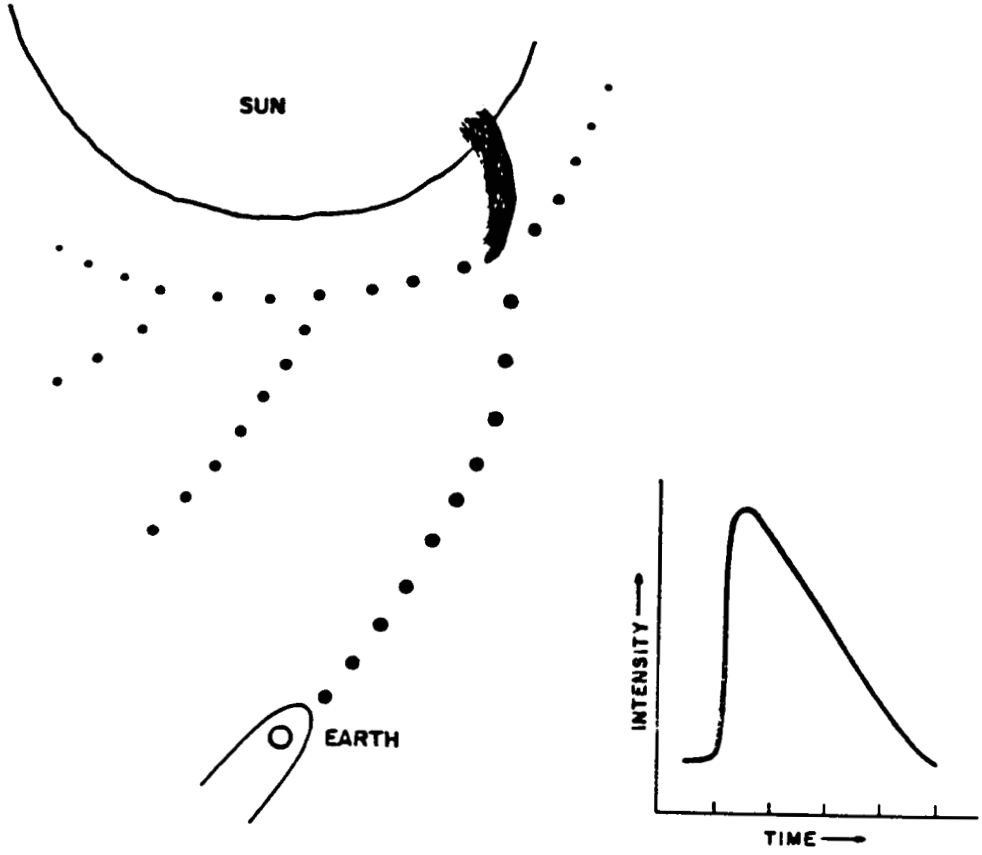

Figure 5. Graphic representation of particle propagation along the interplanetary magnetic field line from the sun to the earth from a solar flare at the "footpoint" of the field line. The larger the dot, the larger the flux. A typical intensity/time profile for this event, as measured at the earth, is shown on the right.

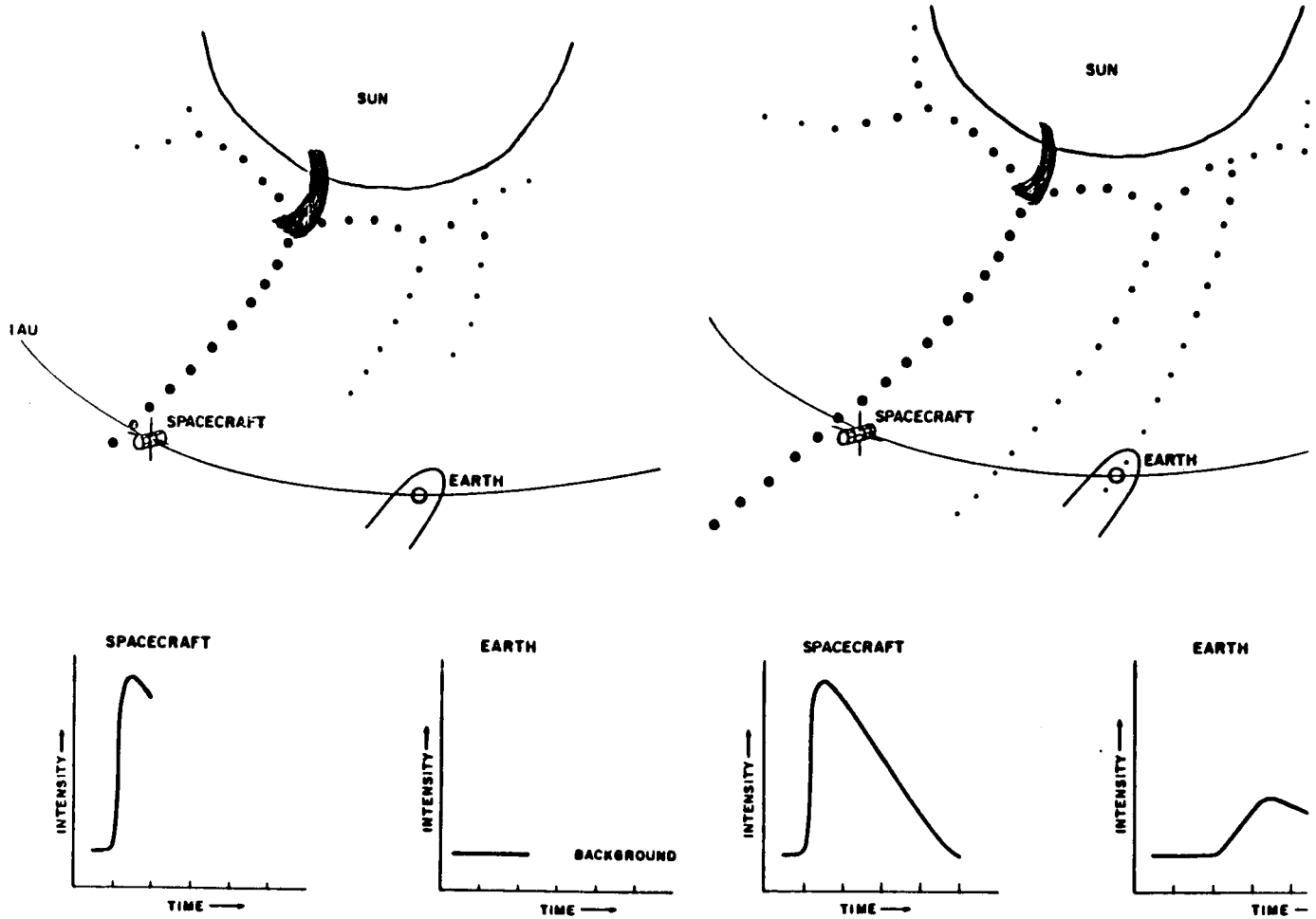

Figure 6. Part A. Solar particle propagation along the interplanetary magnetic field line from a hypothetical flare east of the sun-earth line to a satellite at 1 AU. The larger the dots, the larger the flux. Coronal propagation and particle transport along other field lines are also indicated by smaller dots. The bottom section of Part A on the left side shows the initial intensity/time profile at the spacecraft directly connected to the flare site via the interplanetary magnetic field line; the right side shows coincidental background flux as measured by a satellite at the earth. Part B. Solar particle propagation along the interplanetary magnetic field line and in the inner heliosphere from a hypothetical flare east of the sun-earth line to satellites at 1 AU. The larger the dots, the larger the flux. The bottom section of Part B on the left side shows the intensity/time profile of solar particles for the entire event as measured at the spacecraft directly connected to the flare site via the interplanetary magnetic field line; the right side shows the intensity/time profile of solar particles for the entire event as measured by identical instrumentation on an earth-orbiting spacecraft in the interplanetary medium.

Figure 6 illustrates the particle flux in the inner heliosphere from a flare to the east of the earth-sun line. In Part A the maximum flux (shown by the large dots) would be along the interplanetary magnetic field line from the flare location to the hypothetical spacecraft located at one Astronomical Unit. While particles from this flare are propagating along the field line to the satellite, they are also propagating, albeit with a reduced intensity, through the solar corona to other field lines. Those particles which reach the interplanetary field line connecting the earth with the sun have started to propagate along this field line to the earth; however, as seen from the lower section of this figure the particle intensity at the earth is still at the background level whereas at the spacecraft the maximum intensity has already been measured. The top section of Part B illustrates the particle intensity in the inner heliosphere a few hours later when both the spacecraft to the left, and a hypothetical spacecraft at the earth, would be responding to an enhanced solar particle flux. The lower section of this panel shows the intensity/time profiles which would have been recorded by both spacecraft during this event. The spacecraft at the earth would have recorded a later onset time, slower rise time, smaller maximum flux, and longer decay time than the spacecraft located along the field line connected to the flare site.

At times major flares can populate the entire inner heliosphere with solar particles as illustrated in Figure 7. On 8 and 9 August 1970 particle increases on the Pioneers 8 and 9 space probes together with the small increase on the IMP 5 satellite at the earth could not be associated with any solar activity on the visible hemisphere of the sun; however, Dodson-Prince et al. (1977) noted that active region 10882, which produced particle events on 13 and 14 August 1970, was on the invisible hemisphere of the sun about three days before east limb passage. Since Pioneer 9 had the largest maximum increase on 8 August, and Pioneer 8 had a smaller increase with maximum intensity on 9 August, a possible flare located approximately 40° behind the east limb was assumed to be the source of this particle event. The small increase observed on IMP 5 is consistent with this flare location.

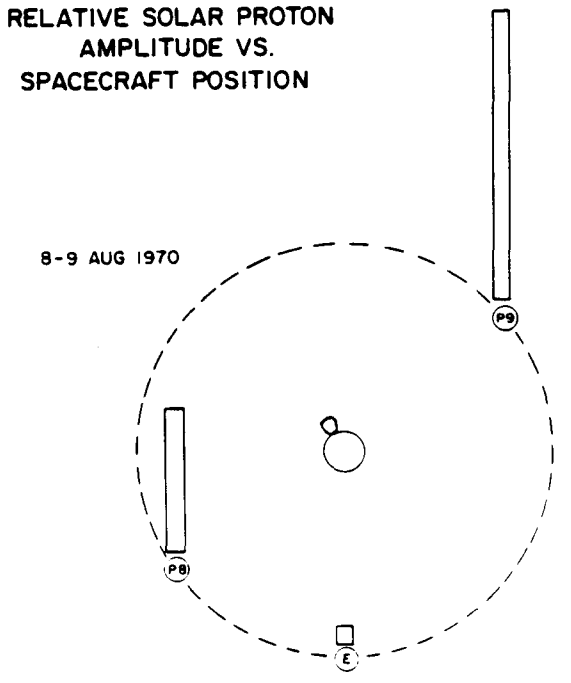

Figure 7. Relative solar particle intensity (on a log scale) as measured on Pioneer 9, Pioneer 8 and IMP 5 (at the earth) for the particle event of 8-9 August 1970. The bars representing the particle flux are placed at the location of the indicated spacecraft. This event has been attributed to a solar flare approximately 40° behind the east limb of the sun. The Pioneer measurements were for particles above 14 MeV; the IMP measurements were for particles above 10 MeV.

4. SPECIFIC EXAMPLES

Figures 8 and 9 illustrate specific examples of intensity/time profiles as measured at the earth during June 1972. Figure 8 shows the particle event on 8 June 1972 as detected on the earth-orbiting Explorer 43. This event exhibited a rapid rise and fast decay associated with a flare to the west of the sun-earth line and possibly close to the west limb. Solar flare observations did not indicate any flare that could be reasonably associated with this particle event. Examination of data from the Pioneer 6 and 10 space probes coupled with the knowledge that an active particle producing region had just rotated over the western limb of the sun led to the assignment of a flare in this region as the possible producer of this particle event (Shea and Smart, 1975).

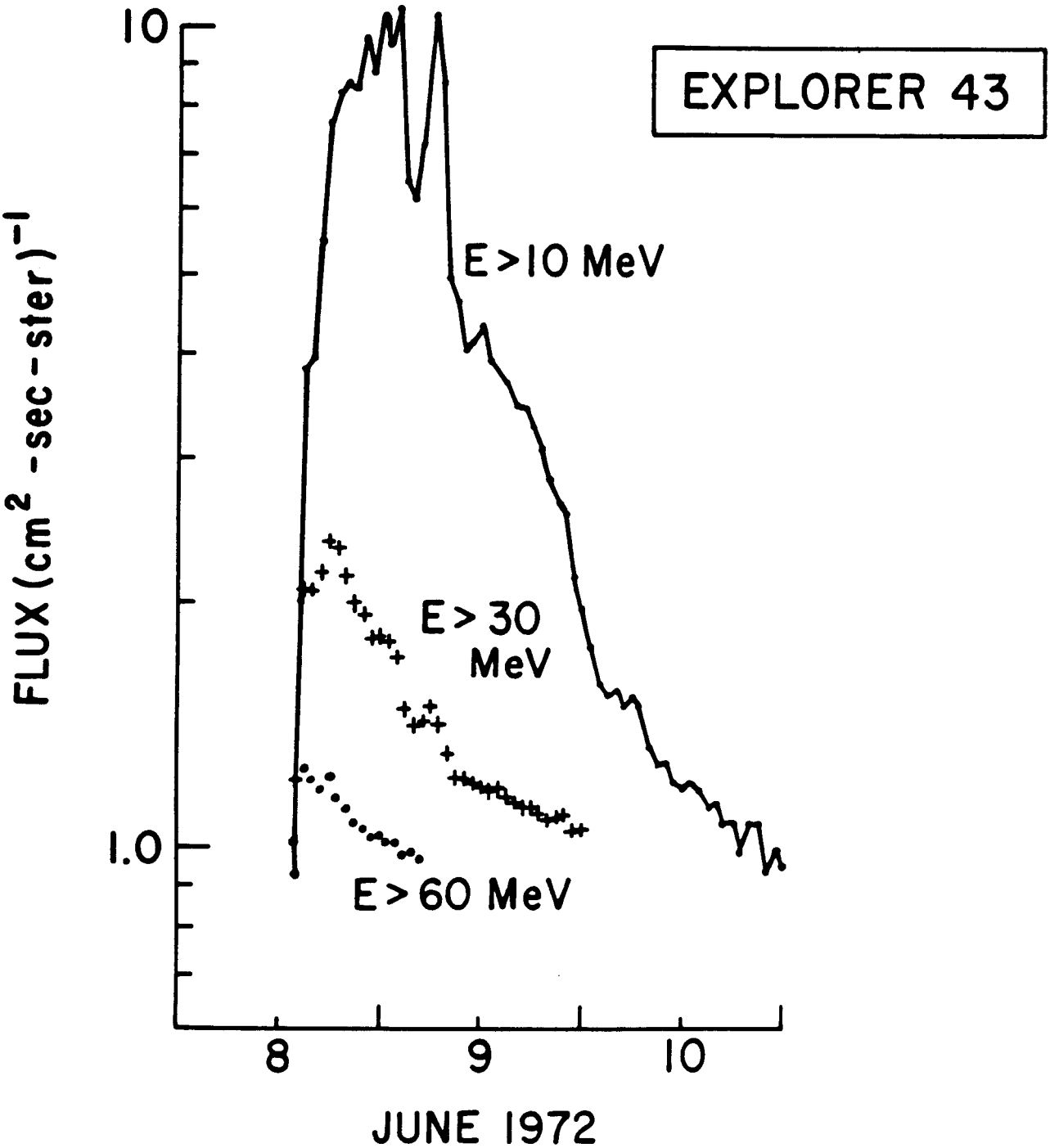

Figure 8. Intensity/time profiles for three proton channels on the Explorer 43 spacecraft for the event with onset on 8 June 1972.

Another particle event occurred later in the same month as shown in Figure 9. There were two possibilities for the solar activity associated with this event - a series of flares near the central meridian of the sun and eastern limb activity which might have been associated with a flare behind the east limb. Because of the large variations in the intensity/time profiles as measured on different spacecraft it has not been possible to associate a specific flare to this event except to assume that more than one solar event on the eastern hemisphere may have contributed to the total flux at the earth. The particle flux profile shown in Figure 9 is indicative of a source region (or regions) to the east of central meridian.

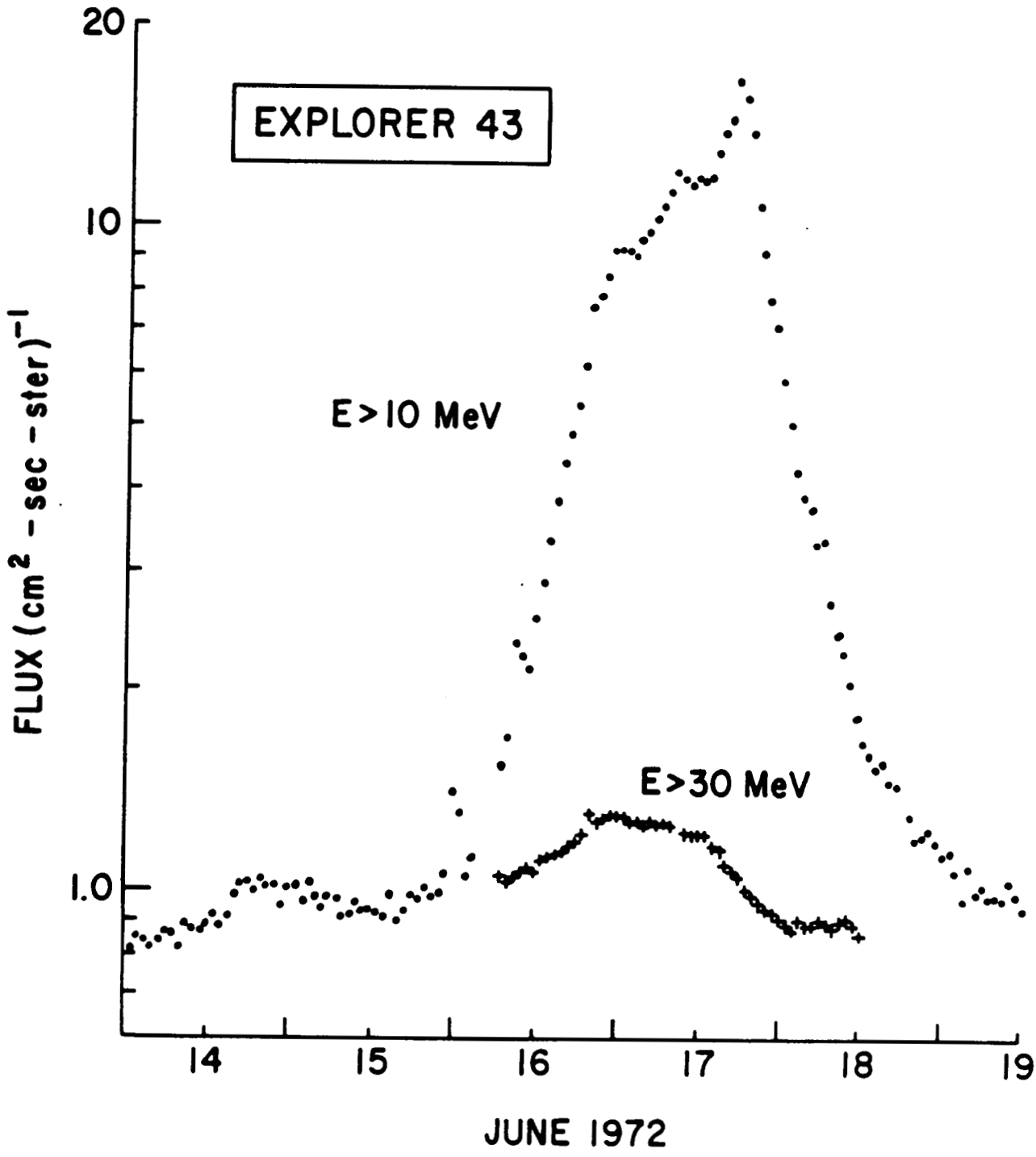

Figure 9. Intensity/time profiles for two proton channels on the Explorer 43 spacecraft for the event with onset on 16 June 1972.

5. DISPELLING POPULAR MYTHS

As in many scientific fields, a certain amount of folklore has been generated which may, or may not, have a factual basis. For example, it is often mentioned that relativistic solar particle events (i.e. the so-called ground-level events) occur on the rising and falling portion of the solar cycle, but not during solar maximum or solar minimum. Inspection of Figure 10 shows that of the 35 relativistic solar particle events between 1956 and 1984, two occurred in 1968 and one in 1979 - both years of sunspot number maximum, and one occurred in 1976 within three months of solar minimum. While most of these events do occur on the rising and falling portions of the solar cycle, a statement that they never occur at solar maximum or minimum is based on mythology.

Another myth which has been dispelled since the era of precise satellite measurements is that solar particle events are always associated with solar flares. First, one should define the term solar particle event which is usually defined as an increase in particle intensity associated with a solar flare. When a specific flare could not be located on the sun in reasonable time association with a particle increase as measured by satellites, a hypothetical flare was often identified as occurring during times of no flare patrol or on the invisible solar disk. With improved resolution of satellite measurements, particle increases have now been associated with disappearing filaments, interplanetary magnetic sector boundary crossings, coronal mass ejections, and acceleration by interplanetary shocks. Although the energies and flux associated with these events are generally relatively small, as shown in Figure 11, there have been exceptions such as the Fermi acceleration of protons to relativistic energies during the August 1972 solar-terrestrial events (Pomerantz and Duggal, 1974).

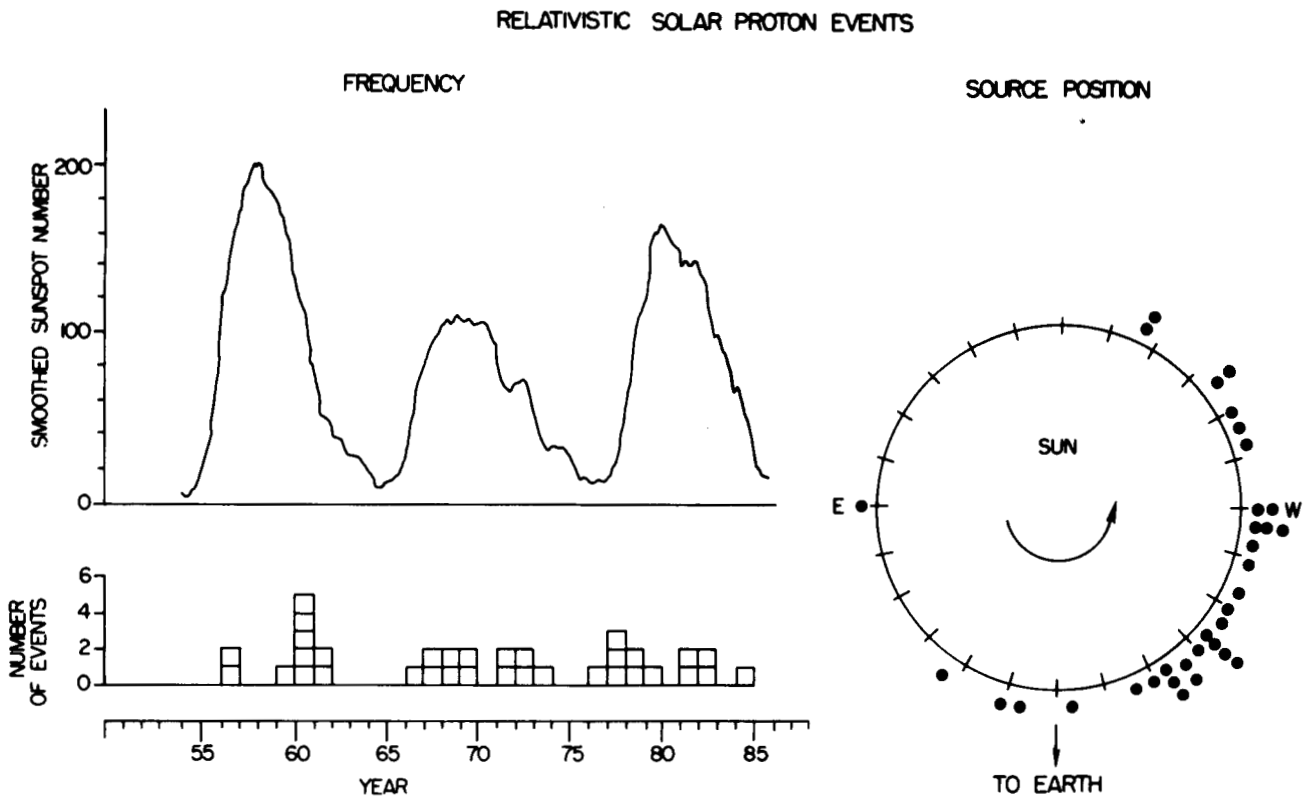

Figure 10. Left Side: Frequency of relativistic solar proton events throughout three solar cycles as shown by the smoothed sunspot number. Right Side: Location on the sun of the flares associated with relativistic solar proton events.

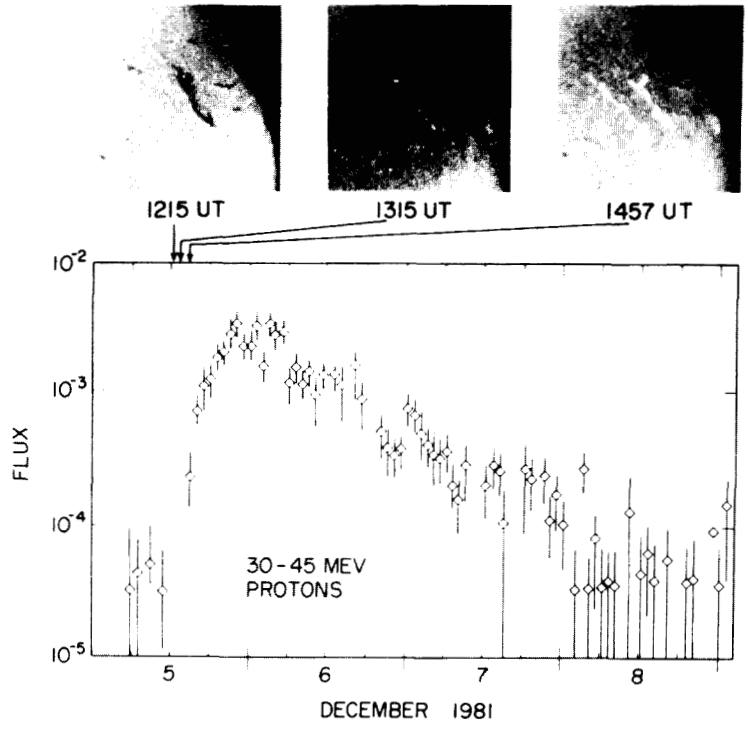

Figure 11. Solar particle increase associated with a disappearing filament on 5 December 1981. (From Kahler, et al., 1986)

6. CONCLUDING REMARKS

Solar particle events can occur at any time in the solar cycle. They come in various sizes and with different intensity/time profiles usually dependent upon the location of the flare with respect to the detection site and the characteristics of the interplanetary medium at the time of the event. There is no guarantee that specific events will or will not occur during a projected mission time frame. The only guidelines that can be given will be generated from statistical studies of ground-based and spacecraft measurements conducted over the past three solar cycles.

REFERENCES

Dodson-Prince, H.W., E.R. Hedeman, and O.D. Mohler, Survey and Comparison of Solar Activity and Energetic Particle Emission in 1970, Air Force Geophysics Laboratory Technical Report, AFGL-TR-77-0222, 1977.

Kahler, S.W., E.W. Cliver, H.V. Cane, R.E. McGuire, R.G. Stone, and N.R. Sheeley, Jr., Solar filament eruptions and energetic particle events, Astrophys. J., 302, 504, 1986.

Pomerantz, M.A., and S.P. Duggal, Interplanetary acceleration of solar cosmic rays to relativistic energy, J. Geophys. Res., 79, 913, 1974.

Shea, M.A., and D.F. Smart, An analysis of the solar particle data obtained during CINOF, in Results Obtained During the Campaign for Integrated Observations of Solar Flares (CINOF), edited by M.A. Shea and D.F. Smart, Air Force Cambridge Research Laboratories Technical Report No. AFCRL-TR-75-0437, 1975.

Smart, D.F., Predicting the arrival times of solar particles, Proceedings of the JPL Workshop in the Interplanetary Charged Particle Environment (this publication), 1988.

Composition of Solar Particle Events

E.C. Stone

(Title Only)

N89-28461

THE RADIAL DEPENDENCE OF THE SOLAR ENERGETIC PARTICLE FLUX

D. C. HAMILTON, Dept. of Physics and Astronomy/Institute for Physical Science and Technology, University of Maryland, College Park, MD 20742 USA

ABSTRACT

We discuss the radial dependence of the peak flux and the fluence of solar flare produced energetic particles under the assumption that they propagate diffusively in the heliosphere.

MODEL

There is considerable evidence that in many cases the propagation of solar energetic particles can be described by Parker's spherically symmetric transport equation which includes the effects of diffusion, convection, and adiabatic energy loss in the expanding solar wind (Parker, 1965).

$$\frac{\partial U}{\partial t} + \frac{1}{r^2}\frac{\partial}{\partial r}\left(r^2 VU - r^2 K_r \frac{\partial U}{\partial r}\right) - \frac{2V}{3r}\frac{\partial}{\partial T}\left(\alpha T U\right) = 0 \qquad (1)$$

where $U(r,T,t)$ = differential number density
V = solar wind speed
K_r = radial diffusion coefficient
T = particle kinetic energy
$\alpha = (T + 2m_o c^2)/(T + m_o c^2)$

The omnidirectional flux is then

$$j = vU/4\pi \qquad (2)$$

where v = particle speed.

Equation (1) has generally been solved under the assumptions that

$$K_r = K_o r^b \qquad (3)$$

where K_o = diffusion coefficient at 1 AU and
r = radial distance in AU.

When the differential number density is expressed as a power law in kinetic energy, $U = U_o T^{-\gamma}$, the explicit energy dependence of (1) can be eliminated. Even with these assumptions, analytic solutions to (1) have been found only for special cases of the radial dependence of K_r:

b = 1 (Fisk and Axford, 1968) and b = 0 (Lupton and Stone, 1973). Therefore (1) is usually solved numerically (Webb and Quenby, 1973; Ng and Gleeson, 1975; Hamilton, 1977; Zwickl and Webber, 1977). Examples of numerical solutions to (1) are shown in Fig. 1.

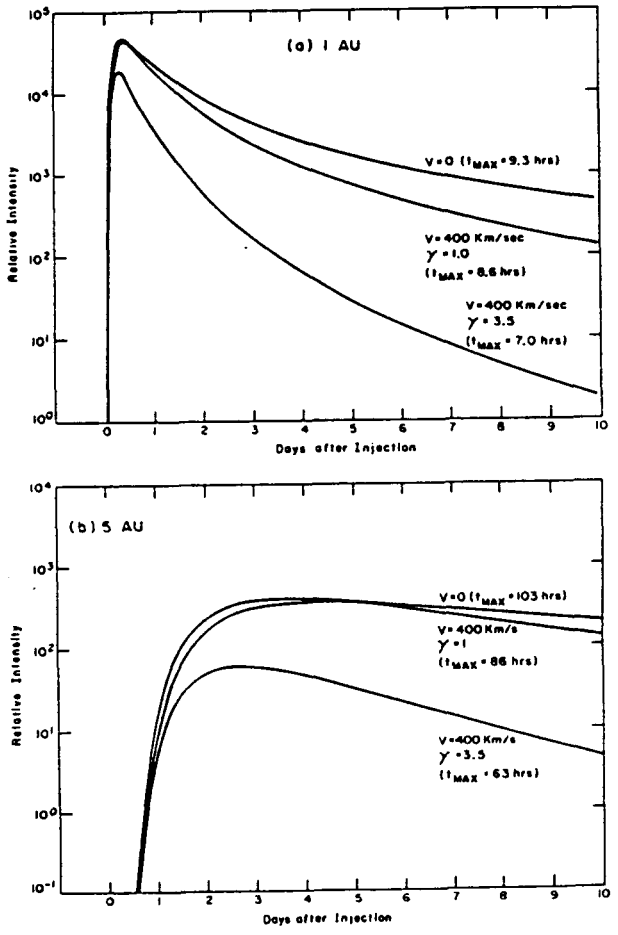

Fig. 1. Intensity-time profiles at (a) 1 AU and (b) 5 AU from a numerical solution of (1) for K_o=1.5 x 10^{21} cm^2/s and b=0.5, values typical for 10 MeV protons. The three curves correspond to diffusion only (V=0), diffusion + convection (V=400 km/s, γ=1.0), and diffusion + convection + adiabatic deceleration (V=400 km/s, γ=3.5). (From Hamilton, 1981).

If the effects of convection and energy loss are removed from (1) (by setting V = 0, for example), then a pure diffusion equation results, and a solution has been given by Parker (1963) for any value of the radial index b. For the case of 3-dimensional space,

$$U(r,t) \propto \left(\frac{1}{K_o t} \right)^{\frac{3}{2-b}} \exp \left(- \frac{r^{2-b}}{(2-b)^2 K_o t} \right) \quad (5)$$

Of interest are the radial dependences of the time to maximum intensity, the maximum flux, and the fluence.

$$t_{max} = \frac{r^{2-b}}{3K_o(2-b)} \quad (6)$$

$$j_{max} \propto r^{-3} \qquad \text{(independent of } K_o \text{ or b)} \quad (7)$$

$$F = \int_0^\infty j(r,t)\, dt \qquad \text{(fluence)}$$

$$F \propto r^{-(b+1)} \quad (8)$$

These analytic solutions to the pure diffusion equation are useful for comparison with numerical solutions to the complete transport equation, but generally they do not agree well with observations of solar energetic particles at moderate energies (< 100 MeV). At these energies the effects of convection and energy loss become important. Including these additional terms reduces t_{max} and produces a more rapid decrease of j_{max} and F with increasing r.

OBSERVATIONS

Observations of solar energetic particles beyond 1 AU have been made with the Pioneer 10/11 and Voyager 1/2 spacecraft. Observations inside 1 AU have been reported from Helios 1/2. We review here the two studies which used simultaneous observations at two or more radial distances to deduce radial propagation parameters.

The power law index b of the radial diffusion coefficient has been determined for several events. Hamilton (1977) analyzed 11-67 MeV protons in solar particle events covering the radial range 1-6 AU. His values for b ranged from 0.3 to 0.5 with the trend towards the smaller value at larger radial distances. Beeck et al. (1987) studied protons and heavier ions over a somewhat lower energy range (0.4-27 MeV/nuc) for two particle events covering the radial range 0.65-1.9 AU. Their value for b ranged from 0.5 to 0.7. In both of these studies, b was deduced by fitting t_{max} at two or three radial distances.

To summarize these results, a value of $b = 0.5 \pm 0.2$ covers all six events studied, with a trend to vary from $b = 0.7$ near 1 AU to $b = 0.3$ near 5 AU. Other observations at larger radial distances

indicate a further reduction to b ≈ 0 or somewhat less by 10 AU (Webber and Goeman, 1979). This variation of b with r of course implies that K_r is not really a simple power law in r. Nevertheless, it is a useful approximation over limited radial ranges.

From (6), we expect $t_{max} \propto r^{1.5}$ for b = 0.5 in the pure diffusion approximation, and this is close to what is observed. The radial dependence of t_{max} is only slightly weaker than this (Hamilton, 1977). Equation (7) predicts an r^{-3} dependence for j_{max}. The solution to (1), on the other hand, gives an $r^{-3.2}$ dependence for parameters typical for 30-67 MeV protons and $r^{-3.3}$ to $r^{-3.5}$ for 11-20 MeV protons depending on the spectral index γ. The more rapid decrease of j_{max} with r results largely from energy loss and thus is more important at lower energies and for larger values of γ.

Hamilton(1977) also studied two events for which the maximum flux fell off more rapidly with radial distance ($r^{-3.8}$ to $r^{-4.0}$). These events were observed in solar wind rarefaction regions in which the flux tube cross section increases more rapidly with r than $\propto r^2$ as is appropriate for 3-dimensional isotropic space. Parker (1963) has shown this more rapid flux tube expansion results in a more rapid decrease of j_{max} with increasing r.

To my knowledge, no observations of the radial dependence of the particle fluence have been reported. To make an estimate we may be guided once again by the pure diffusion approximation. Equation (8) would then suggest a $r^{-1.5}$ dependence for b = 0.5. Including effects of convection and energy loss causes a more rapid decrease. A resonable estimate is $F \propto r^{-2}$ to $r^{-2.5}$.

APPLICABILITY OF RESULTS

The model discussed above applies to a situation of spherical symmetry with istropic diffusion. Ng and Gleeson (1971) have shown, however, that the model (Eq. 1) applies anywhere within the flux tube connected to the flare site even though diffusion parallel to the interplanetary magnetic field is much more rapid than that perpendicular to it.

The particle events selected for the two studies cited above were some of the very few observed when two or more spacecraft at different radial distances have simultaneously been well-connected to a flare site. In most events, the rapid particle intensity decrease away from the best connected field line causes large flux differences at separated spacecraft in addition to any radial dependence. Thus the radial dependences in j_{max} and F cited above will rarely be observed in individual events except for fortuitously located spacecraft. On the other hand, these predictions may be useful on a statistical basis in extrapolating from the large data base collected at 1 AU.

Finally, we note that there are particle events in which there is very little interplanetary scattering, particularly inside of 1 AU

(e.g. Bieber et al., 1980). These "scatter free" events are not described by (1). However for most of the large events in the 1-100 MeV energy range, (1) generally appears to be a good approximation.

This work was supported in part by NASA under subcontract JHU 601620 between The Johns Hopkins University and the University of Maryland.

REFERENCES

Beeck, J., G.M. Mason, D.C. Hamilton, G. Wibberenz, H. Kunow, D. Hovestadt, and B. Klecker 1987. A multispacecraft study of the injection and transport of solar energetic particles. Astrophys. J. 322:1052.

Bieber, J.W., J.A. Earl, G. Green, H. Kunow, R. Müller-Mellin, and G. Wibberenz 1980. Interplanetary pitch angle scattering and coronal transport of solar energetic particles: new information from Helios. J. Geophys. Res. 85:2313.

Fisk, L.A., and W.I. Axford 1968. Effects of energy changes on solar cosmic rays. J. Geophys. Res. 73:4396.

Hamilton, D.C. 1977. The radial transport of energetic solar flare particles from 1 to 6 AU. J. Geophys. Res. 82:2157.

Hamilton, D.C. 1981. Dynamics of solar cosmic ray events: processes at large heliocentric distances (>1 AU). Adv. Space Res. 1:25.

Lupton, J.E., and E.C. Stone 1973. Solar flare particle propagation: Comparison of a new analytic solution with spacecraft measurements. J. Geophys. Res. 78:1007.

Ng, C.K., and L.J. Gleeson 1971. The propagation of solar cosmic ray bursts. Solar Phys. 20:166.

Ng, C.K., and L.J. Gleeson 1975. Propagation of solar-flare cosmic rays along corotating interplanetary flux-tubes. Solar Phys. 43:475.

Parker, E.N. 1963. Interplanetary Dynamical Processes. (New York: Interscience), pp. 214-219.

Parker, E.N. 1965. The passage of energetic charged particles through interplanetary space. Planet. Space Sci. 13:9.

Webber, W.R., and R.A. Goeman 1979. Solar proton propagation characteristics out to 16 AU. Proc. 16th Intl. Cosmic Ray Conf. 5:334.

Webb, S., and J.J. Quenby 1973. A comparison of theoretical and experimental estimates of the solar proton diffusion coefficient during three flare events. Solar Phys. 29:477.

Zwickl, R.D., and W. R. Webber 1977. Solar particle propagation from 1 to 5 AU. Solar Phys. 54:457.

SOLAR PROTON EVENT FORECASTS

G.R. Heckman
NOAA R/E/SE2
325 Broadway
Boulder, Colorado 80303

ABSTRACT

The United States operates a space weather service to provide information on space hazards including solar proton events to federal government agencies and other users who operate systems that are affected by disturbances in the upper atmosphere and interplanetary environment. The observation and prediction of solar proton events has been continuous through solar cycle 21 (1976-1986), establishing a base of experience that can be used in providing similar support to space operations in the 1990's. The observations, indices, alerts, and forecasts used in the service are described in this paper. Also provided is a short summary of the experience obtained from making proton event predictions in solar cycle 21 including the years 1976-1986.

1. INTRODUCTION

Forecasts, alerts and summaries of the salient characteristics of solar proton events are available as part of the real time space environment services provided by the National Oceanic and Atmospheric Administration and the U.S.A.F. Air Weather Service. The two agencies jointly operate the Space Environment Services Center (SESC) in Boulder, Colorado to provide space weather information to operations and missions affected by disturbances in the space environment. The solar proton information is part of a larger set of environmental information including solar flares, solar mass ejections and solar coronal holes, the state of the geomagnetic field, and ionospheric information. The following sections describe the observations, reduced data, alerts, and forecasts that are used in providing solar proton event information.

Solar flares are outbursts of energy that occur sporadically on the sun. They usually (but not always) occur in conjunction with the passage of large sunspot groups across the face of the sun. Flares are associated with areas of enhanced solar magnetic field. At the time of solar flares, the background electromagnetic radiation of the sun may be increased by factors of 1000 or more as measured in visible light, radio noise detectors, and x-ray flux sensors. In fact, the most common methods of scaling the intensity of flares use the increase in visible light or x-rays to assign an importance rating to each flare. Sometimes a flare is followed by an enhancement of energetic particles including protons, electrons, and heavier ions in the interplanetary space near the earth. Such enhancements are commonly called solar proton events since the predominance of the monitoring of the particles has been of the protons. The proton events are of interest to space operations because of the increased radiation exposure to both equipment and people in space. One form of the hazard is the degradation of materials due to increased radiation dose. Another hazard is the upset of spacecraft electronics by the passage of heavy ions through the electronic assemblies. Both the solar flare electromagnetic radiation and solar proton events may interfere with communications with interplanetary spacecraft. Sometimes proton events are observed without a solar flare occurrence. Several possibilities account for such events. Flares may occur beyond the visible limb of the sun, and the particles are guided to the earth by the spiral in the interplanetary magnetic field that connects the earth to the sun, and which is distorted from a radial shape by the rotation of the sun about its north-south axis. Other proton events may be produced by other kinds of solar activity, especially by a phenomenon called solar mass ejection which may occur with or independent of solar flares. Larger proton events are all associated with solar flares, so the flares are used as a precursor to predict the proton event since the propagation time of the particles from the sun to the earth is greater than that of the electromagnetic radiation. The following sections describe the experience of the SESC in observing solar flares and solar proton events, and in using simple models.

2. OBSERVATIONS

In lieu of actual measurements of energetic particle fluxes in the solar wind, the space environment services rely on real time data from satellites in locations where the shielding effect of the earth's magnetic field is minimal for protons with energies above approximately 10 MeV. The fluxes measured and reduced from these satellites are representative of the solar produced fluxes in the interplanetary space at heliospheric longitudes in the vicinity of the earth. Energetic particle observations routinely available to the SESC are summarized in table 2.1.

Table 2.1. Particle observations available to the SESC in real time

Satellite or monitor	Location	Particle type	Energy measured (MeV)	Number of of channels
GOES (1)	Geo	Protons	0.6-500	8
		Alpha	3.8-500	6
		Electrons	>2	1
NOAA (1)	Polar	Protons	.03-215	8
		Ions		1
Thule Neutron Monitor	Geomag-	Protons and ions	>500	1

(1) GOES and NOAA Satellites are operated by the NOAA National Environmental Satellite and Data Information Service and include a set of Space Environment Monitors (SEM).

In the past, arrangements have been made with NASA to obtain real time particle fluxes from any of several interplanetary spacecraft, in order to provide information on energetic particle fluxes in other parts of the solar system. When available, these data have been used by the SESC in assessing conditions and making forecasts. Such cooperation began with the Pioneer 6 spacecraft and continued through the period when International Sun Earth Explorer (ISEE) 3 data was provided to NASA, to the SESC, and thence to the Air Force Global Weather Center in real time. Currently, ad hoc arrangements are made with NASA Operations Centers to obtain special reports from satellites such as the currently operating Pioneer spacecraft.

Other data are available in real time and are used to assess the level of solar activity and to make forecasts of individual solar proton events. These observations are summarized in table 2.2.

Table 2.2. Other observations available to the SESC (1)

Observation	Source	Wavelength
Whole sun x-ray flux	GOES GOES	1-8 Angstrom 0.5-4 Angstrom
Solar chromospheric real time patrol	SOON (2)	Hydrogen-alpha
Solar Radio Noise Patrol	RSTN (3)	606-8800 MHz 8-80 MHz
Solar white light patrol	SOON	
Solar magnetograms	Various	
Geomagnetic indices	Various	

(1) Real time data in the SESC are handled by the Space Environment Laboratory Data Acquisition and Display System (SELDADS), which receives 1100 data sets on a continuous basis from a variety of sources (Cruickshank, et. al., 1988)

(2) The Solar Optical Observing Network (SOON) is operated by the U.S.A.F. in cooperation with the Australian Department of Science and NOAA.

(3) The Radio Solar Telescope Network (RSTN) is also operated by the U.S.A.F. in cooperation with the Australian Department of Science and NOAA.

3. DEFINITIONS

Solar proton events are most generally defined as any increase in fluxes of protons or ions from the sun as measured in the vicinity of the earth. SESC uses a specific definition for a solar proton event in order to simplify communications with users of the service. Real time data displays are routinely available in the SESC and to users for several particle energy thresholds. Alerts of an increase are available for several of these thresholds. Table 3.1 summarizes these definitions and thresholds that are particularly relevant for proton event observation and prediction as of the beginning of solar cycle 22.

Table 3.1. Definitions and thresholds for proton event observation and prediction

Use	Energy threshold or energy range	Flux threshold
Solar Proton Event (definition)	>10 MeV	10 protons cm^{-2} $s^{-1}st^{-1}$
Standard proton displays	>10 MeV flux >30 MeV flux >60 MeV flux >100 Mev flux @ 50 MeV flux @ 10 MeV flux	No threshold; all data displayed
Class X solar flare (definition)	1-8 Angstrom flux	$>10^{-4}$ W m^{-2}
Class M solar flare (definition)	1-8 Angstrom flux	10^{-5} to 10^{-4} W m^{-2}
Standard x-ray displays	1-8 Angstrom flux 0.5-4 Angstrom flux	No threshold; all data displayed

4. SERVICES AVAILABLE

Table 4.1 summarizes the services available from the SESC relevant to the operation of satellites and experiments in space.

Table 4.1 Summary of real time alerts, data, and forecasts for use in space operations

Service	Types of phenomena included
Alerts	Solar proton events Solar flares Solar proton increases at other energy levels Geomagnetic storms Other phenomena
Plots	Standard proton displays
Indices and summaries	Proton fluences Geomagnetic indices Tabulation of solar flares Tabulation of solar mass ejections
Forecasts	Solar proton events Solar flares Geomagnetic indices

5. SOLAR PROTON EVENT OCCURRENCE IN SOLAR CYCLE 22 (1976-1986)

As expected from the classification system, class X flares occur less frequently than class M flares and proton events are even less frequent. Both M and X flares may produce proton events (as defined here) so that the ratio of proton events to flares is the order of a few percent. The operational problem of proton event prediction then becomes primarily a problem of eliminating false alarms. The immediate question when a flare occurs is whether it, as normal, will not produce a proton event or whether it is one of the rarer flares that are followed by a proton event. In solar cycle 21, there were approximately 3300 class M flares, 550 class X flares and 60 proton events. The exact count of events of each type depend on the separation of new events when an earlier one is still in progress.

6. PREDICTIONS OF PROTON EVENTS IN SOLAR CYCLE 21

6.1 Predictions of proton events after a flare occurs

By using characteristics of a solar flare including its electromagnetic radiation and its location on the sun, a more specific prediction can be made of the time and intensity of the proton event. Algorithms for making such predictions were developed during solar cycle 20 (Smart, 1979). The algorithm used in SESC was developed specifically for making radiation predictions for the Apollo lunar missions. It uses observed characteristics of proton events combined with first order models of energetic protons in the interplanetary space (Burlaga, 1967). It was originally oriented to 30 MeV protons but was adjusted to 10 Mev to meet the standard proton event definition that began to be used in 1976. It incorporated the use of soft x-ray emission that was available from the GOES x-ray ionization chambers (Grubb, 1975). The primary assumptions used in the SESC prediction algorithm are summarized as follows (Heckman, 1979):

a. Occurrence of a soft x-ray event is the basis for predicting a proton event.

b. The algorithm predicts a start time, peak flux, a rise time, and a probability of occurrence.

c. The intensity of the proton event is proportional to the peak x-ray flux and type of rise and decay (slow rise and decay is more productive than an impulsive event).

d. The intensity of the proton event is highest when the earth is well connected magnetically to the flare location.

e. The intensity is scaled downward by a factor e^{-1} for each radian the flare is displaced from a direct connection.

f. A history of energetic flares in the region in the 48 hours prior to the most recent flare will increase the predicted event size.

h. The predicted rise time is a minimum of approximately 2 hours for well connected flares and rises to 50 hours for poorly connected events.

Evaluation of the forecasts for cycle 21 has been done in the SESC. For 2180 flares, the forecast was for "no proton event" and no event occurred. In 47 cases, an event was predicted and did occur. In 14 cases, no event was predicted but one did occur. Four of these unpredicted events had a peak flux over 100 protons cm^{-2} s^{-1} st^{-1}, a threshold that would realistically define a proton event for space radiation and spacecraft operational purposes. In the case of a forecast for an event, but where none occurred, 19 times the forecast flux was greater than 100 protons

cm^{-2} s^{-1} st^{-1} but the event did not occur. These numbers indicate the major aspect of proton event occurrence; 96 percent of all flares do not produce a significant proton event at the earth. The first goal of a prediction program is the elimination of these events so they are not treated as false alarms. By using the model, the false alarm rate drops from a 96 percent rate assuming all flares will produce a proton event, to 46 percent false alarms wherein no event occurred when the model had predicted one. The complementary problem is that of missed events (not forecasting one but having one occur anyway). Using the SESC model for solar cycle 21, after a forecast is made for no proton event, less than one percent of the flares actually produced one.

6.2 Forecasts of proton events for one, two, and three days in advance

Since the rise times of proton events are of the order of a few hours, the forecast of an event with longer lead times is more difficult since the responsible flare must also be forecast. SESC does make forecasts of proton events on a longer time scale in the form of a probability of occurrence of a proton event for each 24 hour period in the forecast. The forecasts are analogous to the probability of precipitation in the weather forecasts. Verification of the accuracy of the forecasts indicates they are mostly useful as a guide in identifying periods when proton events may occur, but currently are not of sufficient accuracy for use in specific decision making.

7. ACCESS TO PREDICTIONS AND REAL TIME OBSERVATIONS IN SOLAR CYCLE 22

Mission operators who require support for proton event observations and forecasts can gain access to the SESC services by several methods, depending on the rapidity and level of information that is needed. Table 7.1 summarizes the common methods of accessing the services.

Table 7.1 Access to SESC services for solar proton event information

Services	Method of distribution
Alerts	Telephone call initiated by SESC Receipt of a satellite broadcast from SESC to user's computer system
Proton flux rates	Direct access to SELDADS computer system Receipt of a satellite broadcast
Short term forecasts	Receipt of telephone call from SESC Receipt of a satellite broadcast
Activity summaries	Call to SESC computer bulletin board system Subscription to the "Preliminary Report and Forecast of Solar Geophysical Data" Receipt of daily forecasts and activity summaries distributed over teletype networks
Discussion of current space weather conditions	Call to SESC forecast console and speak to duty forecaster or duty solar technician

To obtain further information, the relevant telephone numbers as of 1988 are given in table 7.2.

Table 7.2 Telephone numbers to call for access to proton event services

Position	Commercial	Federal Telephone Service
Chief Forecaster	(303) 497-3204	320-3204
Duty Forecast	(303) 497-3171	320-3171
SELDADS System Manager	(303) 497-3780	320-3780
Satellite Broadcast Manager	(303) 497-3188	320-3188
Bulletin Board Service	(303) 497-5000	320-5000

8. FUTURE IMPROVEMENTS

As solar cycle 22 progresses into the 1990's, improvements will be added to the SESC proton event services. A new solar patrol instrument that makes images of the sun in x-rays (Solar X-ray Imager (SXI)) will provide improved coverage over present solar flare patrols that currently are blind approximately 20 percent of the time because of bad weather at the ground based observatories. The SXI will also improve observations of events beyond the limbs of the sun and observations of the solar coronal structures that influence the acceleration and release of high energy particles into the solar wind. Particles that contribute to solar proton event fluxes are also accelerated in the solar wind by strong shocks propagating outward from the sun. Instrumentation to detect and measure such shocks would improve the predictions of this aspect of solar proton events. Images obtained by Interplanetary Scintillation telescopes will become available to the SESC in the next few years and may be useful for this detection. Improvements to the prediction routines will also be made which incorporate knowledge gained about energetic particle events over solar cycle 21.

REFERENCES

Burlaga, L.F., Anisotropic diffusion of solar cosmic rays, J. Geophys. Res., 72, 4449.

Cruickshank, C. M., editor, Space Environment Laboratory Data Acquisition and Display System, NOAA Technical Memorandum ERL SEL-76, 1988.

Grubb, R. N., The SMS/GOES Space Environment Monitor Subsystem, NOAA Technical Memorandum, ERL SEL-42, 1975.

Heckman, G. R., Predictions of the Space Environment Services Center, Solar Terrestrial Predictions Proceedings, Boulder, 322-329, 1979.

Hirman, J. W., G.R. Heckman, M. S. Greer, and J. B. Smith, Solar and geomagnetic activity during Solar Cycle 21 and implications for Cycle 22, EOS, 1988, in press.

Smart, D. F., and M.A. Shea, PPS76 - A computerized "event mode" solar proton forecasting technique, Solar Terrestrial Predictions Proceedings, Boulder, 406-427, 1979.

Wagner, W.J., R.N. Grubb, G. R. Heckman, and P. J. Mulligan, The Solar X-ray Imagers (SXI) on NOAA's GOES, Bull. Amer. Astron. Soc., 19, 923.

PREDICTING THE ARRIVAL TIMES OF SOLAR PARTICLES

D. F. Smart
Air Force Geophysics Laboratory
Bedford, Massachusetts, 01731, USA

N89-28463

ABSTRACT

A procedure has been developed to generate a computerized time-intensity profile of the solar proton intensity expected at the earth after the occurrence of a significant solar flare on the sun. This procedure is a combination of many pieces of independent research and theoretical results. Many of the concepts used were first reported by Smart and Shea (1979) and are summarized by Smart and Shea (1985). Extracts from the general procedure that relate to predicting the expected onset time and time of maximum at the earth after the occurrence of a solar flare are presented.

1. CONCEPTS INVOLVED

Solar energetic particles are assumed to be accelerated in solar active regions from the available coronal material during solar flare events. After the initial acceleration there may be further acceleration of the energetic particle population that interacts with shocks, but these subjects are beyond the scope of this paper. The X-ray, radio and optical emissions during the solar flare event are the indicators (perhaps secondary manifestations) that proton acceleration is occurring. The solar protons emitted from the inner solar corona at a "favorable" position may intercept the earth. In organizing solar energetic ion data it is very useful to use the gross features of the interplanetary magnetic field topology illustrated in Figure 1 (see Roelof; 1973, 1975, 1976; Roelof and Krimigis, 1973; Reinhard et al., 1986) which is determined by the solar wind outflow and the rotation of the sun.

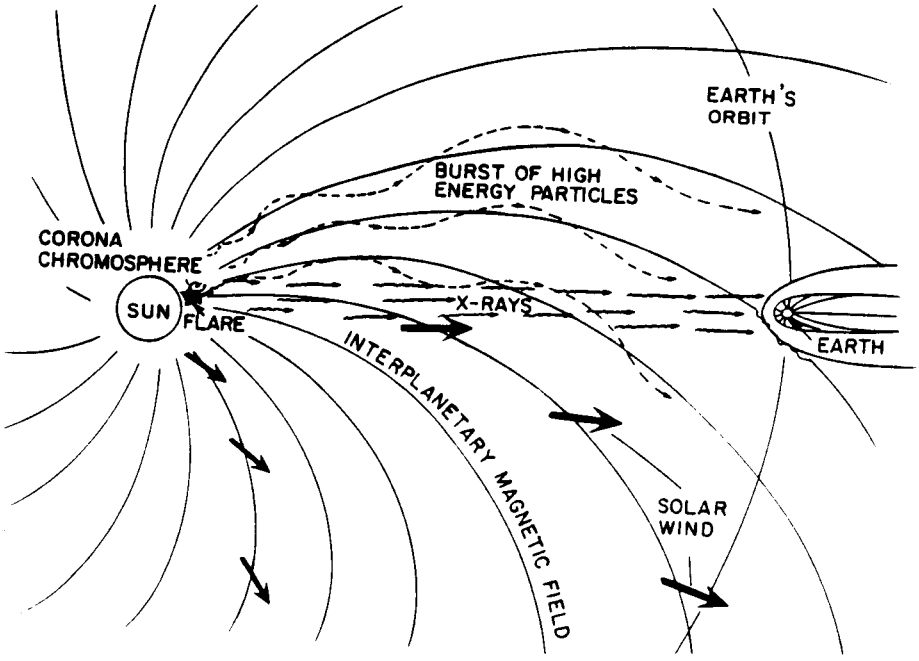

Figure 1. Illustration of the sun and the gross characteristics of the idealized structure of the interplanetary medium.

Once the solar flare accelerated energetic ions arrive at the earth, we can generalize the characteristics of the time-intensity profile observed at any energy above the solar wind domain as illustrated in Figure 2. First there is a propagation delay from the time of the solar flare until the first particles are observed at the earth. After the initial onset of particles, there is a rise in the solar proton flux until a maximum flux is observed, and after the time of the maximum solar proton intensity, there is a slow general exponential decay of the particle flux to background levels. The shape of an individual event may be distorted by features which happen to be present in the interplanetary medium at the time of the solar particle event, and the decay of the solar particle event may be further disturbed by travelling interplanetary shocks, but the general features are always recognizable.

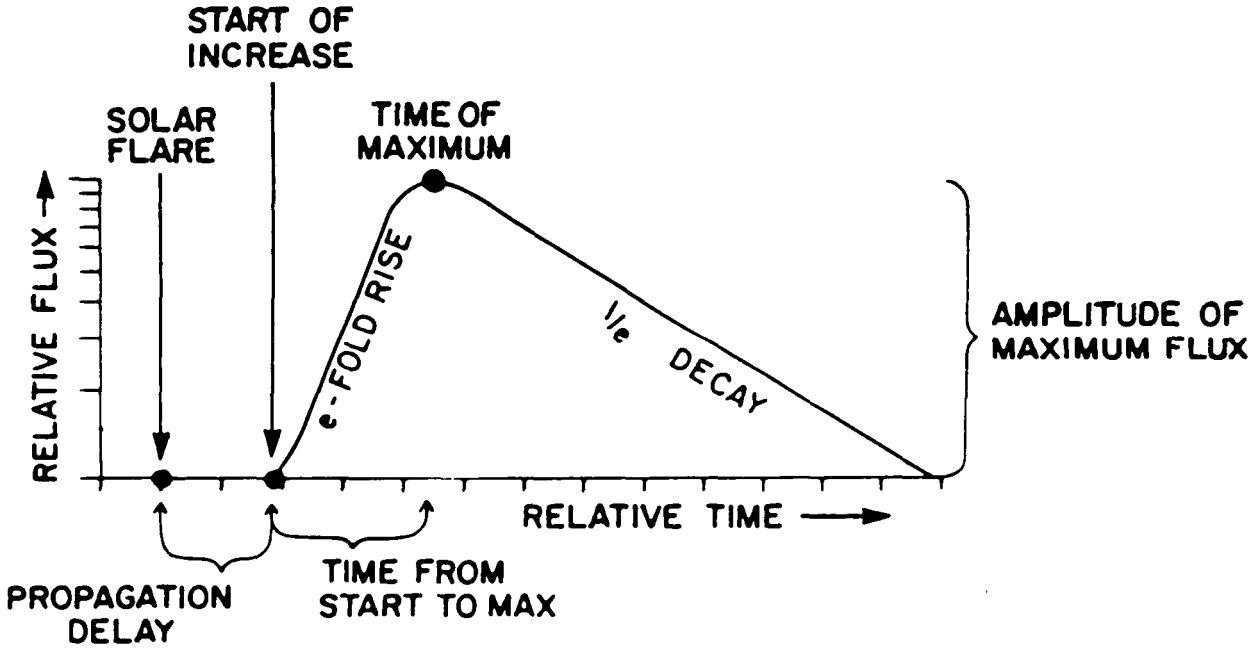

Figure 2. Illustration of the general characteristics of solar proton events.

2. SOLAR PARTICLE PROPAGATION TO THE EARTH

From examining the solar proton data acquired during the past three solar cycles, we can generalize and separate the propagation of solar protons from the flare site to the earth into two distinct and independent phases. The first phase is diffusion from the flare site through the solar corona to the "foot" of the Archimedean spiral path formed by the interplanetary magnetic field line between the sun and the earth. The maximum possible flux is presumed to be at the solar flare site and it is further assumed that there is a gradient in the solar corona extending from the flare site. This gradient attenuates the maximum particle intensity as the angular distance from the flare site increases. The second phase is the propagation in the interplanetary medium from the sun to the earth along the interplanetary magnetic field lines. Both of these phases are illustrated in Figure 3.

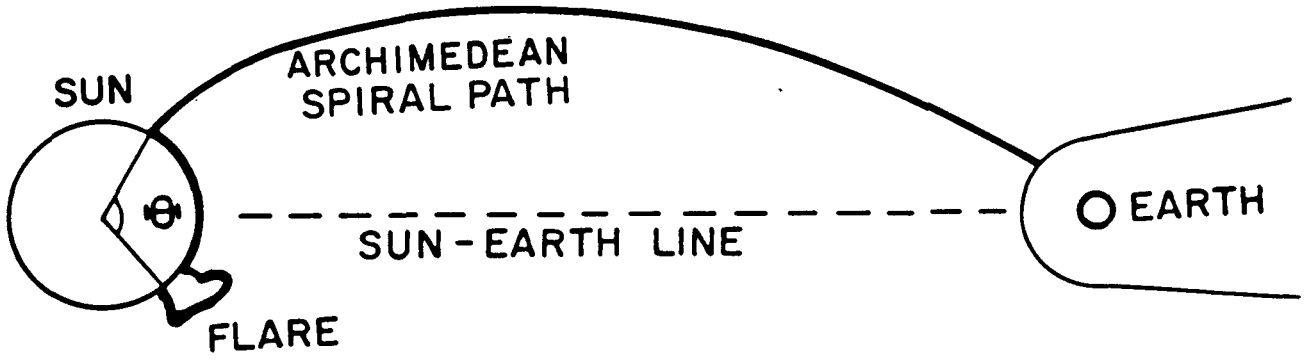

Figure 3. Illustration of the propagation concept. The coronal propagation distance is illustrated by the heavy arc on the sun. Interplanetary propagation proceeds along the interplanetary magnetic field lines which for a constant speed solar wind forms an Archimedean spiral path from the sun to the earth.

2.1 Propagation in the Solar Corona

The concepts we have used for the propagation of solar protons in the solar corona are similar to those originally advanced by Reinhard and Wibberenz (1974). We make very few assumptions as to the manner of coronal transport except that some stochastic processes dominate the particle transport between their source at the flare site and their release point along an interplanetary magnetic field line. In this context we take the fundamental elements of solar particle diffusion theory as developed by early researchers (e.g., Reid, 1964; Axford, 1965; Krimigis, 1965; Burlaga, 1967) and assume that almost all of the major diffusive effects occur in the solar corona. For events observed at the earth, the distance the solar particles travel in the solar corona from the presumed source (i.e. the solar flare site) to the foot of the Archimedean spiral path from the sun to the earth is designated by the symbol Θ.

We assume that coronal propagation is a function of Θ. From diffusion theory we would expect it to be proportional to Θ^2. (See Wibberenz (1974) for a discussion of diffusion theory relating to coronal propagation.) For large values of Θ the propagation delay time to the earth is dominated by the coronal diffusion rather than interplanetary propagation. Some of the early satellite observed data containing onset times of particle events at the earth are those of Barouch et al. (1971), and Lanzerotti (1973); later data sets tend to confirm the general trends noted by the earlier investigators. When these data sets are organized in a heliographic coordinate system they show that the minimum time from the flare onset to particle detection at the earth occurs in a broad range of heliolongitudes around 60 degrees west of central meridian and that the longest times between the associated flare and the onset of particles observed at the earth are for eastern heliolongitude flares.

The distribution of onset times expected for 30 MeV protons for nominal solar wind speeds is shown in Figure 4. The data points shown on the figure are taken from Barouch et al. (1971) and indicate typical variations that may be expected. The minimum in the figure corresponds to a flare at the "foot point" of the Archimedean spiral path between the sun and the earth (57 degrees west of central meridian). To our prejudiced eye, a reasonable fit to the onset data at any specific energy has the functional form of $4\ \Theta^2$.

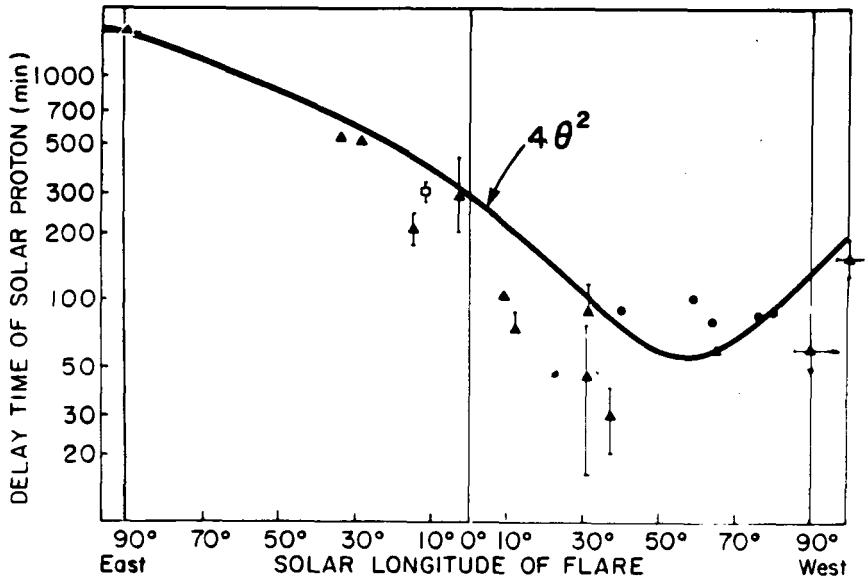

Figure 4. Distribution of onset time of 30 MeV protons observed at the earth as a function of solar longitude. The data points are the measurements of Barouch et al. (1971)

2.2 Propagation in the Interplanetary Medium

After the particles propagate through the solar corona and are released into the interplanetary medium, they essentially propagate along the interplanetary magnetic field lines. During this phase of their propagation we assume that their mean free path length is of the order of 0.1 to 0.3 AU. We make the simplest possible assumptions regarding transport in the interplanetary medium as follows:

a. The particles travel essentially along the interplanetary magnetic field lines with a velocity which is a function of the particle energy.
b. Diffusion perpendicular to the interplanetary magnetic field is assumed to be negligible.
c. The minimum distance to travel from the sun to the earth is the distance along the Archimedean spiral path. The length of the Archimedean spiral path can be obtained by integration of the polar form of the Archimedean spiral equation.

The minimum interplanetary propagation time will be for particles that essentially travel along the interplanetary magnetic field lines with very little scattering, so for scatter free onsets the propagation time from the sun to the earth will be the distance traveled (i.e. the length of the Archimedean spiral path), divided by the particle velocity. After the initial onset it is reasonable to expect that some scattering has taken place and that some aspects of diffusion theory are applicable. The time for the propagation of any specified ion along this path is merely the Archimedean spiral path distance divided by the velocity which is determined by the kinetic energy of the ion. Almost all theories involving differential transport show that the time of maximum is proportional to the square of the distance traveled. (See Wibberenz, 1974.)

The distribution of the observed time of maximum as a function of heliolongitude is illustrated in Figure 5. The data points are from Van Hollebeke et al. (1975) and show the typical range of variations that can be expected. The minimum in the curve corresponds to a flare at the "foot point" of 57 degrees for the Archimedean spiral path between the earth and the sun computed from a nominal solar wind of 404 km/sec. Other data sets (e.g., Reinhard and Wibberenz, 1974) can be plotted in this manner and illustrate the same general characteristics.

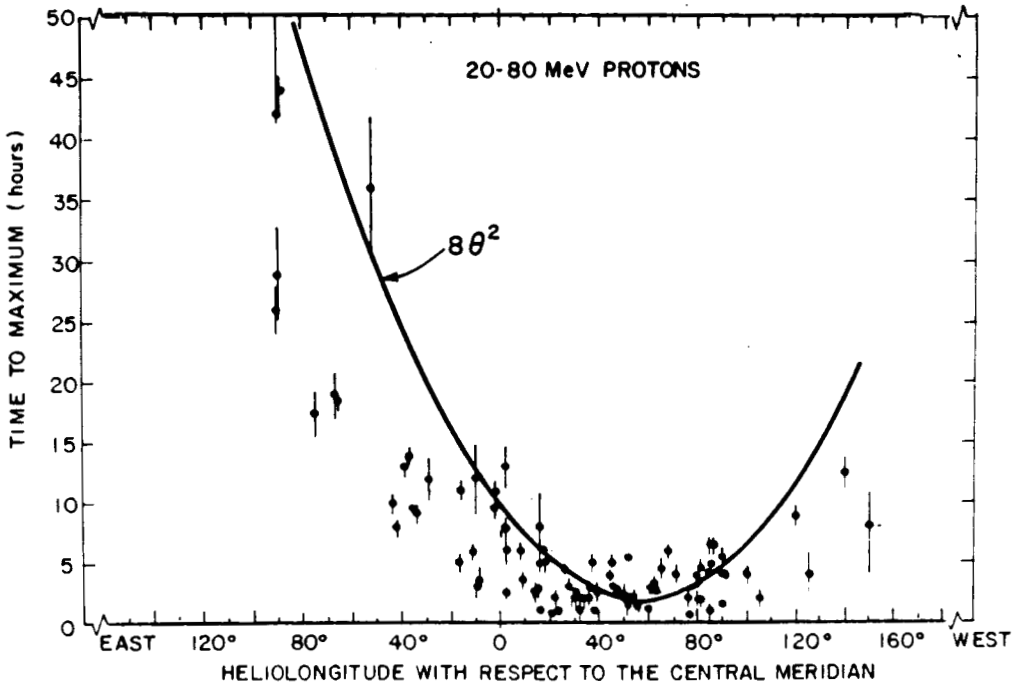

Figure 5. The time from onset to the maximum 20 - 80 MeV proton flux as a function of the heliolongitude of the associated solar flare. The data points are from Van Hollebeke et al. (1975) and the (heavy solid line) is the 8 Θ^2 curve for a nominal solar wind speed.

As a result of diffusion in the solar corona from the flare site to the "foot" of the Archimedean spiral, and the inherent assumption that some stochastic processes are operating, we would expect that there is a solar particle gradient existing in the solar corona such that the proton intensity decreases as a function of distance from the flare site. There is some observational evidence for the existence of such a gradient (Gold et al., 1975; McCracken and Rao, 1970; Roelof et al., 1975; McCracken et al., 1971; Roelof, 1976). The observational evidence suggests that the gradient may vary from case to case. We assume that the gradient from the presumed particle source (i.e. the flare location) to the release point of solar protons observable at the earth (i.e. the "foot" of the Archimedean spiral of the interplanetary magnetic field line between the earth and the sun) is a factor of 10 per radian. Therefore, an observer at one astronomical unit who is connected via the interplanetary magnetic field line to the heliographic longitude of the flaring region would observe the maximum possible particle intensity. An observer whose interplanetary magnetic field connection is at a distance of Θ from the flaring location would observe a flux that has been attenuated by propagation through the coronal gradient over the heliocentric distance in the corona between the flare position and the solar equatorial longitude of the foot point of the Archimedean spiral path from the sun to the earth.

2.3 Event Decay

The decaying portion of the event can be modeled after the principles of collimated convection (Roelof, 1973). After making a number of simplifying assumptions (some of which are that the particle flux can be represented by a simple power law, the anisotropy of the particle flux is small, the magnitude of the interplanetary magnetic field falls off as r^{-2}, and that the particle flux gradient is field aligned and small), a 1/e decay constant can be derived which is a function of the distance along the Archimedean spiral path, the solar wind velocity, and differential energy spectral exponent.

3. HEAVY ION EVENTS

The same principles involved for organizing and estimating the proton (ions with Z=1) arrival and time-intensity profiles are also applicable to heavy ions. These data are conveniently organized by kinetic energy or momentum per unit charge (particle rigidity). It is reasonable to assume that the same principles of coronal propagation and interplanetary propagation apply to all ions independent of the mass or atomic charge. There is a major problem in anticipating the flux or fluence in finding a simple common factor for the elemental abundance ratios. There have been a number of papers reporting the variation of the elemental abundances in solar particle events; see Lin (1987), Mason (1987), and Shea (1987) for recent reviews. A general summary may be that "small" events may have the greatest variability in elemental composition. The elemental abundance ratios seem to have a slight variation according to the energy of the measurement. This may be a reflection of the "size" of the particle event since small particle events would not have many heavy ions at high energies. The hydrogen to helium ratios are the most variable even for "large" events; the heavier elemental abundance ratios seem to be in general agreement with the ratios expected from normal coronal material organized by the first ionization potential. Unfortunately, most of the solar particle data currently available are for protons. So as an expediency, it is required, at least as an interim measure, to estimate the probable heavy ion fluence from the observed or expected proton fluence, except for the relatively few recent cases where the heavy ion flux data have been measured by spacecraft. A table of solar particle element abundance ratios normalized to hydrogen is presented in Table 1.

4. EXTRAORDINARY SOLAR PARTICLE EVENTS

In a discussion of the expected solar particle environment, there is always some discussion of the extraordinary solar particle event or a worst case model. The view of this author is that the extraordinary event, such as the August 1972 sequence of events, is the result of a sequence of occurrences which contribute to the unusually large effect. The 4 August 1972 solar particle event is an outstanding example. This is a sequence of strong converging interplanetary shock structures and a large solar particle event. The extraordinary flux of solar particles observed on 4 August 1972 was the result of a large injection of solar particles from a 3B solar flare at 0413 UT into a region of space where the converging interplanetary shock structures re-accelerated what was a substantial solar particle population into an extraordinary solar particle population. (See Lee (1988) for a more detailed discussion of shock acceleration.) The solar proton time-intensity history of early August 1972 is shown in Figure 6. The results expected from the principles described earlier in this paper are illustrated by the thick gray lines in the figure. It is worth noting that after the interplanetary shock had moved beyond the orbit of the earth, late on 5 August, the event followed our model quite well. The extraordinary flux and extraordinary hard spectrum are present only during the time when the earth is between the two converging interplanetary shocks which are re-accelerating the particle population. This time period, from about 05 UT to about 20 UT, is illustrated by the shaded portion of Figure 6.

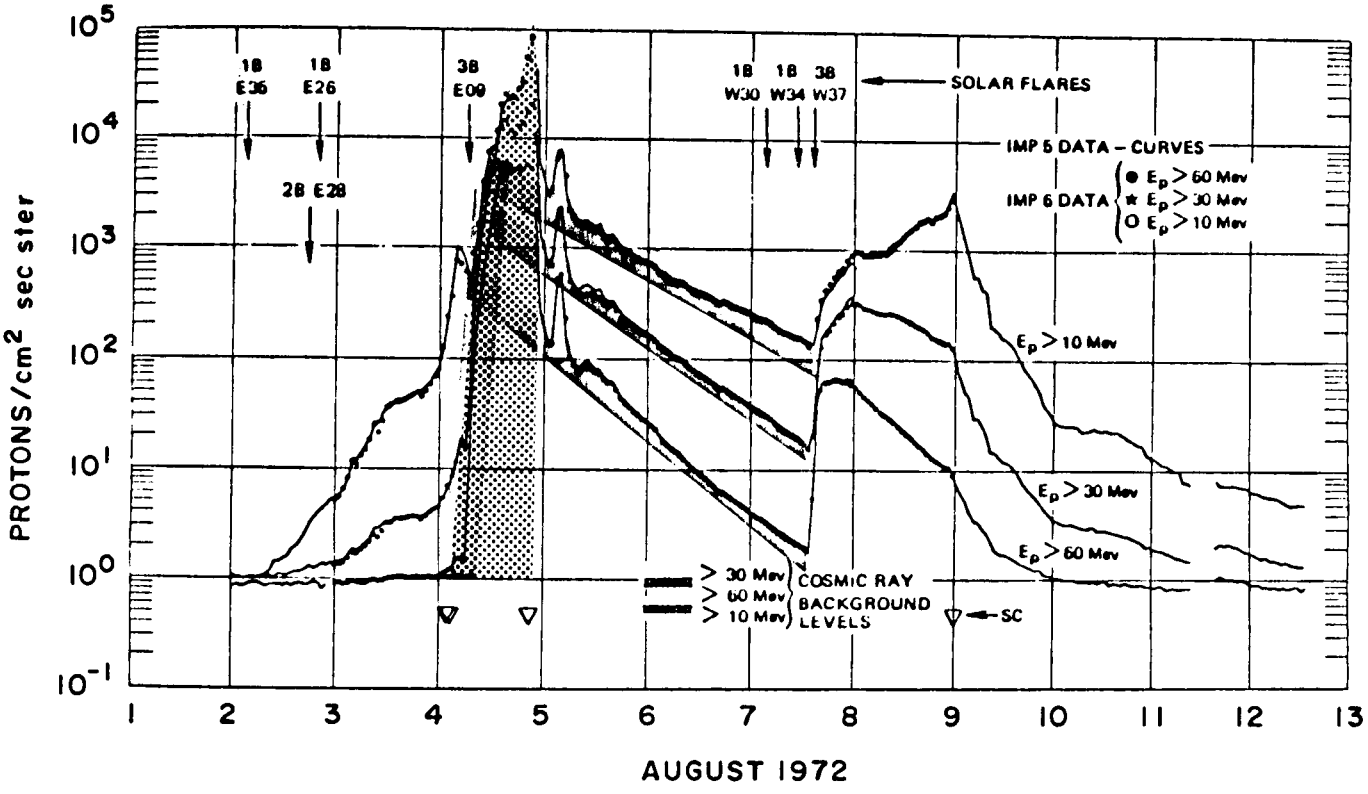

Figure 6. The solar proton time-intensity profile observed for the August 1972 sequence of events. Note the extraordinary hard spectrum and high flux during the time when the earth was between the two converging interplanetary shocks (the second shock overtaking the first).

Table 1. Normalized Elemental Abundances of Solar Energetic Particle Events

NORMALIZED SOLAR ENERGETIC PARTICLE ABUNDANCES

		Adams Mason (1980) 1 MeV		Gloeckler (1979) 1-20 MeV		Cook et al. (1984) 10 MeV		McGuire et al. (1986) 6.7-15 MeV	
1	H	1.0		1.0		1.0		1.0	
2	He	2.2	E-2	1.5	E-2			1.5	E-2
3	Li			1.0	E-7	4.8	E-8	2.8	E-6
4	Be			1.5	E-7	6.0	E-9	1.4	E-7
5	B			1.5	E-7	1.2	E-8	1.4	E-7
6	C	1.6	E-4	1.2	E-4	9.6	E-5	1.3	E-4
7	N	3.8	E-5	2.8	E-5	2.7	E-5	3.7	E-5
8	O	3.2	E-4	2.2	E-4	2.2	E-4	2.8	E-4
9	F			4.3	E-7	1.0	E-8	1.4	E-7
10	Ne	5.1	E-5	3.5	E-5	3.1	E-5	3.6	E-5
11	Na	1.6	E-6	3.5	E-6	2.6	E-6	2.4	E-6
12	Mg	4.8	E-5	3.9	E-5	4.3	E-5	5.2	E-5
13	Al	3.5	E-6	3.5	E-6	3.1	E-6	3.3	E-6
14	Si	3.8	E-5	2.8	E-5	3.5	E-5	4.2	E-5
15	P	2.3	E-7	4.3	E-7	1.7	E-7	4.0	E-7
16	S	1.8	E-5	5.7	E-6	7.8	E-6	6.5	E-6
17	Cl	1.7	E-7			7.1	E-8		
18	Ar	3.9	E-6	8.7	E-7	7.3	E-7	4.6	E-6
19	K	1.3	E-7			1.0	E-7		
20	Ca	2.3	E-6	2.6	E-6	3.1	E-6	3.2	E-6
21	Sc					7.8	E-9		
22	Ti	1.0	E-7			1.2	E-7		
23	V					1.2	E-8		
24	Cr	5.7	E-7			5.0	E-7		
25	Mn	4.2	E-7			1.8	E-7		
26	Fe	4.1	E-5	3.3	E-5	3.4	E-5		
27	Co	1.0	E-7			4.8	E-7		
28	Ni	2.2	E-6			1.2	E-6		
29						1.4	E-8		
30						3.8	E-8		

REFERENCES

Adams, J. H. Jr., R. Silberberg, and C. H. Tsao, Cosmic Ray Effects on Microelectronics, Part 1: The near-earth particle environment, NRL Memorandum Report 4506, Naval Research Laboratory, Washington, D. C., August 25, 1981. (ADA103897)

Axford, W. I., Anisotropic diffusion of solar cosmic rays, Planet. Space Sci., 13, 1301, 1965.

Barouch, E., M. Gros, and P. Masse, The solar longitude dependence of proton event delay, Sol. Phys., 19, 483, 1971.

Burlaga, L. F., Anisotropic diffusion of solar cosmic rays, J. Geophys. Res., 72, 4449, 1967.

Cook, W. R., E. C. Stone and R. E. Vogt, Elemental composition of solar energetic particles, Astrophy. J., 297, 827, 1984.

Gloeckler, G. Composition of energetic particle population in interplanetary space, Reviews of Geophysics, 17, 569, 1979.

Gold, R. E., E. C. Roelof, J. T. Nolte and A. S. Krieger, Relation of large-scale coronal x-ray structure and cosmic rays: 5. Solar wind and coronal influence on a Forbrush decrease lasting one solar rotation, Proc. 14th International Cosmic Ray Conference (Munich), 3, 1095, 1975.

Krimigis, S. M., Interplanetary diffusion model for the time behavior of intensity in a solar cosmic ray event, J. Geophys. Res., 70, 2943, 1965.

Lanzerotti, L. J., Coronal propagation of low-energy solar protons, J. Geophys. Res., 78, 3942, 1973.

Lee, M. A., Particles accelerated by shocks in the heliosphere, these proceedings, 1988.

Lin, R. P., Solar particle acceleration and propagation, Reviews of Geophysics, 25, 676, 1987.

Mason G. M., L. A. Fisk, D. Hovestadt, and G. Gloeckler, A survey of $\sim$ 1 Mev nucleon^{-1} solar flare particle abundances, $1 < Z < 26$, during the 1973-1977 solar minimum period, Astrophy. J., 239, 1070, 1980.

Mason, G. M., The composition of galactic cosmic rays and solar energetic particles, Reviews of Geophysics, 25, 685, 1987.

McCracken, K. G., and U. R. Rao, Solar cosmic ray phenomena, Space Science Reviews, 11, 155, 1970.

McCracken, K. G., U. R. Rao, R. P. Bukata, and E. P. Keath, The decay phase of solar flare events, Sol. Phys., 18, 100, 1971.

McGuire, R. E., T. T. Von Rosenvinge and F. B. McDonald, The composition of solar energetic particles, Astrophy. J., 301, 938, 1986.

Reid, G. C., A diffusive model for the initial phase of a solar proton event, J. Geophys. Res., 69, 2659, 1964.

Reinhard, R., E. C. Roelof and R. E. Gold, Separation and analysis of temporal and spatial variations in the 10 April 1969 solar flare particle event, in The Sun and the Heliosphere in Three Dimensions, edited by R. G. Marsden, Proceedings of the XIX ESLAB symposium, Astrophysics and Space Science Library, p. 123, D. Reidel Publishing Co., Dordecht, 1986.

Reinhard, R., and G. Wibberenz, Propagation of flare protons in the solar atmosphere, Sol. Phys., 36, 473, 1974.

Roelof, E. C., New aspects of interplanetary propagation revealed by 0.3 MeV solar proton events in 1967, in: Solar-Terrestrial Relations, p. 411, University of Calgary, Canada, 1973.

Roelof, E. C., Scatter-free collimated convection and cosmic-ray transport at 1 AU. Proc. 14th International Cosmic Ray Conference (Munich), 5, 1716, 1975.

Roelof, E. C., Solar particle emission, in: Physics of Solar Planetary Environments, 1, p. 214, Published by the American Geophysical Union, Washington, D.C., USA, 1976.

Roelof, E. C., R. E. Gold, S. M. Krimigis, A. S. Krieger, J. T. Nolte, P. S. McIntosh, A. J. Lazarus and J. D. Sullivan, Relation of large-scale coronal X-ray structure and cosmic rays: 2. Coronal control of interplanetary injection of 300 keV solar protons. Proc. 14th International Cosmic Ray Conference (Munich), 5, 1704, 1975.

Roelof, E. C. and S. M. Krimigis, Analysis and synthesis of coronal and interplanetary energetic particle, plasma and magnetic field observations over three solar rotations, J. Geophys. Res., 78, 5375, 1973.

Shea, M. A., Cosmic rays, solar and interplanetary physics; Overview of cosmic ray, solar, and interplanetary research (1983-1987), Reviews of Geophysics, 25, 641, 1987.

Smart, D. F., and M. A. Shea, PPS76- a computerized "event mode" solar proton forecasting technique, in Solar Terrestrial Prediction Proceedings, edited by R. F. Donnelly, U. S. Department of Commerce, NOAA/ERL, 1, p. 406, 1979.

Smart, D. F., and M. A. Shea, Galactic cosmic radiation and solar energetic particles, Chapter 6 in the Handbook of Geophysics and the Space Environment, edited by A. S. Jursa, Air Force Geophysics Laboratory, Bedford, Ma, 1985.

Van Hollebeke, M. A. I., L. S. Ma Sung, and F. B. McDonald, The variation of solar proton energy spectra and size distribution with heliolongitude, Sol. Phys., 41, 189, 1975.

Wibberenz, G., Interplanetary magnetic fields and the propagation of cosmic rays, J. Geophys., 40, 667, 1974.

PARTICLES ACCELERATED BY SHOCKS IN THE HELIOSPHERE

MARTIN A. LEE, Institute for the Study of Earth, Oceans and Space, University of New Hampshire, Durham, NH 03824

ABSTRACT

The populations of energetic ions accelerated by shocks in the heliosphere are reviewed briefly. Characteristic spectra and representative fluxes are given.

INTRODUCTION

Shocks accelerate energetic ions throughout the heliosphere. Travelling interplanetary shocks, presumably generated by solar flares or coronal transients, produce energetic storm particle (ESP) events. The forward and reverse shocks bounding corotating interaction regions (CIRs) in the solar wind accelerate the corotating ion events. Planetary bow shocks at Earth, Jupiter, and Saturn accelerate the diffuse upstream ion distributions. The seed particles in all cases are either solar wind ions or solar flare ions, with the possible addition of leaked magnetospheric ions at planetary bow shocks. In most cases, however, these shocks are not efficient producers of energetic particles above 1 MeV/nucleon.

The locations of these populations in the heliosphere are indicated schematically in Figure 1. Also shown is the cosmic ray anomalous component, described elsewhere in this volume, which is presumably accelerated at the solar wind termination shock and propagates back into the inner heliosphere with reduced intensity. Solar flare ions are also indicated with possible origin at a coronal shock; they are also described elsewhere in this volume. Finally, for completeness the interstellar and cometary pickup ions are shown. Although they are energetic with respect to the solar wind thermal distribution their energies in the spacecraft frame are comparable with the $\sim$ 1 keV/nucleon energy of the solar wind and are of little interest in this report.

COROTATING ION EVENTS

The forward and reverse shocks bounding CIRs generally form by 3-4 AU during solar minimum conditions when a polar coronal hole extends to mid latitudes and produces a fast solar wind stream there. The shocks presumably extend as identifiable shocks to 10-15 AU where they criss-cross, merge and dissipate. They may extend to 20°-30° latitude. Although these shocks can be long-lived (over several solar rotations), they are weak, quasi-perpendicular (which tends to inhibit injection of solar wind ions into the acceleration process) and their ion acceleration is partially balanced by adiabatic deceleration of the ions in the diverging solar wind. The differential intensity spectrum of accelerated ions beyond $\sim$1 MeV/nucleon is proportional to exp $(-v/v_o)$ where v is speed and $v_o \sim 0.01 - 0.03c$, and a typical maximum proton flux (i.e. at the shock at $\sim$ 5-10 AU) at 1 MeV is 10 protons cm^{-2} s^{-1} str^{-1} MeV^{-1}. The corotating ion events are described in detail by McDonald et al. (1976), Barnes and Simpson (1976), Marshall and Stone (1977), Pesses, van Allen and Goertz (1978), Van Hollebeke et al. (1978), Gloeckler et al. (1979), Mewaldt et al. (1979), and Fisk and Lee (1980).

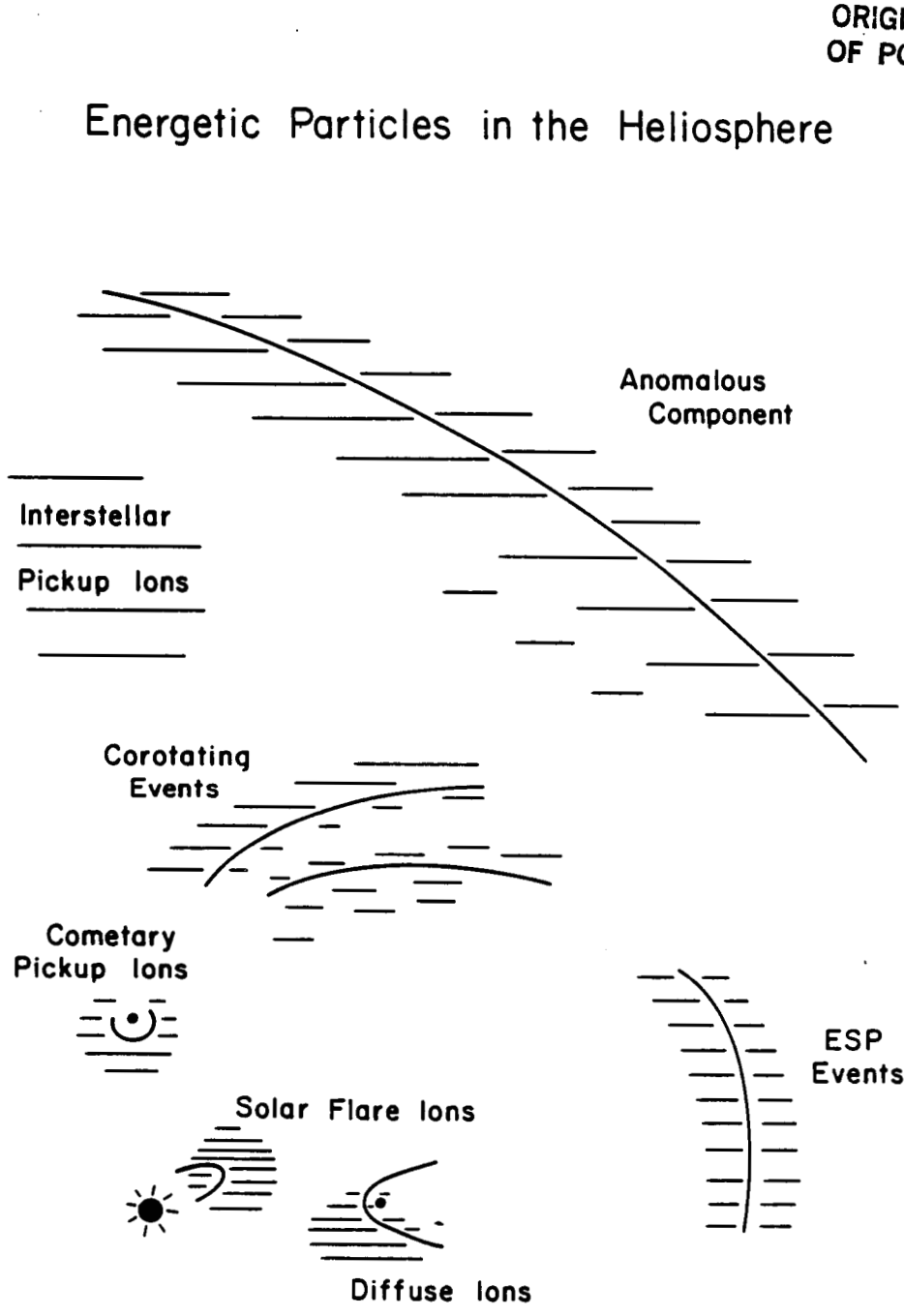

Fig. 1. A schematic diagram of energetic particle populations in the heliosphere.

DIFFUSE ION EVENTS

Planetary bow shocks are strong near their nose but their limited size ($\sim$ 20 R_E at Earth and $\sim$ 100 R_J at Jupiter) limits acceleration efficiency. At Earth beyond $\sim$20 keV per charge the distribution function of diffuse upstream ions is proportional to $\exp(-E/E_0)$ where E is energy per charge and $E_0 \sim$ 15-25 keV per charge. A typical maximum differential flux at 20 keV at the shock is 4000 protons $cm^{-2}\ s^{-1}\ str^{-1}$

keV^{-1}. The ion intensity decays with distance from Earth's bow shock with a scalelength of ~ 10-20 R_E depending on energy. At Jupiter the maximum differential intensity appears to be ~ 20 protons cm^{-2} s^{-1} str^{-1} keV^{-1} at 100 keV, with a similarly soft exponential spectrum. Good references on the diffuse ions are Ipavich et al. (1979, 1981), Gosling et al. (1979), Eastman et al. (1981), Lee (1982), Mitchell and Roelof (1983), Wibberenz et al. (1985), Zwickl et al. (1981), Baker et al. (1984), and Smith and Lee (1986).

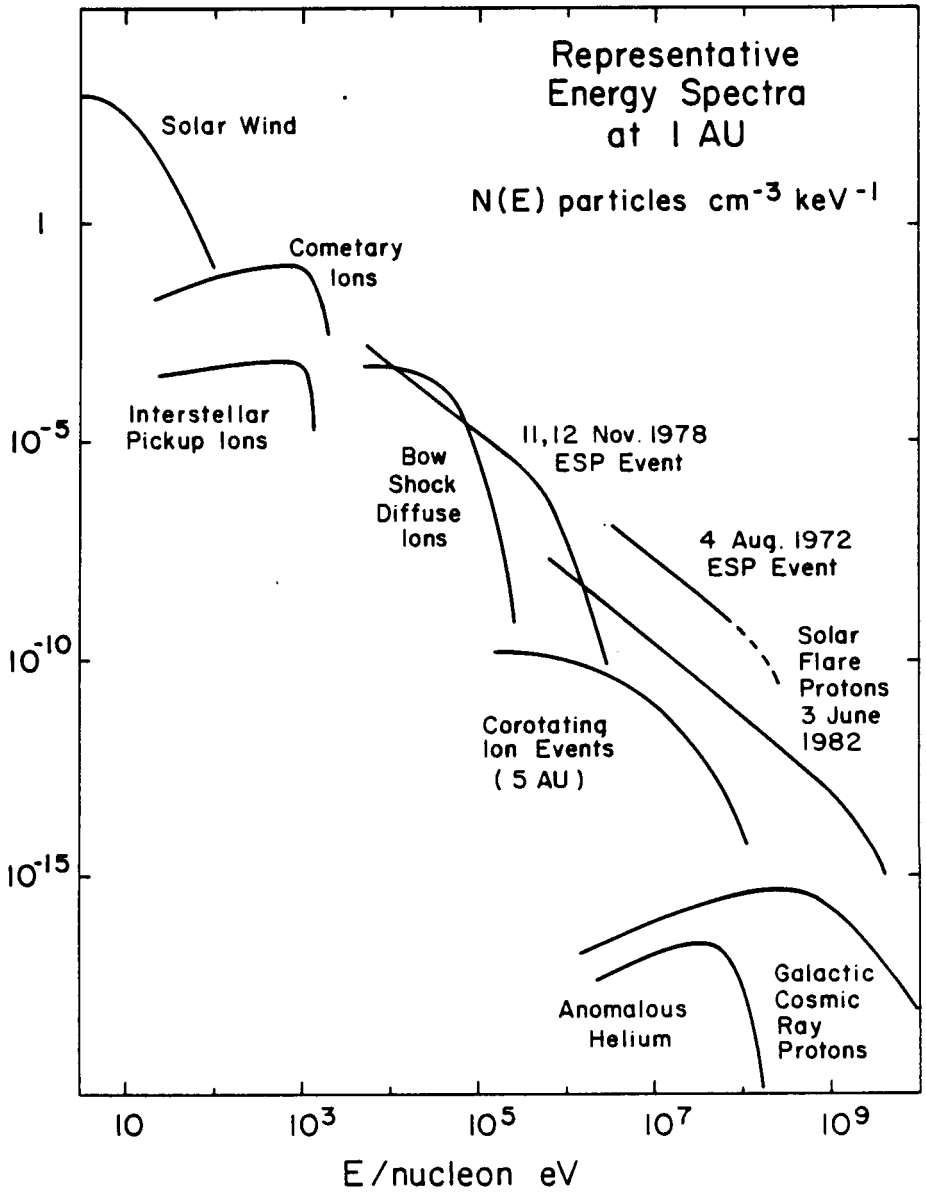

Fig. 2. Representative and particular energy spectra of energetic particle populations at 1 AU (the corotating ion spectrum is at 5AU).

ENERGETIC STORM PARTICLE (ESP) EVENTS

Energetic storm particle events are more variable and difficult to characterize. Interplanetary travelling shocks enhance the background solar flare ion distribution, particularly at quasi-perpendicular shocks, but the enhancement is generally small in comparison with the flare event itself. A few strong quasi-parallel shocks can accelerate solar wind ions (these are so-called "supercritical" shocks), creating very large enhancements at low energies, but finite shock lifetime at $\sim$ 1AU limits the enhancement to energies $\lesssim$ 500 keV/nucleon. For example, the large event of 11,12 November 1978 produced a maximum differential flux of 2000 protons $cm^{-2}\ s^{-1}\ str^{-1}\ keV^{-1}$ at 30 keV at 1 AU with a differential flux power law, $\propto E^{-1.1}$, up to energies of about 200 keV. However, occasionally a very strong shock can produce huge enhancements at 1 AU. The shock on 4 August 1972 was such a shock (Yates et al., 1974; Eichler, 1981). This huge variation is apparently caused by nonlinearity in the injection rate as a function of shock strength and in the acceleration timescale (due to excitation of ion-excited waves), and perhaps in the solar flare seed particle population. Useful references on ESP events are Bryant et al. (1962), Rao et al. (1967), Sarris and Van Allen (1974), Scholer et al. (1983), Lee (1983), Van Nes et al. (1984), Sarris et al. (1984), Kennel et al. (1984a,b, 1986), Tsurutani and Lin (1985), and Bavassano-Cattaneo et al. (1986).

REPRESENTATIVE SPECTRA

Representative and particular ion spectra in units of particles $cm^{-3}\ keV^{-1}$ are shown in Figure 2. It is clear that the energetic particle environment within the heliosphere covers a huge range of energies and differential intensities. All spectra with the exception of that for the corotating ion events are at 1AU. For purposes of comparison with the shock-associated energetic ion events, the spectra of the solar wind protons, cometary water-group pickup ions, interstellar pickup helium, the large solar flare proton event of 3 June 1982, anomalous cosmic ray helium, and galactic cosmic ray protons are also indicated.

SUMMARY

The heliosphere is rich in its populations of shock-accelerated energetic ions. Nevertheless at energies greater than 1 MeV/nucleon they would appear to be dominated by large solar flare ion events in the inner heliosphere. At $\sim$ 5AU, however, during solar minimum conditions, the corotating ion events tend to dominate solar flare events. Diffuse ions at planetary bow shocks have negligible intensities at energies $\gtrsim$ 1 MeV/nucleon. Interplanetary travelling shocks can enhance the solar flare ion flux as an ESP event, but the enhancements are generally not large at energies $\gtrsim$ 1 MeV/nucleon. Occasionally an ESP event can have a substantial intensity at energies $\gtrsim$ 1 MeV/nucleon as shown for the 4 August 1972 event in Figure 2.

Acknowledgements

The author wishes to thank Dr. Joan Feynman for her efforts in organizing the Workshop on the Interplanetary Charged Particle

Environment. This work was supported, in part, by NSF Grant ATM-8513363, NASA Grant NAG 5-728, and NASA Solar Terrestrial Theory Program Grant NAGW-76.

REFERENCES

Baker, D.N., R.D. Zwickl, S.M. Krimigis, J.F. Carbary, and M.H. Acuña 1984. Energetic particle transport in the upstream region of Jupiter: Voyager results. J. Geophys. Res., 89: 3775.

Barnes, C.W., and J.A. Simpson 1976. Evidence for interplanetary acceleration of nucleons in corotating interaction regions. Astrophys. J. 210: L91.

Bavassano-Cattaneo, M.B., B.T. Tsurutani, E.J. Smith, and R.P. Lin 1986. Subcritical and supercritical interplanetary shocks: magnetic field and energetic particle observations. J. Geophys. Res. 91: 11929.

Bryant, D.A., T.L. Cline, U.D. Desai, and F.B. McDonald 1962. Explorer 12 observations of solar cosmic rays and energetic storm particles after the solar flares of September 28, 1961. J. Geophys. Res. 67: 4983.

Eastman, T.E., R.R. Anderson, L.A. Frank, and G.K. Parks 1981. Upstream particles observed in the earth's foreshock region. J. Geophys. Res. 86: 4379.

Eichler, D. 1981. A cosmic-ray-mediated shock in the solar system. Astrophys. J. 247: 1089.

Fisk, L.A., and M.A. Lee 1980. Shock acceleration of energetic particles in corotating interaction regions in the solar wind. Astrophys. J. 237: 620.

Gloeckler, G., D. Hovestadt, and L.A. Fisk 1979. Observed distribution functions of H, He, C, O and Fe in corotating energetic particle streams: implications for interplanetary acceleration and propagation. Astrophys. J. 230: L191.

Gosling, J.T., J.R. Asbridge, S.J. Bame and W.C. Feldman 1979. Ion acceleration at the earth's bow shock: a review of observations in the upstream region. In Particle Acceleration Mechanisms in Astrophysics, AIP Conference Proceedings, No. 56, AIP, New York.

Ipavich, F.M., G. Gloeckler, C.Y. Fan, L.A. Fisk, D. Hovestadt, B. Klecker, J.J. O'Gallagher, and M. Scholer 1979. Initial observations of low energy charged particles near the earth's bow shock on ISEE 1. Space Sci. Rev. 23: 93.

Ipavich, F.M., A.B. Galvin, G. Gloeckler, M. Scholer, and D. Hovestadt 1981. A statistical survey of ions observed upstream of the earth's bow shock: energy spectra, composition, and spatial variation. J. Geophys. Res. 86: 4337.

Kennel, C.F., et al. 1984a. Plasma and energetic particle structure upstream of a quasi-parallel interplanetary shock. J. Geophys. Res. 89: 5419.

Kennel, C.F., et al. 1984b. Structure of the November 12, 1978 quasi-parallel interplanetary shock. J. Geophys. Res. 89: 5436.

Kennel, C.F., F.V. Coroniti, F.L. Scarf, W.A. Livesey, C.T. Russell, E.J. Smith, K.P. Wenzel, and M. Scholer 1986. A test of Lee's quasi-linear theory of ion acceleration by interplanetary traveling shocks. J. Geophys. Res. 91: 11917.

Lee, M.A. 1982. Coupled hydromagnetic wave excitation and ion acceleration upstream of the earth's bow shock. J. Geophys. Res. 87: 5063.

Lee, M.A. 1983. Coupled hydromagnetic wave excitation and ion acceleration at interplanetary traveling shocks. J. Geophys. Res. 88: 6109.

Marshall, F.E., and E.C. Stone 1977. Persistent sunward flow of 1.6 MeV protons at 1 AU. Geophys. Res. Lett. 4: 57.

McDonald, F.B., B.J. Teegarden, J.H. Trainor, T.T. von Rosenvinge, and W.R. Webber 1976. The interplanetary acceleration of energetic nucleons. Astrophys. J. 203: L149.

Mewaldt, R.A., E.C. Stone, and R.E. Vogt 1979. Characteristics of the spectra of protons and α particles in recurrent events at 1 AU. Geophys. Res. Lett. 6: 589.

Mitchell, D.G., and E.C. Roelof 1983. Dependence of 50 - keV upstream ion events at IMP 7&8 upon magnetic field bow shock geometry. J. Geophys. Res. 88: 5623.

Pesses, M.E., J.A. Van Allen, and C.K. Goertz 1978. Energetic protons associated with interplanetary active regions 1-5 AU from the sun. J. Geophys. Res. 83: 553.

Rao, U.R., K.G. McCracken, and R.P. Bukata 1967. Cosmic-ray propagation processes, 2, the energetic storm-particle event. J. Geophys. Res. 72: 4325.

Sarris, E.T., and J.A. Van Allen 1974. Effects of interplanetary shock waves on energetic charged particles. J. Geophys. Res. 79: 4157.

Sarris, E.T., G.C. Anagnostopoulos, and P.C. Trochoutsos 1984. On the E-W asymmetry and the generation of ESP events. Sol. Phys. 93: 195.

Scholer, M., F.M. Ipavich, G. Gloeckler, and D. Hovestadt 1983. Acceleration of low-energy protons and α particles at interplanetary shock waves. J. Geophys. Res. 88: 1977.

Smith, C.W., and M.A. Lee 1986. Coupled hydromagnetic wave excitation and ion acceleration upstream of the Jovian bow shock. J. Geophys. Res. 91: 81.

Tsurutani, B.T., and R.P. Lin 1985. Acceleration of >47 keV ions and > 2 keV electrons by interplanetary shocks at 1 AU. J. Geophys. Res. 90:1.

Van Hollebeke, M.A.I., F.B. McDonald, J.H. Trainor, and T.T. von Rosenvinge 1978. The radial variation of corotating energetic particle streams in the inner and outer solar system. J. Geophys. Res. 83: 4723.

van Nes, P., R. Reinhard, T.R. Sanderson, K.-P. Wenzel, and R.D. Zwickl 1984. The energy spectrum of 35- to 1600- keV protons associated with interplanetary shocks. J. Geophys. Res. 89: 2122.

Wibberenz, G., F. Zöllich, and H.M. Fischer 1985. Dynamics of intense upstream ion events. J. Geophys. Res. 90: 283.

Yates, G.K., L. Katz, B. Sellers, and F.A. Hanser 1974. Interplanetary particle fluxes observed by OV 5-6 satellite. In Correlated Interplanetary and Magnetospheric Observations, ed. D.E. Page (Dordrecht: Reidel), p. 597.

Zwickl, R.D., S.M. Krimigis, J.F. Carbary, E.P. Keath, T.P. Armstrong, D.C. Hamilton, and G. Gloeckler 1981. Energetic particle events (>30 keV) of Jovian origin observed by Voyager 1 and 2 in interplanetary space. J. Geophys. Res. 86: 8125.

High-Energy Particles Very Near the Sun

B.E. Goldstein
Jet Propulsion Laboratory
California Institute of Technology
Pasadena, CA 91109

NASA's long range plans include a Solar Probe (Star Probe) mission in which a spacecraft is placed in an eccentric orbit with perihelion at four solar radii. As part of the study effort for this mission, a Solar Probe Environment Workshop was sponsored by JPL. The report of this committee was issued in September 1978 as JPL Publication 78-64. The situation with respect to understanding of the near-solar energetic particle environment has not changed substantially since that time. The best reference therefore is the JPL 78-64 document. We provide a brief abstract of this document below.

There are considerable uncertainties in the models of solar energetic particle release and transport. The committee addressed this problem by using different modelling techniques when possible to provide a cross-check on the estimates. These models were used to extrapolate observation at 1 AU to the vicinity of the Sun. Additionally, the occurrence of a flare of a given magnitude must be estimated on a statistical basis. Therefore, it is possible to state a likelihood that the fluxes and fluences will be less than a certain magnitude, but in the event of an extremely large solar flare (occurrence of perhaps once a decade, e.g., August 4, 1972) it is likely that the hazard would be insurmountable.

A reasonable mission plan would require that there be no more than a 1% chance that the peak fluxes and fluences encountered near the Sun exceed those of the Jupiter flyby. For protons of energy greater than 20 MeV, the report estimates that there is a maximum 1% chance of encountering a flux of 3×10^6 $cm^{-2}sec^{-1}$ during the solar flyby, which is close to the Jupiter level. The maximum fluence at the 1% likelihood level is 2×10^{11} cm^{-2}, less than the fluence predicted for the Jupiter phase of the mission.

The solar energetic electron flux above 1/2 MeV is about 7 times larger than the proton flux above 20 MeV, whereas at Jupiter the comparable ratio is 100. Thus, energetic electrons should not be a problem at the Sun.

It might be concluded that a flyby of the Sun is less hazardous than a flyby of Jupiter. This is not necessarily the case. First, it has been assumed that the spacecraft will not fly through any closed field line particle-trapping regions. Additionally, one could meet an extremely large but rare flare. One flare per decade may emit on the order of 10^{36} energetic protons, which would yield fluxes and fluences at the Solar Probe of 6×10^7 $cm^{-2}sec^{-1}$ and 10^{12} cm^{-2} respectively. In making the above estimates, it was assumed that particles travel adiabatically from the Sun to the Earth; if there are mechanisms that cause energy loss near the Sun, the fluxes and fluences could be higher than estimated. Third, the flux of low energy particles (protons of about 1 MeV) at 1 AU is observed to last for many days with long injection times. Therefore, the probable flux of low energy particles may not simply scale as the observed energy near the peak of events.

In summary, a brief first look indicates that the near-solar particle environment is not a worse hazard than Jupiter.

GALACTIC COSMIC RAYS

Elemental Composition and Energy Spectra of Galactic Cosmic Rays

R. A. Mewaldt
California Institute of Technology
Pasadena, CA 91125

ABSTRACT

A brief review is presented of the major features of the elemental composition and energy spectra of galactic cosmic rays. The requirements for phenomenological models of cosmic ray composition and energy spectra are discussed, and possible improvements to an existing model are suggested.

1. INTRODUCTION

Over the past forty years, but especially during the past decade or so, a variety of spacecraft and balloon instruments have combined to measure the composition of galactic cosmic rays over essentially the entire periodic table (nuclear charge Z = 1 to 92), and the energy spectrum of abundant cosmic ray species from ~10 MeV/nuc to ~100 GeV/nuc. In this report we discuss aspects of these measurements that are relevant to phenomenological models of cosmic ray composition and its dependence on energy. Adams et al. (1981; see also Adams, 1986) have produced such a model and we suggest some minor improvements and updates that might be made to this model in an effort to improve its accuracy.

This report constitutes a written version of a presentation made at the *Workshop on the Interplanetary Charged Particle Environment* held at the Jet Propulsion Laroratory in March, 1987. The purpose of this workshop was to review current models of the interplanetary particle environment, in an effort to evaluate their accuracy and improve their predictive capability. Among the applications of such models are evaluations of the effects of energetic charged particles on microelectronic devices carried on spacecraft, and their effect on man in space.

2. COSMIC RAY COMPOSITION

Several experiments over the past decade or so have led to significant improvements in in our knowledge of the composition of galactic cosmic rays. There are now accurate measurements of the relative abundances of all elements from H to Zn (Z = 1 to 30; see, e.g., Engelmann et al., 1983, 1985; Dwyer and Meyer, 1985, 1987; Garcia-Munoz and Simpson, 1979). For the ultra-heavy (UH) elements with Z > 30, the recent HEAO-3 and Ariel missions (Stone et al., 1987; Fowler et al., 1985) have provided abundances of adjacent pairs of even and odd nuclei up to Z = 60, while for the upper one-third of the periodic table the abundances of various groups of charges have been reported. For recent reviews of

these and other measurements see Simpson (1983) Mewaldt (1983), Meyer (1985), and Mason (1987).

Figure 1 and Table 1 summarize the relative elemental composition from Z = 1 to 92, normalized to Si = 10^6. Note that the relative flux spans more than 10 decades in intensity. To a rough approximation the relative abundances of the major elements in cosmic rays are in proportion to their distribution in solar system material, but there are also significant differences from the solar composition, including the great enhancement of "secondary" nuclei produced in cosmic rays by fragmentation (e.g., Li, Be, and B); the relative depletion (by a factor of ~5) of elements with high first ionization potential in cosmic rays (e.g., C, N, O, Ne, Ar); and the underabundance of H and He relative to heavier elements.

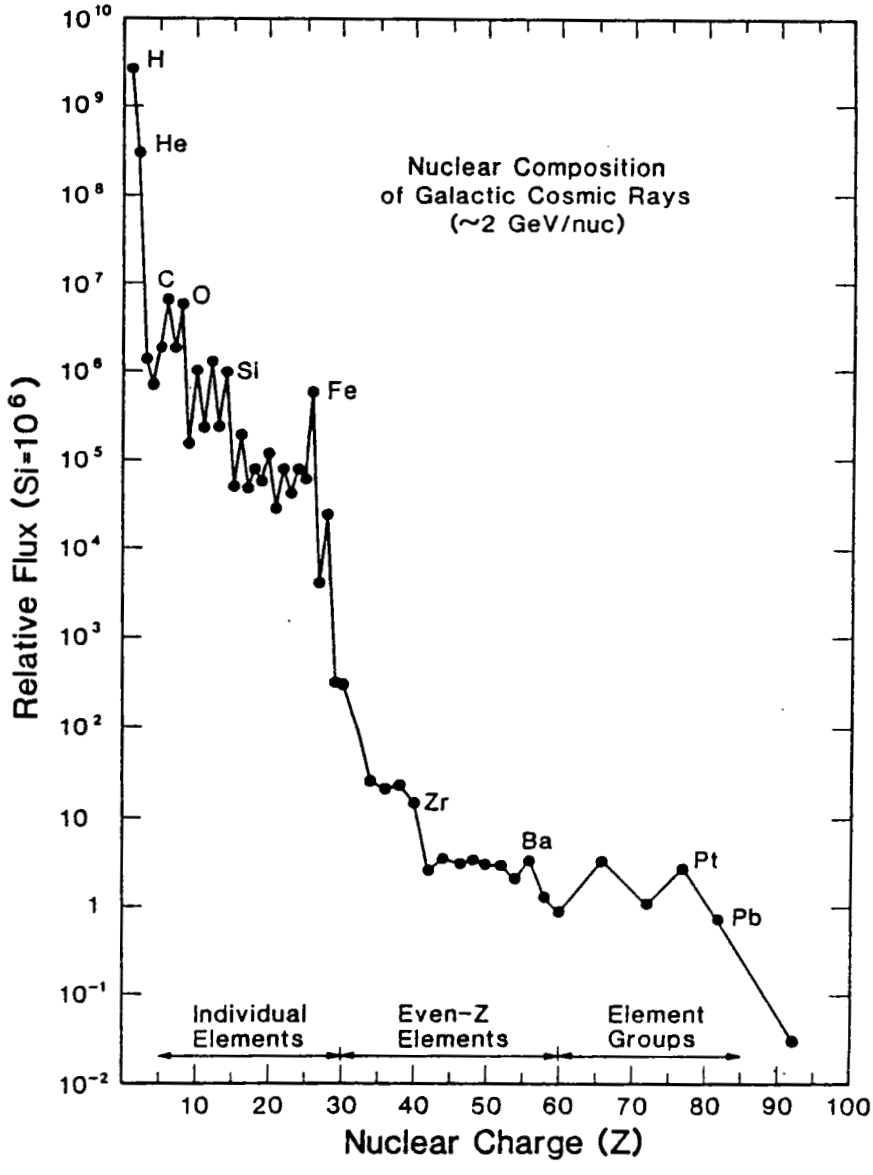

Figure 1: The relative flux of cosmic rays as a function of nuclear charge Z (see also Table 1).

Table 1 - Elemental Composition of Galactic Cosmic Rays (~1 GeV/nucleon)[+]

Nuclear Charge Z	Relative Abundance (Si = 1000*)	Nuclear Charge Z	Relative Abundance (Si = 10^6)*
1	3×10^6	29	381±88
2	$2.7 \pm 0.6 \times 10^5$	30	393±35
3	1360±30	31-32	63±12
4	670±20	33-34	26.4±2.3
5	1920±143	35-36	20.6±1.4
6	6400±211	37-38	22.4±1.4
7	1820±58	39-41	14.5±1.1
8	5930±107	42	2.4±0.5
9	143±7.4	43-44	3.6±0.6
10	993±26	45-46	3.0±0.5
11	224±8	47-48	3.4±0.5
12	1240±28	49-50	3.0±0.5
13	224±8	51-52	3.0±0.5
14	1000	53-54	2.1±0.4
15	51.1±3.5	55-56	3.4±0.5
16	189±8	57-58	1.3±0.3
17	47.1±3.4	59-60	0.9±0.3
18	79.5±4.9	62-69	3.5±0.4
19	57.0±3.7	70-73	1.1+0.4-0.3
20	124.4±6.3	74-80	2.7±0.4
21	28.5±2.6	81-83	0.6+0.3-0.2
22	82.1±4.8	90-96	0.03+.04-.03
23	41.0±3.3		
24	80.9±5.0		
25	59.9±4.1		
26	587±17		
27	3.3±0.5		
28	29.6±0.6		

+ Based on Binns et al. (1982), Byrnak et al. (1983), Dwyer and Meyer (1985), Engelmann et al. (1983), Lezniak and Webber (1978), and Stone et al. (1987). Uncertainties in the relative abundance of widely separated charges may be somewhat greater than indicated.

* Note that the normalization is Si=10^6 for Z≥29 and Si=1000 for Z≤28.

In Figure 2 we show the "integral composition" of cosmic rays, the integrated flux of elements heavier than a given nuclear charge. Note in particular that the flux of the UH elements, which constitute the upper 2/3 of the periodic table, amount to only ~0.1% of that of Fe (Z = 26). In problems involving the effect of cosmic rays on micro-electronic devices there is often a threshold energy loss for a given device, such that only cosmic rays of a certain charge or greater are capable of triggering the device, since energy loss is proportional to Z^2. Figure 2 demonstrates the advantages of a high threshold, and shows that phenomenological models of cosmic ray composition should, at the very least, characterize accurately the abundance and energy spectra of certain key elements that represent significant increases or "breaks" in this integral distribution (e.g., H, He, O, Si, and Fe).

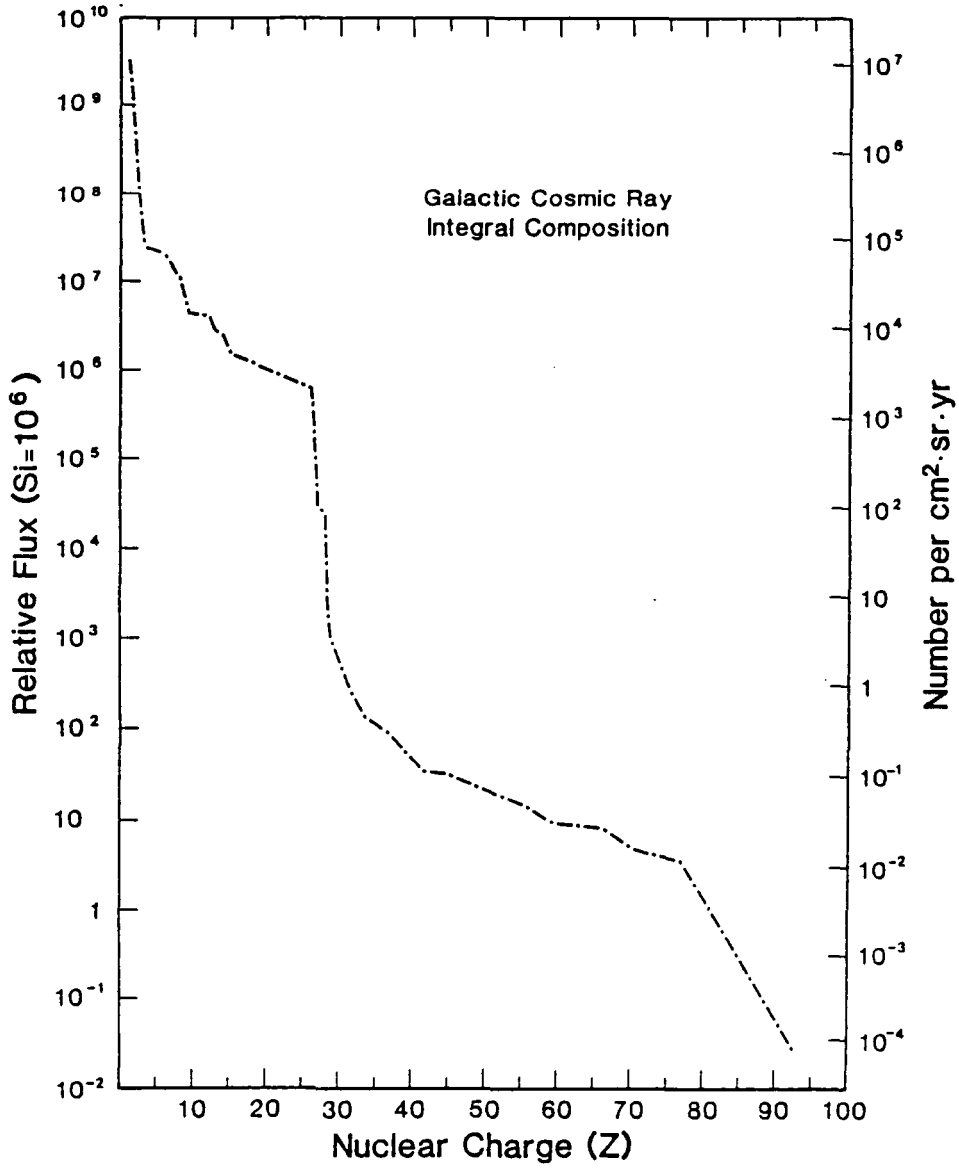

Figure 2: The relative flux of cosmic rays heavier than a given nuclear charge, as obtained by integrating the data shown in Figure 1.

3. ENERGY DEPENDENCE OF THE COMPOSITION

To a good approximation, the composition of cosmic rays can be considered independent of energy if the particle energy is measured in units of energy per nucleon (equivalent to comparing the composition at the same velocity). There are, however, some important differences. Figure 3 compares the composition measured at 0.2 and 15 GeV/nuc to that at ~2 GeV/nuc. The most obvious difference at 15 GeV/nuc is the generally lower abundance of "secondary" nuclei relative to primary nuclei, indicating that higher energy cosmic-ray nuclei (those with energies > several GeV/nuc) have passed through less material subsequent to their acceleration (see, e.g., Ormes and Protheroe, 1983). A possibly related feature is that the abundance of heavier "primary" nuclei such as Fe is more abundant at high energy.

The N_z(15 GeV/nuc)/N_z(2 GeV/nuc) ratio in Figure 3 is an indication of the extent to which the energy spectra of the various elements differ. Engelmann et al. (1983, see also Juliusson et al., 1983) have fit power laws in total energy/nucleon to the spectra of elements with $4 \leq Z \leq 28$ from ~0.8 to 25 GeV/nuc. This particular spectral shape gives a good approximation to the observed spectra of "primary" elements from ~2 to 10 GeV/nuc; at lower energies the (time dependent) effects of solar modulation are particularly important. They found that the typical spectral index for "secondary" elements over this energy range was steeper than that for primaries by about $\Delta\gamma \simeq 0.2$.

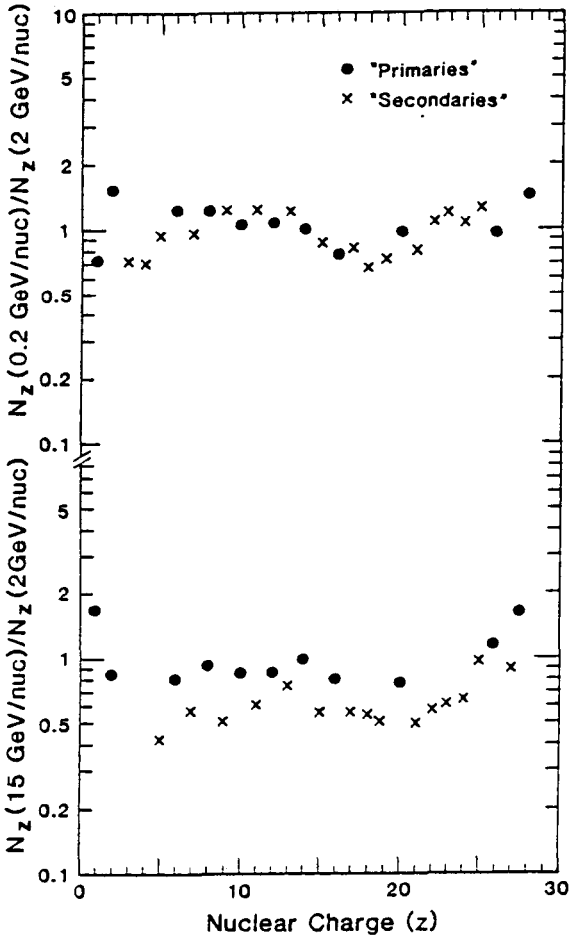

Figure 3: (Top) Comparison of the cosmic ray elemental composition measured at ~0.2 GeV/nuc (Garcia-Munoz and Simpson, 1979) relative to that at ~2 GeV/nuc Engelmann et al., 1983); (Bottom) Comparison of the ~15 GeV/nuc composition (Engelmann et al., 1983) with that measured at 2 GeV/nuc. Elements that are mainly of "secondary" origin, produced by cosmic ray collisions with the interstellar gas, are differentiated from "primary" species accelerated by cosmic ray sources.

At lower energies (0.2 GeV/nuc, see Figure 3) the differences in composition (from 2 GeV/nuc) are somewhat more difficult to characterize; they are likely due in part to the energy dependence of the various fragmentation cross sections, which vary more with energy below ~1 GeV/nucleon. Note that neither H or He seems to fit with the pattern of heavier nuclei. This is perhaps not surprising for H, since it has a different charge to mass ratio. It should also be pointed out, however, that even though H and He are the most abundant elements in cosmic rays, in many cases their abundance relative to heavier nuclei in less certain than the relative composition of heavier nuclei. This is because most of the experiments that measure the composition of heavy nuclei do not measure H and He (and vice versa) because of dynamic range considerations.

4. ENERGY SPECTRA

Figure 4 shows energy spectra for four abundant elements spanning several decades in energy/nucleon, up to the highest energies so far measured. At high energies ($\gtrsim 5$ GeV/nuc) the spectra approach the well known power law ($\sim E^{-2.7}$, where E is kinetic energy/nuc); at lower energies the effects of solar modulation are evident, and the intensity varies significantly over the solar cycle. These four

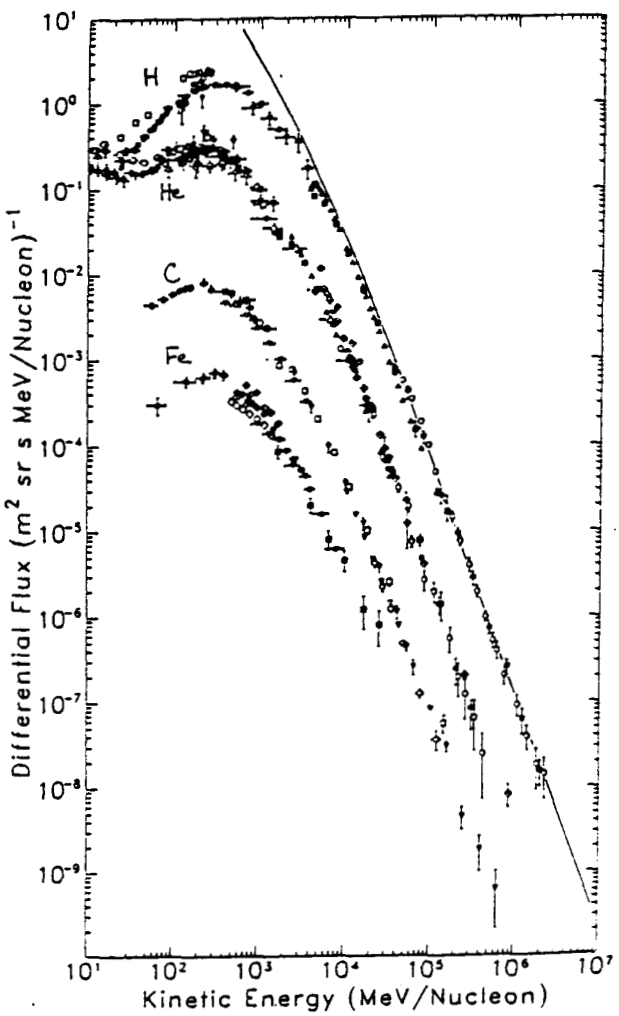

Figure 4: Measured cosmic ray energy spectra for the elements H, He, C, and Fe (from Simpson, 1983).

elements are among the most important to characterize accurately in phenomenological models of cosmic rays. Here again it is evident that all of these elements have approximately the same spectral shape, although the enhanced abundance of Fe at high energy and the relative depletion of H at lower energies is also evident.

At energies below ~100 MeV/nucleon, the composition becomes more complex, as indicated in Figure 5. The solar minimum spectra of several elements, especially He, N, O, and Ne contain anomalous enhancements at energies below ~50 MeV/nuc. This so-called "anomalous" cosmic ray (ACR) component has a separate origin from the higher energy galactic cosmic ray component. Its composition, and its spatial and temporal behavior was discussed at this workshop by Cummings (1987; see also the workshop summary by Mewaldt et al., 1987).

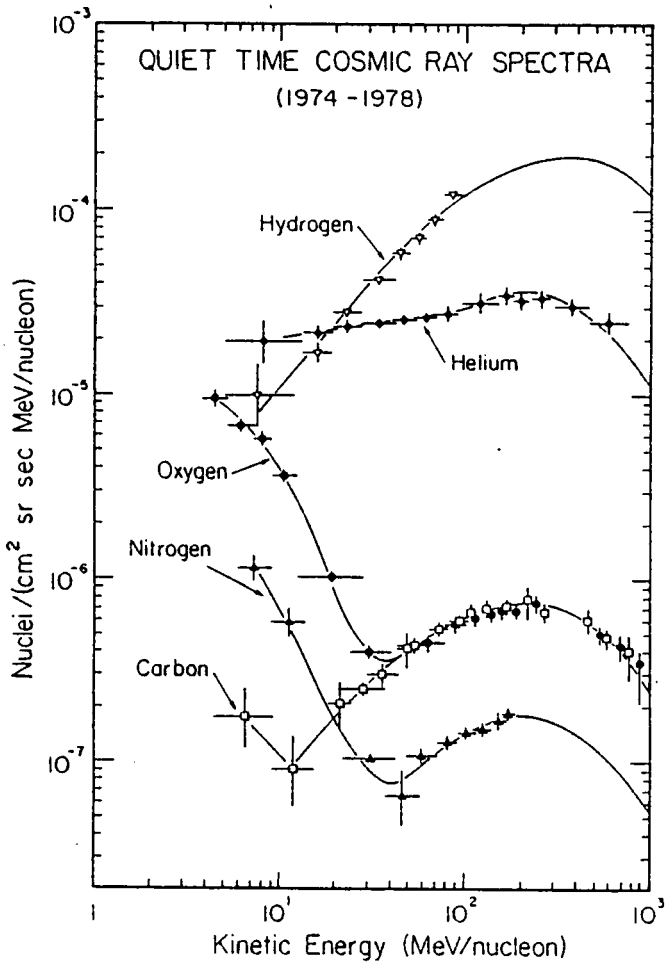

Figure 5: Quiet-time energy spectra for the elements H, He, C, N, and O measured at 1 AU over the solar minimum period from 1974 to 1978 (from Mewaldt et al., 1984). Note the "anomalous" enhancements in the low-energy spectra of He, N, and O. The data are from the Caltech and Chicago experiments on IMP-7 and IMP-8.

Figure 6 shows integral energy spectra for H and He (from Webber and Lezniak, 1974) appropriate to solar minimum. This figure demonstrates that the bulk of cosmic rays are in the energy range below a few GeV/nuc, and it is therefore this region that must be most accurately represented in modeling cosmic ray energy spectra. Unfortunately, this region is also the most sensitive to solar modulation effects. Note that only a few % of cosmic rays have energies $\gtrsim$ GeV/nuc. Figure 6 also demonstrates that H and He do not have exactly the same spectral shape (see also Figure 4).

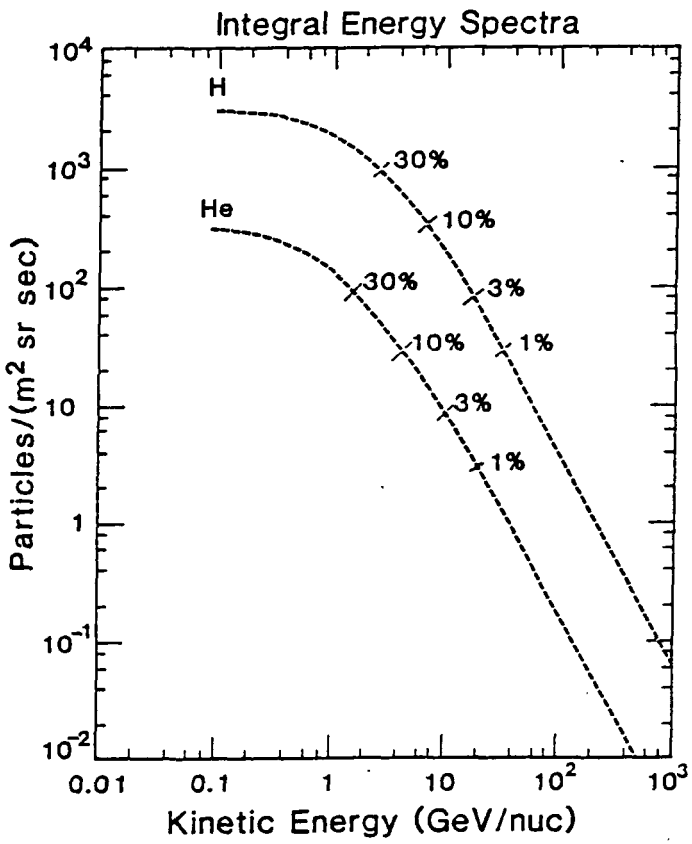

Figure 6: Integral energy spectra of H and He measured at solar minimum (adapted from Webber and Lezniak, 1974).

5. REQUIREMENTS FOR PHENOMENOLOGICAL COSMIC RAY MODELS

We discuss here the minimum requirements that should enter into phenomenological models of the composition and energy spectra of cosmic rays if the available data are to be represented in a reasonably accurate fashion.

a) Elemental Abundances: As a minimum the relative composition of elements with $1 \leq Z \leq 28$ with a typical energy of $\sim$1 to 2 GeV/nuc should be included. If relevant to the application, the composition up through $Z \simeq 92$ can also now be easily included (e.g., Table 1). For the heaviest elements, where only charge groups have been measured, it would be possible to make a reasonable breakdown of the abundances of the charge group into individual elements using the results of a cosmic ray propagation model (see, e.g., Brewster et al., 1983).

b) Energy Spectra of Selected Species: There are at least four key primary species, H, He, C, and Fe, for which a differential energy spectrum (at solar minimum) is needed. There should also be at least one "generic" secondary spectrum to take into account the secondary/primary differences indicated in Figure 3.

c) Energy Spectra for other Elements: One method to obtain the energy spectra of other elements would be to use the relative composition from item (a) (e.g., Table 1) and choose the spectrum (from (b)) that is closest in shape. Thus, for example, the elements can be divided into the following five (minimum) groups:

H
He
C (C, O, Ne, Mg, Si, S)
Fe (Ca, and all $25 \leq Z \leq 92$)
"Secondary" (Li, Be, B, N, F, Na, Al, P
$Z = 17\text{-}19$, $Z = 21\text{-}24$)

d) Solar Cycle Dependence: To model the effects of solar modulation on the energy spectra there could be an energy and time dependent modulation factor scaled from observed neutron monitor rates (see, e.g., Mewaldt et al., 1987). Another possibility is to tabulate both solar minimum and solar maximum spectra for the various key species and then interpolate between these spectra using an observed (or predicted) neutron monitor rate.

e) Extrapolation to the Outer Heliosphere: Measurements by Pioneer and Voyager show that the composition of cosmic rays is only weakly dependent on distance from the Sun, with the exception of the anomalous cosmic ray component, which has a somewhat larger radial gradient than normal galactic cosmic rays, and thus becomes more important in the outer heliosphere. Because of the energy dependence of cosmic ray gradients, low energy cosmic rays gradually become relatively more numerous in the outer heliosphere (see the reports at this workshop by McKibben and Mewaldt et al.)

f) Mean Mass: Finally, a mean mass should be defined for each element based on the results of a cosmic ray propagation model that takes into account the source composition, nuclear interactions, and solar modulation. The mean mass parameter is needed to calculate various range-energy and rigidity-dependent effects.

The model of Adams et al. (1981; updated in Adams, 1986) is an example of a phenomenological model of cosmic rays like that described above which was derived for the near-Earth environment. This model does meet the various requirements described above and appears to provide a reasonably accurate characterization of cosmic ray composition and energy spectra. Since this model was last revised, there have been several new measurements reported that should be reviewed and, if appropriate, taken into account. For example, recent measurements of the energy spectra of H and He have been reported by Garcia-Munoz et al. (1987) and Webber et al. (1987a, 1987b). In the GeV/nuc energy range, the French-Danish experiment on HEAO-3 (Engelmann et al., 1985) and the balloon

experiment of Dwyer and Meyer (1985, 1987) have provided precise measurements of the energy spectra of elements with $4 \leq Z \leq 28$. There is also new data HEAO-3 for both $Z=20$ to 28 and $Z>30$ nuclei (Binns et al., 1987, Stone et al., 1987). Incorporation of these recent results is suggested mainly for completeness; while they should improve the accuracy of the model, it does not appear likely that these updates will make a significant difference in the predictions of the model for most applications.

In addition, the following other improvements to the model of Adams et al. should also be considered. Their model uses the energy spectrum of He as a reference spectrum for elements with $3 \leq Z \leq 16$. However the He spectrum is contaminated by "anomalous" He at energies below $\sim$100 MeV/nucleon, and, in addition, a significant fraction of He is known to be ^{3}He (see, e.g., Mewaldt, 1986), which has a different charge to mass ratio. For these reasons we suggest that the carbon spectrum be used as a reference for these light elements.

Perhaps the major uncertainty in the Adams et al. model is associated with the difficulty of predicting the time dependence of the cosmic ray flux due to solar modulation effects. A possible solution to this problem is discussed in the report by Mewaldt et al. (1987).

6. SUMMARY AND CONCLUSIONS

Available measurements now allow for a reasonably precise description of galactic cosmic ray composition and energy spectra. Thus, the relative composition of species with $1 \leq Z \leq 30$ is now known to $\sim$10% accuracy, while the accuracy of measurements of $Z > 30$ nuclei is perhaps more like $\sim$20-30%. When combined with available knowledge of the energy spectra, quantities such as the integral flux of (relatively abundant) species above (e.g.) some cutoff rigidity can now be modeled to an accuracy of $\sim$20% at solar minimum conditions. Because the model of Adams et al. appears to do a very reasonable job of accounting for cosmic ray composition and energy spectra, only minor updates and improvements to this aspect of the model are recommended; there is no apparent reason (within the context of this workshop) to derive a new model. The largest uncertainty in such descriptive models of cosmic rays results from the difficulty of predicting the level of solar modulation at some particular future time period, the effects of which are greatest at low energy. It is in this area of the temporal description of cosmic ray energy spectra that efforts at improvement can most profitably be directed.

Acknowledgements: This work was supported in part by NASA under grants NGR 05-002-160 and NAG5-722.

REFERENCES

Adams, J. H. Jr., Cosmic ray effects on microelectronics, part IV: *NRL Memorandum Report 5901* 1986.

Adams, J. H. Jr., R. Silberberg, and C. H. Tsao, Cosmic ray effects on microelectronics, part I: the near-earth particle environment, *NRL Memorandum Report 4506,* 1981.

Binns, W. R., R. K. Fickle, T. L. Garrard, M. H. Israel, J. Klarmann, E. C. Stone, and C. J. Waddington, The abundance of the actnides in the cosmic radiation as measured on HEAO-3, *Astrophys. J., 261,* L117, 1982.

Binns, W. R., T. L. Garrard, M. H. Israel, Micheal D. Jones, M. P. Kamionkowski, J. Klarmann, E. C. Stone, and C. J. Waddington, Cosmic ray energy spectra between ten and several hundred GeV/amu for elements between $_{18}$Ar and $_{28}$Ni - results from HEAO-3, submitted to the *Astrophys. J.,* 1987.

Brewster, N. R., P. S. Freier, and C. J. Waddington, The propagation of ultraheavy cosmic ray nuclei, *Astrophys. J., 264,* 324, 1983.

Brynak, B., N. Lund, I. L. Rasmussen, M. Rotenburg, J. Engelmann, P Goret, and E. Juliusson, The abundance of the elements with $Z > 26$ in the cosmic radiation, *Proc. 18th Internat. Cosmic Ray Conf., 2,* 29, 1983.

Cummings, A. C., reported at this workshop, 1987.

Dwyer, R. and P. Meyer, Cosmic-ray elemental abundances for 1-10 GeV per nucleon for boron through nickel, submitted to the *20th Internat. Cosmic Ray Conf.,* Paper OG 4.1-1, 1987.

Dwyer, R. and P. Meyer, Composition of cosmic ray nuclei from boron to nickel for 1200 to 2400 MeV per nucleon, *Astrophys. J., 294,* 441, 1985.

Engelmann, J. J., P. Goret, E. Juliusson, L. Koch-Miramond, P. Masse, A. Soutoul, B. Byrnak, N. Lund, B. Peters, I. L. Rasmussen, M. Rotenberg, and N. J. Westergaard, Elemental composition of cosmic rays from Be to Ni as measured by the French-Danish instrument on HEAO-3, *Proc. 18th Internat. Cosmic Ray Conf., 2,* 17, 1983.

Englemann, J. J., P. Goret, E. Juliusson, L. Koch-Miramond, N. Lund, P. Masse, I. L. Rasmussen, and A. Soutoul, Source energy spectra of heavy cosmic ray nuclei as derived from the French-Danish experiment on HEAO-3, *Astron. Astrophys., 148,* 12, 1985.

Fowler, P. H., M. R. W. Masheder, R. T. Moses, R. N. F. Walker, A. Worley, and A. M. Gay, Ariel VI measurements of ultra-heavy cosmic ray fluxes in the region $Z > 48$, *Proc. 19th Internat. Cosmic Ray Conf., 2,* 119, 1985.

Garcia-Munoz, M., and J. A. Simpson, The elemental abundances of hydrogen through nickel in the low energy cosmic rays, *Proc. 16th Internat. Cosmic Ray Conf., 1,* 270, 1979.

Garcia-Munoz, M., K. R. Pyle, and J. A. Simpson, The anomalous helium component in the heliosphere: The 1 AU spectra during the cosmic ray recovery from the 1981 solar maximum, submitted to the *20th Internat. Cosmic Ray Conf.,* paper SH 6.4-11, 1987.

Juliusson, E., J. J. Engelmann, J. Jorrand, L. Koch-Miramond, N. Lund, I. L. Rasmussen, and M. Rotenberg, The galactic cosmic ray enery spectra as measured by the French-Danish instrument on HEAO-3, *Proc. 18th Intl. Cosmic*

Ray Conf., 2, 21, 1983.
Lezniak, J. A., and W. R. Webber, *Astrophys. J., 223,* 676, 1978.
Mason, G. M., The composition of galactic cosmic rays and solar energetic particles, to be published in *Rev. Geophys. Space Phys.,* 1987.
Mewaldt, R. A., The elemental and isotopic composition of galactic cosmic ray nuclei, *Rev. Geophys. Space Phys., 21,* 295, 1983.
Mewaldt, R. A., A. C. Cummings, J. H. Adams, Jr., P. Evenson, W. Fillius, J. R. Jokipii, R. B. McKibben, and P. A. Robinson, Jr., Toward a descriptive model of galactic cosmic rays in the heliosphere, presented at this workshop, 1987.
Mewaldt, R. A., J. D. Spalding, and E. C. Stone, The isotopic composition of the anomalous low energy cosmic rays, *Astrophys. J., 283,* 450, 1984.
Mewaldt, R. A., ^{3}He in galactic cosmic rays, *Astrophys. J., 311,* 979, 1986.
Meyer, J.-P., Galactic cosmic ray composition, *Proc. 19th Intl. Cosmic Ray Conf., 9,* 141, 1985.
Ormes, J. F. and R. J. Protheroe, Implications of HEAO 3 data for the acceleration and propagation of galactic cosmic rays, *Astrophys. J., 272,* 756, 1983.
Simpson, J. A., Elemental and isotopic composition of the galactic cosmic rays, *Ann. Rev. Nucl. and Particle Sci.,* ed. J. D. Jackson, H. E. Grove, and R. Y. Schwitters, (Pala Alto: Annual Reviews Inc.), *33,* 706, 1983.
Stone, E. C., C. J. Waddington, W. R. Binns, T. L. Garrard, P. S. Gibner, M. H. Israel, M. P. Kertzman, J. Klarmann, and B. J. Newport, The abundance of ultraheavy elements in the cosmic radiation, submitted to the *20th Internat. Cosmic Ray Conf.,* paper OG4.3-1, 1987.
Webber, W. R., R. L. Golden, and R. A. Mewaldt, A re-examination of the cosmic ray helium spectrum and the ^{3}He/^{4}He ratio at high energies, *Astrophys. J. 312,* 178, 1987a.
Webber, W. R., R. L. Golden, and S. A. Stephans, Cosmic ray proton and helium spectra from 5 -2000 GV measured with a magnetic spectrometer, sumitted to the *20th International Cosmic Ray Conference,* paper OG 4.1-2, 1987b.
Webber, W. R., and J. A. Lezniak, The comparative spectra of cosmic ray protons and helium nuclei, *Astrophys. Space Sci., 30,* 361, 1974.

THE ANOMALOUS COSMIC-RAY COMPONENT

A. C. Cummings and E. C. Stone

California Institute of Technology, Pasadena, CA 91125 USA

This brief report is intended to update the "anomalous component" section of the summary report of the galactic cosmic-ray working group (Mewaldt et al., 1987), which was drafted at the March 1987 *Workshop on the Interplanetary Charged Particle Environment* at the Jet Propulsion Laboratory. The description of the spectrum of the anomalous cosmic-ray component is contained in section 3.3 of that report. That description is based on data analyzed through day 310 of 1986, and in it we proposed that the energy spectrum of the various species of the anomalous component could be derived by scaling from two generic spectra. Two generic spectra were required because the energy spectrum of the anomalous component changed shape near the time of the solar magnetic field reversal in 1980. These two generic spectra are shown in Figure 2 of the summary report.

We also indicated in the summary report that "it remains to be seen, however, whether the spectrum over the next few years will maintain this new shape or will return to its 1972-1977 shape." Therefore, we have continued to monitor the energy spectrum to see whether or not the new spectral shape is truly characteristic of the new magnetic polarity epoch of the Sun. We now find evidence that it is not.

In Figure 1 we show fourteen 52-day average composite anomalous spectra from the middle of 1985 to the latest available data. The last four spectra (periods 11 - 14) have been added after the Workshop results were incorporated into the summary report. The dashed line is the spectrum from the last solar minimum period, normalized to the current spectrum at higher energies. It appears that the spectrum changed after period 10. For example, from period 10 to 14 the peak energy shifts by near-

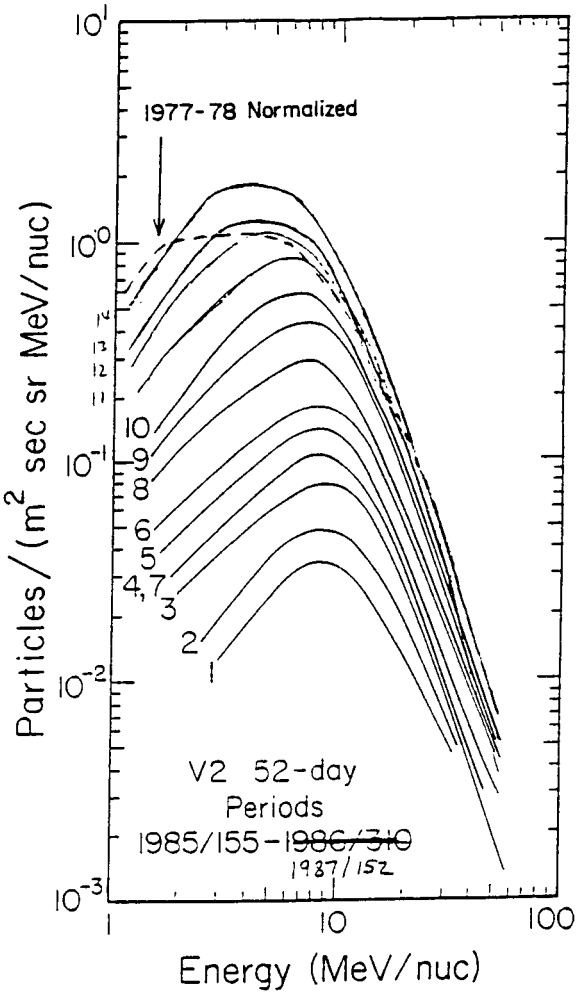

Figure 1.

ly a factor of 2 to lower energies. This peak energy is still higher than at the last solar minimum, by ~30 to 50%, and the spectrum appears to be somewhat differently shaped. However, since the recent changes have been rapid, we caution that we must still wait to see how the spectrum evolves over the next year or so before we can make definitive statements about the spectral shape of the anomalous component. Certainly, it appears incorrect to say that there are only two generic shapes for the spectrum. A more accurate description at this time would be: it appears that the spectral shape changed in ~1980, remained approximately unchanged for ~6 years, and is now undergoing a rather rapid evolution back toward the shape it had in 1977-78. For future updates, please contact the authors.

Acknowledgements. We are grateful for the contributions of R. E. Vogt in his tenure as Principal Investigator for the Cosmic Ray System (CRS) on the Voyager spacecraft. We also appreciate the contributions of the other Voyager CRS team members at Caltech and the Goddard Space Flight Center. This work was supported in part by NASA under contract NAS 7-918 and grant NGR 05-002-160.

References

Mewaldt, Cummings, Adams, Jr., Evenson, Fillius, Jokipii, McKibben, and Robinson, Toward a descriptive model of galactic cosmic rays in the heliosphere, Summary report of the galactic cosmic-ray working group of the *Workshop on the Interplanetary Charged Particle Environment,* JPL, March, 1987.

GRADIENTS OF GALACTIC COSMIC RAYS AND ANOMALOUS COMPONENTS

R. B. McKIBBEN
Enrico Fermi Institute, University of Chicago
933 E. 56th St., Chicago, Ill., 60637

ABSTRACT

Measurements of radial and latitudinal gradients of galactic cosmic rays and anomalous components now cover radii from 0.3 to 40 AU from the sun and latitudes up to 30° above the ecliptic plane for particle energies from ~10 MeV/n up to relativistic energies. The most accurate measurements cover the period 1972-1987, which includes more than one full 11 year cycle of solar activity. Radial gradients for galactic cosmic rays of all energies and species are small ($\lesssim$ 10%/AU), and variable in time, reaching a minimum of near 0%/AU out to 30 AU for some species at solar maximum. Gradients for anomalous components are larger, of order 15%/AU, may show similar time variability, and are relatively independent of particle species and energy. Latitude gradients have only recently been measured unambiguously by the Voyager 1 and 2 spacecraft. For the period 1985-86 the intensity decreased away from the ecliptic for all species and energies. For galactic cosmic rays, the measured gradients are ~0.5%/degree near 20 AU, while for anomalous components the gradients are larger, ranging from 3-6%/degree. Comparison with a similar measurement for anomalous helium in 1975-76 suggests that the latitude gradients for anomalous components have changed sign between 1975 and 1985. For galactic cosmic rays, the available evidence suggests no change in sign of the latitudinal gradient for relativistic particles.

INTRODUCTION

After many years of measurements by sensors on the ground, in high altitude balloons, and on spacecraft, the cosmic radiation environment of the earth is well characterized (e.g. Adams, 1986). At low energies ($\lesssim$ few GeV) the cosmic ray intensity observed at earth is much lower than that which exists in the interstellar medium. The intensity reduction is a result of the process of solar modulation, which is caused by the interaction of cosmic rays with the interplanetary magnetic fields carried outward from the sun by the solar wind. The modulated intensity is determined by a balance between inward diffusion of the cosmic rays through the irregular interplanetary magnetic fields, gradient and curvature drifts as a result of the non-uniform nature of the fields, outward convection by the solar wind, and cooling, or adiabatic deceleration, of the cosmic ray gas as a result of its coupling to the diverging solar wind (see, for example, Quenby, 1984). Above a few GeV/nucleon the effects of modulation on the intensity are small, but cosmic rays with interstellar energies below a few hundred MeV/nucleon are effectively excluded from the inner heliosphere by modulation. As seen from Figure 1, which shows the intensity of relativistic cosmic rays as measured by the Climax neutron monitor and the monthly sunspot number, the cosmic ray intensity in the heliosphere is highest at the minimum of the 11-year solar activity cycle. However, observations from 1 to near 40 AU in near-solar-minimum conditions show that even at solar minimum the intensity at low energies is strongly affected by modulation.

As a result of the modulation, we have very little reliable information concerning the interstellar intensities and spectra of galactic cosmic rays at energies below ~1 GeV/nucleon.

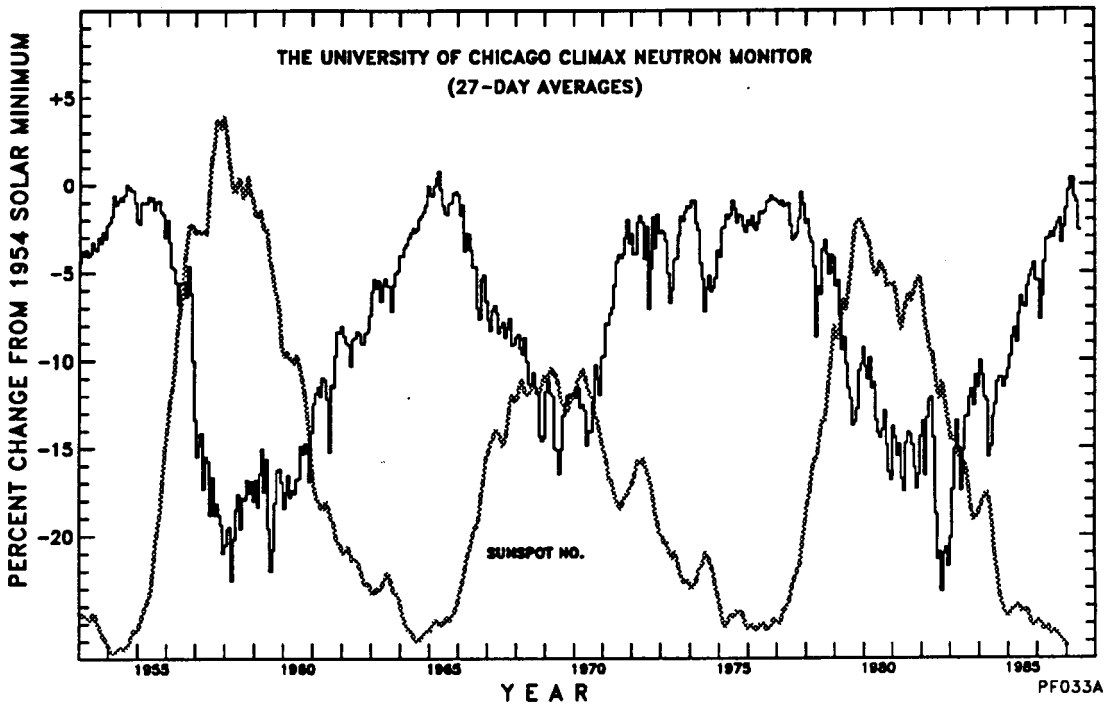

Figure 1. Monthly average Climax neutron monitor counting rate and smoothed sunspot number.

Such information as does exist is based on comparison of the modulated electron spectrum observed at 1 AU with the interstellar electron spectrum deduced from analysis of radio observations of synchrotron emission in the galactic magnetic field. Such a comparison makes it possible to deduce the strength of the modulation and, given a model for the modulation process, to "demodulate" the observed nucleonic cosmic ray spectrum. For example, Evenson et al. (1983) have found that an interstellar proton spectrum of the form

$$\frac{dJ}{dE} = 3.73 \times 10^{9}[T+1335-835\exp(-T/1000)]^{-2.75} \quad (s\ m^2\ sr\ MeV/n)^{-1} \qquad (1)$$

provides a satisfactory fit to observed modulated intensities when used with a quasi-steady, spherically symmetric model of modulation. The analysis does not lead to a unique form for the interstellar spectrum, however. For example, Figure 2 , compiled by Garcia-Munoz, Pyle, and Simpson (private communication, 1987), shows three different interstellar proton and helium spectra that have recently been proposed as consistent with modulated spectra at 1 AU. Partly because of this uncertainty, we cannot now deduce accurately either the location of the boundary or the intensity at the boundary for particle energies $\lesssim 1$ GeV.

As part of an experimental program to determine the mechanisms of modulation and the physical scale of the modulation region, measurement of radial and latitudinal gradients of galactic cosmic rays has been a principal activity of experimental cosmic ray physics since the first spacecraft left the orbit of earth. By far the most productive period for such measurements has been the period from the launch of Pioneer 10 in 1972 until the present. In this period, various spacecraft have explored the heliosphere over a radial range from the orbit of Mercury to ~40 AU from the sun, and over a latitude range from near the ecliptic to ~30° north latitude. Figure 3 shows ecliptic projections of the trajectories of the Voyager and Pioneer spacecraft, which have performed the most extensive exploration of the heliosphere. Whereas before these missions estimates of the radius of the modulation region in the heliosphere had been in the neighborhood of 10 AU, current estimates range from ~ 50 AU to more than 100 AU.

The goal of this paper is to summarize what we currently know concerning the spatial and temporal variations of the galactic cosmic ray intensity and of the anomalous components, which are nuclei of He, N, O, and Ne, (and, more recently reported, of C and Ar (Cummings and Stone, 1987)) observed at energies $\lesssim$100 MeV/nucleon and believed to be accelerated in the outer regions of the heliosphere. While I have tried to represent fairly the results of all current work, as this workshop was intended primarily to provide guidance for spacecraft and mission design, I have not attempted to present as exhaustive a survey as would be found in more thorough review articles such as those recently prepared by McKibben (1987) or Quenby (1984). I have further restricted the scope of this review to nuclei below a few GeV/nucleon, which are the most significant from the point of view of producing single event upsets or latchups in circuit devices, and, with a few exceptions, to the period 1975 to 1987, which includes one complete 11 year cycle of solar activity. This is a period in which measurements were available from a number of spacecraft at significant distances (several AU) from the orbit of earth, so that the effects on the values of gradients of systematic errors in the intensity measurements at the various spacecraft is minimized.

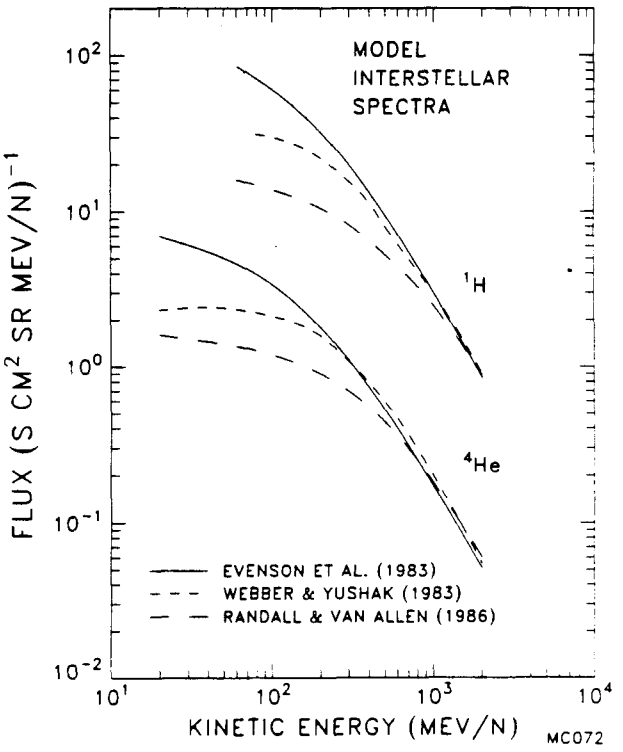

Figure 2. Estimated interstellar cosmic ray proton and helium spectra

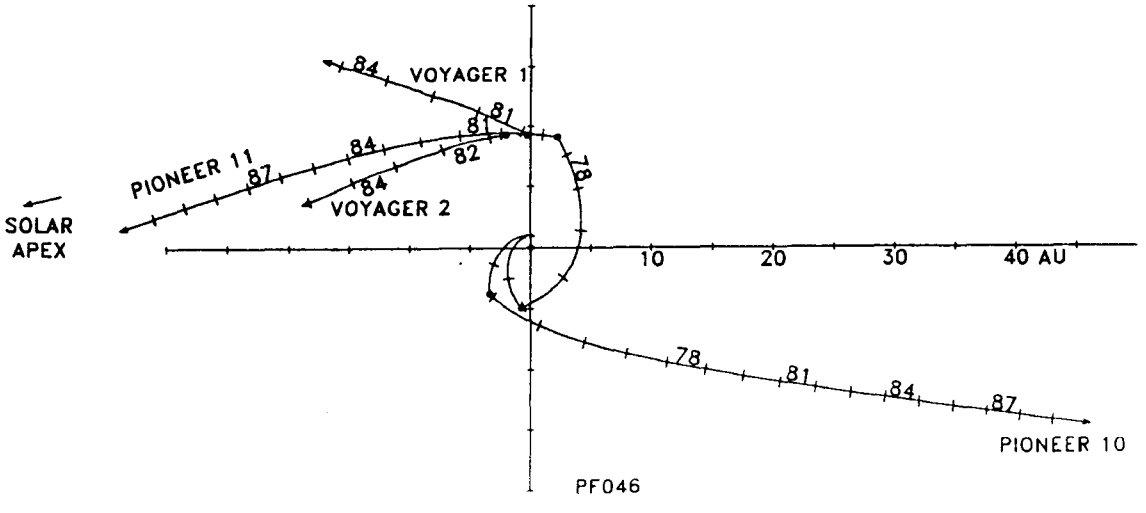

Figure 3. Pioneer 10/11 and Voyager 1/2 trajectories projected on the ecliptic.

THEORETICAL EXPECTATIONS

The theory of galactic cosmic ray modulation is well developed. The governing equations were first written down by E.N. Parker (1965) and have not been fundamentally modified since. However, the critical parameters which govern the modulated intensity remain poorly known. These parameters include, for example, the size of the modulation region and the values, spatial, and energy dependences of the components of the interplanetary diffusion tensor. As a result, the use of the equations has been more explanatory than predictive, and theoretical arguments concerning the relative importance of the terms describing the physical processes of modulation remain unsettled.

Historically, most analysis of galactic cosmic ray modulation and of spatial intensity gradients has been performed in the context of a quasi-steady, spherically symmetric modulation model. For such a model, latitude gradients, by definition, do not exist, and the predictions for the radial gradient G_r are particularly simple, being given at any point in the heliosphere by

$$G_r(r,T) = C(T)V_{SW}/\kappa(r,T) \qquad (2)$$

where κ is the effective radial interplanetary diffusion coefficient at radius r, V_{SW} is the solar wind velocity, and C(T) is the Compton-Getting factor at kinetic energy T MeV/nucleon. C(T) in turn is given by

$$C(T) = (2-\alpha\gamma)/3 \qquad (3)$$

where γ is the power law spectral index of the cosmic ray spectrum for the particles of interest at energy T, $\alpha = (T+2mc^2)/(T+mc^2)$, and mc^2 is the nucleon rest energy. Since below ~100 MeV/n, the modulated galactic cosmic ray spectra take the form $dJ/dT \propto T^{+1}$, $C(T) \cong 0$ at these low energies, and gradients are expected to be small. For anomalous components, $\gamma < +1$, so that gradients for these species should be larger, as is observed. $\gamma<+1$ for higher energy galactic cosmic rays as well, so that larger gradients might be expected. However, at higher energies, κ is larger than at low energies, so that the gradients remain small.

Although equation (2) offers useful guidance as to the systematics of the dependence of radial gradients on particle energy through knowledge of the spectral form, in practice the diffusion coefficient, κ, is so poorly known as a function of position and energy that useful numerical predictions for the value of G_r can not be obtained. Furthermore, equation (2) is based on a greatly oversimplified model of modulation. More realistic models incorporate time dependence (e.g. O'Gallagher and Mazlyar, 1976; Perko and Fisk, 1983), departures from spherical symmetry (e.g. Newkirk and Fisk, 1985), and the influence of gradient and curvature drifts (e.g. Jokipii, 1986; Potgieter and Moraal, 1985).

A unique feature of models for modulation which incorporate drifts is sensitivity of the modulated cosmic ray intensity to the sign of the dipole component of the solar magnetic field, which reverses near maximum solar activity approximately every 11 years. The last reversal occurred in 1980 (Webb et al., 1984). A number of qualitative and semi-quantitative predictions can be made concerning the behavior of the spectra, intensities and gradients of galactic cosmic rays and anomalous components upon reversal of the solar dipole magnetic field (e.g. Jokipii, 1986; Potgieter and Moraal, 1985). Most such predictions lie outside the scope of this report, but two that are relevant are a) that for the sign of the dipole field pertaining after 1980, radial gradients should be larger than for the period of opposite polarity (~1970-80), and b) that upon reversal of the solar dipole field gradients in latitude should at least change markedly, and in some cases change sign. As will be demonstrated below, observations do not show the predicted increase in radial gradients, but they do appear to show a reversal of latitude gradients for at least some particle species.

Unfortunately, for all of the more sophisticated (and realistic) models involving time dependence, drifts, or other effects of non-spherical symmetry, in order to obtain

quantitative predictions it is necessary to make assumptions concerning heliospheric structure in regions for which little or no information exists. Furthermore, the models are in general so complex that results can be obtained only by numerical solution of specific cases. As a result, the predictions of these models, especially for regions not yet explored, are likely to undergo significant changes as we learn more about the structure of the helisophere.

OBSERVATIONS

RADIAL GRADIENTS OF THE INTEGRAL INTENSITY (E $\gtrsim$100 MeV/n)

The most frequently reported measurement of a gradient for the galactic cosmic ray intensity is for the integral intensity above a threshold energy, usually of the order of ~100 MeV/n. Because most of the cosmic ray intensity is at energies well above 100 MeV/n, for the modulated cosmic ray spectrum the mean energy of particles contributing to the integral intensity is of the order of 2 GeV. The gradient measurements are of two types, based either on counting rates from a single, shielded detector which responds to all particles with sufficient energy to penetrate the shielding, or on coincidence counting rates from multidetector cosmic ray telescopes which respond to particles with sufficient energy to penetrate the complete stack of detectors in the telescope. The latter generally provide a higher quality measurement since the requirement for mutiple detector firings suppresses many forms of background, and since pulse height analysis is usually available from one or more detectors in the telescope to allow the particles contributing to the counting rate to be identified, background contributions to be estimated, and gains and discriminator settings to be monitored. Furthermore, especially for experiments on the Voyager and Pioneer spacecraft, the RTG power sources provide a gamma ray backgound that grows with time. Gradient analyses based on single detector counting rates must take great pains to avoid confusing the effects of the increasing background with the effects of a radial gradient (see, for example, Van Allen and Randall, 1985, for a thorough discussion of this problem).

In Figure 4 we show as a function of time measurements of the radial gradient of the integral intensity reported by the University of Chicago using cosmic ray telescopes on board Pioneer 10 and various IMP spacecraft at 1 AU. Figure 4A shows the 27 day averages of the intensity, I, measured at the two observing points, and Figure 4B shows the radial gradient, G_r, calculated as

$$G_r = \frac{\ln[\, I(P10)/I(IMP)]}{[R(10)-1]} \qquad (4)$$

where R(10) is the radial position of Pioneer 10. In order to minimize the effect of propagating disturbances in the solar wind on the gradient, it has become customary to compare Pioneer and IMP counting rates at times shifted by the propagation time for the solar wind from 1 AU to the position of Pioneer 10. This procedure has the effect of removing some of the larger temporal fluctuations in the measured gradient, but has little effect on the long-term average value of the gradient.

From Figure 4, it is clear that temporal fluctuations of the intensity in response to variations in solar activity have been comparable to the total effect of the radial gradient on the Pioneer intensity up to the present time. Therefore, it is possible to measure gradients only by comparison of well matched counting rates at two locations. It is also clear that the value of the gradient itself varies in response to the solar activity cycle. The largest average gradient, amounting to ~4%/AU, was observed early in the Pioneer 10 mission during a period of extended near-solar-minimum conditions. This large value was confirmed by Pioneer 11 measurements, and by a similar measurement from the GSFC/UNH telescope, also on Pioneer 10. The largest value observed subsequently was ~3%/AU near solar maximum in 1981-83.

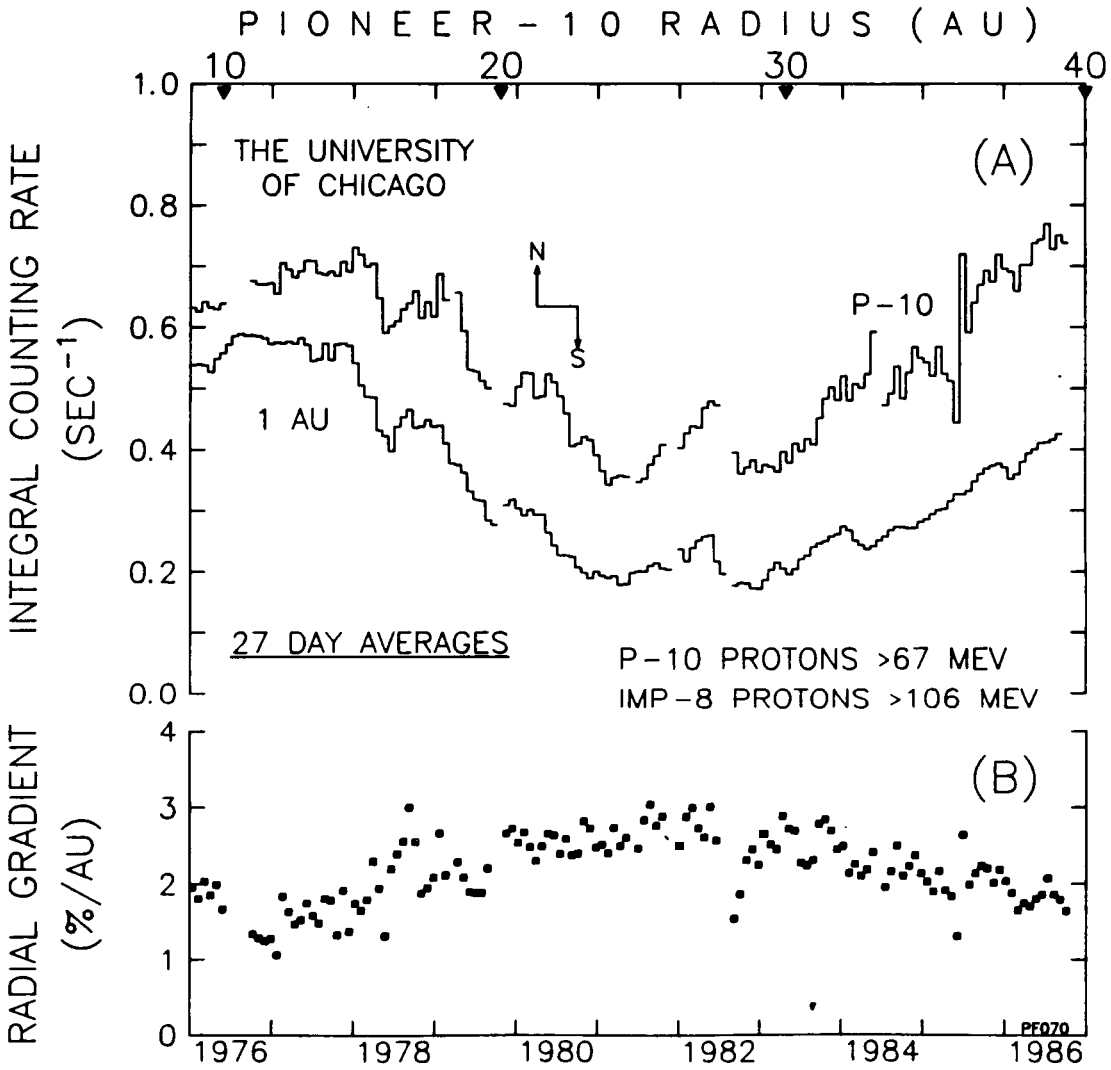

Figure 4. Integral intensities and radial gradients from Pioneer 10 and IMP 8. Reversal of the solar magnetic polarity is indicated in 1980.

For comparison, values of the integral gradient measured in each year for the period 1975-1986 reported by the University of Chicago and by other investigators are listed in Table 1. As values of the gradients were not generally reported on a yearly basis, the entries in the Table are in some cases fairly crude averages derived from published figures. They should be sufficiently accurate to indicate the trends of the data, but the original references should be consulted if greater accuracy is desired. The measurements of Lopate et al. (1987) and of Webber and Lockwood (1987) make use of coincidence counting rates from multi-detector telescopes. The other measurements are based on single detector counting rates. The agreement between the measurements is in general reasonably good, and it is clear that the value of the integral gradient is no larger than a few per cent per AU.

Note that at the time of the reversal of the solar dipole field in 1980, no significant changes in the gradient were observed, and that the value of ~1.5-2%/AU observed in the present near-solar-minimum conditions is not larger than that observed in the previous solar minimum. Both observations are inconsistent with the predictions of drift-dominated modulation models.

Table 1. Integral Radial Gradients (E>100MeV)
(Per cent/AU)

	Lopate et al. (1987)	Webber & Lockwood (1987)	Van Allen & Randall (1985)	Fillius† et al. (1985)	Venkatesan et al. (1986)	Max. Radius (AU)	
	P-10 IMP-8	P-10,11 VGR-1,2 IMP-8	P-10,11	P-10,11	VGR-2 IMP-8	VGR-2	P-10
1975			2.06±0.2*	1.4±0.2			8.9
1976	1.6±0.4	-----	"	1.5±0.3			11.7
1977	1.6±0.3	2.77±0.35	"	1.5±0.3		1.8	14.7
1978	2.1±0.4	2.81±0.37	"	1.9±0.1		4.7	17.5
1979	2.3±0.4	-----	"	1.9±0.2		6.1	20.5
1980	2.5±0.2	3.16±0.31	"	1.8±0.1		7.8	23.3
1981	2.7±0.3	3.15±0.30	"	1.7±0.1	3.7±0.3	9.7	26.2
1982	2.7±0.3	-----	"	1.5±0.3	3.0±1.0	10.7	28.5
1983	2.5±0.3	2.19±0.20	"	1.3±0.2	2.8±0.7	13.0	31.7
1984	2.2±0.2	1.78±0.12	"	1.1±0.1	2.3±0.7	15.9	34.5
1985	2.0±0.2	1.77±0.25	"			18.6	37.2
1986	1.8±0.2					21.0	40.0

† M1 detector, yearly values estimated from Fig. 3 of reference.
* Mean value only quoted for 1972-1985.
Variations in range 0-4%/AU reported but not identified as to time of occurrence.

The temporal variations in the value of the gradient are not well understood, and thus future behavior of the gradient cannot be confidently predicted. Also, there is no compelling evidence for changes in the value of the gradient as a function of radius. Therefore, for guidance in design, a conservative approach would be to assume no radial dependence and adopt a value of 4%/AU, equal to the largest persistent gradient measured since 1972. An upper limit on the intensity that can be reached is set by the interstellar spectrum. For the spectrum of Evenson et al. (1983) this corresponds to a flux of ~1.6 (sec cm^2 sr)$^{-1}$ above 100 MeV/n. Starting from the intensity measured at Pioneer 10 at 40 AU in 1987, with a radial gradient of 4%/AU the interstellar intensity would be reached at a radius of ~65-70 AU, whereas with the measured ~2%/AU gradient the interstellar intensity would be attained at a radius of ~90-100 AU.

3.2 RADIAL GRADIENTS IN DIFFERENTIAL ENERGY WINDOWS

Less frequently reported, but more useful for tests of modulation theory, are gradients of the intensity of particles identified as to particle species and energy. Measurement of such "differential gradients" requires use of cosmic ray telescopes in which particles can be brought to rest, or at least significantly slowed, and thus identified by charge and energy per nucleon. As for the integral gradients, it is important to compare measurements at 1 AU and at larger radii that are well matched in terms of energy and particle species. Such measurements are at present available only from the University of Chicago and GSFC/UNH telescopes on Pioneer 10 and 11 (and IMP 8) and from the CRS telescopes on Voyager 1 and 2.

In Figure 5 we show a sample of data for 2 energy ranges each for protons and helium from the University of Chicago telescopes on Pioneer 10 and IMP 8, taken from Lopate et al. (1987). The lower half of each panel contains simultaneous intensity measurements from each spacecraft for the given species and energy range, while the upper half contains the radial

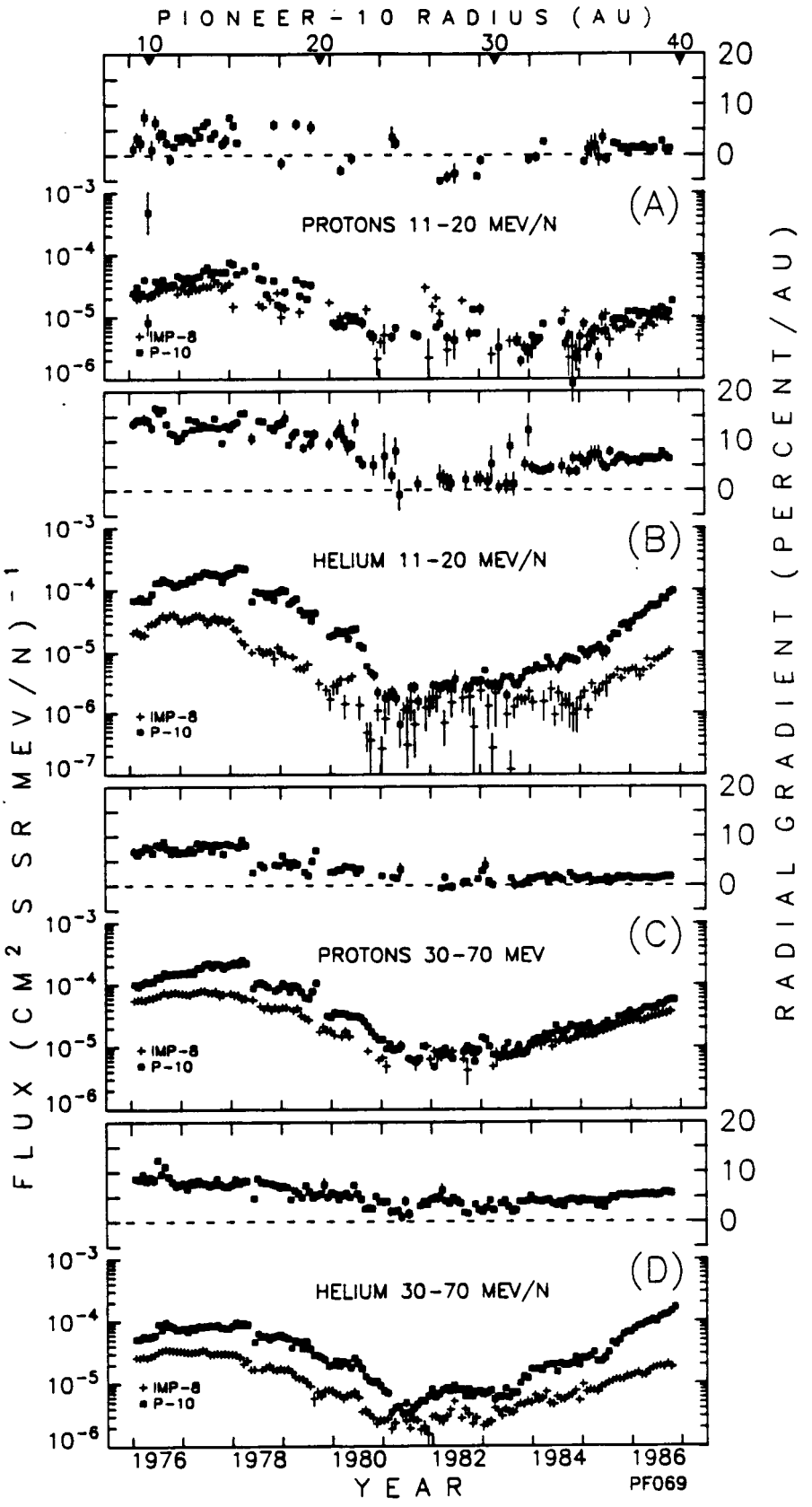

Figure 5. Fluxes and radial gradients for protons and helium in differential energy windows.

gradient computed, as for the integral gradients, by comparing propagation-shifted measurements from Pioneer 10 and IMP. The protons represent a pure galactic component, whereas the helium energy ranges contain a strong admixture of the anomalous helium component except for the period near maximum solar modulation. The radial position of Pioneer 10 is indicated along the top axis. Sample snapshots of the radial dependence of the intensity taken from the same data set at yearly intervals are shown in Figure 6, together with the estimated interstellar intensity for galactic cosmic rays of the same energy and charge, based on the interstellar spectra of Evenson et al. (1983). For the helium, which contains the anomalous component, the estimated interstellar density shown is most likely much smaller than the intensity of the anomalous component near the boundary. The upper limit to the intensity of anomalous components at the boundary is set by the energy density of the solar wind and interplanetary magnetic field at the boundary.

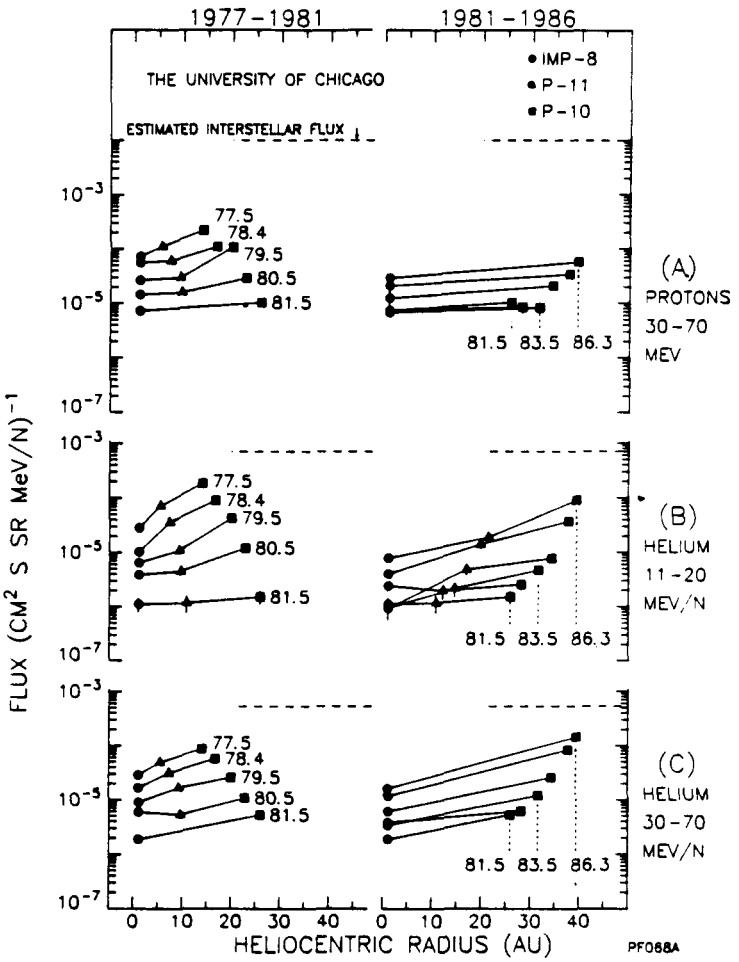

Figure 6. Yearly snapshots of low energy proton and helium flux vs. radius.

In all four panels of Figure 5, the magnitude of temporal variations in response to the solar activity cycle exceeds the magnitude of the effects due to the radial gradient between 1 and 40 AU. Thus, once again, comparison of measurements at two different radii is required for measurement of a gradient. Furthermore, the gradients themselves exhibit strong time dependence. Most striking is the near disappearance of the radial gradient for low energy galactic protons during the period of maximum solar modulation, and the strong reduction in the value of the gradient for the mixed anomalous and galactic helium. Such an effect was not anticipated from available modulation models. The reduction of the helium gradient appears to coincide with the disappearance of the anomalous helium spectrum at Pioneer 10 and with the reversal of the solar dipole polarity, both of which occurred in 1980. As is discussed elsewhere in these proceedings (Cummings, 1987; Jokipii, 1987; Mewaldt et al, 1987), models of modulation incorporating drifts provide reason to expect significant changes in the anomalous component spectra upon reversal of the solar magnetic polarity. However, they do not predict disappearance of the radial gradient. Furthermore, in contradiction to the observations, such models in general predict that in the approach to the new solar minimum in 1987, radial gradients should be larger than in the solar minimum of the 1970's.

Other measurements for differential radial gradients for these and for other energy intervals and species have been reported by McDonald et al. (1986) for protons and helium in energy intervals up to 380 MeV/nucleon, and for anomalous oxygen by Lopate et al. (1987) and Cummings et al. (1987a, b). Table 2 contains a selection of these observations for the years

Table 2. Differential Radial Gradients

Species	Energy Range (MeV/n)	Measured Gradients (Per cent/AU) 1977	1982	1986	Reference
Protons	11-20	4.2±1.6	-3.7±1.6*	1.5±0.5	A
Protons	29-67	7.7±0.8	0.7±1.2	1.5±0.2	A
	30-55	8±3**	2.5±1.5**	2.5±1.5**	B
Protons	140-240	6.5±5.5**	3±3*?	3.5±0.5	B
Helium†	11-20	12.2±0.2	-1.5±2.4	5.9±0.6	A
	10-21	17±5**	3±1**	5.0±0.5	B
Helium†	29-67	7.6±0.6	3.6±1.4	5.5±0.2	A
	30-55	10±5**	3.0±0.5**	5.7±1.3**	B
Helium	150-380	4.5±2.5**	4.0±0.5**	3±1**	B
Carbon	21-37	---	----	~2	A
Oxygen†	5.4-8.5	---	----	15.5±2.1	C
	8.5-13.9	---	----	15.3±2.0	C
	13.9-30.6	---	----	12.3±2.3	C
	24-43	---	----	~8	A

Notes

* Possible Solar Contamination

** Corresponds to range of values quoted.

† Contains anomalous component

References

A) Lopate et al. (1987)

B) McDonald et al. (1986)

C) Cummings et al. (1987b)

1977, 1982, and 1986, corresponding to periods before, during, and after the most recent maximum in the 11 year solar modulation cycle. Agreement between the various measurements is in general excellent.

If the observed gradients for galactic cosmic rays are extended in radius, the radius at which the estimated interstellar intensity is attained varies strongly with the phase of the solar cycle. For example, for 1977 and before, the 29-67 MeV proton observations suggest that the boundary would be reached near 50 AU, but in 1986, the observed gradient suggests that the boundary lies near 300 AU. These numbers should not be taken seriously, however, for it is likely that the radial gradient depends strongly on radius in some region near the boundary. There are some indications of a radial dependence for the radial gradients in observations made between Pioneer 10, Voyager 2, and 1 AU and reported by McDonald et al. (1986), but it is so far difficult to organize the observed variations into a systematic model that might allow general conclusions and predictions to be made concerning radial dependence of the gradients.

The observational situation for differential gradients may be summarized by the statement that radial gradients for galactic cosmic rays at low energy ($E \tilde{<} 100$ MeV/n) are always small ($\tilde{<} 10\%$/AU) and positive. Gradients for anomalous component species are

somewhat larger, of the order of 15%/AU, independent of species. Gradients of galactic cosmic rays show temporal variations associated with changes in the level of solar activity, but these changes are not well understood in terms of current models. Therefore, it is not possible to predict with any confidence the behavior of the gradients in future phases of the solar activity cycle.

GRADIENTS IN HELIOSPHERIC LATITUDE

Recently, measurement of gradients in heliospheric latitude has become a very active area of research. In part this is because current modulation models tend to emphasize the importance of conditions at moderate and high latitudes for determining the modulated intensity near the ecliptic, and in part this is because two spacecraft, Voyager 1 and Pioneer 11, are significantly above the ecliptic, at ~30° and 17° latitude, respectively, so that direct measurements of latitude gradients are possible.

Ground based or earth-orbit observations have also been used to measure gradients in latitude with respect to the heliospheric "equatorial" current sheet which separates positive and negative magnetic polarity in the solar wind, and which drift-dominated models of modulation suggest may be the crucial symmetry plane for modulation of cosmic rays. Since the current sheet usually has a large inclination to the ecliptic, an observer at earth may sample a large range in magnetic latitude in the course of one solar rotation. For integral intensity measurements made with neutron monitors (mean energy ≡ a few GeV), Newkirk and Fisk (1985), and Newkirk et al. (1985, 1986) have performed an extensive study of gradients with respect to the current sheet, using K-coronameter observations to infer the inclination of the sheet. Newkirk et al. (1986) have also extended the measurement of latitude gradients to lower energies by applying the same techniques they used for the integral measurement to spacecraft observations. For the integral flux, for the years 1973-77, and, in preliminary work, 1984, they find a persistent average negative gradient of ~2.7%/AU (~0.05%/degree) at 1 AU to latitudes of ±30°. They further find that the magnitude of the gradient depends upon rigidity approximately as $P^{-\alpha}$ where α is in the range $0.72 < \alpha < 0.86$. Drift-dominated models of modulation predict that near the current sheet, the average latitudinal gradient should be negative for all phases of the solar cycle, and the observed magnitude is consistent with the choice of reasonable parameters in such models (e.g. Jokipii and Kota, 1986). However, a significant change in magnitude should have been expected after 1980, which, at least in the preliminary analysis of the observations, does not seem to have occurred.

Using direct measurements of the integral intensity from Voyager 1 at high latitude and Voyager 2 near the ecliptic, Christon et al. (1985, 1986a) have used a complex multi-parameter analysis to deduce the existence of a negative gradient of ~2%/AU (~0.5%/degree) away from the current sheet near a radius of 15 AU in 1981-83. In data obtained from these spacecraft after mid-1985, clear evidence for a latitude gradient appears even without sophisticated analysis, since the intensity measured by both integral and differential energy channels on Voyager 1 at latitudes >25° has been lower than that at Voyager 2 near the ecliptic, despite the fact that Voyager 1 is about 6 AU further from the sun than Voyager 2, and that radial gradients measured between spacecraft in the ecliptic continued to be positive outwards (Christon et al., 1986b; McDonald and Lal, 1986; Cummings et al., 1987a, b). Appearance of these large and unambiguous latitude gradients appears to have been associated with a decrease in the inclination of the current sheet to below the latitude of Voyager 1 (e.g. Christon et al., 1986b).

For galactic cosmic rays, the gradients in latitude are reported to be of order 0.5%/degree, with little dependence on particle rigidity (McDonald and Lal, 1986). For anomalous components, the gradients appear to be much larger, of order 3-4%/degree and 1-2% degree for anomalous oxygen and anomalous helium, respectively, in late 1985 - early 1986 (Cummings et al., 1987a) and 3-6%/degree for both species later in 1986 at radii near 28 AU (Cummings et al., 1987b). In terms of models of modulation, it is possible to interpret these

results using either drift-dominated or drift-free models of modulation, in the latter case appealing to an observed positive gradient in solar wind velocity away from the current sheet (Newkirk and Fisk, 1985). Drift-free models would predict a negative gradient for both signs of the solar magnetic polarity, whereas drift-dominated models might predict a reversal in sign of the gradient upon reversal of the polarity, depending on the particle species and energy and the latitude range sampled.

Prior to the recent Voyager observations, the only positive reported measurement of a latitude gradient is that performed with Pioneer 11 in 1975-76, when the spacecraft rose to a heliographic latitude of 16° at a radius of ~4 AU (Bastian et al., 1979; McKibben et al, 1979). In these observations, evidence for a latitude gradient of ~2-3%/degree positive away from the ecliptic plane was reported. The correlation between intensity and latitude was significant to >4σ, but temporal variations could not be excluded absolutely as a source for the effect. Nevertheless, the existence of a positive latitude gradient for the anomalous helium provided the simplest interpretation of the observations. No statistically significant latitude gradients were found for galactic cosmic ray protons or for the integral intensity of galactic cosmic rays.

If the interpretation of the Pioneer 11 observations as a latitude gradient is correct, then these observations show a reversal of the latitude gradient, at least for the anomalous helium, in two successive solar activity cycles, consistent with predictions of drift-dominated models. Thus, it may be expected that following the field reversal anticipated in ~1991, latitude gradients for anomalous components may again be positive away from the ecliptic. It is risky to extend this conclusion to galactic cosmic rays, however, for the anomalous components most likely are accelerated in a localized region within the heliosphere, whereas galactic cosmic rays are incident uniformly and isotropically on the boundary of the modulation region. Thus, the effects of modulation on the galactic and anomalous component cosmic rays differ significantly. Indeed the only experimental reports of latitude gradients for galactic cosmic rays prior to the 1980 field reversal suggest no change in the sign of the latitude gradient (Fisk and Newkirk, 1985;, Newkirk et al., 1985, 1986).

In summary, the most solid evidence for the existence of latitude gradients to date is that provided by Voyager 1/2 observations for the period after 1985. The gradients are larger for anomalous components (~3-6%/degree) than for galactic cosmic rays (~0.5%/degree), and are relatively independent of rigidity for galactic cosmic rays. For the anomalous helium, a previous measurement by Pioneer 11 in 1975-76 suggests that the sign of the latitude gradient reversed between 1976 and 1985. No such conclusion is warranted at present for galactic cosmic rays. Extension of these observations to latitudes higher than the 30° attained by Voyager 1 would be very uncertain.

SUMMARY

At the present time, experimental knowledge of cosmic ray radial and latitudinal gradients covers the region from 0.3 to 40 AU, and latitudes from the ecliptic northward to 30°. In this region, the radial gradients are small (<10%/AU for galactic cosmic rays of all energies, ~15%/AU for anomalous components) and variable in time. Latitude gradients for anomalous components are of the order of 3 - 6 %/degree and appear to be sensitive to the polarity of the solar dipole magnetic field, being negative for the current polarity, and positive for the polarity of the last solar cycle (~1970-1980). Latitude gradients for galactic cosmic rays are smaller (~0.5%/degree), and have only recently been measured for the first time, so that their sensitivity to the solar magnetic polarity is unknown. While the values observed are consistent with currently available theoretical models, neither the time variability nor the values of the gradients could have been reliably predicted from the models. The location of the boundary of the modulation region remains unknown, and extrapolation of the measured gradients to larger (or smaller) radii, to higher latitudes, or to later times is difficult to do with confidence. If such extrapolation is required, recommended

values for radial and latitude gradients based on currently available observations are given by Mewaldt et al. (1987), who have summarized the findings of this workshop.

ACKNOWLEDGMENTS

It is a pleasure to thank J. A. Simpson for his support and encouragement, and M. Garcia-Munoz and K. R. Pyle for many useful discussions. This work was supported in part by NASA/Ames Grant NAG 2-380 and NASA Grant NGL 14-001-006. The Climax neutron monitor is supported by NSF Grant ATM 86-20160.

REFERENCES

Adams, J. H., Jr. Cosmic ray effects on micro-electronics, part 4, NRL Memorandum Report 5901, Naval Research Laboratory, Washington, D. C., 1986.

Bastian, T. S., R. B. McKibben, K. R. Pyle, and J. A. Simpson, Variations in the intensity of galactic cosmic rays and anomalous helium as a function of solar latitude, Proc. XVIth Int'l Cosmic Ray Conf. (Kyoto), 12, 318, 1979.

Christon, S. P., A. C. Cummings, E. C. Stone, K. W. Behannon, and L. F. Burlaga, Differential measurement of cosmic ray gradient with respect to interplanetary current sheet, Proc. XIXth Int'l Cosmic Ray Conf. (La Jolla), 4, 445. 1985.

Christon, S. P., A. C. Cummings, E. C. Stone, K. W. Behannon, L. F. Burlaga, J. R. Jokipii, and J. Kota, Differential measurement and model calculation of cosmic ray latitudinal gradient with respect to the heliospheric current sheet, J. Geophys. Res., 91, 2867, 1986a.

Christon, S. P., E. C. Stone, and J. T. Hoeksema, Evidence for a latitudinal gradient of the cosmic ray intensity associated with a change in the tilt of the heliospheric current sheet, Geophys. Res. Letters, 13, 777, 1986b.

Cummings, A. C., Time and space variation of the anomalous component, These proceedings, 1987.

Cummings, A. C., and E. C. Stone, Elemental composition of the anomalous cosmic ray component, Proc. XXth Int'l Cosmic Ray Conf. (Moscow), 3, 413, 1987.

Cummings, A. C., E. C. Stone, and W. R. Webber, Latitudinal and radial gradients of anomalous and galactic cosmic rays in the outer heliosphere, Geophys. Res. Letters, 14, 174, 1987a.

Cummings, A. C., R. A. Mewaldt, and E. C. Stone, Large -scale radial gradient of anomalous cosmic-ray oxygen from 1 to ~30 AU, Proc. XXth Int'l Cosmic Ray Conf. (Moscow), 3, 425, 1987b.

Evenson, P. M., M. Garcia-Munoz, P. Meyer, K. R. Pyle, and J. A. Simpson, A quantitative test for solar modulation theory: The proton, helium, and electron spectra from 1965-1979, Astrophys. J. (Letters), 275, L15, 1983.

Fillius, W., I. Axford, and D. Wood, Time and energy dependence of the cosmic ray gradient in the outer heliosphere, Proc. XIXth Int'l Cosmic Ray Conf. (La Jolla), 5, 189, 1985.

Jokipii, J. R., Effects of three-dimensional heliospheric structures on cosmic ray modulation,in The Sun and the Heliosphere in Three Dimensions, edited by R.G. Marsden, p. 375, D. Reidel, Dordrecht, Holland, 1986.

Jokipii, J. R., and J. Kota, Cosmic rays near the heliospheric current sheet 2. An ensemble approach comparing theory and observation, J. Geophys. Res., 91, 2885, 1986.

Jokipii, J. R., Galactic cosmic rays in 3-D, These proceedings, 1987.

Lopate, C. L., R. B. McKibben, K. R. Pyle, and J. A. Simpson, Radial gradients of galactic cosmic rays to ~40 AU during declining solar activity, Proc. XXth Int'l Cosmic Ray Conf. (Moscow), 3, 409, 1987.

Mewaldt, R. A., A. C. Cummings, J. H. Adams, Jr., P. Evenson, W. Fillius, J. R. Jokipii, R. B. McKibben, and P. A. Robinson, Jr., Toward a descriptive model of galactic cosmic rays in the heliosphere, These proceedings, 1987.

McDonald, F. B., and N. Lal, Variations of galactic cosmic rays with heliolatitude in the outer heliosphere, Geophys. Res. Letters, 13, 781, 1986.

McDonald, F. B., T. T. von Rosenvinge, N. Lal, J. H. Trainor, and P. Schuster, The recovery phase of galactic cosmic ray modulation in the outer heliosphere, Geophys. Res. Letters, 13, 785, 1986.

McKibben, R. B., Galactic cosmic rays and anomalous components in the heliosphere, Rev. Geophys., 25, 711, 1987.

McKibben, R. B., K. R. Pyle, and J. A. Simpson, The solar latitude and radial dependence of the anomalous cosmic-ray helium component, Astophys. J. (Letters), 227, L147, 1979.

Newkirk, G. Jr., and L. A. Fisk, Variation of cosmic rays and solar wind properties with respect to the heliospheric current sheet 1. Five GeV protons and solar wind speed, J. Geophys. Res., 90, 3391, 1985.

Newkirk, G. Jr., J. A. Lockwood, M. Garcia-Munoz, and J. A. Simpson, Latitudinal gradients of cosmic rays and the polarity reversal of the heliospheric magnetic field: A preliminary evaluation, Proc. XIXth Int'l Cosmic Ray Conf. (La Jolla), 4, 469. 1985.

Newkirk, G. Jr., J. Asbridge, J. A. Lockwood, M. Garcia-Munoz, and J. A. Simpson, Variation of cosmic ray and solar wind properties with respect to the heliospheric current sheet 2. Rigidity dependence of the latitudinal gradient of cosmic rays at 1 AU, J. Geophys. Res., 91, 2879, 1986.

O'Gallagher , J. J., and G. S. Mazlyar, III, A dynamic model for the time evolution of the modulated cosmic ray spectrum, J. Geophys. Res., 81, 1319, 1976.

Parker, E. N., The passage of energetic charged particles through interplanetary space, Plan. Sp. Sci., 13, 9, 1965.

Perko, J. S., and L. A. Fisk, Solar modulation of galactic cosmic rays 5. Time dependent modulation, J. Geophys. Res., 88, 9033, 1983.

Potgieter, M. S., and H. Moraal, A drift model for the modulation of galactic cosmic rays, Astrophys. J., 294, 425, 1985.

Quenby, J. J., The theory of cosmic ray modulation, Sp. Sci. Rev., 37, 201, 1984.

Randall, B. A., and J. A. Van Allen, Heliocentric radius of the cosmic ray modulation boundary, Geophys. Res. Letters, 13, 628, 1986.

Van Allen, J. A., and B. A. Randall, Interplanetary cosmic ray intensity: 1972-1984 and out to 32 AU, J. Geophys. Res., 90, 1399, 1985.

Venkatesan, D., R. B. Decker, and S. M. Krimigis, Measurement of radial and latitudinal gradients of cosmic ray intensity during the decreasing phase of sunspot cycle 21, in The Sun and the Heliosphere in Three Dimensions, edited by R.G. Marsden, p. 389, D. Reidel, Dordrecht, Holland, 1986.

Webb, D. F., J. M. Davis, and P. S. McIntosh, Observations of the reappearance of polar coronal holes and the reversal of the polar magnetic field, Solar Phys., 92, 109, 1984.

Webber, W. R. and J. A. Lockwood, Interplanetary radial cosmic-ray gradients and their implication for a possible large modulation effect at the heliospheric boundary, Astrophys. J., 317, 534, 1987.

Webber, W. R. and S. M. Yushak, A measurement of the energy spectra and relative abundance of the cosmic ray H and He isotopes over a broad energy range, Astrophys. J., 275, 391, 1983.

TIME VARIATION OF GALACTIC COSMIC RAYS

Paul Evenson

Bartol Research Institute
University of Delaware
Newark, Delaware 19716

Abstract. Time variations in the flux of galactic cosmic rays are the result of changing conditions in the solar wind. Maximum cosmic ray fluxes, which occur when solar activity is at a minimum, are well defined. Reductions from this maximum level are typically systematic and predictable but on occasion are rapid and unexpected. Models relating the flux level at lower energy to that at neutron monitor energy are typically accurate to 20 percent of the total excursion at that energy. Other models, relating flux to observables such as sunspot number, flare frequency, and current sheet tilt are phenomenological but nevertheless can be quite accurate.

Introduction. By definition, galactic cosmic rays are charged particles, electrons and nuclei, which occupy the local region of interstellar space. Unlike photons, the charged cosmic rays cannot travel in straight lines through the magnetic fields (typically one microgauss) which permeate the galaxy. Particles of energy less than about 10 GeV, which are the only ones numerous enough to contribute significantly to the radiation background of a spacecraft, have radii of curvature in this field which are small compared to the dimensions of the solar system and tiny compared even to the distance to the nearest star.

Therefore even though these particles have speeds near that of light their convoluted paths in the interstellar medium are such as to completely randomize their directions and smooth out any fluctuations in density. On the timescale of a human lifetime it is inconceivable that there could be any detectable time variation in the fluxes of these particles.

However, as Figure 1 shows, fluxes of galactic particles which penetrate into the solar system exhibit substantial time variations. Particles of different species and/or different energies show obviously related but nevertheless distinctly different variations. It is my aim in this paper to provide a brief and qualitative discussion of the causes of time variability of galactic cosmic radiation. I hope that I cause no offense by choosing not to give references in the text. Instead I present a list of suggestions for further reading chosen in part because they contain extensive references to the literature.

Solar Modulation. The variability, or modulation, of the galactic cosmic ray fluxes was recognized some time ago as related to the general eleven year cycle of solar activity, hence the term "Solar Modulation." Figure 1 shows approximately one complete cycle of this activity and illustrates the inverse nature of the relationship. Sunspots, solar flares, and the like were at a maximum during the years 1980-1982 while the fluxes of cosmic rays were at a minimum. A naive explanation, that the extra "stuff" coming off the sun at solar maximum somehow drives the cosmic rays out of the solar system, is very close to the truth. Beyond this point however intuition fails and the details of the process are the subject of much scientific research and debate.

Cosmic ray particle density and the particle density in the solar wind are so low that the particles almost never physically collide with one another. All of the

interactions take place through electromagnetic interactions. The electromagnetic fields can be described mathematically in many ways; generally they are described in terms of Fourier components or waves. Because they propagate in an anisotropic, conductive medium, these waves in turn cannot be completely characterized by pointlike measurements from spacecraft. Further, they are almost invisible to remote sensing techniques such as radio sounding although analysis of fluctuations in spacecraft telemetry signals does provide important input into the problem. If a precise, time dependent model of the electromagnetic fields within the heliosphere were available calculation of solar modulation would be only a numerical problem, albeit a complex one, much in the fashion of calculating global weather. In practice, particle observations are often used as the basis for constructing approximate models of the electromagnetic fields.

In order to understand the propagation of cosmic rays in the heliosphere three processes must be considered: diffusion, convection, and adiabatic deceleration. To understand these, consider Figure 2, a highly schematic representation of the heliosphere, or sphere of influence of the sun. The boundary of the heliosphere, which may or may not be sharp, is the surface where the expanding and weakening solar wind can no longer push back the interstellar medium. Because the sun is moving with respect to the interstellar medium it is likely that the boundary is not spherical at all. Estimates of the distance to the boundary have been historically very consistent -- always approximately twice the distance to the furthest spacecraft. Hence, in 1987, most people would place the boundary at approximately 100 AU (one Astronomical Unit is the average earth-sun separation).

Cosmic rays individually have high energies but their total energy content is low compared to the particles which make up the solar wind. Therefore they play little role in the dynamics of the solar wind and are only weakly coupled to the waves created by the lower energy particles. The boundary as such, even if it is sharp, is scarcely seen by the cosmic rays as a barrier; the weakly interacting cosmic rays respond only to the bulk properties of the medium within which they propagate.

Hence the picture of the heliosphere given in Figure 2. The solar wind is seen by the cosmic rays as a collection of radially moving scattering centers that are irregularities and fluctuations in the interplanetary magnetic field. The cosmic rays **diffuse** in this sea of scattering centers, a process which can be characterized by a mean free path, the numerical value of which is typically 0.3 AU at the location of the earth. The process is similar to molecules of perfume diffusing from an open bottle through the air in a room. If the solar wind were not flowing, eventually cosmic rays would diffuse until the intensity throughout the heliosphere became the same as that in interstellar space.

But the solar wind is not stationary, it flows outward at approximately 400 km/second. This flow results in the **convection** of the cosmic rays which are diffusing in the rest frame of the solar wind. One could liken this to aiming a fan at the perfume bottle. This could reduce or even eliminate the scent at some locations depending on the relation of the flow speed to the rate of diffusion.

The wind is expanding as it moves out so cosmic rays trapped in the expansion are in effect cooled much as a gas is cooled by adiabatic expansion against a piston. This process, termed **adiabatic deceleration,** makes modulation complex, as the energy losses are large (hundreds of MeV for a 1 GeV proton) and the flux of particles is strongly energy dependent. The paradoxical nature of this effect can best be seen by noting that at lower energies, where the flux increases with increasing energy, adiabatic deceleration represents a net source of particles at a given energy, rather than a net

sink. This idea, that there can be apparent sources of particles deep within the heliosphere must be kept in mind when trying to understand radial gradient measurements.

One final point is worthy of some note. The previous discussion has treated the scattering centers as if they were interplanetary billiard balls scattering cosmic marbles. Such a view is useful to some level, but at a deeper level leads to contradictions which I only mention but do not explore. Under a Galilean transformation a billiard ball is still a billiard ball, so one may treat the scattering in a convenient frame and then transform trivially to another frame moving uniformly with respect to the first. Magnetic fields, even in the non-relativistic limit of a Galilean transformation, do not stay simply as magnetic fields, they change slightly in magnitude and electric fields appear. (That is why dynamos work.) In the solar wind the process is further complicated by the fact that there is no overall rest frame. Because of the expansion, a small volume element of the solar wind is not only expanding itself but its center has a net motion with respect to the centers of other volume elements.

Magnetic Fields on the Sun. To understand the magnetic field in the heliosphere it is useful to know a little about the structure of the sun. The energy of the sun is thought to be generated in the central regions, approximately confined to a sphere with a radius one quarter that of the sun (and thus within only about 2% of the volume of the sun). The heat is transported by (radiative) conduction most of the way to the surface. About 85% of the way to the surface the method of heat transport switches to convection. Currents generated by the convective motion in this outer layer of the sun probably support the surface magnetic field. At the surface, the field is highly complex, with regions of positive and negative polarity found in both hemispheres. Only at altitudes of a solar radius or more has the dipole component begun to dominate the field, giving a net polarity to an entire hemisphere. In contrast, the currents producing the earth's field lie deep within the planet, so that at the surface the dipole component is already dominant. Again in contrast to the earth, where changes and reversals of the field take place on timescales of millenia, the magnetic field of the sun reverses its polarity every eleven years, during the period of maximum solar activity. Thus the eleven year solar cycle should more properly be viewed as half of a 22 year cycle. Subtle effects of the 22 year cycle are the subject of intensive study at the present time.

The Solar Wind. "Solar Wind" is the name given to the continuous flow of plasma from the sun outward into the heliosphere. The solar wind has its origin in the hot corona, or outer atmosphere of the sun which is so dramatically visible at the time of total eclipses. The hot coronal plasma expands against the force of gravity in a process that has many similarities to the operation of a rocket nozzle. Thermal energy is converted to bulk motion with such high efficiency that the solar wind is highly supersonic. For solar wind protons, the random motion contains only about 10% of the energy of the bulk flow, which has a typical velocity of 400 km/second. The motion of individual solar wind particles is almost purely radial, however it is important to note that the locus of particles which have come from the same area of the sun forms a spiral pattern exactly like that from a garden sprinkler (Figure 3).

Interplanetary Magnetic Fields. Even though the solar wind plasma is tenuous (about 1 per cm^3 at the orbit of earth) the conductivity is high enough that magnetic fields are "frozen in": their decay or diffusion rate is slow compared to the time it takes the solar wind to reach the heliospheric boundary. The dominant source of the magnetic field is the dipole component of the solar field which threads through the corona

where the solar wind is forming. As a result of this process, it can be shown that the field lines in the corona are drawn out into the solar wind and end up following the loci of the particles flowing from one region of the sun. Thus the field forms the familiar Parker spiral shown in Figure 3. Typical field amplitudes at the orbit of earth are a few nanotesla.

Cosmic rays propagate mainly along these field lines. Therefore the picture is not quite so simple as shown in Figure 2; the boundary is much further away along the path the cosmic ray must take. It is of course irregularities in this magnetic field which provide the scattering which results in the diffusion of the cosmic rays. Some of these irregularities are remnants of the irregularity of the solar source of the plasma, but others are undoubtedly generated by various types of plasma processes as the solar wind propagates through the heliosphere.

Observational Data. Cosmic ray fluxes vary greatly with energy and particle species. They are also to a good approximation isotropic, in that any detector has a counting rate independent of its direction of view. Flux and energy units in common use are chosen in a way which best exhibits the systematic nature of the energy and composition variability. Particle energies are measured in electron volts (eV), which is the amount of energy required to move a unit electric charge (such as an electron) through a potential of one volt. Cosmic rays are relativistic particles, so it is convenient to refer to the mass in terms of an equivalent energy, a proton therefore has a "mass" of 931 MeV (properly MeV/c^2) and an electron 511 keV. It is an observational fact that the relative abundances of cosmic ray nuclei are nearly constant as a function of velocity, which for relativistic nuclei is most commonly described as kinetic energy per unit rest mass. For practical purposes the mass difference between neutrons and proton and that due to nuclear binding energy are insignificant. The mass of a nucleus is therefore conveniently characterized by the number of nucleons (A) and the usual velocity unit becomes kinetic energy per nucleon.

For particles propagating in magnetic fields the best ordering parameter is rigidity (momentum per unit charge). In a magnetic field not changing in time this parameter completely determines the trajectory of the particle; the velocity determines only how fast the particle traverses the trajectory. Momentum, p (in the units MeV/c) is calculated relativistically from kinetic energy, E, and rest mass, m, by the formula

$$p^2 = E^2 - 2Em$$

Rigidity, expressed in a unit commonly called the volt, but bearing only a distant relationship to the ordinary volt, is the total momentum of the particle divided by the net charge. With the exception of the so called anomalous component cosmic ray nuclei are fully stripped and the net charge is the atomic number Z. For electrons of cosmic ray energies the total energy, kinetic energy, momentum, and rigidity are approximately equal numerically.

Cosmic ray flux is measured as the number of particles striking a unit area per unit time from a unit solid angle. A flat detector of area s cm^2 sensitive to particles from one side receives particles from a half sphere, or 2π steradians. Because of projection effects the net **geometry factor** of such a detector is only $s\pi$ cm^2-steradian. At low energies relevant to spacecraft radiation dose the flux of cosmic rays is almost always given as a differential spectrum, a number of particles within a stated interval about the stated energy. Both the energy and the energy differential are often given in terms of energy per nucleon so some care must be taken when using a published spectrum to calculate total dose; extra factors of the number of nucleons can easily be lost.

The most readily available continuous cosmic ray data come from neutron monitors. These ground based detectors are sensitive to the fragments produced by primary cosmic rays as they strike the atmosphere. Cosmic rays must have energies upwards of 1 GeV before the secondaries they produce can strike the ground, therefore the neutron monitors provide information only about the higher energy particles. The earth's magnetic field also screens out cosmic rays. At the equator only particles with rigidities over 20 GV are able to get in, while near the poles the neutron monitor response is limited by the atmosphere.

It is therefore possible in principle to get accurate spectra from 1 GeV to 20 GeV or so for protons (the dominant component) using ground based data. In practice it is difficult to normalize the data properly from one station to the next, therefore such spectra are not readily available. Current research using neutron monitors is done with time variations from individual stations or matched pairs of stations looking for effects at the level of tenths of a percent. Modulation models can be successfully linked to a few selected stations as the behavior of the spectrum is quite regular to the accuracy required to estimate dose. Extrapolation of the neutron monitor data via appropriate models to lower energies is quite successful, although it is possible to have errors as large as a factor of two in flux under certain circumstances.

Below 1 GeV, data on cosmic rays are obtained from spacecraft and sometimes balloons. Normally spectra for protons and helium below 150 MeV/nucleon can be obtained, with an integration time of about ten days, for almost any date desired. The energy range 150MeV/n to 1 GeV/n is poorly monitored on a routine basis, but interpolation between lower energy data and neutron monitors is generally accurate to 20% or better.

Absolute Level of Modulation. Although cosmic electrons contribute little to the total dose, and measurements of their flux are sparse, they provide the one direct link to the region outside the heliosphere from which the absolute amount of solar modulation may be calculated. Microwave synchrotron radiation produced by the electrons as they spiral around the interstellar magnetic field can be detected and measured quantitatively by earth based radiotelescopes. These data can in turn be used to estimate the electron flux outside the heliosphere, the so-called Local Interstellar Spectrum or LIS. Figure 4 shows the electron LIS together with an electron spectrum obtained at earth during 1977, a year representative of maximum electron fluxes at earth. Note particularly the large amount of modulation which is present at energies below 1 GeV even at this time of solar minimum. Estimates of modulation model parameters (see below) are made by comparing the model calculation (line through data points) with the data while keeping the input spectrum at the heliospheric boundary constant and equal to that deduced from the radio data.

Modulation Models. Transport of cosmic rays through the interplanetary medium is described mathematically by an equation of the Fokker-Planck type which relates the three fundamental processes, diffusion, convection, and adiabatic deceleration discussed above. Obtaining practically useful solutions of this equation remains a difficult task because of the need to deal with spatial anisotropies and inhomogeneities of the interplanetary medium. Even if these effects are included in the mathematical solution, data of sufficient accuracy are not available over enough of the solar system to permit a truly *ab initio* calculation. Solutions are generally obtained by numerical methods, most of which have many free parameters. In practice most of these parameters must be fixed at nominal values and only a few varied to obtain agreement with the data.

Typically the diffusion coefficient as a function of momentum and position and the distance to the boundary are taken as adjustable parameters.

Figure 5 illustrates such a modulation model. In this figure are plotted data and model fits showing the range of variation observed in the spectrum of cosmic ray protons. Modulation measured by the electrons is used to trace back from the observed proton spectrum to the presumed local interstellar spectrum (LIS). Success of the model therefore corresponds to recovering the same LIS during periods of different modulation amplitude. I should note that the LIS in Figures 4-6, including the electron LIS, have been refined over the years to provide the best overall fit to all observations. (Modifications made to the electron LIS are within the quoted error limits of the radio measurements.) One further point to note in Figure 5 is that the high level of solar activity which reduces the cosmic ray fluxes in 1982 compared with 1977 leaves its mark in the form of greatly increased fluxes of low energy particles.

Figure 6, illustrating the modulation of cosmic ray helium, is in many respects similar to Figure 5. The shapes of the LIS are nearly identical when plotted as a function of energy per nucleon (velocity). The overall shape and behavior of the modulated spectra are similar and a component of solar flare helium is clearly visible during 1982. However there are some key points of difference as well. Effects of modulation are smaller on helium at the same energy per nucleon than they are on protons because helium nuclei are more rigid, having twice the charge but four times the mass of the protons. At low energies the so called anomalous component of helium stands out in the 1977 data. Anomalous cosmic rays are most probably singly charged ions produced by sunlight falling on neutral atoms of the interstellar medium which enter the solar system because of the proper motion of the sun with respect to the local gas cloud. These ions are accelerated to high energies by a process which is not well understood. Their anomalous properties with respect to modulation are due to their high rigidity (from their low net charge) and the fact that they are injected deep within the modulation region rather than having to diffuse in from the boundary. (Before the particles are ionized they do not interact significantly with the solar wind and propagate freely through the magnetic fields.)

Model Weaknesses. Often attempts are made to construct models relating cosmic ray flux to observables such as sunspot number, flare frequency, and current sheet tilt. All of these are correlated with each other in some general way so the models do a good job with general trends but in detail tend to predict the past much better than they predict the future. Current models of modulation do provide a systematic basis for calculating fluxes and spectra of many particles based on a few direct cosmic ray observations.

To date it has been observed that maximum cosmic ray fluxes, which occur when solar activity is at a minimum, are well defined and reproducible from one solar cycle to the next. Reductions from this maximum level are typically systematic, slow and predictable in a general sense but on occasion are rapid and unexpected. Most rapid fluctuations are reductions in flux (Forbush decreases) so conservative calculations can be based on the nominal model. Of course the real danger of an upward fluctuation comes from solar flare particles which are not considered in this paper.

Models that do a good job of ordering observations at one location seldom permit accurate extrapolations to flux levels elsewhere in the solar system. This may be due to fundamental problems with the physics of the models. Small differences in the behavior of positive and negative particles may be a symptom of large scale particle

drifts, possibly associated with the magnetic neutral sheet separating the regions of opposite magnetic polarity. On the other hand, the models may be sound but the model parameters may vary with radial distance and distance from the ecliptic in ways which are not currently understood.

Summary. Current modulation models are quite good at reproducing the relative modulation amplitudes near the earth of most of the cosmic rays. By using a few key indicators, such as neutron monitor measurements and low energy proton data, flux levels of other components can be calculated to an accuracy of 20%. These calculations unfortunately do not usually give good predictions of the flux at other locations in the heliosphere.

Acknowledgements. This paper is based on a talk given at the Workshop on the Interplanetary Charged Particle Environment, held at JPL on March 16 and 17, 1987. I would like to thank John Simpson, Peter Meyer, Roger Pyle, and Moises Garcia-Munoz for their assistance in supplying data and model fits for the figures, and Leo Krawczyk for technical assistance in preparing the figures. Preparation of this paper was supported in part by NASA Grant NAG-5-374 and NSF Grant ATM86-03192.

Bibliography. The following are suggested to the reader who would like a more detailed and technical treatment of the process of solar modulation. This list is not intended to be exhaustive in itself, however the publications cited contain within them references to most of the significant literature on the subject.

Bieber, J. W., P. Evenson, and W. H. Matthaeus, Magnetic helicity of the IMF and the solar modulation of cosmic rays, *Geophys. Res. Lett., 14*, 864-867, 1987.

Evenson, P., M. Garcia-Munoz, P. Meyer, K. R. Pyle, and J. A. Simpson, A quantitative test of solar modulation theory: The proton, helium and electron spectra from 1965 through 1979, *Astrophys. J. Lett., 275* L15, 1983.

Fisk, L. A., Solar modulation of galactic cosmic rays, 2, *J. Geophys. Res., 80*, 1701, 1971.

Garcia-Munoz, M., P. Meyer, K. R. Pyle, J. A. Simpson, and P. Evenson, The dependence of solar modulation on the sign of the cosmic ray particle charge, *J. Geophys. Res., 91*, 2858-2866, 1986.

Jokipii, J. R., Cosmic ray propagation I: Charged particles in a random magnetic field, *Astrophys. J., 146*, 480-487, 1966.

Jokipii, J. R., E. H. Levy, and W. B. Hubbard, Effects of particle drift on cosmic ray transport I: General properties, application to solar modulation, *Astrophys. J., 213*, 861-868, 1977.

Mc Kibben, R. B., Galactic Cosmic Rays and Anomalous Components in the Heliosphere, *Reviews of Geophysics, 25*, 711-722, 1987.

Parker, E.N., *Interplanetary Dynamical Processes*, New York: Interscience, 1963

Shea, M. A., Solar-Planetary Relationships: Cosmic Rays, Solar and Interplanetary Physics, *Reviews of Geophysics, 25,* 641-650, 1987.

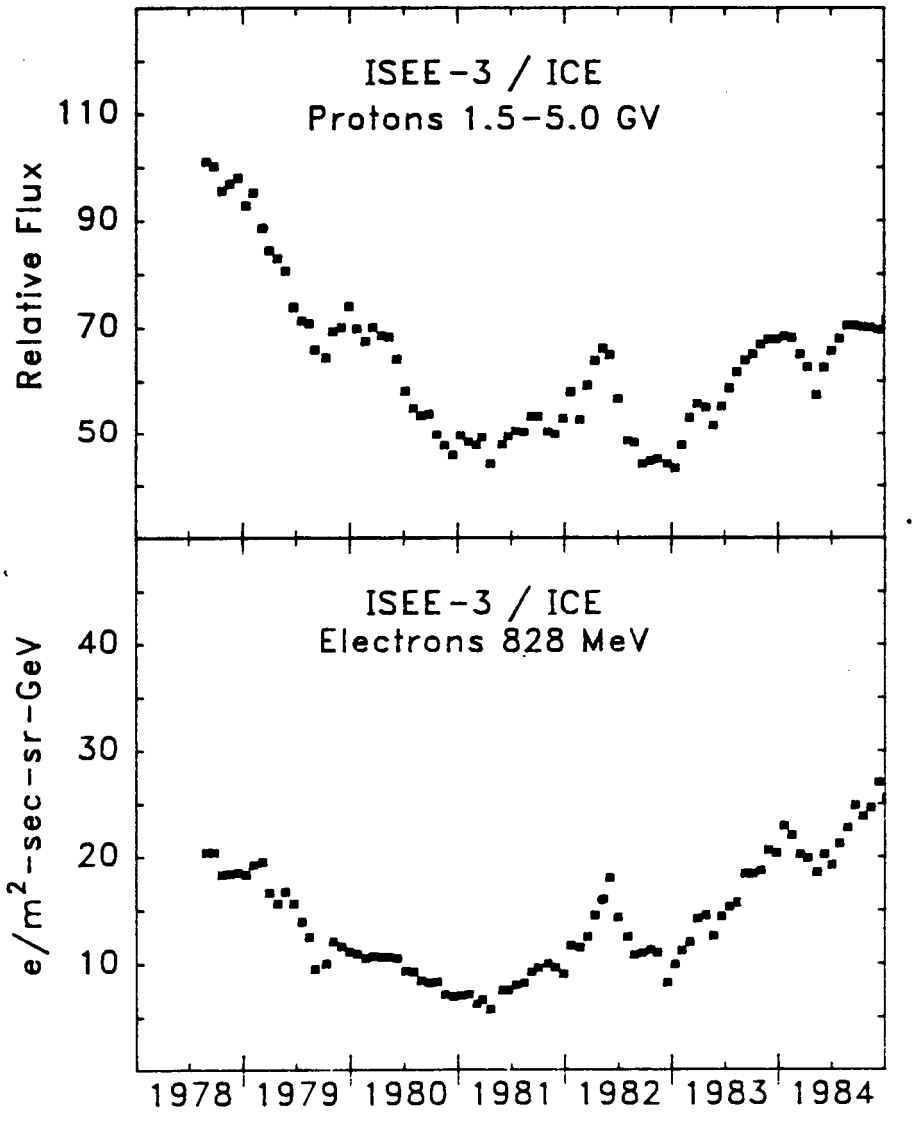

Figure 1. Time variability of galactic cosmic ray proton and electron fluxes. Overall similarity is apparent but close observation shows differences which depend on energy and charge sign.

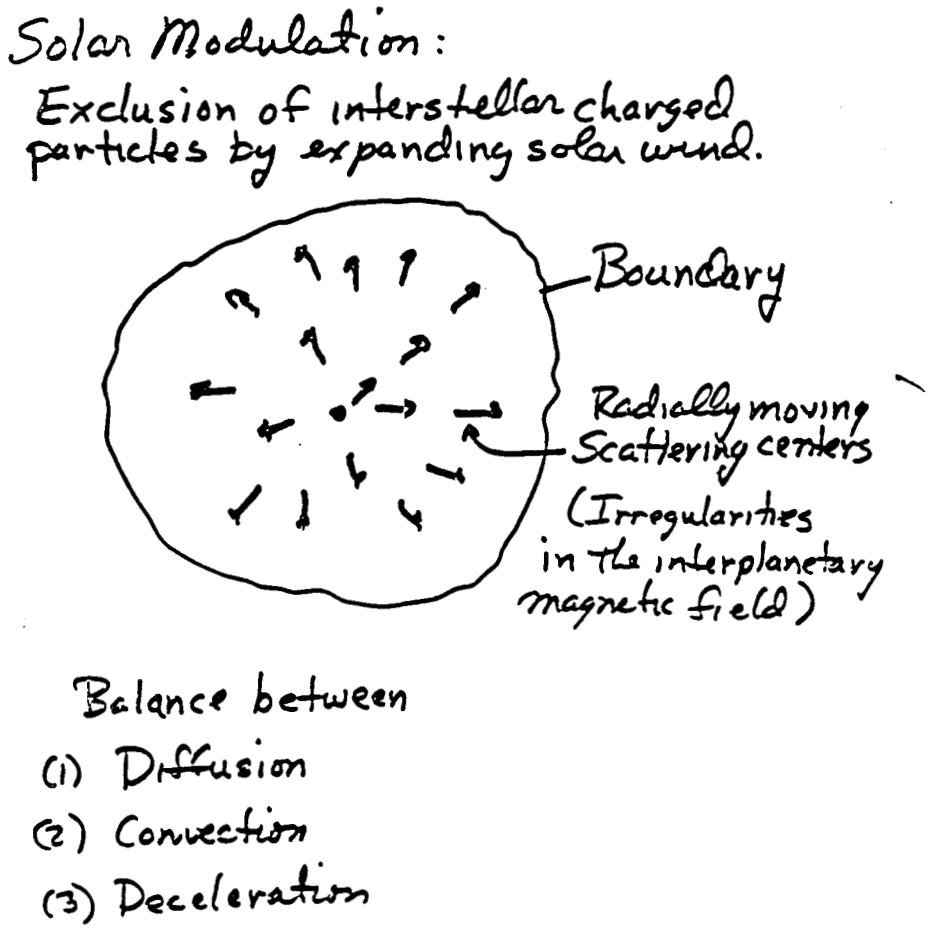

Figure 2. Schematic representation of solar modulation. Details are discussed in the text and references.

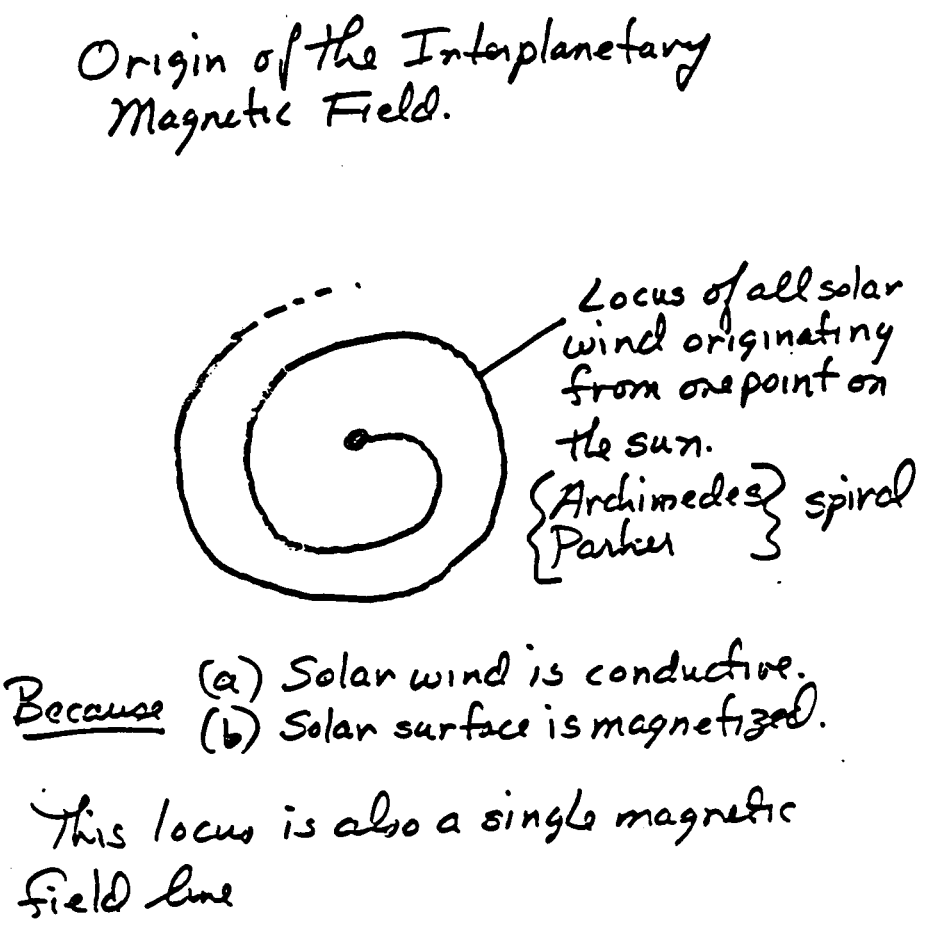

Figure 3. Interplanetary magnetic field has the same shape above and below the solar equator but opposite polarity as the dipole field is drawn out by the solar wind.

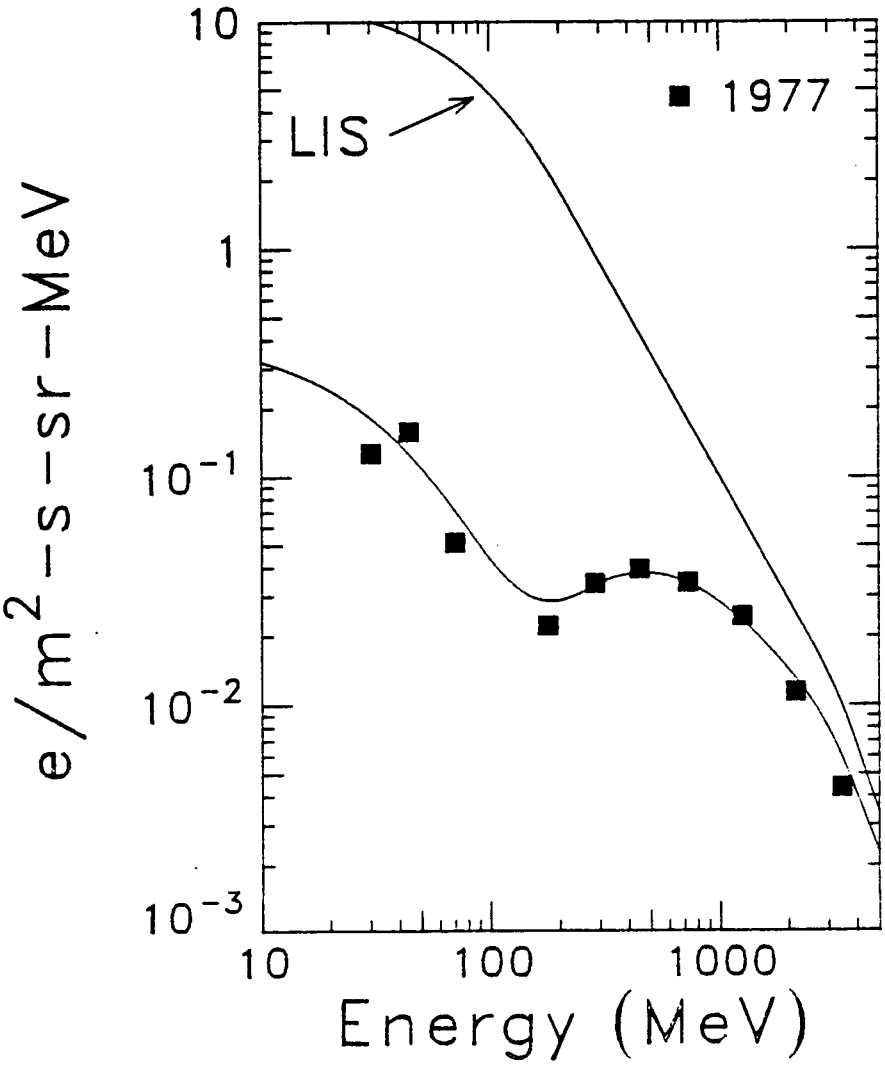

Figure 4. Comparing measured electron fluxes with the Local Interstellar Spectrum (LIS) deduced from radio data gives the only absolute measurement of the total amount of solar modulation. The 1977 electron spectrum shown is representative of maximum electron fluxes near Earth.

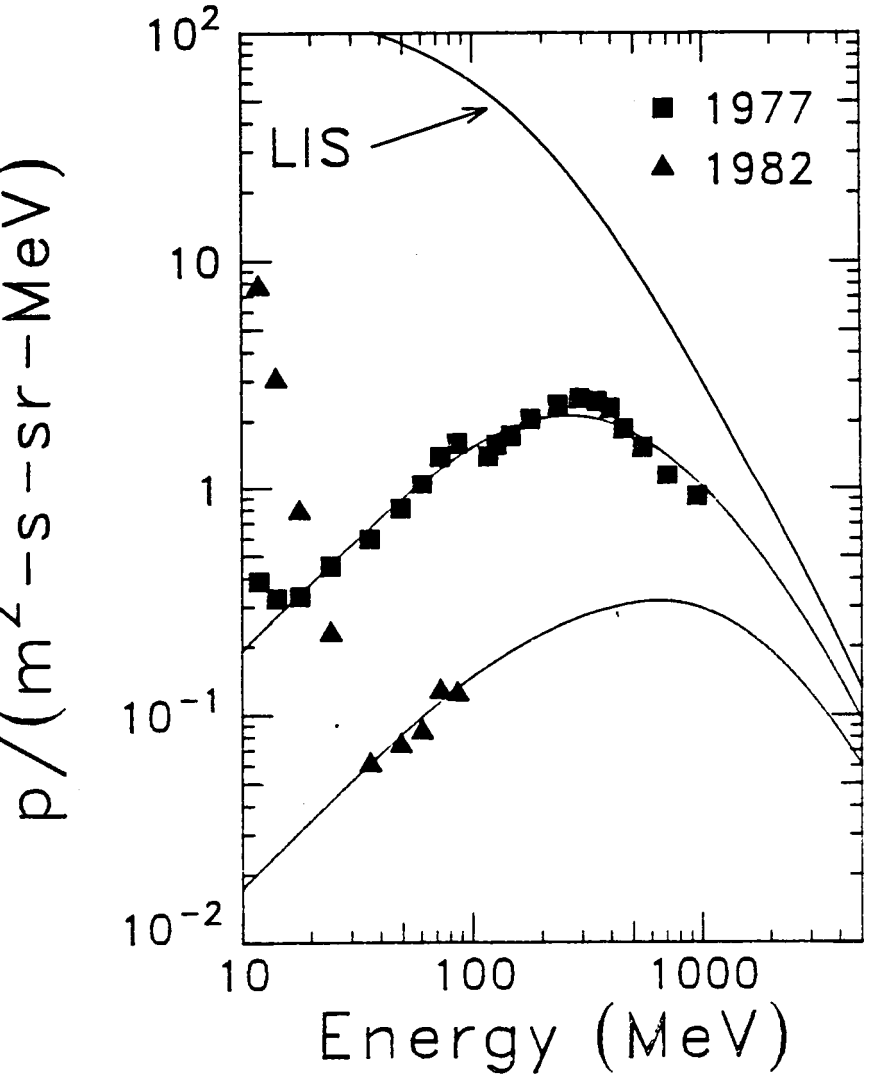

Figure 5. Comparison of maximum and minimum proton fluxes with model fits. The LIS for protons is an output of the model: the one shown here gives consistent results over the observed range of modulation.

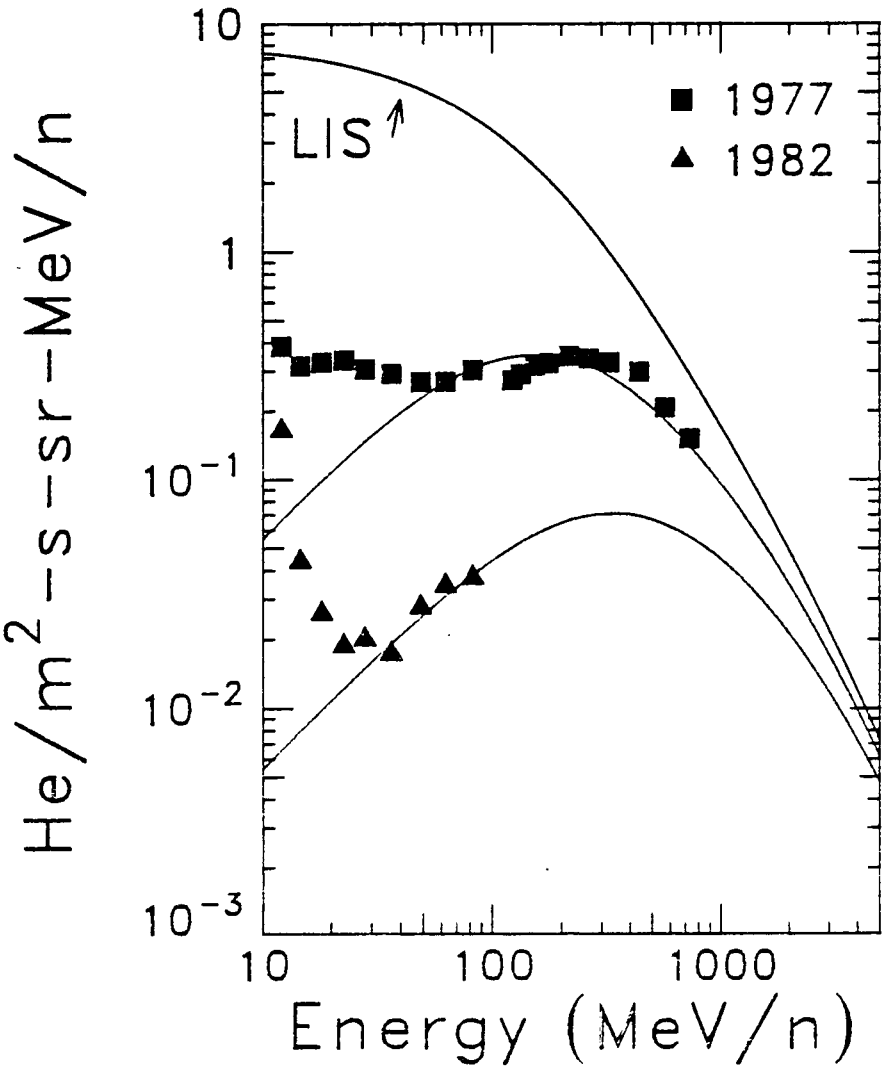

Figure 6. Helium data for comparison with the proton data in the previous figure. Subtle differences are discussed in the text.

GALACTIC COSMIC RAYS IN THREE DIMENSIONS

Summary
by
J. R. Jokipii
University of Arizona, Tucson, AZ 85721

Galactic cosmic rays are energetic particles with energies in the range from roughly 100 keV up to as high as 10^{20} electron volts. The maximum intensity in the spectrum is at an energy of approximately 1 GeV. These cosmic rays come from outside the solar system, and are influenced by the solar wind as they come into the inner solar system. The magnetic field of the Sun is dragged out by the solar wind to form an Archimedean spiral. This field impedes the access of the cosmic rays to the inner solar system and causes "solar modulation" of galactic cosmic rays with a variety of time scales. The dominant changes are 11-year and 22-year cyclic changes associated with changes in the solar wind and its magnetic field, in conjunction with the sun spot cycle.

A reasonably complete understanding of this process is now available. The energetic particles random walk through the turbulent magnetic field of the solar wind, tending to fill the inner solar system. This inward random walk of the particles is opposed by their outward convection with the solar wind, cooling or energy loss due to radial expansion of the wind and the drifts of the particles in the large scale magnetic structure.

A very adequate fundamental transport equation has been derived.

There are currently two basic approaches to this theory.

The first is the ad hoc assumption that drifts are unimportant. In this case spherically symmetric solutions and neglect of latitude gradients is sufficient.

The second mechanism is based on following the consequences of a reasonable extrapolation of our observations near the ecliptic to the unexplored high heliographic latitudes. These calculations show a fundamental importance of particle drift and latitudinal effects. In fact, one can show that the drifts, energy change, convection, and diffusion are all of the same general order of magnitude. There are significant variations of cosmic rays both with heliospheric radius and with heliospheric latitude. Moreover, these variations change dramatically over the sun spot cycle. A fundamental new result is that whereas the cosmic ray intensity increased with distance away from the heliospheric current sheet during the last sun spot minimum, during the present sun spot minimum the intensity decreases away from the heliospheric current sheet. This idea has support in recent observations.

A general conclusion is that the cosmic rays increase with increasing distance from the Sun at approximately 2%/a.u. There is a strong correlation of the cosmic ray

intensity with distance with the tilt of the heliospheric current sheet. Moreover, we find that the variation of the cosmic rays with time changes in alternate sun spot cycles.

Finally, it seems that during alternate sun spot minima (1965 and 1985) the cosmic rays access to the inner solar system was along the equatorial current sheet, whereas in 1975 the cosmic rays came in over the poles.

The recently discovered anomalous component of cosmic rays is very much related to this whole problem, and probably corresponds to particles being accelerated at the termination of the solar wind at some 50-100 astronomical units from the sun.

In summary, many predictions of the models remain controversial in detail. Nonetheless, it appears now that we can expect more cosmic rays over the poles in the next sunspot cycle, and the intensity will continue to increase with heliocentric radius out to the interstellar medium.

LIST OF PARTICIPANTS

J.H. Adams Jr.
Naval Research Laboratory
Washington, D.C. 20375

T.P. Armstrong
Dept. of Physics and Astronomy
University of Kansas
Lawrence, KS 66045

D.L. Chenette
Aerospace Corporation
2350 East El Segundo Blvd.
El Segundo, CA 90245

A.C. Cummings
California Institute of Technology
Pasadena, CA 91125

L. Dao-Gibner
Syscon
Pasadena, CA 91109

W.F. Dietrich
Aerospace Corporation
2350 East El Segundo Blvd.
El Segundo, CA 90245

P. Evenson
Bartol Research Foundation
University of Delaware
Newark, DE 19711

J. Feynman
Jet Propulsion Laboratory
California Institute of Technology
4800 Oak Grove Drive
Pasadena, CA 91109

PARTICIPANTS (cont)

W. Fillius
University of California, San Diego
La Jolla, CA 92093

S.B. Gabriel
Jet Propulsion Laboratory
California Institute of Technology
4800 Oak Grove Drive
Pasadena, CA 91109

B.E. Goldstein
Jet Propulsion Laboratory
California Institute of Technology
4800 Oak Grove Drive
Pasadena, CA 91109

D.C. Hamilton
University of Maryland
College Park, MD 20742

G.R. Heckman
NOAA/ERL/SEL
325 Broadway
Boulder, CO 80303

J.R. Jokipii
University of Arizona
Tucson, AZ 85721

A. Konradi
NASA/Johnson Space Center
Houston, TX 77058

M.A. Lee
University of New Hampshire
Durham, NH 03824

R.B. McKibben
Enrico Fermi Institute
University of Chicago
Chicago, IL 60637

PARTICIPANTS (cont)

R.A. Mewaldt
California Institute of Technology
Pasadena, CA 91125

D.S. Nachtwey
NASA/Johnson Space Center
Houston, TX 77058

P.A. Robinson, Jr.
Jet Propulsion Laboratory
California Institute of Technology
4800 Oak Grove Drive
Pasadena, CA 91109

E.C. Roelof
Applied Physics Laboratory
Johns Hopkins University
Johns Hopkins Road
Laurel, MD 20810

M.A. Shea
Air Force Geophysics Laboratory
Hanscom AFB
Bedford, MA 01731

S. Silverman
Dept. of Physics
Boston College
Chestnut Hill, MA 02173

D.F. Smart
Air Force Geophysics Laboratory
Hanscom AFB
Bedford, MA 01731

E.C. Stone
California Institute of Technology
Pasadena, CA 91125

21997C

TECHNICAL REPORT STANDARD TITLE PAGE

1. Report No. 88-28	2. Government Accession No.	3. Recipient's Catalog No.
4. Title and Subtitle Interplanetary Particle Environment: Proceedings of a Conference		5. Report Date April 15, 1988 6. Performing Organization Code
7. Author(s) Joan Feynman and Stephen Gabriel (editors)		8. Performing Organization Report No.
9. Performing Organization Name and Address JET PROPULSION LABORATORY California Institute of Technology 4800 Oak Grove Drive Pasadena, California 91109		10. Work Unit No. 11. Contract or Grant No. NAS7-918 13. Type of Report and Period Covered JPL External Publication
12. Sponsoring Agency Name and Address NATIONAL AERONAUTICS AND SPACE ADMINISTRATION Washington, D.C. 20546		14. Sponsoring Agency Code
15. Supplementary Notes		

16. Abstract A workshop entitled the Interplanetary Charged Particle Environment was held at the Jet Propulsion Laboratory (JPL) on March 16 and 17, 1987. The purpose of the Workshop was to define the environment that will be seen by spacecraft operating in the 1990s. It focused on those particles that are involved in single event upset, latch-up, total dose and displacement damage in spacecraft microelectronic parts. Several problems specific to Magellan were also discussed because of the sensitivity of some electronic parts to single-event phenomena. Scientists and engineers representing over a dozen institutions took part in the meeting.

The workshop consisted of two major activities, reviews of the current state of knowledge and the formation of working groups and the drafting of their reports. Fifteen presentations were made during the first part of the meeting. Two working groups were then convened, one on solar events and particles accelerated by shocks within the heliosphere and the other on galactic cosmic rays. The working groups made recommendations as to what models should now be used in the assessment of interplanetary particle environments and also recommended what steps should be taken in the future to upgrade the environmental models. This volume contains the reports of the working groups, presentations or extended abstracts of presentations given at the meeting, and a list of the participants.

17. Key Words (Selected by Author(s))	18. Distribution Statement
Reliability; Astrophysics; Solar Physics; Space Radiation	Unclassified -- Unlimited

19. Security Classif. (of this report)	20. Security Classif. (of this page)	21. No. of Pages	22. P
Unclassfied	Unclassified	167	